State of Oregon
Oregon Department of Geology and Mineral Industries
Brad Avy, State Geologist

GEOLOGIC MAP 125

GEOLOGIC MAP OF THE BURNS BUTTE 7.5' QUADRANGLE, HARNEY COUNTY, OREGON

Jason D. McClaughry[1], Carlie J. M. Duda[2], and Mark L. Ferns[3]

2020

[1] Jason.McClaughry@oregon.gov; Oregon Department of Geology and Mineral Industries, Baker City Field Office, Baker County Courthouse, 1995 3rd Street, Suite 130, Baker City, OR 97814
[2] Oregon Department of Geology and Mineral Industries, 800 NE Oregon Street, Suite 965, Portland, OR 97232
[3] Oregon Department of Geology and Mineral Industries, Baker City Field Office; retired.

NOTICE

This manuscript is submitted for publication with the understanding that the United States Government is authorized to reproduce and distribute reprints for governmental use. The views and conclusions contained in this document are those of the authors and should not be interpreted as necessarily representing the official policies, either expressed or implied, of the U.S. government.

This product is for informational purposes and may not have been prepared for or be suitable for legal, engineering, or surveying purposes. Users of this information should review or consult the primary data and information sources to ascertain the usability of the information. This publication cannot substitute for site-specific investigations by qualified practitioners. Site-specific data may give results that differ from the results shown in the publication.

Cover photograph: A view looking northeast into the Willow Creek valley in the west-central part of the Burns Butte 7.5′ quadrangle, Harney County, Oregon (43.582108, −119.222403 WGS84 geographic coordinates; 4827859mN, 320572mE WGS84 UTM Zone 11 coordinates*). The outcrops here expose a faulted sequence of trachyandesite lavas (Tmat) overlain by the 7.1 Ma Rattlesnake Tuff (Tmtr). Photo credit: Jason D. McClaughry, 2019.*

Expires: 12/1/2021

Oregon Department of Geology and Mineral Industries Geologic Map 125
Published in conformance with ORS 516.030.

For additional information:
Administrative Offices
800 NE Oregon Street, Suite 965
Portland, OR 97232
Telephone (971) 673-1555
Fax (971) 673-1562
https://www.oregongeology.org
https://www.oregon.gov/dogami

TABLE OF CONTENTS

LIST OF FIGURES

LIST OF TABLES

GEODATABASE

BB2020_GeMS_v10.7.gdb

See the appendix for geodatabase description. See the digital publication folder for files. Geodatabase is Esri® version 10.7 format. Metadata is embedded in the geodatabase and shapefiles and is also provided as separate .xml format files.

SHAPEFILES AND SPREADSHEETS

Shapefiles

Geochemistry: BB2020_Geochemistry.shp
Geochronology: BB2020_Geochronology.shp
Orientation: BB2020_Orientation.shp
Reference map: BB2020_RefMap.shp
Wells: BB2020_Wells.shp
Cross Section Lines: BB2020_XSectionLine.shp

Spreadsheets (Microsoft® Excel®)

BB2020_DATA.xlsx master file contains sheets:

Geochemistry: BB2020_Geochemistry
Geochronology: BB2020_Geochronology
Orientation: BB2020_Orientation
Wells: BB2020_Wells

MAP PLATE

Plate 1. Geologic map of the Burns Butte 7.5' quadrangle, Harney County, Oregon, scale 1:24,000

1.0 INTRODUCTION

The geology of the Burns Butte 7.5' quadrangle was mapped by the Oregon Department of Geology and Mineral Industries (DOGAMI) during 2019 and 2020 (**Figure 1-1**; Plate 1). This mapping is part of a multi-year geologic study of the Harney Basin, designated a high priority by the Oregon Geologic Mapping Advisory Committee (OGMAC). Key objectives of this project are to 1) provide an updated and spatially accurate geologic framework for the quadrangle, referred to as the map area in the following report; 2) correlate lithologic units to surrounding areas; 3) improve the understanding of the structural and lithologic controls on groundwater aquifers; and 4) describe the occurrence of geologic resources (aggregate, industrial, mineral, and energy) and geologic hazards within the map area. This study was supported in part by a grant from the STATEMAP component of the National Cooperative Geologic Mapping Program (G19AC00160). Additional funds were provided by the State of Oregon.

The core products of this study are this report, an accompanying geologic map and cross sections (Plate 1), an Esri ArcGIS™ geodatabase, and Microsoft Excel® spreadsheets tabulating point data. The geodatabase presents the new geologic mapping in a digital format consistent with the U.S. Geological Survey (USGS) National Cooperative Geologic Mapping Program (NCGMP) Geologic Map Schema (GeMS), version 2.7 (U.S. Geological Survey, 2010; U.S. Geological Survey, 2018). This geodatabase contains spatial information, including geologic polygons, contacts, structures, geochemistry, geochronology, bedding, and water well data, as well as data about each geologic unit such as age, lithology, mineralogy, and structure. Digitization at scales of 1:8,000 or better was accomplished using a combination of 1-m lidar digital elevation models (DEMs) and 1-m 2016 National Agriculture Imagery Program (NAIP) digital orthophotos. Surficial and bedrock geologic units contained in the geodatabase are depicted on the map plate at a scale of 1:24,000. Both the geodatabase and the digital geologic map are supported by this report, which describes the geology in detail.

Collectively, this work refines our understanding of geologic conditions that control the distribution, quantity, and quality of groundwater resources, the distribution of terrain susceptible to landslides, the nature of seismic hazards, and the distribution of potential aggregate sources and other mineral resources in the Burns Butte 7.5′ quadrangle. New detailed geologic data presented here also provide a basis for future geologic, geohydrologic, and geohazard studies in the greater Harney Basin.

Figure 1-1. Location map of the Burns Butte 7.5′ quadrangle (*following page*), showing the status of geologic mapping completed, in progress, and planned in the Harney Basin. Deep pink area encompasses 2019 to 2020 geologic mapping in the Burns Butte 7.5′ quadrangle (this study). Blue quadrangles were mapped by DOGAMI with funding from STATEMAP between 2015 and 2019 (R.A. Houston, unpublished mapping, 2015; Niewendorp and others, 2018; Houston and others, 2018; McClaughry and others, 2019). Yellow quadrangles include geologic maps completed by the USGS (Minor and others, 1987a,b; Johnson, 1994, 1996; Sherrod and Johnson, 1994). Orange quadrangles include geologic mapping completed or in progress by Portland State University (EdMap). Light pink quadrangles include targets of future geologic mapping by DOGAMI. Blue line is the Harney Basin hydrologic boundary. Asterisks are landmarks and labeled as follows: AL – Alkali Lake; AR – Antelope Reservoir; BV – Bear Valley; BR – Beulah Reservoir; BC – Buchanan; BB – Burns Butte; CH – Capehart Lake; CR – Castle Rock; CW – Cow Lakes; CN – Crane; CG – Cougar Mountain; CM – Cottonwood Mountain; CL – Crump Lake; DC – Diamond Craters; DM – Dry Mountain; GB – Glass Buttes; GL – Goose Lake; HL – Harney Lake; HM – Horsehead Mountain; IR – Ingle Mountain; IM – Iron Mountain; JC – Jordan Craters; JR – Juniper Ridge; LA – Lake Abert; LO – Lake Owyhee; LW – Lawen; LJ – Little Juniper Mountain; LV – Logan Valley; ML – Malheur Lake; MNWR – Malheur National Wildlife Refuge; NHS – Neil Hot Springs; SL – Silver Lake; SM – Sheep Mountain; WM – Wagontire Mountain; WRP – Wrights Point; WR – Warm Springs Reservoir.

Figure 1-1. (Location map of the Burns Butte 7.5′ quadrangle – caption on previous page)

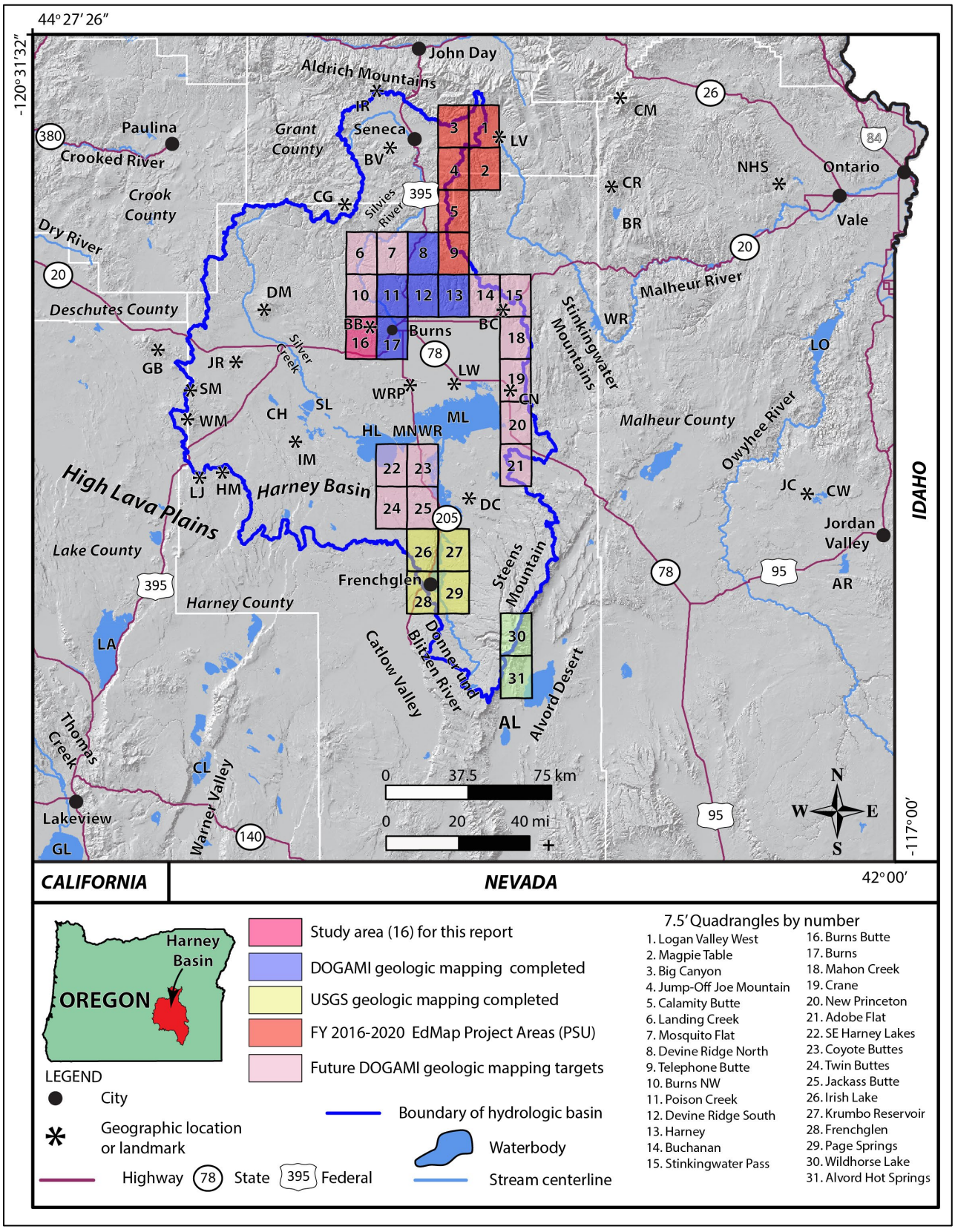

2.0 GEOGRAPHIC AND GEOLOGIC SETTING

The Burns Butte 7.5′ quadrangle is located in the north-central part of the Harney Basin of southeastern Oregon (**Figure 1-1**). The Harney Basin, encompassing approximately 13,566 km^2 (5,247 mi^2), is a hydraulically closed basin fed by several creeks and rivers, including Silver Creek, Silvies River, and the Donner und Blitzen River (**Figure 1-1**). These waterways drain into numerous plains, marshes, and seasonal to permanent lakes, including Harney and Malheur lakes, which lie near the geographic center of the basin. Topographic relief is substantial, ranging from a high of 2,967 m (9,733 ft) at the summit of Steens Mountain to a low of 1,248 m (4,093 ft) at Harney Lake in the center of the basin. Climate in this region is semi-arid, and precipitation (rainfall and snow) varies greatly from year to year.

The Harney Basin is a major physiographic feature in southeastern Oregon lying at the east end of the High Lava Plains (HLP) and along the southern margin of the Blue Mountains Province (BMP; Dicken, 1965; Walker, 1977; **Figure 2-1**). The southern part of the basin, south of the Brothers fault zone (BFZ), includes the northern part of the Basin and Range Province (BRP). The Owyhee Uplands border the Harney Basin on the east (**Figure 2-1**).

The BMP includes the pre-Cenozoic Baker, Wallowa, Olds Ferry, and Izee terranes. These units are exposed along the core and flanks of the east-west trending Aldrich and Strawberry Mountain ranges in the northern part of the Harney Basin (Brooks and Vallier, 1978; **Figure 1-1**, **Figure 2-1**, **Figure 2-2**). Pre-Cenozoic terranes (Olds Ferry-Izee terrane in this area) form an extensive, south-southeast-dipping block that plunges beneath the Harney Basin (Plate 1, cross section A-A′). Deeply eroded pre-Cenozoic rocks in the northern part of the Harney Basin are variably covered by late Oligocene to early Miocene (~24 to 22 Ma) calc-alkaline lavas (Niewendorp and others, 2018; Houston and others, 2018), early to middle Miocene tholeiitic Columbia River flood basalt, and middle Miocene calc-alkaline lavas of the Strawberry Volcanics. The ~16 Ma Picture Gorge Basalt of the Columbia River Basalt Group occurs over a large area of north-central Oregon, extending south into the northern part of the Harney Basin (Cahoon and others, 2020).

The northern extent of the BRP, forming the southern part of the Harney Basin, comprises a series of regional fault blocks that include north-trending Steens Mountain (**Figure 1-1**, **Figure 2-1**, **Figure 2-2**). The volcanic sequence in the southern Harney Basin includes late Oligocene and early Miocene calc-alkaline volcanic rocks (~26 to 22 Ma; Minor and others, 1987a,b; Langer, 1991; Scarberry and others, 2009), early to middle Miocene tholeiitic Columbia River flood basalts, intercalated middle Miocene ash-flow tuffs, and overlying olivine basalt flows. Flows of the ~17 to 16.5 Ma Steens Basalt (Camp and others, 2013; Kasbohm and Schoene, 2018; Moore and others, 2018), forming part of this southern volcanic sequence, are the earliest lavas to erupt as part of the Columbia River Basalt Group. Steens flows cover much of southeastern Oregon and parts of southwestern Idaho to northern Nevada, and likely underlie a significant portion of the southern to central part of the Harney Basin (**Figure 2-2**). Large-displacement (>150 m [>500 feet]), north-northeast to northwest-trending normal faults (e.g., Winter Rim fault, Abert Rim fault, Hart Mountain fault, Steens Mountain fault) characterize the Basin and Range Province in Oregon. Colgan and others (2008) proposed northwest Basin and Range Province experienced a two-stage slip history with extensional uplift of ranges, occurring between 14 and 8 Ma and again at ~4 to 3 Ma. Scarberry and others (2009) demonstrated activity on the Abert Rim fault and associated NW-striking faults after ~9 Ma and before ~7.5 Ma. The Abert Rim fault propagated northward after 7 Ma to a linkage with NW-striking faults forming the Brothers fault zone.

The HLP transects the central part of the Harney Basin, forming a late Cenozoic volcanic upland, continuous and gradational into the BRP. Volcanic rocks exposed in the HLP younger than 12 Ma are

strongly bimodal, including relatively equal volumes of thin primitive basalt flows and rhyolitic tuffs and domes (MacLeod and others, 1976; Jordan and others, 2004; Scarberry and others, 2009; Ford and others, 2013). Rhyolitic rocks, in general, successively young to the northwest, toward Newberry Volcano (MacLeod and others, 1976). Basaltic flows, as young as latest Holocene, are present in the southern part of the Harney Basin (e.g., Diamond Craters) (**Figure 1-1**, **Figure 2-2**). The BFZ lies across the southern part of the Harney Basin as a wide diffuse zone interpreted as an intracontinental transform fault separating the extended crust of the BRP from comparatively un-extended BM crust to the north (Walker, 1969; Lawrence, 1976; **Figure 2-1**). The Steens fault zone (Personius and Haller, 2016) extends across the eastern end of the BFZ, while the western end is buried by a ~ 80 ka Newberry flow (Macleod and Sherrod, 1992; Jordan and others, 2004). Lawrence (1976) described the BFZ as a series of longer (as much as 20 km [12.4 miles]), discontinuous en echelon faults (Reidel shears) trending ~N. 50° W. and less abundant shorter (5 km [3.1 miles]) N. 30° E. faults expressed as horst and graben structures (Lawrence, 1976). Faults in the BFZ largely dip steeply northeast, with a down-on-the-northeast sense of offset. Iademarco (2009), Trench (2008), and Trench and others (2012) suggested en echelon faults in the BFZ formed from ~7 Ma to 5 Ma. Trench (2008) suggested east-west extension in the BRP transitions into the BFZ by way of dextral oblique strike-slip horsetail fractures and structural clockwise rotation about a pole located in northeastern Oregon.

Three voluminous, locally erupted late Miocene ash-flow tuffs are widely exposed across the Harney Basin (**Figure 2-2**; **Figure 2-3**). These units include the 9.74 Ma Devine Canyon Ash-flow Tuff , 8.4 Ma Prater Creek Ash-flow Tuff (**Tmtp**), and 7.1 Ma Rattlesnake Tuff (**Tmtr**) (Walker, 1979; Streck, 1994; Streck and Grunder, 1995, 2008; Jordan and others, 2004; Ford and others, 2013). Marginal to their vent areas, these successive cliff- and bench-forming ash-flow tuffs are locally separated from one another by intervening, poorly exposed tuff beds and tuffaceous sedimentary rocks (**Tmst**). The Rattlesnake Tuff (**Tmtr**) is the youngest and largest of the three late Miocene Harney Basin tuffs, having an estimated eruptive volume >280 km^3 (>67 mi^3) and outcrops covering an area >35,000 km^2 (>13,500 mi^2) (Streck and Grunder, 1995; **Figure 2-3**). The Devine Canyon Ash-flow Tuff is the oldest and second most widespread of the late Miocene tuffs with an eruptive volume estimated at 250 to 300 km^3 (60 to 72 mi^3) and outcrops covering an area >30,800 km^2 (>11,891 mi^2) (Isom, 2017). The intermediate age Prater Creek Ash-flow Tuff (**Tmtp**) is the smallest of the three late Miocene tuffs, having an eruptive volume of ~200 km^3 (~48 mi^3) and outcrops covering an area of ~9,615 km^2 (~3,713 mi^2) (Greene, 1973; Parker, 1974; Streck and Ferns, 2004). The type sections for these ash-flow tuffs are in Devine Canyon, located along the eastern edge of the Poison Creek 7.5′ quadrangle (Walker, 1979; McClaughry and others, 2019).

Caldera sources for the three late Miocene Harney Basin ash-flow tuffs (Devine Canyon, Prater, Rattlesnake) have no surface expression (**Figure 2-2**; **Figure 2-3**). Extensive Rattlesnake Tuff (**Tmtr**) outflow deposits originating from the Capehart Lake area completely inundated and largely buried evidence for earlier late Miocene calderas in the Harney Basin (**Figure 2-2**; **Figure 2-3**). Previous studies have inferred the likelihood of source calderas to lie beneath the Harney Basin on the basis of mapped outcrop distribution of tuffs, thickness changes, welding characteristics, distance correlations with pumice-lithic size/shape, and geophysics (Greene, 1973; Parker, 1974; Walker, 1974, 1979; Walker and Nolf, 1981; Streck, 1994; Streck and Grunder, 1995, 2008; Meigs and others, 2009; Cox, 2011; Cox and others, 2013; Ford and others, 2013; Khatiwada and Keller, 2015). **Figure 2-3** illustrates the distribution of late Miocene tuffs across the Harney Basin and shows the locations of postulated source calderas. More recent mapping and characterization of two deep exploration wells penetrating through Rattlesnake Tuff (**Tmtr**) has identified a previously unknown, >427-m-thick (>1,400 ft) section of monotonous rhyolitic tuff (**Tmtpi**) underlying the Burns Butte area (Federal 1-10, CTI; **Table 2-1**) (McClaughry and others, 2019).

The buried rhyolitic tuff (**Tmtpi**) shares a similar stratigraphic position to and is geochemically indistinguishable from surface exposures of the Prater Creek Ash-flow Tuff (**Tmtp**). This linked relationship provides direct evidence that the source vent the Prater Creek Ash-flow Tuff (**Tmtp**) lies concealed beneath the Burns Butte area. McClaughry and others (2019) referred to this cryptic Prater Creek eruptive center as the Silvies River caldera (**Figure 2-3**, Plates 1 and 2).

Tmtpi deposits are spatially associated with a bimodal suite of late Miocene (~8.4 to 7.68 Ma) rhyolitic tuffs (tuff of Wheeler Springs, [**Tmtw**, **Tmtwh**]), exogenous rhyolite domes and flows (rhyolite of Golden Ranch [**Tmrg**], rhyolite of Burns Butte [**Tmrb**]**,** rhyolite intrusive rocks [**Tmri**]), and (7.68 to 7.1 Ma) basaltic trachyandesite and trachyandesite flows, dikes, and vent deposits (**Tmatu, Tmat**, **Tmvt, Tmati**). These rocks define a narrow volcanic field of silicic domes and mafic shield volcanoes lying above caldera-filling tuffs (**Tmtpi**) (Plate 1; McClaughry and others, 2019).

Late Miocene rocks in the Burns Butte 7.5′ quadrangle are locally covered by late Pliocene to Quaternary sedimentary rocks (**QTst**) and basaltic lava flows (**QTbw**), and younger surficial units, including older fan deposits (**Qoaf**), colluvium (**Qc**), fan deposits (**Qaf**), alluvium (**Qa**), marsh and alluvial deposits (**Qma**), and modern fill (**Qf**). Landslide deposits (**Qls**) are also present in some areas. Mima mounds, observed in 1-m lidar DEMs, are a conspicuous surficial feature across surfaces underlain by the Rattlesnake Tuff (**Tmtr**).

Table 2-1. List of oil and gas exploration wells, geothermal test wells, and groundwater observation wells drilled in and adjacent to the Burns Butte 7.5′ quadrangle. See section 6 and McClaughry and others (2019) for detailed well information.

Well Name	Year Drilled	Total Depth (m)	Total Depth (ft)	Type	Cuttings	LAT_NAD83	LONG_NAD83
Dog Mountain	1912	>1,147	>3,763	oil and gas exploration	no	unknown#	
United Company of Oregon, Inc., #1 Fay (HARN 52702) *^	1945	1,166	3,826	oil and gas exploration	yes	43.50400	−118.77003
United Company of Oregon, Inc., Weed and Poteet #1 (HARN 52707) *^	1949	1,976	6,480	oil and gas exploration	no	43.59358	−119.01930
H.C. Voglar No. 1 (HARN 52706) *^	1949	1,387	4,550	oil and gas exploration	no	43.45563	−118.94754
Michael T. Halbouty Federal 1-10 (HARN 52703) *^	1977	2,343	7,684	oil and gas exploration	yes	43.59260	−119.22004
CTI geothermal test well (HARN 50087) ^	1996	596	1,956	geothermal exploration	yes	43.55013	−119.08158
EOARC Observation Well (HARN 52747) ^	2018	171	560	groundwater observation	yes	43.52580	−119.02042

#Buwalda (1921) reported a location 19 km (12 mi) south of Burns near Dog Mountain.

*Additional information is available for these wells from the DOGAMI Oil and Gas Well Log Index — https://www.oregongeology.org/mlrr/oilgas-logs.htm

^Additional information available for these wells from the OWRD Groundwater Information System — https://apps.wrd.state.or.us/apps/gw/gw_info/gw_info_report/gw_details.aspx?gw_site_id=30492 (HARN 52702 #1 Fay); https://apps.wrd.state.or.us/apps/gw/gw_info/gw_info_report/gw_details.aspx?gw_site_id=30497 (HARN 52707 Weed and Poteet); https://apps.wrd.state.or.us/apps/gw/gw_info/gw_info_report/gw_details.aspx?gw_site_id=30496 (HARN 52706 H.C. Voglar No. 1); https://apps.wrd.state.or.us/apps/gw/gw_info/gw_info_report/gw_details.aspx?gw_site_id=30493 (HARN 52703 Federal 1-10); https://apps.wrd.state.or.us/apps/gw/gw_info/gw_info_report/gw_details.aspx?gw_site_id=12735 (HARN 50087 CTI); https://apps.wrd.state.or.us/apps/gw/gw_info/gw_info_report/gw_details.aspx?gw_site_id=31110 (HARN 52747 EOARC).

Figure 2-1. Physiographic province map of Oregon, showing location of the Brothers fault zone, selected Basin and Range faults, and the study area. Abbreviations: CR – Coast Range; HC – High Cascades; KM – Klamath Mountains; WC – Western Cascades; WV – Willamette Valley. Solid black lines demarcate physiographic provinces (after Walker, 1977). Blue lines are selected major Basin and Range type normal faults, showing normal displacement direction (ball and bar on downdropped block). Red line marks the location of the Harney hydrologic basin. Basemap: 10-m hillshade DEM.

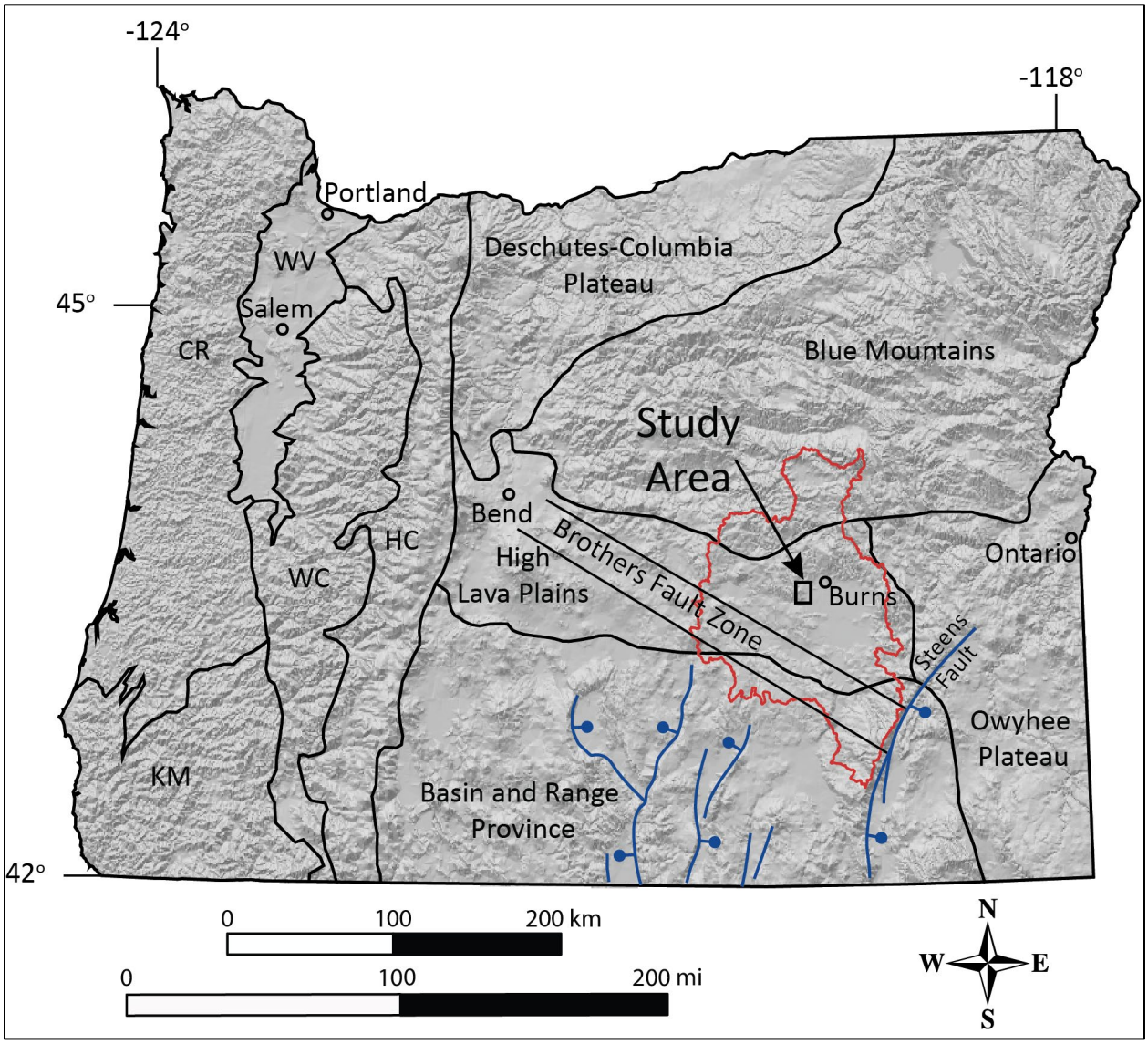

Figure 2-2. Generalized geologic map of southeastern Oregon, after compiled data of Smith and Roe (2015). Red-outlined quadrangle is the map area. The blue line marks the location of the Harney hydrologic basin.

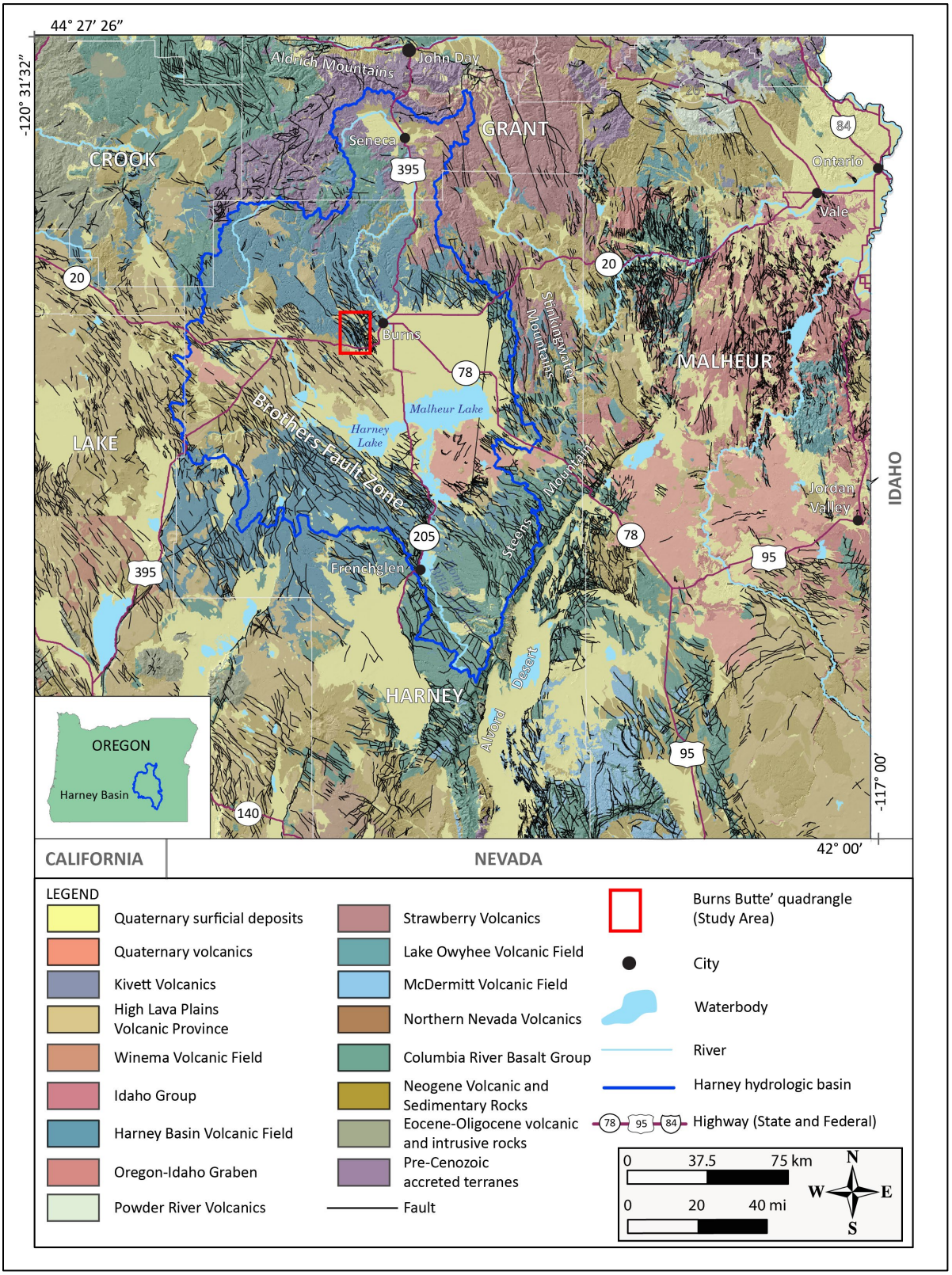

Figure 2-3. Outcrop distribution and proposed source areas for late Miocene tuffs in the Harney Basin (next page). RT – Rattlesnake Tuff (Tmtr), PCT – Prater Creek Ash-flow Tuff (Tmtp), DCT – Devine Canyon Ash-flow Tuff (Tmtd). Estimated distribution outline for RT is from Streck and Grunder (1995), Streck and others (1999), and Streck and Ferns (2004). Estimated unit distribution outlines for the DCT and PCT are from Streck and Ferns (2004) and Isom (2017), modified from Greene (1973) and Walker (1979), respectively. Red, solid to dashed line represents the eastern margin of the Silvies River caldera as defined by McClaughry and others (2019) (see Structure section for further discussion). Abbreviated locations are as described in the caption in Figure 1-1.

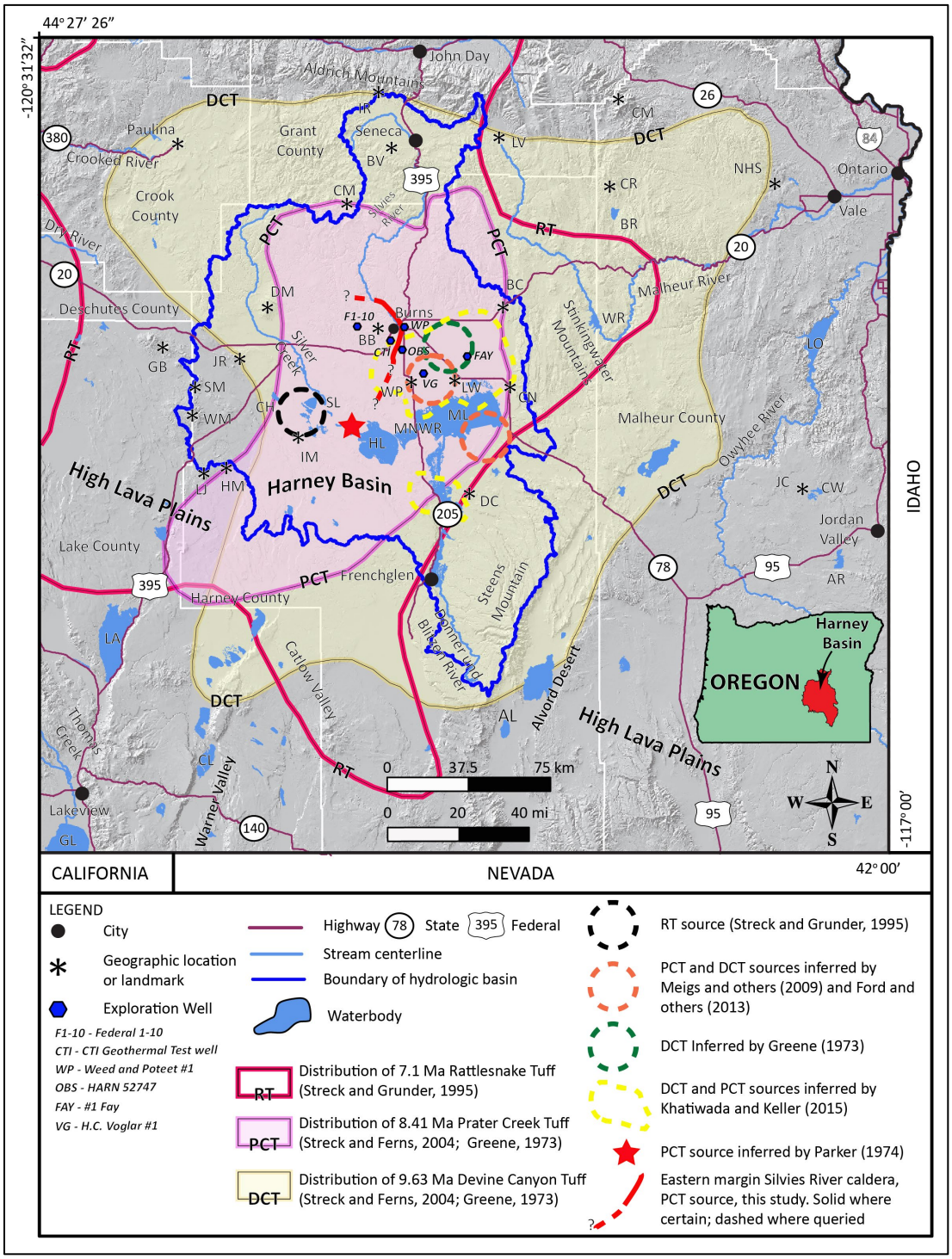

3.0 PREVIOUS WORK

Table 3-1 shows a list of previous regional geologic investigations consulted for work in the Burns Butte 7.5′ quadrangle. Reports and maps listed in **Table 3-1** are organized in chronological order; those shown in bold are geologic maps that lie within the study area. The index map shown in **Figure 3-1** summarizes the sources of previous geologic mapping consulted during this project. Earlier geologic maps and reports displaying the bedrock geology in and adjacent to the study area include those by Piper and others (1939), Greene (1972), Greene and others (1972), Brown and others (1980a,b), Brown (1982), McGrane (1985), Walker and MacLeod (1991), Smith and Roe (2015), S. L. Isom and M. J. Streck (unpublished data, 2017), Niewendorp and others (2018), Houston and others (2018), R. Houston and others (unpublished data, 2016), and M. Cruz and M. J. Streck (unpublished data, 2018). Additional scientific investigations consulted during this study include Russell (1884), Leonard (1970), Walker (1970), Greene (1973), Niem (1974), Lawrence (1976), Walker (1979), Sherrod and Johnson (1994), Sheppard (1994), MacLean (1994), Streck (1994), Streck and Grunder (1995), Johnson (1994, 1996), Jordan (2001), Jordan and others (2002), Camp and others (2003), Jordan and others (2004), Streck and Ferns (2004), Trench (2008), Meigs and others (2009), Milliard (2010), Ford (2012), Boschmann (2012), Ferns and McClaughry (2013), Camp and others (2013), Ford and others (2013), Streck and others (2015), Khatiwada and Keller (2015), and McClaughry and others (2019).

Table 3-1. Partial chronological list of maps and reports on which this study builds. Maps shown in bold lie within or adjacent to the study area. Unpub. is unpublished geologic mapping.

Author	Year	Subject	Scale
Piper and others	**1939**	**Geology and groundwater resources of the Harney Basin**	**1:125,000**
Leonard	1970	Ground-water resources in Harney Valley	na
Walker	1970	Cenozoic ash-flow tuffs of Oregon	na
Greene	**1972**	**Geologic map Burns and West Myrtle-Butte 15′ quadrangles**	**1:62,500**
Greene and others	**1972**	**Geologic map of the Burns quadrangle**	**1:250,000**
Greene	1973	Petrology of the welded tuff of Devine Canyon	na
Niem	1974	Wright's Point, Harney County, Oregon	na
Walker	1979	Revisions to the Cenozoic stratigraphy of Harney Basin	na
Brown and others	**1980a**	**Geothermal resource potential northern Harney Basin**	**1:62,500**
Brown and others	**1980b**	**Geothermal resource potential southern Harney Basin**	**1:62,500**
Brown	**1982**	**Geology/geothermal resources south half Burns 15′ quadrangle**	**1:24,000**
McGrane	1985	Geology of the Idol City area	1:24,000
Walker and MacLeod	1991	Geologic map of Oregon	1:500,00
MacLean	1994	Geochem. Juniper Ridge, Horsehead Mtn., Burns Butte	na
Streck	1994	Volcanology and petrology of the Rattlesnake Tuff	na
Streck and Grunder	1995	Crystallization and welding variations Rattlesnake Tuff	na
Jordan	2001	Basaltic volcanism and tectonism of the High Lava Plains	na
Jordan and others	2002	Bimodal volcanism and tectonism of the High Lava Plains	na
Jordan and others	2004	Geochronology of the High Lava Plains	na
Streck and Ferns	2004	The Rattlesnake Tuff and silicic volcanism	na
Meigs and others	2009	Magmatic and tectonic development of High Lava Plains	na
Cox	2011	controlled-source seismic/gravity study High Lava Plains	na
Ford	2012	Rhyolitic magmatism of the High Lava Plains	na
Ford and others	2013	Bimodal volcanism of the High Lava Plains	na
Cox and others	2013	controlled-source seismic/gravity study High Lava Plains	na
Smith and Roe	2015	Oregon geologic data compilation (OGDC), release 6	variable
Khatiwada and Keller	2015	Geophysical imaging of upper crust Harney Basin	na
Isom	2017	Composition of the Devine Canyon Tuff	na
Isom and Streck	unpub.	Geologic map of the Telephone Butte 7.5′ quadrangle	1:24,000
Cruz and Streck	unpub.	Geologic map of the Calamity Butte 7.5′ quadrangle	1:24,000
Niewendorp and others	**2018**	**Geologic map of the Devine Ridge South 7.5′ quadrangle**	**1:24,000**
Houston and others	**2018**	**Geologic map of the Devine Ridge North 7.5′ quadrangle**	**1:24,000**
R. Houston and others	unpub.	Geologic map of the Harney 7.5′ quadrangle	1:24,000
McClaughry and others	**2019**	**Geologic map of the Poison Creek and Burns 7.5′ quadrangles**	**1:24,000**

Figure 3-1. Sources of geologic maps consulted during the project. See DataSourcePolys feature class in the geodatabase. Blue line marks the location of the Harney hydrologic basin. Basemap: 10-m shaded relief DEM.

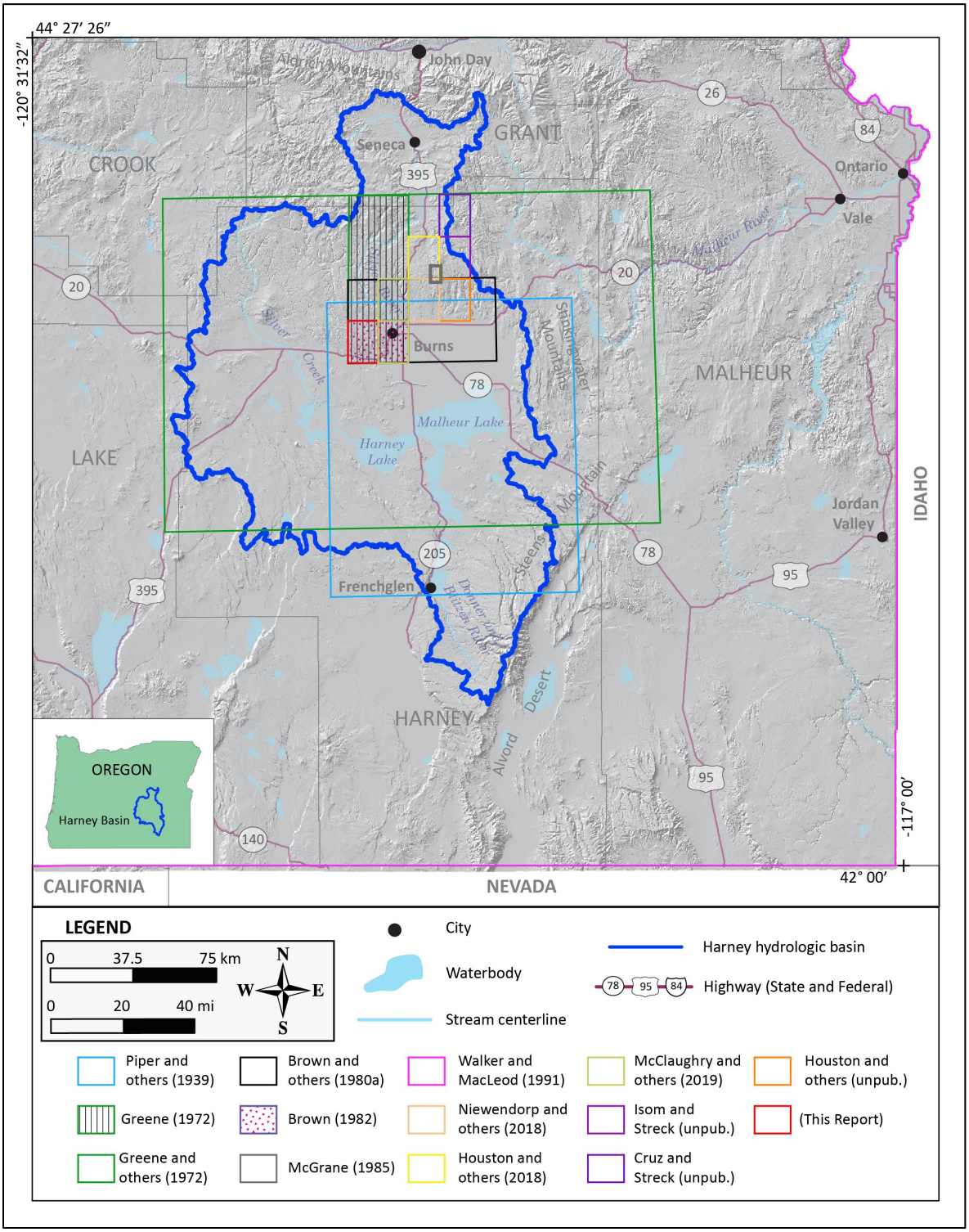

4.0 METHODOLOGY

Mapping presented in this report was collected digitally in the field using a GPS-enabled Apple® iPad® 4, with Esri™ Collector, following standard DOGAMI procedures outlined by Duda and others (2018, 2019). Detailed field mapping used 1-m lidar DEMs (8 pts/m^2), USGS digital raster graphics (DRGs), and digital orthophoto imagery (2016) obtained from Google Earth™ as basemaps. Fieldwork conducted during this study consisted of data collection along roads combined with transects following lithologic contacts and faults across public and private rangelands. Standard geologic methods for collecting samples and measuring attitudes of inclined bedding, geologic features, and faults were employed.

New mapping was compiled with published and unpublished data and was converted into digital format using Esri ArcGIS™ ArcMAP™ GIS software. On-screen digitizing was performed through heads-up digitizing using georeferenced 1-m lidar DEMs, 1:24,000-scale USGS digital raster images (DRGs), USGS 10-m DEMs, and 2016 National Agriculture Imagery Program (NAIP) digital orthophotos. Digitization and the final digital Esri ArcGIS ArcMap format geologic database were completed at a minimum scale of 1:8,000, supported by full 3D visualization of lidar DEMs in Quick Terrain Modeler™ (Duda and others, 2018, 2019). The geologic time scale used is the 2020 (v2020/01), version of the International Stratigraphic Commission's International Chronostratigraphic Chart (https://stratigraphy.org/icschart/ChronostratChart2020-01.pdf) revised from Cohen and others (2013).

In this report, volcanic rocks with fine-grained (<1 mm [0.04 in]; Mackenzie and others, 1997; Le Maitre and others, 2004), average crystal or particle size in the groundmass are characterized in the following manner:

- A "coarse groundmass" if the average crystal or particle size is <1 mm (0.04 in) and can be determined using the naked eye (>~0.5 mm [0.02 in]).
- A "medium groundmass" if crystals of average size cannot be determined by eye but can be distinguished by using a hand lens (>~0.05 mm [0.02 in]).
- A "fine groundmass" if crystals or grains of average size can be determined only by using a microscope (or by hand lens recognition of phyllite-like sparkle or sheen in reflected light, indicating the presence of crystalline groundmass).
- A "glassy groundmass" if the groundmass has (fresh), or originally had (altered), groundmass with the characteristics of glass (conchoidal fracture; sharp, transparent edges; vitreous luster; etc.).
- Mixtures of crystalline and glassy groundmass are described as intersertal; ratios of glass to crystalline materials may be indicated by textural terms including holocrystalline, hypocrystalline, hyalophitic, and hyalopilitic.
- Microphenocrysts are defined as crystals larger than the overall groundmass and < 1 mm across (0.04 in).

Grain size of clastic sedimentary rocks is described following the Wentworth (1922) scale. Hand samples of unconsolidated sediments and clastic sedimentary rocks were compared in the field and/or in the laboratory to graphical representations (comparator) of the Wentworth scale to determine average representative grain size in various parts of a respective sedimentary geologic unit. Colors given for hand-sample descriptions are from the Geological Society of America Rock-Color Chart Committee (1991).

Whole-rock geochemical data are useful in further classifying volcanic rocks, as many lavas are too fine grained and glassy to be adequately characterized by mineralogical criteria alone. Descriptive rock unit names for volcanic rocks are based in part on online British Geological Survey classification schemes (Gillespie and Styles, 1999; Robertson, 1999; Hallsworth and Knox, 1999) and on normalized major

element analyses plotted on the total alkali ($Na_2O + K_2O$) versus silica (SiO_2) diagram (TAS) of Le Bas and others (1986), Le Bas and Streckeisen (1991), and Le Maitre and others (1989, 2004). Whole-rock geochemical samples were prepared and analyzed by X-ray fluorescence (XRF) at the Washington State University GeoAnalytical Lab, Pullman, Washington, under the direction of Dr. Ashley Steiner. Analytical procedures for the Washington State University GeoAnalytical Lab are described by Johnson and others (1999) and are available online at https://environment.wsu.edu/facilities/geoanalytical-lab/technical-notes/. Major element determinations are normalized to a 100-percent total on a volatile-free basis and recalculated with total iron expressed as FeO*.

Our mapping presents three new $^{40}Ar/^{39}Ar$ ages, prepared and analyzed by Dr. Dan Miggins at the College of Oceanic and Atmospheric Sciences, Oregon State University, Corvallis (OSU). The methodology for $^{40}Ar/^{39}Ar$ geochronology at OSU is summarized in Duncan and Keller (2004) and the OSU laboratory website http://geochronology.coas.oregonstate.edu/. The map also includes three additional K-Ar and $^{40}Ar/^{39}Ar$ ages compiled from Fiebelkorn and others (1982) and Jordan and others (2004). For numerical ages assigned to dated units, we use standard conventions in reporting age in millions of years ago (mega-annum, abbreviated Ma) for units > 1 m.y. old.

The magnetic polarity of strongly magnetized lavas was determined at numerous outcrops in the Burns Butte area by using a handheld digital fluxgate magnetometer. Magnetic polarity reversals, commonly preserved by volcanic rocks and readily measured in the field, provide for 1) distinguishing between flow units with normal and reversed magnetic polarity, 2) a check on the permissible age of isotopically dated samples, when compared to the paleomagnetic time scale (Cande and Kent, 1992), and 3) another way to constrain possible depositional ages for some undated strata.

Orientation measurements of geological planes (e.g., inclined bedding) were obtained in the field area by traditional compass and clinometer methods and were compiled from data published by previous workers. Additional bedding measurements were generated from lidar imagery by using a routine and model developed by DOGAMI in Esri ArcGIS™ Model Builder to calculate three-point solutions from lidar bare-earth DEMs. Further details of this process are described in the appendix under the heading Orientation points.

Subsurface geology shown in the geologic cross section on Plate 1 incorporates lithologic descriptions, analyses, and geologic interpretations from 1) oil and gas exploration well logs from the Federal 1-10 well (HARN 52703) and 2) water-well drill records (Appendix). Records of historical oil and gas and geothermal exploration are available online from the DOGAMI Oil and Gas Well Log Index (https://www.oregongeology.org/mlrr/oilgas-logs.htm) and Geothermal Information Layer for Oregon web portal (https://www.oregongeology.org/gtilo/index.htm). Water well logs are available through the Oregon Water Resources Department (OWRD) Groundwater Resource Information Distribution (GRID) system (https://apps.wrd.state.or.us/apps/gw/well_log/). Water wells were not physically located. However, an attempt was made remotely to locate water wells and other drill holes that have well logs archived by OWRD. Approximate locations were estimated by using a combination of sources, including internal OWRD databases of located wells, Google Earth™, taxlot maps, street addresses, and aerial photographs. The accuracy of the locations ranges widely, from errors of 1.1 km (0.7 mi) for wells located only by section and plotted at the section centroid, to a few tens of feet for wells located by address or taxlot number on a city lot with bearing and distance from a corner. A well log ID is queried in the OWRD database (e.g., HARN-51852) to retrieve an image of the well log from the OWRD website (https://apps.wrd.state.or.us/apps/gw/well_log/). A database of 61 well logs with interpreted subsurface geologic units for the Burns Butte 7.5′ quadrangle is provided with the geodatabase.

Microsoft Excel® spreadsheets tabulating geochemical and geochronological analyses, orientation measurements, and water wells are provided as part of this publication. The appendix contains a more detailed explanation of data collection methods and the field list for the spreadsheets mentioned above.

Map coordinates for outcrop photographs are given in report figure captions allowing the interested reader to visit these sites in the field or to visualize them remotely using Google Earth™. Locations are provided in two coordinate systems: 1) Geographic (datum = WGS84, units = decimal degree); and 2) Universal Transverse Mercator (UTM) Zone 11 (datum = WGS84, units = meters). Decimal degree coordinates can be entered into the "Fly to" box (e.g., 45.66132, −121.47123) in the Google Earth™ search toolbar, and Google Earth™ will automatically locate and "fly" to the specified site. UTM coordinates are provided for the reader who would like to more precisely locate and visit sites in the field using a handheld GPS unit.

5.0 EXPLANATION OF MAP UNITS

The terrestrial volcanic and sedimentary bedrock in the Burns Butte 7.5′ quadrangle ranges in age from late Miocene to early Pleistocene (**Figure 5-1**; Plate 1). Bedrock geologic units are locally covered along drainages and on some slopes in the project area by Late Pleistocene and Holocene surficial deposits. Widely separated stratigraphic units were correlated on the basis of apparent stratigraphic position, lithology, and chemical composition. Unit names follow established stratigraphic nomenclature when available, but when formal rock names are lacking, informal names are given on the basis of composition or sites of good exposure. **Figure 5-1** depicts a time-rock chart showing age ranges for late Cenozoic bedrock and surficial units.

5.1 Overview of map units

UPPER CENOZOIC SURFICIAL DEPOSITS

Qf modern fill and construction material (upper Holocene)
Qma marsh and alluvial deposits (Holocene and Upper Pleistocene[?])
Qa alluvium (Holocene and Upper Pleistocene[?])
Qaf fan deposits (Holocene and Upper Pleistocene[?])
Qls landslide deposits (Holocene and Upper Pleistocene[?])
Qc colluvium (Holocene and Upper Pleistocene[?])
Qoaf older fan deposits (Holocene and Pleistocene[?])

Angular Unconformity to Disconformity

UPPER CENOZOIC VOLCANIC AND SEDIMENTARY ROCKS

LOWER PLEISTOCENE TO UPPER MIOCENE SEDIMENTARY ROCKS

Harney Formation

QTst sedimentary rocks (lower Pleistocene[?] to upper Miocene [?])
QTbw Wrights Point Member (Pliocene) 3.29 ± 0.03 Ma ($^{40}Ar/^{39}Ar$; groundmass); 3.69 ± 0.57 Ma ($^{40}Ar/^{39}Ar$; plagioclase)

Angular unconformity to disconformity

UPPER MIOCENE VOLCANIC AND SEDIMENTARY ROCKS

Tmatu basaltic andesite flows and dikes (upper Miocene)

Tmtr Rattlesnake Tuff (upper Miocene) 7.05± 0.01 ($^{40}Ar/^{39}Ar$); 7.093 ± 0.015 Ma ($^{40}Ar/^{39}Ar$)

Tmst tuffaceous sedimentary rocks (upper Miocene)

Tmat basaltic trachyandesite and trachyandesite flows and dikes (upper Miocene)

Tmvt basaltic trachyandesite and trachyandesite vent deposits (upper Miocene)

Tmrb rhyolite of Burns Butte (upper Miocene) 7.68 ± 0.04 Ma ($^{40}Ar/^{39}Ar$); 7.74 ± 0.1 Ma (K-Ar)

Tmrg rhyolite of Golden Ranch (upper Miocene) 8.46 ± 0.03 Ma ($^{40}Ar/^{39}Ar$); 8.03 ± 0.26 Ma (K/Ar)

Tmri rhyolite and trachydacite (upper Miocene)

Tmtwh tuff of Wheeler Springs, non-welded lapilli tuff (upper Miocene)

Tmtw tuff of Wheeler Springs, welded tuff (upper Miocene)

Tmatl basaltic trachyandesite, trachyandesite, and trachydacite flows and dikes (upper Miocene) (cross section only)

Tmtp Prater Creek Ash-flow Tuff (upper Miocene) 8.41 ± 0.16 Ma ($^{40}Ar/^{39}Ar$); 8.48 ± 0.05 Ma ($^{40}Ar/^{39}Ar$)

Tmtpi Prater Creek Ash-flow Tuff, intracaldera unit (upper Miocene) (cross section only) 8.52 ± 0.02 Ma ($^{40}Ar/^{39}Ar$)

Figure 5-1. Time-rock chart for the Burns Butte 7.5' quadrangle showing the 22 geologic units displayed on the geologic map and in cross section on Plate 1.

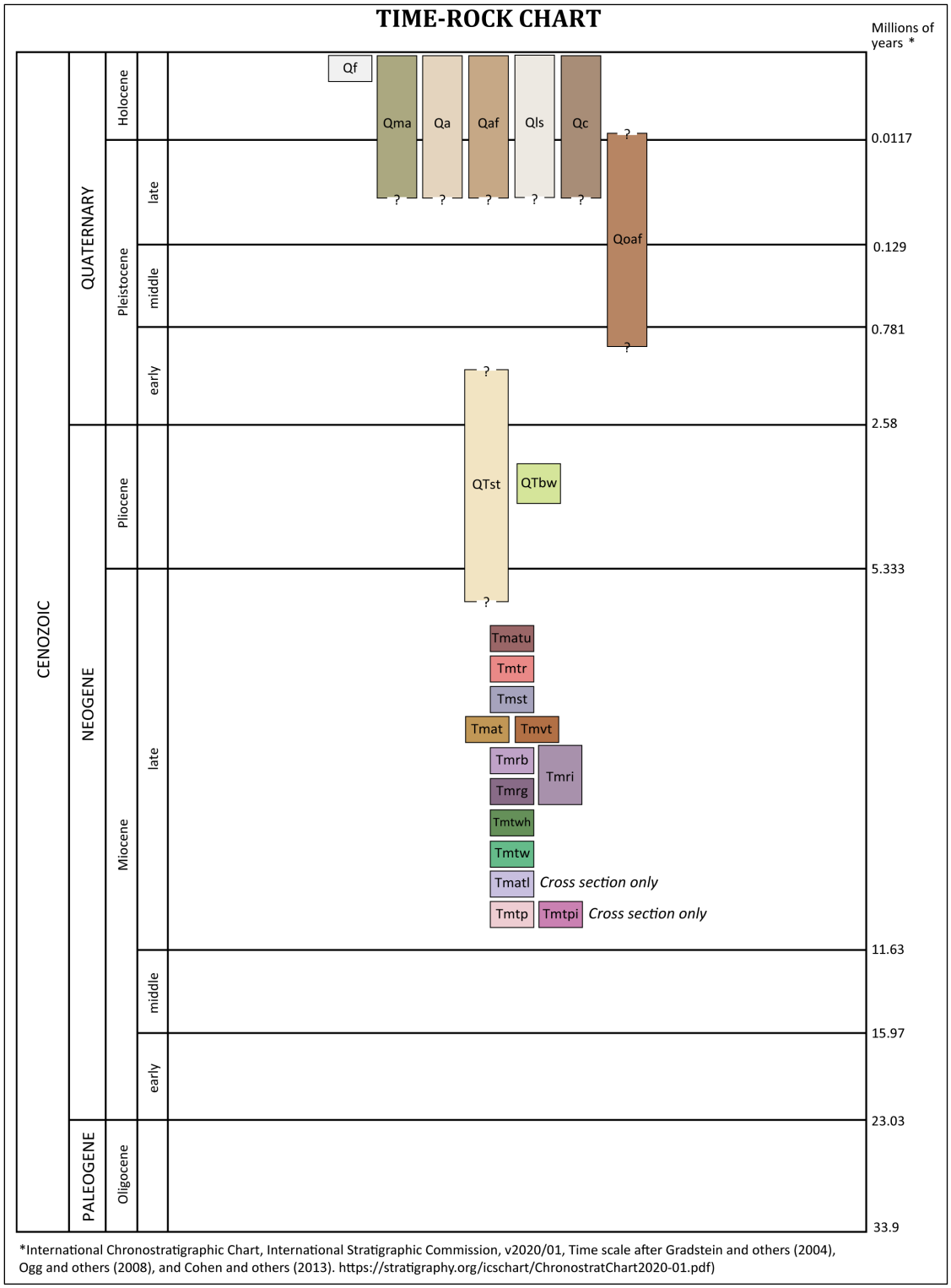

5.2 Upper Cenozoic surficial deposits

Upper Cenozoic sedimentary and volcanic rocks are locally covered by Upper Pleistocene and Holocene surficial deposits in the Burns Butte 7.5′ quadrangle, including alluvial, landslide, and fan deposits (**Figure 5-1**; Plate 1). Surficial units within the project area are delineated on the basis of geomorphologic expressions as interpreted from a combination of field observations, 1-m lidar DEMs, shaded relief raster images, USGS digital raster graphics (DRGs), and digital orthophoto imagery (2016).

Qf **modern fill and construction material (upper Holocene)**—Variable constructed fill deposits of poorly sorted and crudely layered mixed gravel, sand, clay, and other engineered fill (Plate 1). These deposits usually contain rounded to angular clasts ranging from small pebbles to boulders up to several meters across. The orientation of clasts is typically less uniform than is found in naturally occurring imbricated or bedding-parallel gravel. Deposits mapped as modern fill and construction material are generally associated with dams, road embankments (e.g., U.S. Highway 20, Burns-Izee Road), approaches to bridges, rail beds, culvert fills, mined land, and other low-lying areas (Plate 1). Additional artificial fills are present throughout the study area but are at too small a scale to digitize or portray on the map plate. The thickness of fill deposits may locally exceed several meters.

Qma **marsh and alluvial deposits (Holocene and Upper Pleistocene[?])**—Peat and muck interbedded with unconsolidated clay and silt deposited across the broad, low relief and saturated alluvial plain of the northern part of the Harney Valley in the southeast part of the map area (Plate 1). The unit includes some horizons of volcanic ash (Piper and others, 1939). Coarser alluvium composed of sand and gravel occurs along larger valley-traversing streams. The thickness of marsh and alluvial deposits may be up to 27 to 40 m (90 to 130 ft) in this part of the Harney Valley. The unit is assigned a Holocene and Late Pleistocene age on the basis of stratigraphic position. The area covered by marsh and alluvial deposits prior to settlement was originally native meadow and swamp. The area is now extensively reclaimed as serviceable meadowlike ranch and agriculture land (Piper and others, 1939). Partly equivalent to Qal (valley fill) of Piper and others (1939), Qs (sedimentary deposits) of Greene (1972), Greene and others (1972), and Walker (1977), Qs/Qal (alluvium and Holocene sedimentary deposits, undifferentiated) of Brown and others (1980a), and Qal (recent alluvium and sedimentary deposits, undivided) of Brown (1982).

Qa **alluvium (Holocene and Upper Pleistocene[?])**—Unconsolidated gravel, sand, silt, and clay deposited along active stream channels and on adjacent floodplains of Willow Creek, Sage Hen Creek, Brush Canyon, and smaller tributaries (Plate 1). Gravels deposited as imbricated, massive to cross-stratified accumulations on smaller mid-channel islands and bars are the most common type of near-channel alluvium along major tributaries. The unit is composed completely of locally derived volcanic detritus. Thickness of alluvial deposits is generally less than 5 m (16 ft) along smaller upland tributary streams. Beneath Sage Hen Valley, thickness of alluvial deposits may be up to 33 m (100 ft), as determined on the basis of interpretation of well logs (Appendix). Bedrock units are locally exposed in the bottoms of stream channels within areas mapped as unit **Qa**. The unit is assigned a Holocene and Late Pleistocene age on the basis of stratigraphic position and a lack of more precise age indicators. Unit **Qa**, as mapped here, is partly equivalent to Qal (valley fill) of Piper and others (1939), Qal (alluvium) and Qs (sedimentary deposits) of Greene (1972),

Greene and others (1972), and Walker (1977), Qs/Qal (alluvium and Holocene sedimentary deposits, undifferentiated) of Brown and others (1980a), and Qal (recent alluvium and sedimentary deposits, undivided) of Brown (1982).

Qaf **fan deposits (Holocene and Upper Pleistocene[?])**—Unconsolidated, poorly sorted, poorly graded deposits of boulders, cobbles, pebbles, granules, sand, silt, and clay in fan-shaped accumulations at the transition between low-gradient valley floodplains and steeper upland drainages (Plate 1). Individual fans mapped are as small as 0.02 hectares (0.05 acres) along smaller drainages and as large as 40 hectares (98 acres) adjacent to the broader valleys of Willow Creek Flats and Sage Hen Valley. The local thickness of alluvial fan deposits is variable but is probably <15 m (<50 ft). Fan deposits are considered to be Holocene and Late Pleistocene in age on the basis of stratigraphic position and a lack of more precise age indicators. Unit **Qaf**, as mapped here, is partly equivalent to Qal (valley fill) of Piper and others (1939), Qf (alluvial-fan deposits), Qal (alluvium), and Qs (sedimentary deposits) of Greene (1972) and Greene and others (1972), Qf (alluvial-fan deposits) and Qs/Qal (alluvium and Holocene sedimentary deposits, undifferentiated) of Brown and others (1980a), and units Qf (alluvial fan deposits) and Qal (recent alluvium and sedimentary deposits, undivided) of Brown (1982).

Qls **landslide deposits (Holocene and Upper Pleistocene[?])**—Unconsolidated, chaotically mixed masses of rock and soil deposited by landslides (e.g., slides, debris flows, rock avalanches; Plate 1). Landslide terrain is characterized by sloping hummocky surfaces. Slides are often traceable uphill to head scarps or failure surfaces. Individual slides mapped are as small as 0.02 hectares (0.05 acres) and as large as 14.5 hectares (36 acres). Thickness of landslide deposits is highly varied but may be more than several tens of meters. Landslide deposits range in age from Late Pleistocene to those that have been recurrently active in relatively recent time.

Qc **colluvium (Holocene and Upper Pleistocene[?])**—Unconsolidated and unsorted mixtures of locally derived volcanic and sedimentary rock and soil deposited in extensive aprons and as rockfall and talus cones beneath steep slopes (**Figure 5-2**; Plate 1). The unit includes accumulations of colluvial debris in upland drainages and swales. Thick, narrow colluvial wedges covering up to 182 hectares (450 acres) are especially prevalent along the base of curvilinear fault-parallel escarpments and upland areas in the north half of the map area. Thickness of colluvial deposits is highly varied; maximum thickness is several meters. The unit is assigned a Holocene and Late Pleistocene age on the basis of stratigraphic position. Unit **Qc**, as mapped here, is partly equivalent to Qc (colluvium and colluvium blanketed bedrock) of Brown (1982).

Figure 5-2. Example of colluvium (Qc). Extensive aprons of colluvium (Qc) are present below cliff-forming outcrops throughout much of the Burns Butte 7.5' quadrangle, including this part of Willow Creek Flat, in the northeastern part of the map area (43.60706, −119.16418 WGS84 geographic coordinates; 4830507mN, 325346mE WGS84 UTM Zone 11 coordinates). Colluvium (Qc) here extends downslope from cliffs composed of the rhyolite of Burns Butte (Tmrb). View is looking north. Photo credit: Jason D. McClaughry, 2019.

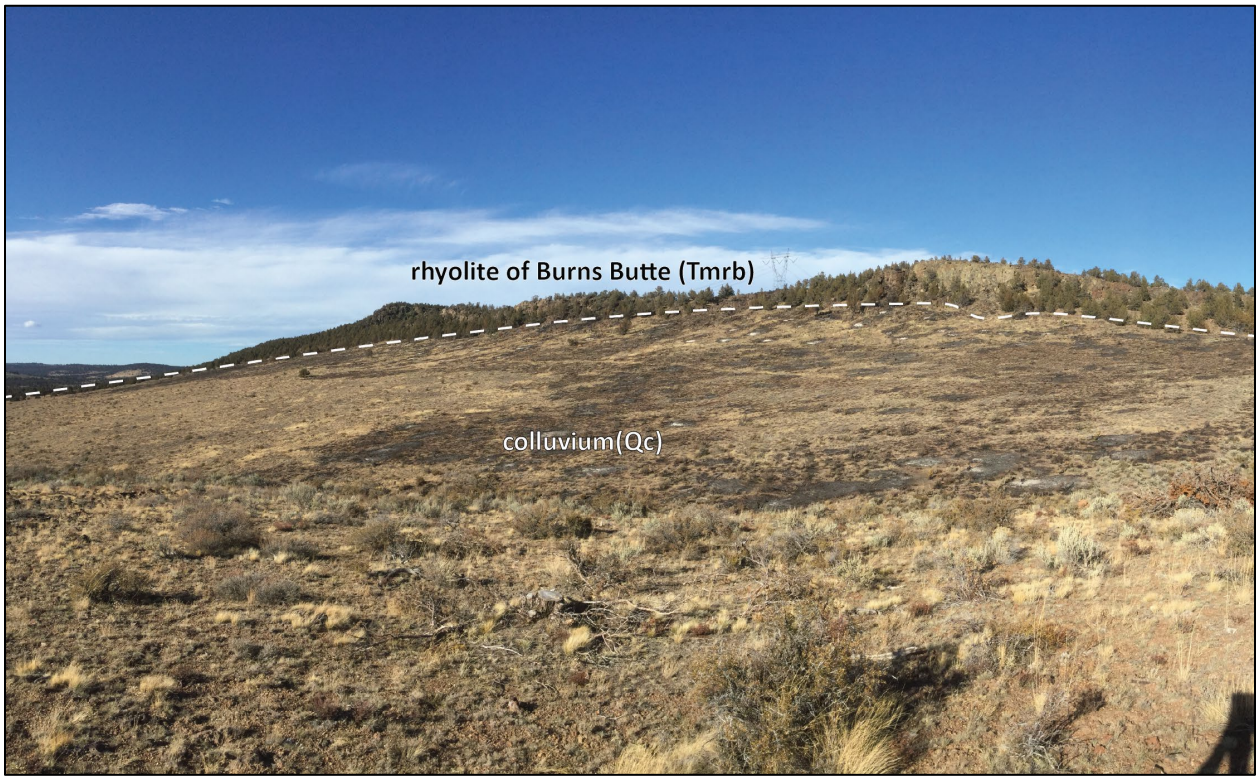

Qoaf **older fan deposits (Holocene and Upper Pleistocene[?])**—Unconsolidated to partly cemented, poorly sorted and poorly graded deposits of cobble- and boulder-dominated gravel, sand, and silt principally found in broad fans fringing upland areas along Sage Hen Creek in the southeastern part of the map area and in Willow Creek Flats in the northeastern part of the map area (Plate 1). Deposits grade down slope from coarse, clay-rich boulder gravels to fine- to medium-grained gravel, sand, and silt. Partial cementing of deposits by caliche ($CaCO_3$) is common. Locally, older alluvial fan deposits are dissected by deeply incised ephemeral, alluvium-filled channels. Thickness of the older alluvial fan deposits ranges between 18 and 30 m (60 to 100 ft). Older alluvial fans are likely Late Pleistocene age on the basis of deeply incised surface channels and stratigraphic position. However, some areas mapped as older alluvial fan deposits are likely to have been active into early Holocene time. Unit **Qoaf**, as mapped here, is partly equivalent to Qf (alluvial fan deposits) of Brown and others (1980a) and Brown (1982).

Angular Unconformity to Disconformity

5.3 Upper Cenozoic volcanic and sedimentary rocks

5.3.1 Lower Pleistocene to Upper Miocene sedimentary rocks

5.3.1.1 Harney Formation

QTst **sedimentary rocks (lower Pleistocene[?] to upper Miocene[?])**—Dissected and deeply eroded remnants of semi-consolidated sedimentary deposits overlying the Rattlesnake Tuff (**Tmtr**) and interfingering with basaltic lava flows (**QTbw**) in the southwestern part of the map area (**Figure 5-3**, **Figure 5-4**; Plate 1). Additional exposures are also present overlying the rhyolite of Burns Butte (**Tmrb**) in the northeastern part of the map area (Plate 1). In the southwest part of the map area, the unit forms low-lying rounded hills and steeper cliff faces chiefly composed of white (N9) to yellowish gray (5GY 8/1) and light gray (N7), massive to stratified deposits of pumiceous-tuffaceous claystone, siltstone, sandstone, pebbly sandstone, and interlayered air-fall tuff (**Figure 5-3**, **Figure 5-4**). Thickness of unit **QTst** is variable in the Burns Butte 7.5′ quadrangle, ranging between 8 and 91 m (25 and 300 ft). The unit is used widely as a source of construction aggregate and crushed stone in the Burns area (McClaughry and others, 2020).

Unit **QTst** is equivalent to the Harney Formation as redefined by Walker (1979). Correlative, in part, to the Harney Formation of Piper and others (1939), QTtg (terrace gravels) of Greene (1972) and Greene and others (1972), QTg (pediment gravel) and QTs (tuffaceous sedimentary rocks) of Walker (1977), and QTsg (Pliocene to Pleistocene[?] tuffaceous sedimentary rocks) of Brown and others (1980a) and Brown (1982). According to Walker (1979), sedimentary rocks equivalent to **QTst** are present in the type section of the Harney Formation at Wright Point, ~6.2 km (~3.8 mi) to the southeast of the Burns 7.5′ quadrangle. The unit is assigned a lower Pleistocene (?) to upper Miocene (?) age on the basis of stratigraphic position.

Figure 5-3. Unit QTst sedimentary rocks exposed at the BLM Wild Horse Corrals in the Burns Butte 7.5′ quadrangle. (A) Roadside exposure of thin-bedded tuffaceous siltstone and pumice-bearing sandstone (43.51731, −119.17507 WGS84 geographic coordinates; 4820561mN, 324205mE WGS84 UTM Zone 11 coordinates). Scale bar is 1 m (3.3 ft) high. View is looking northwest. (B) Close-up view of outcrop in (A) showing planar-stratified sedimentary rocks broken by a number of anastomosing vertical fractures. View is looking west. Scale bar is 0.5 m (1.6 ft) high. Photo credits: Carlie J.M. Duda, 2019.

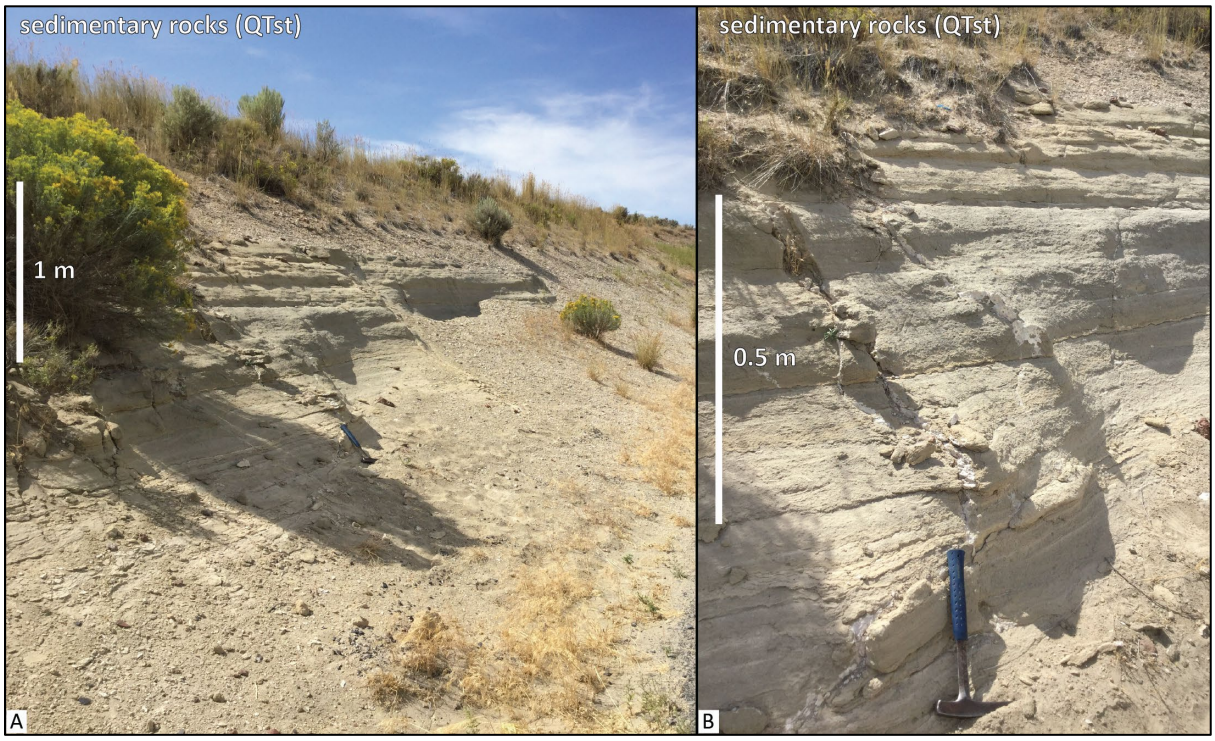

Figure 5-4. Unit QTst sandstone. (A) Ledge-forming, indurated pebbly sandstone exposed beneath lower basalt flows in unit QTbw on the north side of Sage Hen Creek in the southwest part of the map area (43.52783, −119.22579 WGS84 geographic coordinates; 4821839mN, 320137mE WGS84 UTM Zone 11 coordinates). Scale bar is 1 m (3.3 ft) high. (B) Hand sample of pale reddish brown (10R 5/4) indurated, well-sorted, fine- to medium-grained sandstone from the outcrop in (A). Scale bar is 2.5 cm (1 in) high. Photo credits: Jason D. McClaughry, 2019.

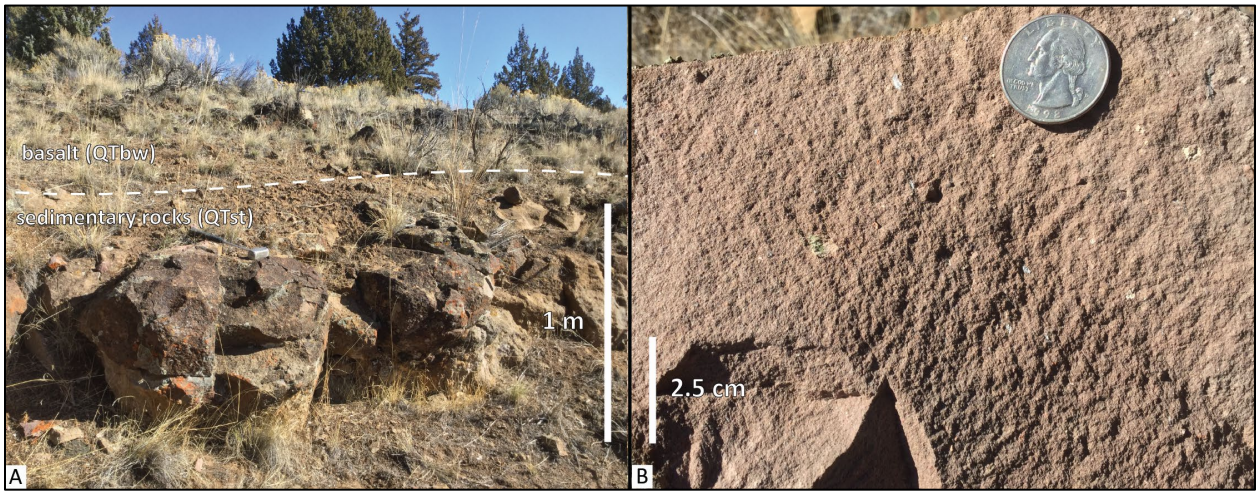

QTbw **Wrights Point Member (Pliocene)—**Olivine basalt lava flows (SiO_2 = 46.16 to 48.06 weight percent; K_2O = 0.35 to 0.74 weight percent; *n* = 5 analyses) both interfingering with and capping sedimentary rocks of unit **QTst** in the southwest corner of the Burns Butte 7.5′ quadrangle (**Figure 5-4**, **Figure 5-5**, **Figure 5-6**; **Figure 5-7, Table 5-1**; Plate 1; Appendix). Chemical compositions are comparable to high-alumina olivine tholeiite (HAOT) (**Figure 5-7**, **Table 5-1**) The unit occurs as multiple thin flows (herein described as lower and upper flows) erupted from different vent complexes, but they are not mapped separately here due to similar appearing lithology and narrow chemical ranges (**Figure 5-7**, **Table 5-1**).

Lower flows of unit **QTbw** are interbedded with sedimentary rocks of unit **QTst**. Flow outcrops are typically poorly exposed as low-relief ledges of massive to crudely columnar-jointed and blocky basalt. The lower flow typically weathers to subrounded boulders up to 0.5 m (1.6 ft) across (**Figure 5-4**, **Figure 5-5**). Lower flows are associated with light brown (5YR 6/4) to pale yellowish orange (10YR 8/6) soils, in contrast with lighter colored white (N9) to light gray (N7) bracketing sedimentary rocks (**Figure 5-5**). Typical hand samples of the lower basalt are grayish black (N2) to medium bluish gray (5B 5/1) and aphyric to sparsely microporphyritic. The basalt contains 3 to 5 percent olivine and <1 percent (vol.) subhedral to anhedral plagioclase microphenocrysts, contained within a fine-grained holocrystalline groundmass of plagioclase, intergranular olivine, subophitic clinopyroxene, and ~5 percent (vol.) rod-shaped opaque minerals (**Figure 5-8a,c,d**).

Plateau-capping **QTbw** lava flows typically crop out as cliff-forming ledges south of U.S. Highway 20 (Plate 1). Upper flows are characterized by blocky meter-scale columns or intervals of thick platy or slabby jointing (**Figure 5-6**). Outcrops typically weather to thick, angular slabs measuring 0.5 to 2 m (1.6 to 6.6 ft) across. The thickness of individual lava flows in the unit ranges between 4.5 to 14 m (15 to 45 ft) in the map area.

Upper plateau capping lavas are medium gray (N5) and aphyric to sparsely microporphyritic. These rocks include 5 to 10 percent (vol.) euhedral to subhedral olivine microphenocrysts ≤1 mm (0.04 in) and 3 to 5 percent euhedral, prismatic plagioclase microphenocrysts and phenocrysts up to 1 cm (0.4 in) contained within a holocrystalline groundmass of seriate plagioclase, intergranular olivine, subophitic clinopyroxene, and opaque minerals (**Figure 5-8b,e,f**). The upper basalt also contains scattered olivine-plagioclase glomerocrysts up to 2 mm (0.08 mm).

Lower flows exposed north of Sage Hen Creek have reversed magnetic polarity (**Figure 5-5**). Plateau-capping outcrops have flows of both normal and reversed magnetic polarity (**Figure 5-6**). The unit is assigned Pliocene on the basis of stratigraphic position and isotopic ages. A groundmass sample from the upper basalt plateau, south of Sage Hen Creek, yielded an $^{40}Ar/^{39}Ar$ plateau age of 3.29 ± 0.03 and a total fusion age of 3.21 ± 0.04 Ma (groundmass; sample 108 BBHC 19; map number G3)**;** an older and less precise $^{40}Ar/^{39}Ar$ plateau age of 3.69 ± 0.57 Ma was determined for plagioclase separates from the same sample (Plate 1; Appendix). **QTbw** basalt flows share an equivalent stratigraphic position, chemical composition, and age to the Wrights Point member of the Harney Formation (Walker, 1979; Brown, 1982) and other high-alumina olivine tholeiite (HAOT) basalts forming a broad plateau cross the west-central part of the Harney Basin (**Figure 2-2**). A basaltic lava capping Wrights Point, 16 km (10 mi) south of Burns, has a reported $^{40}Ar/^{39}Ar$ age of 2.54 ± 0.07 Ma (Jordan and others, 2004), while other plateau-capping HAOT lavas exposed in the western Harney Basin have reported $^{40}Ar/^{39}Ar$ ages of 2.83 ± 0.89 and 2.2 ± 0.04 Ma (Jordan and others., 2004; Streck and Grunder, 2012). The unit is equivalent to QTbw (Wrights Point member) of Brown (1982).

Figure 5-5. Lower basalt flows in unit QTbw, exposed on the north side of Sage Hen Creek in the southwest part of the map area (43.52783, −119.22579 WGS84 geographic coordinates; 4821839mN, 320137mE WGS84 UTM Zone 11 coordinates). Lower flows in unit QTbw are typically poorly exposed, cropping out as low-lying ledges of massive to crudely columnar-jointed and blocky basalt. Lower flows are associated with light brown (5YR 6/4) to pale yellowish orange (10YR 8/6) soils in the field; distribution of individual flows can readily be discerned in 1 m orthophotos by distinct color contrast with lighter colored white (N9) to light gray (N7) interbedded sedimentary rocks. Scale bar is 1 m (3.3 ft) high. Photo credit: Jason D. McClaughry, 2019.

Figure 5-6. Plateau-capping basalt flow in unit QTbw, exposed south of U.S. Highway 20 in the southwest part of the map area (43.51153, −119.23383 WGS84 geographic coordinates; 4820045mN, 319439mE WGS84 UTM Zone 11 coordinates). Upper flows in unit QTbw are typically well exposed, cropping out as cliff-forming ledges of massive to crudely columnar-jointed and blocky basalt. The outcrop corresponds to field site sample 108 BBHC 19 (map no. G3), which has an $^{40}Ar/^{39}Ar$ age of 3.29 ± 0.03. Scale bar is 1 m (3.3 ft) high. Photo credit: Carlie J.M. Duda, 2019.

Figure 5-7. Total alkali ($Na_2O + K_2O$) vs. silica (SiO_2) (TAS) classification showing whole-rock XRF analyses on volcanic rocks in the Burns Butte area (normalized to 100 percent anhydrous). Plot includes 236 analyses obtained for this study and those compiled from previous studies (MacLean, 1994; Ford, 2012; M. Ferns, unpublished data, 2015; R. Houston, unpublished data, 2016; Houston and others, 2018; Niewendorp and others, 2018; McClaughry and others, 2019). TAS graph fields are from Le Bas and others (1986), Le Maitre and others (1989), and Le Maitre and others (2004). Red-dashed line is the dividing line between alkaline (above) and subalkaline/tholeiitic (below) fields after Cox and others (1979).

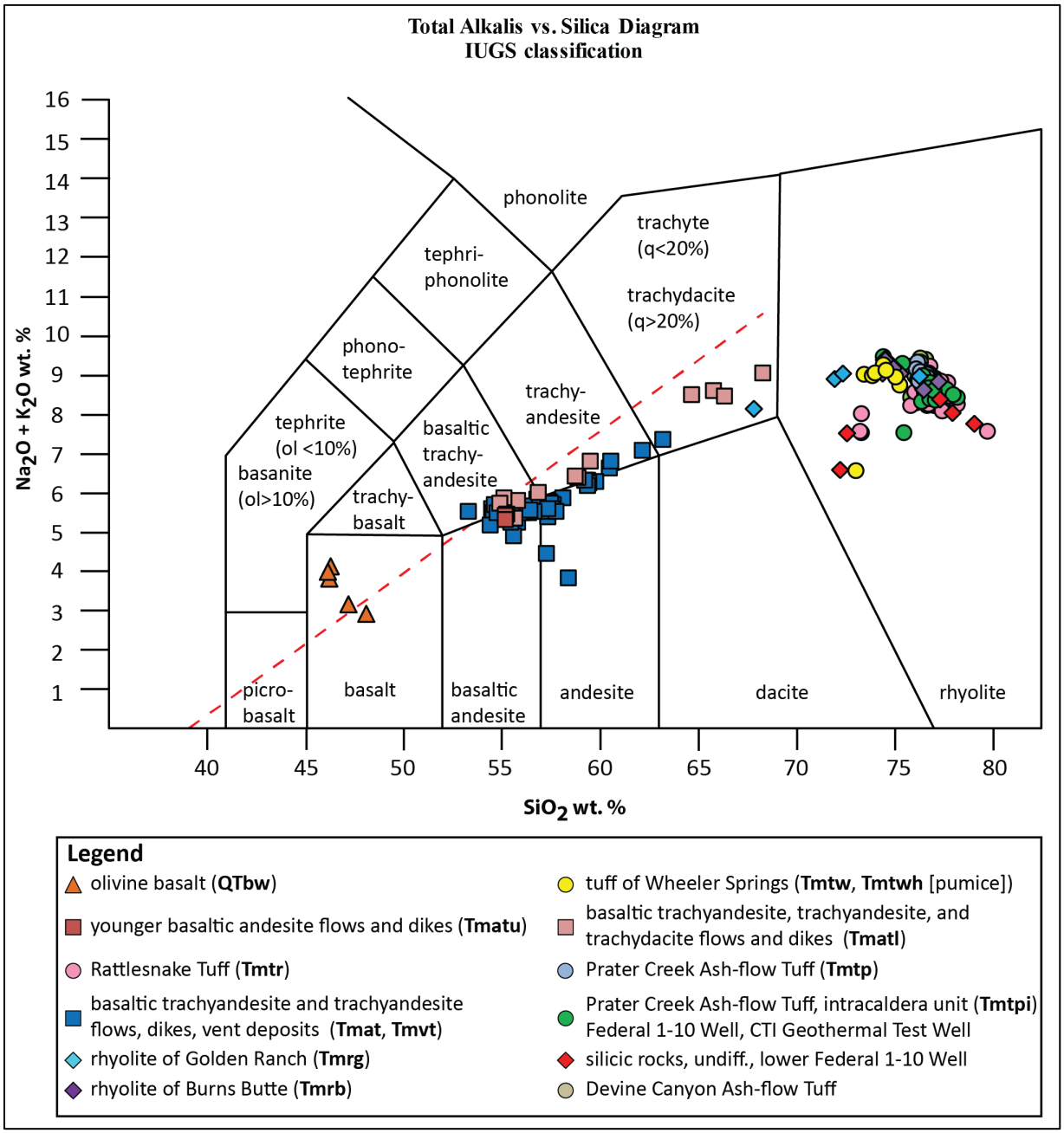

Table 5-1. Representative XRF analyses for lower Pleistocene (?) to upper Miocene (?) basalt flows of unit QTbw sampled from the Burns Butte 7.5' quadrangle.

Sample	107 BBHC 19	108 BBHC 19	106 BBHC 19	105 BBHC 19	268 BBJ 19
Geographic Area	Sage Hen Valley	Sage Hen Valley	Sage Hen Valley	Sage Hen Valley	Sage Hen Valley
Formation	Harney	Harney	Harney	Harney	Harney
Member	Wrights Point	Wrights Point	Wrights Point	Wrights Point	Wrights Point
Map Unit	Wrights Point Member	Wrights Point Member	Wrights Point Member	Wrights Point Member	Wrights Point Member
Label	QTbw	QTbw	QTbw	QTbw	QTbw
UTMNorthingNAD83	4820013	4820045	4820166	4820335	4821840
UTMEastingNAD83	319414	319440	318902	318166	320144
Age (Ma)	nd	3.29 Ma	nd	nd	nd
Map No.	G2	G3	G4	G5	G6
Oxides, weight percent					
SiO_2	48.06	46.16	46.27	46.20	47.21
Al_2O_3	17.63	15.59	15.46	15.90	16.15
TiO_2	1.28	2.97	3.01	2.88	1.85
FeO*	9.82	14.38	14.34	14.01	11.59
MnO	0.17	0.24	0.25	0.23	0.19
CaO	11.18	9.49	9.43	9.65	10.50
MgO	8.69	6.47	6.35	6.71	8.88
K_2O	0.36	0.71	0.74	0.61	0.66
Na_2O	2.58	3.28	3.41	3.21	2.53
P_2O_5	0.23	0.71	0.74	0.60	0.45
LOI	0.00	0.00	0.00	0.00	3.30
Total_I	99.81	99.51	99.72	99.44	96.49
Trace Elements, parts per million					
Ni	143	53	50	58	137
Cr	205	47	44	55	253
Sc	37	37	38	38	33
V	235	347	346	363	232
Ba	188	439	474	426	297
Rb	6	11	12	9	14
Sr	216	282	279	290	257
Zr	97	220	233	194	117
Y	27	47	50	43	32
Nb	6.7	17.5	19.7	15.1	7.3
Ga	16	21	22	20	18
Cu	75	41	52	62	77
Zn	71	117	119	114	86
Pb	2	3	2	3	2
La	7	20	21	18	10
Ce	18	50	52	39	27
Th	1	1	2	0	0
Nd	12	32	34	25	16
U	1	2	1	0	1

Major element determinations have been normalized to a 100-percent total on a volatile-free basis and recalculated with total iron expressed as FeO*; nd - no data or element not analyzed; na - not applicable or no information. LOI, Loss on Ignition; Total_I, original analytical total.

Figure 5-8. Hand sample and thin-section photographs showing textural variations in basalt flows of unit QTbw. (A) Hand sample of lower basalt in unit QTbw, sample 268 BBJ 19 (map no. G6). (B) Hand sample of upper basalt, sample 108 BBHC 19 (map no. G3). Scale bars in A and B are 2.5 cm (1 in) high. (C) Photomicrograph of sample 268 BBJ 19 basalt under cross-polarized light. (D) Same view as (C), under plane-polarized light. (E) Photomicrograph of sample 108 BBHC 19 basalt under cross-polarized light. (F) Same view as (E), under plane-polarized light. Scale bar in photos (C–F) is 1 mm (0.04 in) in length. Abbreviations: px – subophitic pyroxene. Photo credits: (A, C-D) Jason D. McClaughry, 2018; (B) Carlie J.M. Duda, 2019.

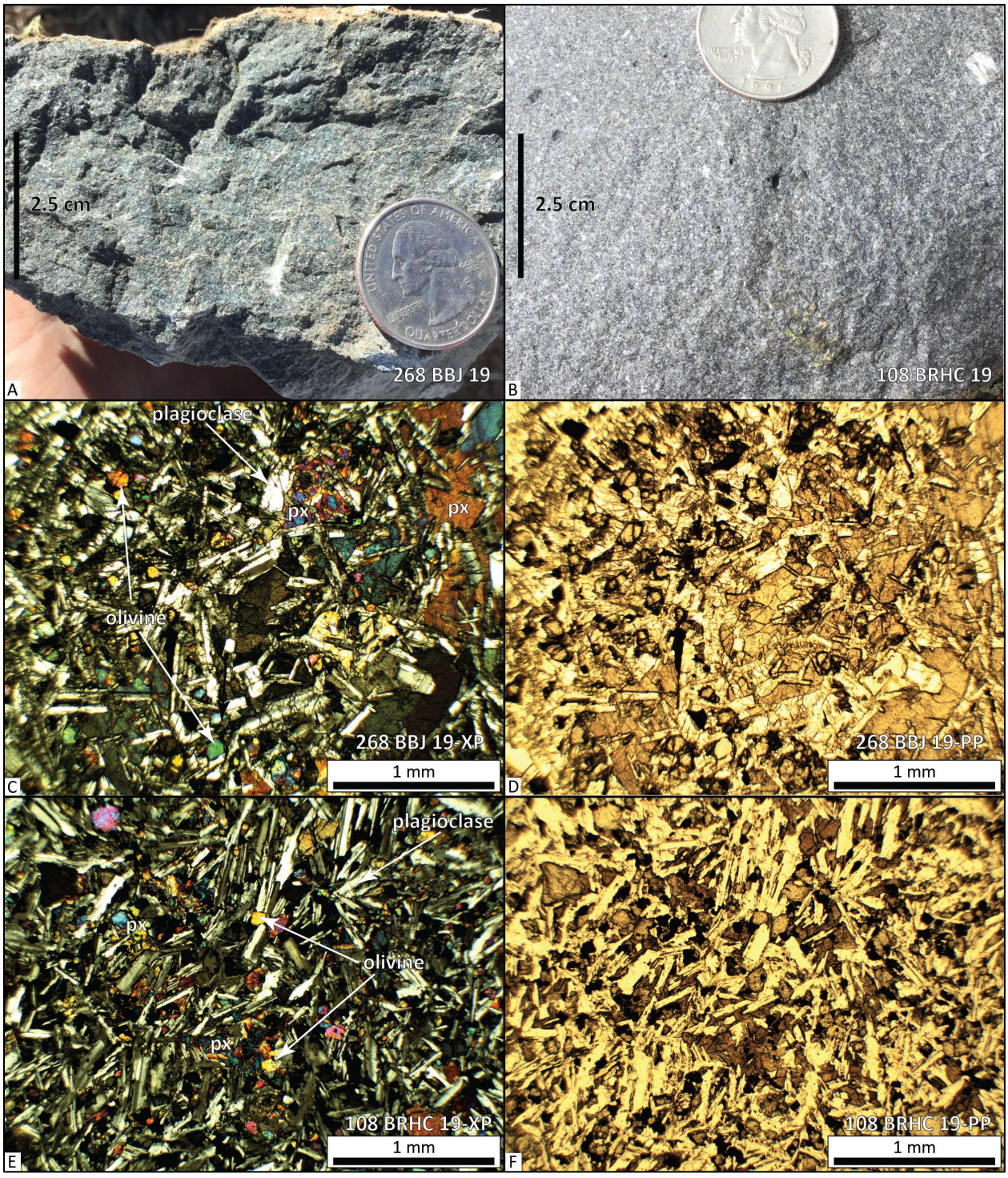

Angular unconformity to disconformity

5.3.2 Upper Miocene volcanic and sedimentary rocks

Upper Miocene stratigraphy in the map area includes a bimodal suite of late Miocene (8.46 to 7.1 Ma) caldera-filling rhyolitic tuffs (**Tmtp**, **Tmtpi**, **Tmtw**, **Tmtwh**), exogenous rhyolite domes and flows (**Tmrg**, **Tmrb**, **Tmri**), and basaltic trachyandesite and trachyandesite flows, dikes, and vent deposits (**Tmatu**, **Tmat**, **Tmvt**, **Tmatl**) (Plate 1). The regionally extensive Rattlesnake Tuff (**Tmtr**) mantles these units throughout the quadrangle (Plate 1). XRF geochemical analyses of whole-rock samples were obtained on 67 samples from the Burns Butte 7.5′ quadrangle (Plate 1; Appendix). Representative major- and trace-element data for upper Miocene units are shown in **Table 5-2**, **Figure 5-7**, and **Figure 5-9** (see geochemical data in geodatabase and appendix).

Figure 5-9. Chemical variation diagram (zirconium versus niobium) showing geochemical groupings for late Miocene volcanic rocks in the Burns-Burns Butte area. Plot includes 231 analyses obtained for this study and those compiled from previous studies (MacLean, 1994; Ford, 2012; M. Ferns, unpublished data, 2015; R. Houston, unpublished data, 2016; Houston and others, 2018; Niewendorp and others, 2018; McClaughry and others, 2019).

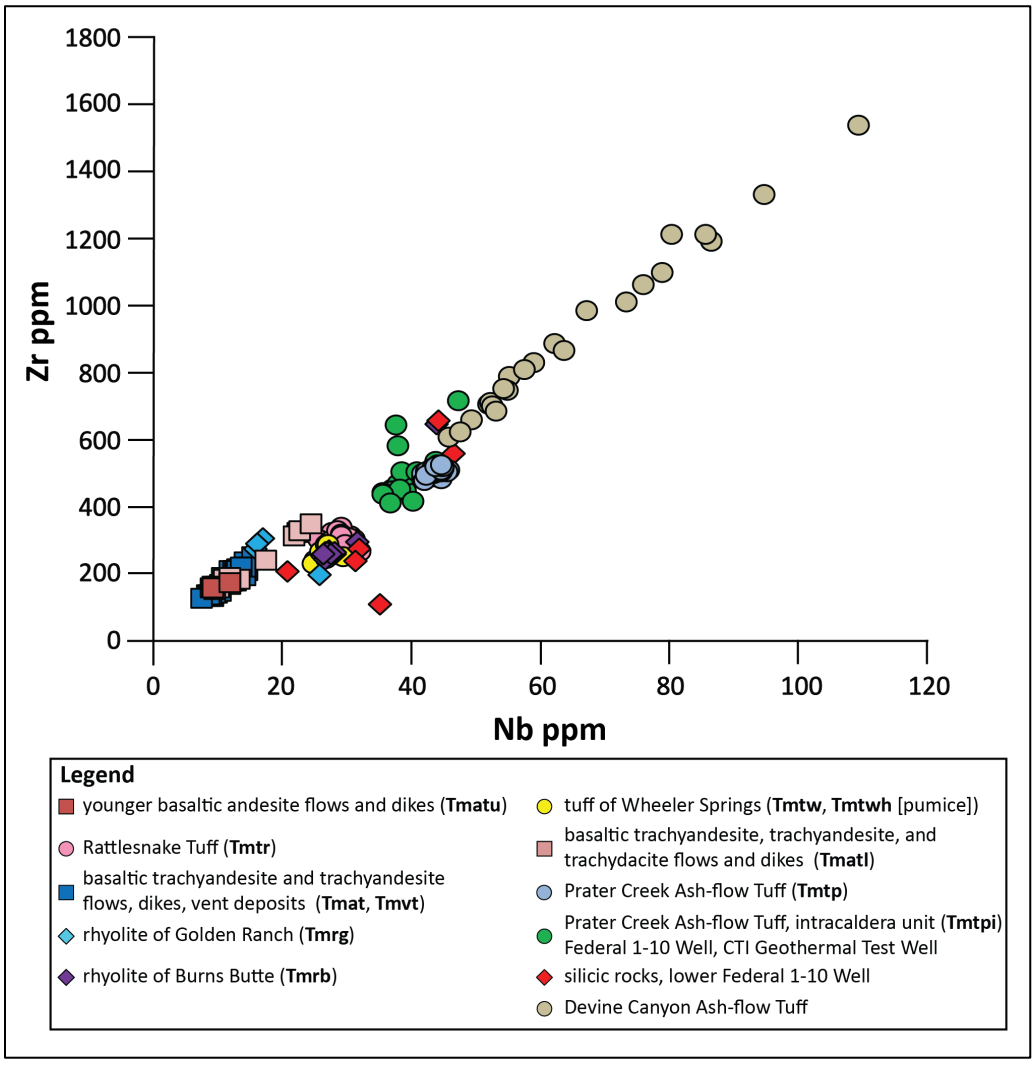

Table 5-2. Representative XRF analyses for late Miocene volcanic rocks sampled from the Burns Butte 7.5' quadrangle (3 tables, part 1 of 3).

Sample	117 BBJ 19	121 BBJ 19	007BBHC 19	093BBHC 19	095BBHC 19	104BBHC 19	F-1-10-460	HBH022-17	146BBHC 19	117BBHC 19	31-BF-15
Geographic Area	Skull Cr. Rd.	Skull Cr. Rd.	Skull Cr. Rd.	W. Willow Cr.	W. Willow Cr.	Halfway-Res. Flat Rd.	Federal 1-10 well	Hines Logging Rd.	Rimrock Spring	Rimrock Spring	Hines Logging Rd.
Formation	na	na	na	na	na	na	na	na	na	na	na
Member	Silvies R. caldera	Silvies R. caldera	Silvies R. caldera	Silvies R. caldera	Silvies R. caldera	Silvies R. caldera	Silvies R. caldera	Silvies R. caldera	Silvies R. caldera	Silvies R. caldera	Silvies R. caldera
Label	Tmatu	Tmatu	Tmatu	Tmat	Tmat	Tmat	Tmat	Tmat	Tmat	Tmat	Tmat
UTM N (NAD83)	4831601	4831250	4832410	4829680	4830039	4826498	4828998	4827549	4829742	4830654	4825585
UTM E (NAD83)	327862	327787	327872	319674	319883	320158	320819	325650	326230	327979	328284
Age (Ma)	nd	nd	nd	nd	nd	nd	nd	nd	nd	nd	nd
Map_No	G66	G65	G68	G55	G58	G17	G29	G22	G56	G63	G11
Oxides, weight percent											
SiO_2	55.21	55.17	55.24	54.80	55.30	62.14	54.48	55.71	55.57	59.79	59.21
Al_2O_3	16.83	17.39	17.29	17.46	16.94	16.17	17.06	16.75	16.84	16.89	16.84
TiO_2	1.30	1.14	1.13	1.18	1.26	1.07	1.34	1.33	1.30	0.97	0.98
FeO*	8.49	8.05	8.16	8.21	8.32	6.11	8.83	8.36	8.47	6.88	7.00
MnO	0.16	0.15	0.15	0.15	0.15	0.12	0.16	0.15	0.15	0.11	0.12
CaO	7.79	7.79	7.85	8.13	7.56	4.80	7.85	7.87	7.70	5.95	6.09
MgO	4.31	4.36	4.22	4.06	4.08	2.16	4.13	3.92	3.95	2.65	2.98
K_2O	1.74	1.83	1.77	1.64	1.75	2.80	1.62	1.79	1.72	2.32	2.27
Na_2O	3.57	3.58	3.67	3.85	4.03	4.28	3.98	3.56	3.70	3.96	4.05
P_2O_5	0.60	0.55	0.52	0.52	0.62	0.35	0.55	0.57	0.60	0.47	0.47
LOI	0.47	0.29	0.57	0.86	0.28	0.61	nd	0.85	0.36	0.55	nd
Total_I	99.28	99.18	99.16	98.88	99.35	98.99	98.13	98.64	99.23	99.18	99.64
Trace Elements, parts per million											
Ni	31	37	37	36	22	16	27	32	28	15	18
Cr	59	55	56	57	39	24	38	56	56	12	11
Sc	23	22	21	24	23	17	25	24	23	17	18
V	181	180	176	202	205	120	216	196	183	151	158
Ba	847	840	816	870	745	1030	698	824	831	961	941
Rb	24	23	23	20	22	56	20	24	21	38	34
Sr	475	556	559	594	529	318	529	434	474	441	445
Zr	170	153	153	125	139	229	128	174	172	184	185
Y	29	24	25	24	27	32	25	28	28	28	27
Nb	12.3	9.6	9.3	7.9	9.9	14.5	9.1	12.6	12.5	11.6	11.6
Ga	18	18	18	18	18	18	19	19	18	19	19
Cu	47	56	78	73	68	47	88	78	67	48	39
Zn	87	87	85	80	84	73	86	89	88	78	81
Pb	6	7	7	7	6	10	5	7	7	10	9
La	28	24	27	21	22	25	20	25	24	28	29
Ce	52	51	49	44	48	54	46	51	55	52	57
Th	2	2	1	2	2	4	2	3	2	3	4
Nd	29	26	25	23	25	28	25	27	29	26	24
U	1	1	1	1	2	3	1	2	2	3	1

Major element determinations have been normalized to a 100-percent total on a volatile-free basis and recalculated with total iron expressed as FeO*; nd - no data or element not analyzed; na - not applicable or no information. LOI, Loss on Ignition; Total_I, original analytical total.

Table 5-2, continued. Representative XRF analyses for late Miocene volcanic rocks sampled from the Burns Butte 7.5' quadrangle (part 2 of 3).

Sample	HP 91-2	112 BBJ 19	250 BBJ 19	148 BRH C19	077 BBHC 19	F-1-10-670	128 BRHC 19	F-1-10-940	F-1-10-1330	F-1-10-1480	F-1-10-1810
Geographic Area	Burns Butte	Skull Cr. Rd.	Willow Cr.	U.S. Highway 20	Willow Cr.	Federal 1-10 well	Wheeler Springs	Federal 1-10 well	Federal 1-10 well	Federal 1-10 well	Federal 1-10 well
Formation	na	na	na	na	na	na	na	na	na	na	na
Member	Silvies R. caldera	Silvies R. caldera	Silvies R. caldera	Silvies R. caldera	Silvies R. caldera	Silvies R. caldera	Silvies R. caldera	Silvies R. caldera	Silvies R. caldera	Silvies R. caldera	Silvies R. caldera
Label	Tmrb	Tmrb	Tmrb	Tmrg	Tmri	Tmtwh	Tmtw	Tmatl	Tmatl	Tmatl	Tmatl
UTMNorthingNAD83	4826230	4832303	4824745	4819903	4823629	4828998	4823965	4824014	4824014	4824014	4828998
UTMEastingNAD83	327414	327110	322941	327016	323623	320819	327145	331853	331853	331853	320819
Age (Ma)	7.68 Ma	nd	nd	8.46 Ma	nd	nd	nd	nd	nd	nd	nd
Map No.	G15	G67	G10	G1	G7	G30	G8	G32	G34	G35	G36
Oxides, weight percent											
SiO_2	74.45	77.20	75.27	71.94	67.79	73.86	74.23	55.81	58.77	56.88	68.28
Al_2O_3	13.52	11.06	13.06	14.43	15.20	13.53	13.63	16.75	17.06	17.33	14.99
TiO_2	0.22	0.16	0.20	0.44	0.65	0.23	0.22	1.36	0.98	1.01	0.53
FeO*	1.52	2.52	1.51	2.42	3.92	1.95	1.71	8.42	6.84	7.21	3.54
MnO	0.04	0.06	0.06	0.04	0.08	0.05	0.04	0.15	0.11	0.13	0.06
CaO	0.68	0.12	0.60	1.31	2.87	0.92	0.65	7.42	6.52	7.37	2.21
MgO	0.16	0.00	0.24	0.43	1.12	0.43	0.15	3.67	2.81	3.55	1.16
K_2O	5.05	4.52	5.00	4.67	3.90	5.22	5	2.07	2.41	2.09	4.73
Na_2O	4.32	4.32	4.04	4.24	4.24	3.77	4.32	3.72	4.02	3.92	4.31
P_2O_5	0.04	0.03	0.03	0.08	0.24	0.04	0.04	0.63	0.48	0.52	0.18
LOI	nd	0.28	0.83	0.65	1.14	4.37	0.35	nd	nd	nd	nd
Total_I	nd	99.44	98.87	98.89	98.55	94.65	99.34	98.01	98.20	96.4	97.46
Trace Elements, parts per million											
Ni	7	1	3	2	8	4	7	21	19	26	10
Cr	1	4	3	3	15	6	4	40	17	49	16
Sc	4	1	4	5	11	6	3	25	18	21	9
V	3	5	7	21	61	14	10	222	157	166	50
Ba	498	65	964	1057	1086	399	614	844	931	866	995
Rb	115	105	114	107	79	106	112	34	44	33	86
Sr	27	4	73	102	213	42	39	457	450	485	139
Zr	293	644	242	304	272	227	273	177	187	157	317
Y	41	80	44	27	35	41	43	28	25	23	36
Nb	31.8	44.0	26.8	17.3	16.2	25.2	27.5	13.6	12.1	10.1	22.8
Ga	16	22	16	16	16	17	17	19	19	17	17
Cu	5	4	7	9	20	8	10	53	38	63	19
Zn	40	132	28	29	51	43	40	86	79	83	48
Pb	17	21	12	12	11	16	17	7	8	8	13
La	41	58	41	26	32	36	42	27	29	23	33
Ce	81	101	69	44	51	76	73	51	54	52	62
Th	11	8	10	9	7	9	10	1	3	2	6
Nd	34	60	33	18	27	30	33	29	24	23	29
U	4	1	3	4	3	3	4	1	2	3	2

Major element determinations have been normalized to a 100-percent total on a volatile-free basis and recalculated with total iron expressed as FeO*; nd - no data or element not analyzed; na - not applicable or no information. LOI, Loss on Ignition; Total_I, original analytical total.

Table 5-2, continued. Representative XRF analyses for late Miocene volcanic rocks sampled from the Burns Butte 7.5' quadrangle (part 3 of 3).

Sample	F-1-10-2290	F-1-10-2680	F-1-10-2830	201 BBJ 19	308 BBJ 19	F-1-10-3040	F-1-10-3220	F-1-10-3730	F-1-10-4150	F-1-10-4270
Geographic Area	Federal 1-10 well	Federal 1-10 well	Federal 1-10 well	Radar Rd.	Willow Cr. Flats	Federal 1-10 well	Federal 1-10 well	Federal 1-10 well	Federal 1-10 well	Federal 1-10 well
Formation	na	na	na	Prater Cr. Tuff	Prater Cr. Tuff	Prater Cr. Tuff	Prater Cr. Tuff	Prater Cr. Tuff	Prater Cr. Tuff	Prater Cr. Tuff
Member	Silvies R. caldera	Silvies R. caldera	Silvies R. caldera	Silvies R. caldera	Silvies R. caldera	Silvies R. caldera	Silvies R. caldera	Silvies R. caldera	Silvies R. caldera	Silvies R. caldera
Label	Tmatl	Tmatl	Tmatl	Tmtp	Tmtp	Tmtpi	Tmtpi	Tmtpi	Tmtpi	Tmtpi
UTM N (NAD83)	4845246	4828998	4846121	4828410	4830560	4828998	4828998	4828998	4828998	4828998
UTM E (NAD83)	331068	320819	328940	326899	325059	320819	320819	320819	320819	320819
Age (Ma)	nd	nd	nd	8.48/8.41 Ma	8.48/8.41Ma	8.52 Ma	nd	nd	nd	nd
Map No.	G39	G41	G42	G27	G61	G43	G44	G45	G46	G47
Oxides, weight percent										
SiO_2	54.94	66.32	59.51	76.64	76.63	77.11	75.44	77.6	78.15	78
Al_2O_3	17.42	15.29	16.32	11.82	11.84	10.79	10.36	11.1	11.16	11.37
TiO_2	1.12	0.81	1.13	0.15	0.14	0.14	0.15	0.12	0.11	0.12
FeO*	8.21	4.29	6.74	2.22	2.24	2.01	2.18	2.14	1.6	1.55
MnO	0.15	0.09	0.12	0.03	0.03	0.05	0.04	0.04	0.03	0.03
CaO	7.49	3.1	5.77	0.08	0.08	1.40	4.05	0.25	0.47	0.37
MgO	4.39	1.42	3.23	0.06	0.08	0.13	0.24	0.1	0.06	0.07
K_2O	1.71	3.82	2.55	4.60	4.62	5.14	4.17	5.02	5.13	4.79
Na_2O	4.03	4.63	4.26	4.40	4.31	3.23	3.34	3.61	3.28	3.69
P_2O_5	0.55	0.23	0.37	0.02	0.03	0.02	0.03	0.01	0.01	0.01
LOI	nd	nd	nd	0.66	0.81	nd	4.45	nd	nd	nd
Total_I	97.04	97.58	97.18	98.95	99.05	97.49	94.89	98.43	97.64	97.73
Trace Elements, parts per million										
Ni	37	7	28	1	2	5	1	1	1	1
Cr	65	14	46	3	3	11	17	3	5	4
Sc	23	12	19	2	2	1	2	1	1	1
V	183	68	137	6	6	17	24	6	5	4
Ba	790	1034	882	69	129	86	110	24	27	23
Rb	20	70	42	102	103	124	100	127	127	121
Sr	465	200	352	9	11	18	59	9	15	10
Zr	149	345	238	514	521	447	431	479	410	408
Y	25	41	33	63	45	59	66	73	68	68
Nb	10	24.9	17.8	44.3	45.0	38.5	36	42	40.5	37.2
Ga	18	18	18	21	22	21	20	22	18	19
Cu	75	14	35	5	6	9	13	5	4	6
Zn	82	52	70	94	88	92	100	116	73	76
Pb	7	9	8	19	19	19	24	18	17	14
La	23	35	27	51	52	50	51	58	49	46
Ce	48	69	55	85	82	100	100	106	96	88
Th	3	6	4	8	8	8	7	8	11	9
Nd	25	33	30	46	44	46	46	48	42	40
U	2	2	3	3	3	4	3	3	2	2

Major element determinations have been normalized to a 100-percent total on a volatile-free basis and recalculated with total iron expressed as FeO*; nd - no data or element not analyzed; na - not applicable or no information. LOI, Loss on Ignition; Total_I, original analytical total.

Tmatu **basaltic andesite flows and dikes (upper Miocene)** — Basaltic andesite lava flows (SiO_2 = 55.16 to 55.23 weight percent; K_2O = 1.73 to 1.83 weight percent; *n* = 3 analyses) exposed above the Rattlesnake Tuff (**Tmtr**) in the northeast corner of the Burns Butte 7.5′ quadrangle (**Figure 5-7**, **Figure 5-9**, **Table 5-2**; Plate 1; Appendix). The unit consists of several ridge-capping lava flows up to 8 m (25 ft) thick. Flow tops are rubbly and highly vesiculated; flow bases are composed of moderate red (5R 4/6) to black (N1) scoriaceous ʻAʻā flow-foot breccia (**Figure 5-10**). Lavas form distinctive bench and cliff outcrops, typically characterized by blocky, platy, or hackly jointing (**Figure 5-10**). The lavas commonly weather to platy slabs and irregular blocks, forming extensive talus slopes beneath cliff-forming outcrops. The composite thickness of flow units is up to 27 m (90 ft). The unit includes several N. 20° E. to N. 70° E. vertical dikes of similar composition cross-cutting the Rattlesnake Tuff (**Tmtr**) in the northeastern most part of the map area (Plate 1).

Typical hand samples are commonly streaked or mottled, medium bluish gray (5B 5/1) to medium dark gray (N4), and aphyric to very sparsely microporphyritic. The rock contains 2 to 3 percent (vol.), subhedral to euhedral, seriate, plagioclase microphenocrysts ≤0.5 mm (0.02 in) and ≤1 percent subhedral olivine microphenocrysts ≤0.5 mm (0.04 in) contained within a hypohyaline groundmass of glass and feldspar microlites (**Figure 5-11a–c**).

Tmatu flows have reversed magnetic polarity and are assigned a late Miocene age on the basis of stratigraphic position above the 7.1 Ma Rattlesnake Tuff (Plate 1). Vents for trachyandesite flows of unit **Tmatu** are located in the in the northeasternmost part of the map area and southeastern part of the Burns NW 7.5′ quadrangle where several N. 20° E. to N. 70° E. vertical dikes of similar composition cross-cut the Rattlesnake Tuff (**Tmtr**) (Plate 1). Partly equivalent to Qbh (late basalt) and Th (Harney Formation) of Piper and others (1939), Ta (andesite) of Greene (1972) and Greene and others (1972), Tob (olivine basalt) and Tmv (mafic vent rocks) of Walker (1977), Tma (andesites) and QTmv (Upper Pliocene mafic vent complexes) of Brown and others (1980a), and unit Tmar (basaltic andesites of Rimrock Springs) of Brown (1982).

Figure 5-10. Trachyandesite flows (Tmatu) exposed above the Rattlesnake Tuff (Tmtr) in the northeast part of the map area (43.61276, −119.13019 WGS84 geographic coordinates; 4831069mN, 328104mE WGS84 UTM Zone 11 coordinates). (A) Upper flows in unit Tmatu are typically well exposed, cropping out as cliff-forming ledges of massive to crudely blocky- to platy-jointed trachyandesite. View is looking east. (B) Close-up view of internally blocky- to horizontally platy-jointed trachyandesite in the outcrop in (A). The lowermost exposed part of the outcrops is a red-oxidized basal flow breccia. Scale bar is 1 m (3.3 ft) high. Photo credits: Carlie J.M. Duda, 2019.

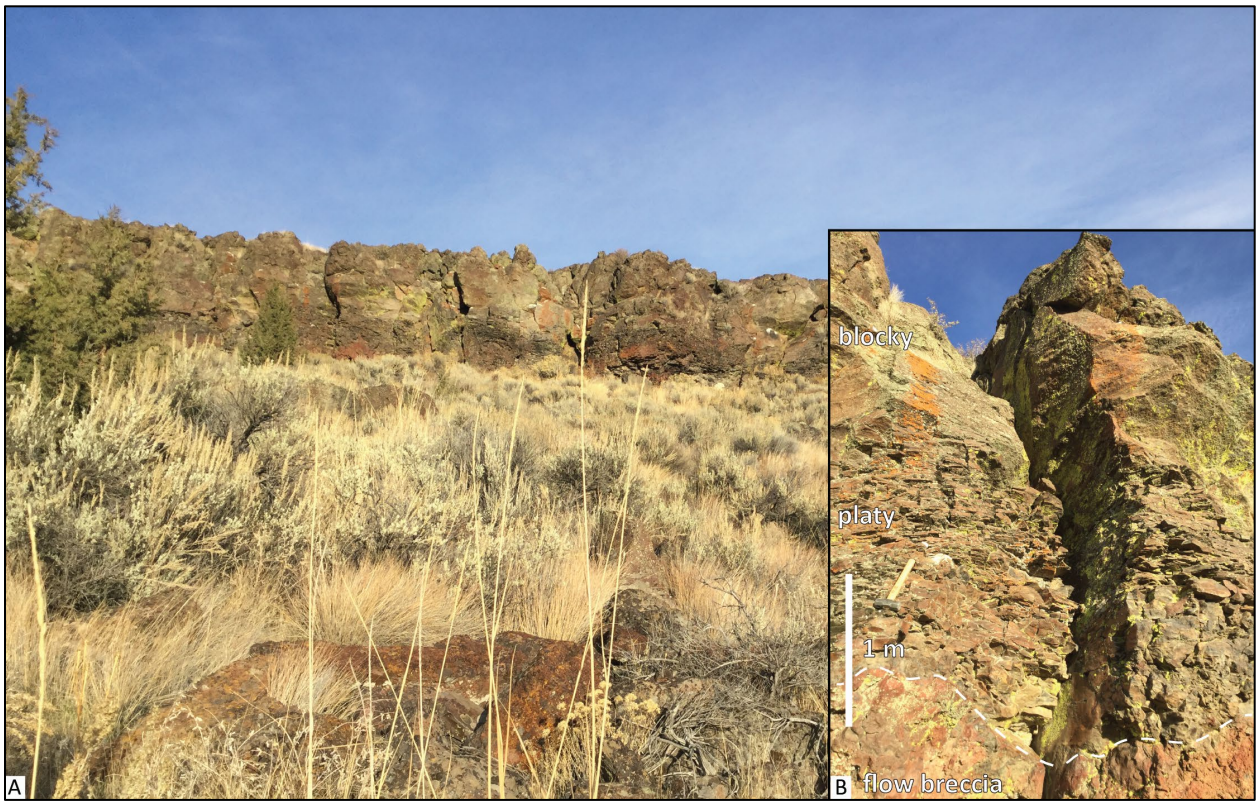

Figure 5-11. Hand sample and thin section photographs from unit Tmatu. (A) Hand sample of aphyric trachyandesite (Tmatu), Sample 117 BBJ 19 (map no. G64). Scale bar in A is 2.5 cm (1 in) high. (B) Photomicrograph of sample 117 BBJ 19 under cross-polarized light. (C) Same view as (B), under plane-polarized light. Scale bar in (B)-(C) is 1 mm (0.04 in) in length. Photo credits: Jason D. McClaughry, 2019.

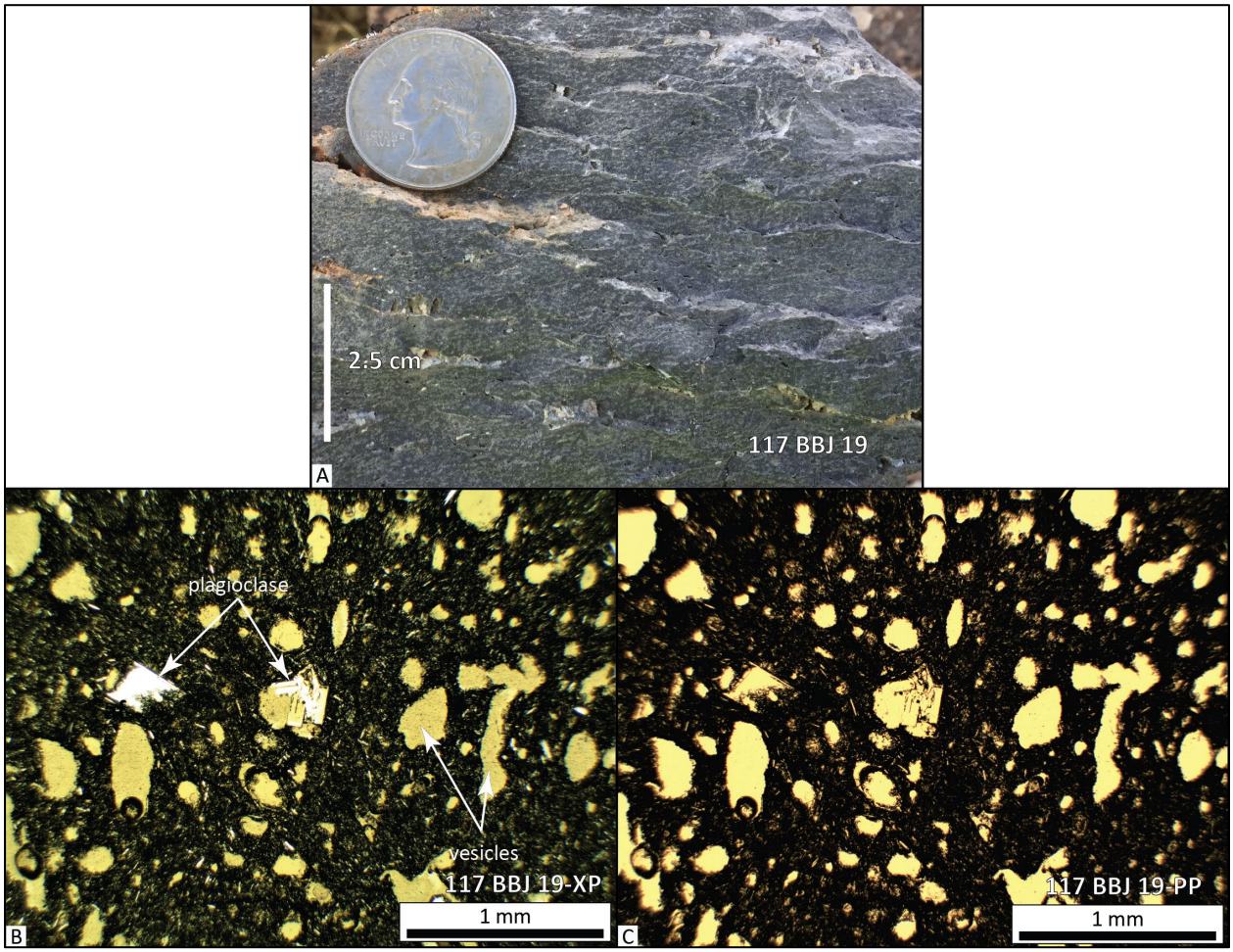

Tmtr **Rattlesnake Tuff (upper Miocene)**—Vitric, phenocryst-poor, pumice- and lithic-rich rhyolitic tuff (SiO_2 = 75.84 to 78.18 weight percent; *n* = 33 samples outside map area) forming an extensive cover across older upper Miocene rocks in the map area (Plate 1; **Figure 5-7**, **Figure 5-9**, **Figure 5-12**, **Figure 5-13**). Over much of the map area, the unit forms distinctive cliffs and rimrock that can be easily traced in 1-m lidar DEMs and air photographs (**Figure 5-12**). The Rattlesnake Tuff (**Tmtr**) abruptly thickens and thins across the map area, draped across an irregular distribution of underlying late Miocene units. South of West Willow Creek, Rattlesnake Tuff (**Tmtr**) onlaps southwest-dipping (10° to 20° SE.) basaltic trachyandesite to trachyandesite lavas (**Tmat**), vent deposits (**Tmvt**), and rhyolite (**Tmrb**; **Tmrg**) along a northwest-trending up-faulted ridge (**Figure 5-12**, **Figure 5-13**, Plate 1). Thickness of the Rattlesnake Tuff (**Tmtr**) along this ridge ranges from <1 m (3.3 ft) to as much as 45 m (148 ft), thickening to the south (Plate 1, cross section A-A′). South and west of Burns Butte, the Rattlesnake Tuff (**Tmtr**) directly overlies the rhyolite of Burns Butte (**Tmrb**), rhyolite of Golden Ranch (**Tmrg**), and tuff of Wheeler Springs (**Tmtw**; **Tmtwh**)

(**Figure 5-13**). Along Willow Creek, directly west of Burns Butte, the Rattlesnake Tuff (**Tmtr**) attains a maximum thickness >76 m (250 ft) (Plate 1).

The Rattlesnake Tuff (**Tmtr**) in the map area occurs as a single cooling unit, often cropping out as several distinct ledges. Individual ledges display both vertical and lateral variations in welding and crystallization facies; not all facies are present at all localities. Welding facies of the Rattlesnake Tuff (**Tmtr**) in the map area are consistent with those defined by Streck (1994) and Streck and Grunder (1995) including 1) a basal strongly welded tuff (vitrophyre), 2) partially welded tuff with fiamme, and 3) partially welded tuff with pumice (**Figure 5-14**). Partially welded tuff contains devitrified, moderately to completely flattened black, white, and banded fiamme up to 10 cm (3.9 in) in diameter (**Figure 5-14a–c**). Poly-compositional lithics consist of angular, moderate reddish brown (10R 4/6) fragments as much as 1 cm (0.5 in) in length that are supported in a devitrified glass shard and crystal groundmass.

The thickest sections of the Rattlesnake Tuff exposed in the central and southern parts of the Burns Butte 7.5′ quadrangle are associated with a thick basal zone of lithophysae, a crystallization facies overprinting pervasively devitrified, partially welded tuff (**Figure 5-14d**, **Figure 5-15**, **Figure 5-16**; Plate 1). Individual lithophysae are 1 to 3 cm (0.4 to 1.1 in) across, with the concentration of lithophysae increasing upsection. The lithophysal zone grades upward to hackly jointed, massively bedded partially welded vitric tuff with a eutaxitic texture defined by aligned fiamme (**Figure 5-14b**).

Zones defined by partially welded tuff with fiamme and partially welded tuff with pumice form rugged, prominent cliffs and ridge caps typically weathering to tightly packed boulder- to pebble-sized, platy, angular fragments. Adjacent talus slopes are often mantled by toppled meter-scale boulders. Lithophysal horizons also form prominent bench and cliff features. However, unlike partially welded zones, these rocks weather to angular, cobble- to sand-sized fragments with occasional meter-sized blocks spalled from more extensive outcrops (**Figure 5-15**, **Figure 5-16**).

Typical hand samples of the Rattlesnake Tuff (**Tmtr**) are very pale orange (10YR 8/2), to very light gray (N7), to medium gray (N5), and light brownish gray (5YR 6/1), and aphyric to very sparsely porphyritic. Phenocryst content is ≤1 percent (vol.) for the bulk tuff. The tuff (**Tmtr**) contains microphenocrysts and phenocrysts ≤2 mm (0.01 in) of clear, subhedral to euhedral anorthoclase and sanidine, clear, subhedral plagioclase, clear, subhedral quartz, and dusky green (5G 3/2), anhedral clinopyroxene (ferrohedenbergite), distributed within a vitric groundmass (**Figure 5-14a–f**). The original vitroclastic texture of the tuff (**Tmtr**) is retained but is locally overprinted by very fine elongated crystals forming axiolitic structures.

The Rattlesnake Tuff (**Tmtr**) has reversed magnetic polarity (Parker, 1974; Thormahlen, 1984; Smith, 1986a,b; Streck, 1994) and is assigned a late Miocene age on the basis of stratigraphic position and $^{40}Ar/^{39}Ar$ ages of 7.05 ± 0.01 (sanidine from pumice; sample HP-91-12; Streck, 1994; Streck and Grunder, 1995) and 7.093 ± 0.015 Ma (sanidine; sample HP-91-12; Jordan and others, 2004). Unit (**Tmtr**) is equivalent to the Rattlesnake Ash-flow Tuff formally described by Walker (1979) and later renamed to Rattlesnake Tuff by Streck and Grunder (1995).

Figure 5-12. Stratigraphic relationships between the Rattlesnake Tuff (Tmtr), trachyandesite (Tmat), and the rhyolite of Burnes Butte (Tmrb) along Willow Creek (*following page*). (A) View looking northwest toward West Willow Creek, where a northwest-trending fault-bounded ridge exposes a succession of 7.68 to 7.1 Ma trachyandesite lavas (Tmat) overlain by the 7.1 Ma Rattlesnake Tuff (Tmtr) (43.57219, −119.20663 WGS84 geographic coordinates; 4826724mN, 321816mE WGS84 UTM Zone 11 coordinates). Black-outlined yellow circle is the location of the Michael T. Halbouty Federal 1-10 oil and gas exploration well drilled between June and September 1977. Total depth of the Federal 1-10 well is 2,343 m (7,684 ft). See section 6 for more details on the Federal 1-10 well. Labels U and D refer to relative up and down movement of fault blocks, respectively. (B) View looking northwest along the same northwest-trending fault-bounded ridge shown in (A) (43.55854, −119.19199 WGS84 geographic coordinates; 4825176mN, 322959mE WGS84 UTM Zone 11 coordinates). At this location, 1.9 km (1.2 mi) southeast of photo (A), the Rattlesnake Tuff (Tmtr) transitions from directly overlying a section of trachyandesite (Tmat) and the 7.68 Ma rhyolite of Burnes Butte (Tmrb), to directly overlying the rhyolite of Burns Butte (Tmrb). South and east of the location marked with an X, unit Tmat lavas are absent in the stratigraphic section. Dashed lines are geologic contacts; solid white line represents a fault trace. Photo credits: Jason D. McClaughry, 2019.

Figure 5-12. (Stratigraphic relationships between the Rattlesnake Tuff (Tmtr), trachyandesite (Tmat), and the rhyolite of Burnes Butte (Tmrb) – caption on previous page)

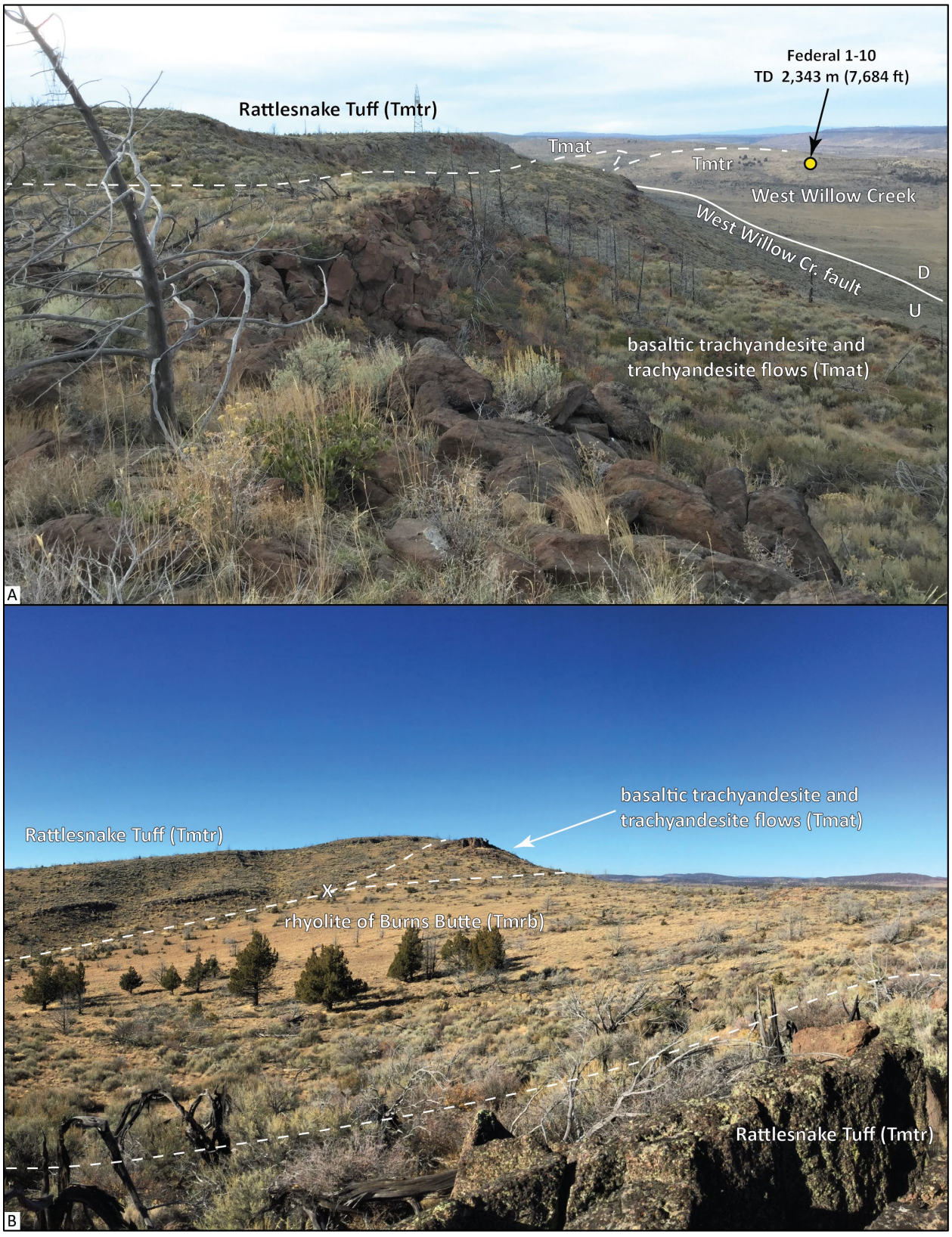

Figure 5-13. Stratigraphic relationships of late Miocene units (43.55466, −119.19209 WGS84 geographic coordinates; 4824745mN, 322939mE WGS84 UTM Zone 11 coordinates). Along Willow Creek, the 7.68 Ma rhyolite of Burns Butte (Tmrb) is overlain by undated trachydacite breccia of unit Tmri. The section is onlapped by the younger 7.1 Ma Rattlesnake Tuff (Tmtr). A north-northeast-trending normal fault offsets the stratigraphic section in a down-on-the-northeast sense on the northeast side of the ridge. Dashed lines are geologic contacts; solid white line represents a fault trace. Labels U and D refer to relative up and down movement of fault blocks, respectively. View is looking southeast across Willow Creek canyon. Streamflow of Willow Creek is from left to right in the photograph. Photo credits: Jason D. McClaughry, 2019.

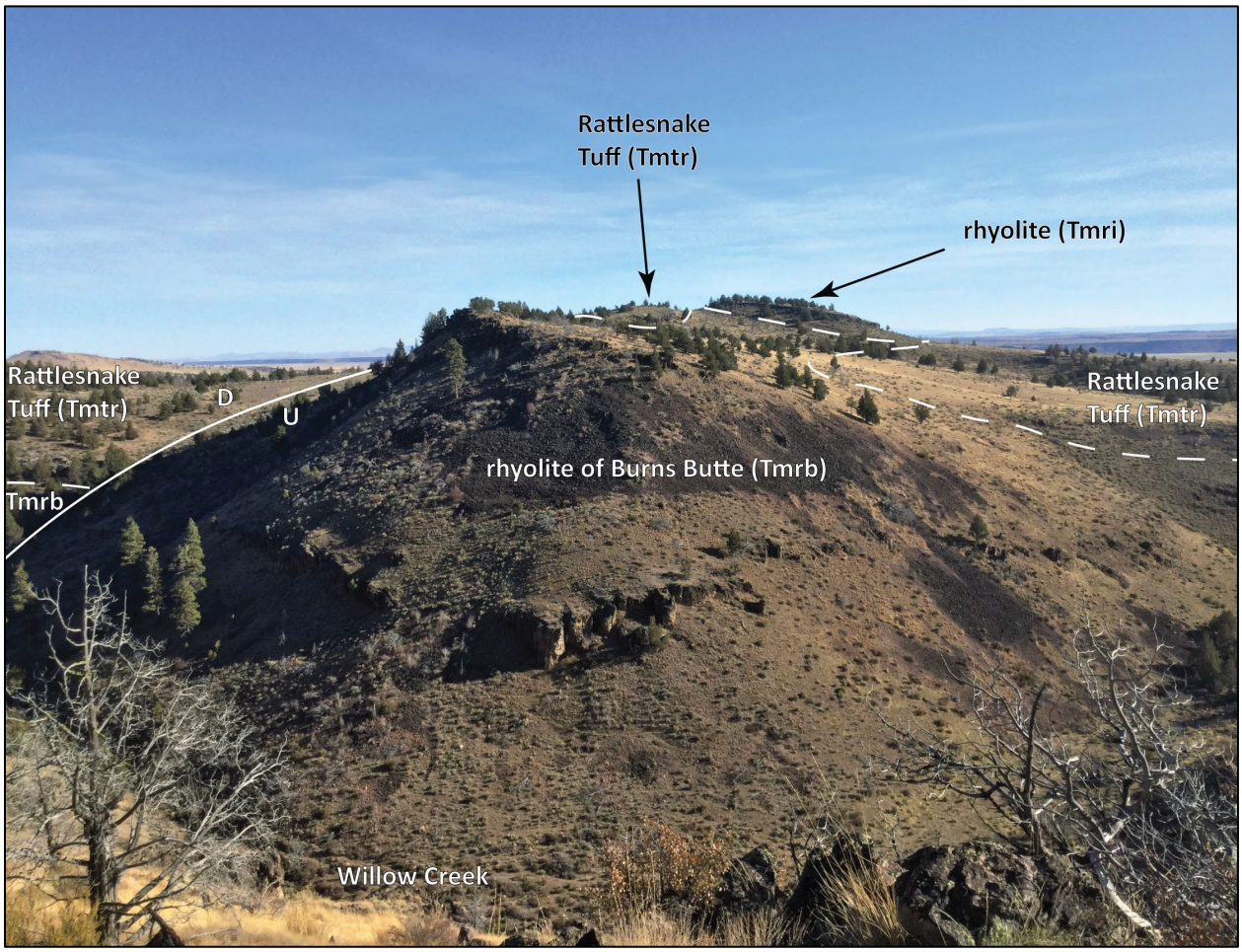

Figure 5-14. Hand sample and thin-section photographs showing textural variations in the Rattlesnake Tuff (Tmtr) in the Burns Butte 7.5' quadrangle and vicinity. (A) Partially welded tuff with pumice, sample 85 PCBJ 18 (43.64153, −119.05989 WGS84 geographic coordinates; 4834121mN, 333856mE WGS84 UTM Zone 11 coordinates). (B) Strongly welded tuff with fiamme, sample 28 BBJ 19 (43.53699, −119.21224 WGS84 geographic coordinates; 4822826mN, 321259mE WGS84 UTM Zone 11 coordinates). (C) Partially welded tuff with banded pumice and fiamme, sample 94 PCBJ 18 (43.60339, −119.134756 WGS84 geographic coordinates; 4830037mN, 327709mE WGS84 UTM Zone 11 coordinates). (D) Lithophysal tuff, sample 58 BBJ 19 (43.57625, −119.24168 WGS84 geographic coordinates; 4827250mN, 318998mE WGS84 UTM Zone 11 coordinates). Scale bar in A–D is 2.5 cm (1 in) high. (E) Photomicrograph of a mafic lithic fragment surrounded by glass shards displaying compaction foliation under cross-polarized light. Scale bar is 1 mm (0.04 in) in length (sample HAH0170-16) (F) Same view as (E), under plane-polarized light. Abbreviations: af - alkali feldspar, qtz - quartz, Lithic Frag. - lithic fragment. Photo credits: (A–D) Jason D. McClaughry, 2018; (E-F) Robert A. Houston, 2017.

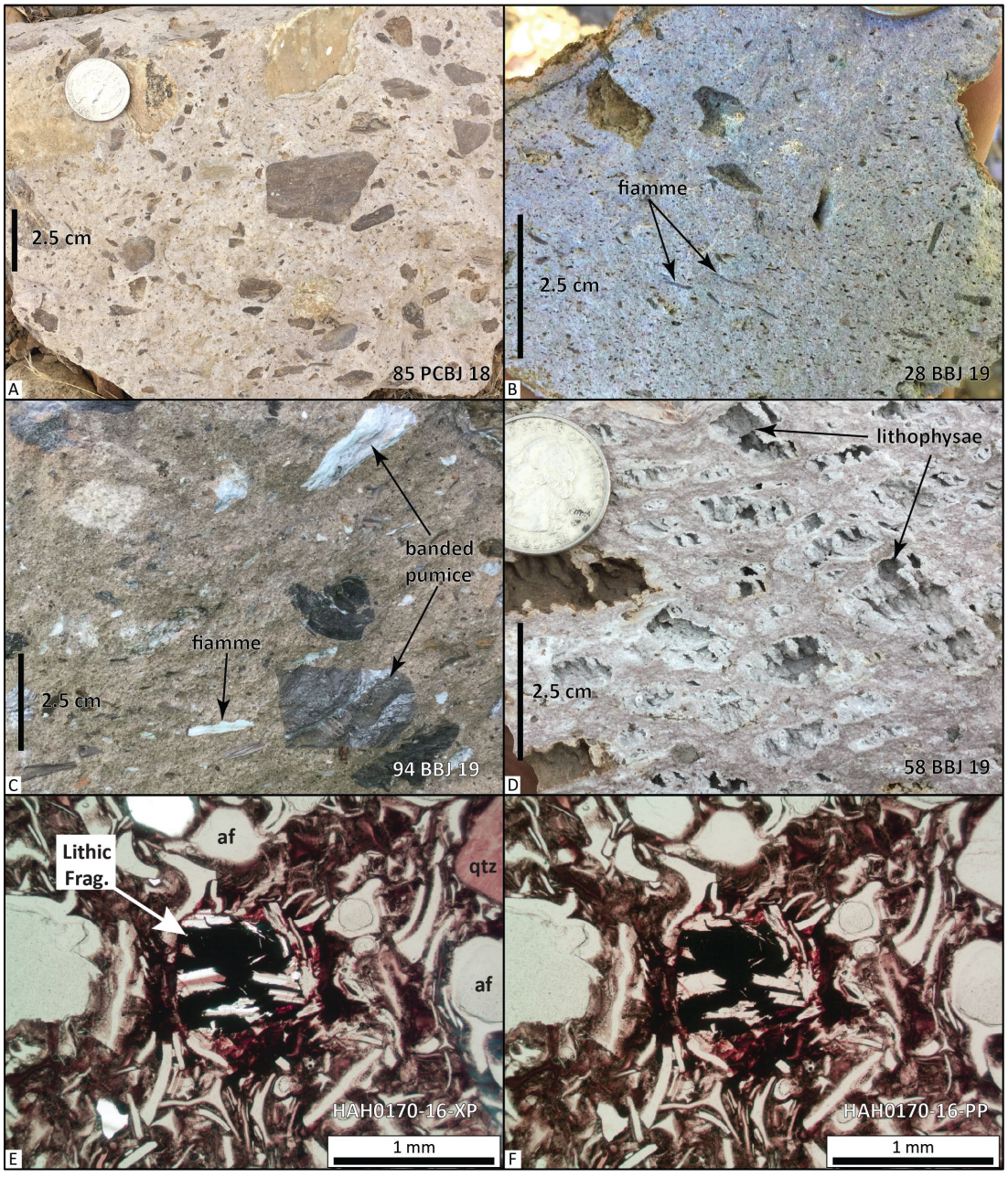

Figure 5-15. Rattlesnake Tuff (Tmtr) exposed in Willow Creek canyon in the south-central part of the map area. (43.54066, −119.19329 WGS84 geographic coordinates; 4823193mN, 322801mE WGS84 UTM Zone 11 coordinates). Ledge-forming exposures here are 10 to 15 m (30 to 50 ft) high and composed of lithophysal Rattlesnake Tuff (Tmtr). View is looking south. Scale bar is 2 m (6.6 ft) high. Photo credit: Carlie J.M. Duda, 2019.

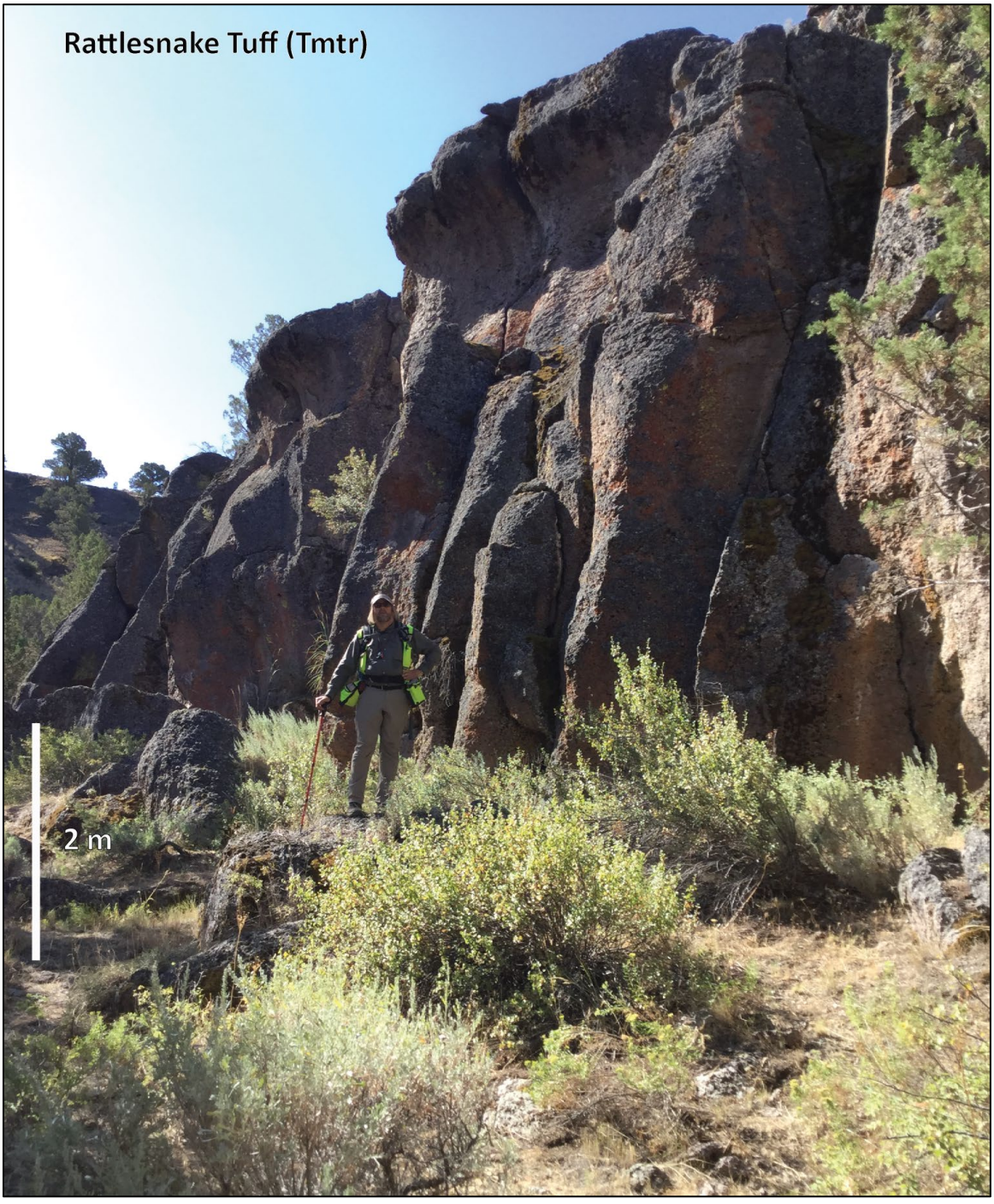

Figure 5-16. Rattlesnake Tuff (Tmtr) exposed west of Burns Butte in the central part of the map area. (43.57554, −119.18325 WGS84 geographic coordinates; 4827046mN, 323714mE WGS84 UTM Zone 11 coordinates). (A) Low-lying, ledge-forming exposures here are composed of lithophysal Rattlesnake Tuff (Tmtr). View is looking east. Scale bar is 1 m (3.3 ft) high. (B) Close-up of the outcrop in (A) showing lithophysal Rattlesnake Tuff (Tmtr) with abundant flattened pumice fiamme. Scale bar is 10 cm (4 in) high. Photo credits: Jason D. McClaughry, 2019.

Tmst **tuffaceous sedimentary rocks (upper Miocene)**—Tuffaceous mudstone, siltstone, sandstone, conglomerate and fluvially reworked tuff beds, pumice tuff, and air-fall tuff exposed beneath the Rattlesnake Tuff (**Tmtr**) in the northeast part of the map area (Plate 1). Tuffaceous sedimentary rocks (**Tmst**) are assigned a late Miocene age on the basis of stratigraphic position and bracketing by precisely dated tuff marker beds. Unit **Tmst** is partly equivalent to units Td (Danforth Formation) of Piper and others (1939), Tst (sedimentary rocks) of Greene (1972), sedimentary rocks overlying Tdv (welded tuff of Devine Canyon) of Greene (1972) and Greene and others (1972), Tst (tuffaceous sedimentary rocks and tuff) of Walker (1977), and Tmst-1, -2, and -3 (tuffaceous sedimentary rocks) of Brown and others (1980a).

Tmat **basaltic trachyandesite and trachyandesite flows and dikes (upper Miocene)**— Multiple flows of basaltic trachyandesite (SiO_2 = 54.43 to 56.67 weight percent; K_2O = 1.52 to 1.98 weight percent; *n* = 14 analyses) and trachyandesite (SiO_2 = 59.21 to 63.19 weight percent; K_2O = 2.24 to 3.54 weight percent; *n* = 7 analyses) exposed beneath the Rattlesnake Tuff (**Tmtr**) in a series of footwall blocks in the north half of the Burns Butte 7.5′ quadrangle (Plate 1; **Figure 5-7**, **Figure 5-9**, **Figure 5-12**; **Table 5-2**; Appendix). The unit consists of 1- to 10-m-thick (3.3 to 33 ft) grayish black (N2) dense and commonly distinctly flow-banded lava flows with rubbly, highly vesiculated flow tops. The base of flows is locally defined by moderate red (5R 4/6) to black (N1) scoriaceous ‘A‘ā flow-foot breccia (**Figure 5-17a**). Dense, non-vesicular lavas form distinctive bench and cliff-forming outcrops; they are typically characterized by blocky, platy, or hackly jointing (**Figure 5-17a**). Lavas commonly weather to platy slabs and irregular blocks, forming extensive talus slopes beneath cliff-forming outcrops (**Figure 5-12**). The composite maximum thickness of the unit in the area of the Federal 1-10 well is ~145 m (476 ft ft). Construction aggregate is obtained from several quarry sites hosted within this unit in the map area (Plate 1).

The unit includes several flow sequences erupted from different vent complexes, but they are not mapped separately here due to similar appearing lithology and narrow chemical ranges (**Figure 5-7**, **Figure 5-9**, **Figure 5-18**, **Table 5-2**). Typical basaltic trachyandesite or trachyandesite hand samples are commonly streaked or mottled, medium bluish gray (5B 5/1), light bluish gray (5B 7/1), dusky blue (5PB 3/2), or very light gray (N8) and aphyric to very sparsely microporphyritic with blocky plagioclase and pyroxene microphenocrysts <1 mm (<0.04 in) across contained within a fine-grained crystalline groundmass of trachytic plagioclase microlites. Lithologic variations may be dense and non-vesicular to highly vesicular, commonly showing flow banding (**Figure 5-18a,b**). Hand samples obtained from unit **Tmat** flows in the map area have a range of petrographic textures in the map area including the following: 1) Sample 14 BBJ 19, collected 2.3 km (1.4 mi) southeast of the Federal 1-10 well, is petrographically aphyric to sparsely microporphyritic with <1 percent subhedral to euhedral plagioclase microphenocrysts <0.5 mm (0.02 in) and <1 percent anhedral to subhedral clinopyroxene microphenocrysts <0.5 mm (0.02 in) contained within a very fine-grained, hypocrystalline groundmass of trachytic plagioclase and intersertal glass (**Figure 5-18c,d**). The groundmass is locally hyalophitic where glass encloses groundmass plagioclase. 2) Sample 46 BBJ 19, collected 2.5 km (1.5 mi) west of the Federal 1-10 well, is petrographically aphyric to microporphyritic with 3 to 5 percent subhedral to euhedral, seriate, plagioclase and clinopyroxene microphenocrysts <1 mm (0.04 in), <1 percent olivine microphenocrysts up to 1 to 2 mm (0.04 to 0.08 in), and <1 percent glomerocrysts (plagioclase + clinopyroxene ± olivine) contained within a hypohyaline groundmass of glass and feldspar microlites (**Figure 5-18e,f**). Feldspar microlites are

trachytically aligned, wrapping around single crystals and crystal clots. Plagioclase display characteristic albite twinning or penetration twinning and are zoned. 3) Sample 117 BBHC 19, collected 0.3 km (0.2 mi) northeast of Rimrock Springs, is petrographically aphyric to very sparsely microporphyritic with < 1 percent subhedral to euhedral, plagioclase and clinopyroxene microphenocrysts < 0.5 mm (0.02 in), contained within a hypohyaline groundmass of glass and feldspar microlites. Feldspar microlites are trachytic, wrapping around single crystals and crystal clots.

Unit **Tmat** has reversed magnetic polarity and are assigned a late Miocene age on the basis of stratigraphic position above the 7.68 Ma rhyolite of Burns Butte (**Tmrb**) and below the 7.1 Ma Rattlesnake Tuff (**Tmtr**) (Plate 1). Brown (1982) reported a K/Ar age of 8.6 ± 0.3 Ma from this unit east of Burns Butte (Brown's Taw unit), but the reported age is considered too old on the basis of stratigraphic position and more precise ages obtained on bracketing units. **Tmat** flows dated by Brown (1982) lie stratigraphically above and infill erosional topography formed on the 7.68 Ma rhyolite of Burns Butte (**Tmrb**), west of the city of Burns. Along U.S. Highway 20, in the southwestern part of the Burns 7.5′ quadrangle flows (**Tmat**) and vent deposits (**Tmvt**) overlie the 8.46 Ma rhyolite of Golden Ranch (**Tmrb**) (see Plate 2 in McClaughry and others, 2019).

Basaltic trachyandesite and trachyandesite flows in the map area were erupted from still extant cinder- and dike-capped vents (**Tmvt**) exposed in a narrow belt of high buttes extending between Willow Creek Flats on the north and U.S. Highway 20 in the southwest corner of the Burns 7.5′ quadrangle (Plate 1; see Plate 2 in McClaughry and others, 2019). Other vent areas (**Tmvt**) for unit **Tmat** are exposed in the vicinity of the Federal 1-10 well (**Figure 5-17b**) in the northwest part of the Burns Butte 7.5′ quadrangle and west of the Silvies River in the Poison Creek 7.5′ quadrangle (McClaughry and others, 2019). Partly equivalent to Qbh (late basalt) and Th (Harney Formation) of Piper and others (1939), Ta (andesite) and QTmv (mafic vent complexes) of Greene (1972) and Greene and others (1972), Tob (olivine basalt) and Tmv (mafic vent rocks) of Walker (1977), Tma (andesites) and QTmv (Upper Pliocene mafic vent complexes) of Brown and others (1980a), and units Tmar (basaltic andesites of Rimrock Springs) and Taw (basaltic andesites of Willow Creek) of Brown (1982).

Figure 5-17. Basaltic trachyandesite flows (Tmat) exposed in the Burns Butte 7.5′ quadrangle and vicinity. (A) Cliff-forming outcrop of platy- to blocky-jointed trachyandesite exposed in the northeast part of the Burns Butte 7.5′ quadrangle (43.59918, −119.15172 WGS84 geographic coordinates; 4829605mN, 326328mE, WGS84 UTM Zone 11 coordinates). The lower exposed meter of this outcrop consists of a red-oxidized, scoriaceous flow base. The flow base, in turn, directly overlies a red-oxidized, glassy, welded basaltic tuff. View is looking north. Scale bar is 2 m (6.6 ft) high. (B) View looking northwest to a vent complex capped by a dense, red-oxidized lava of unit Tmat (43.59099, −119.24906 WGS84 geographic coordinates; 4828903mN, 318447mE, WGS84 UTM Zone 11 coordinates). The lower parts of the vent complex are composed of loosely consolidated cinders forming part of unit Tmvt. The outcrop lies just to the west of the Burns Butte 7.5′ quadrangle in the upper part of West Willow Creek. Dashed lines are geologic contacts. Photo credits: (A) Jason D. McClaughry, 2019; (B) Carlie J.M. Duda, 2019.

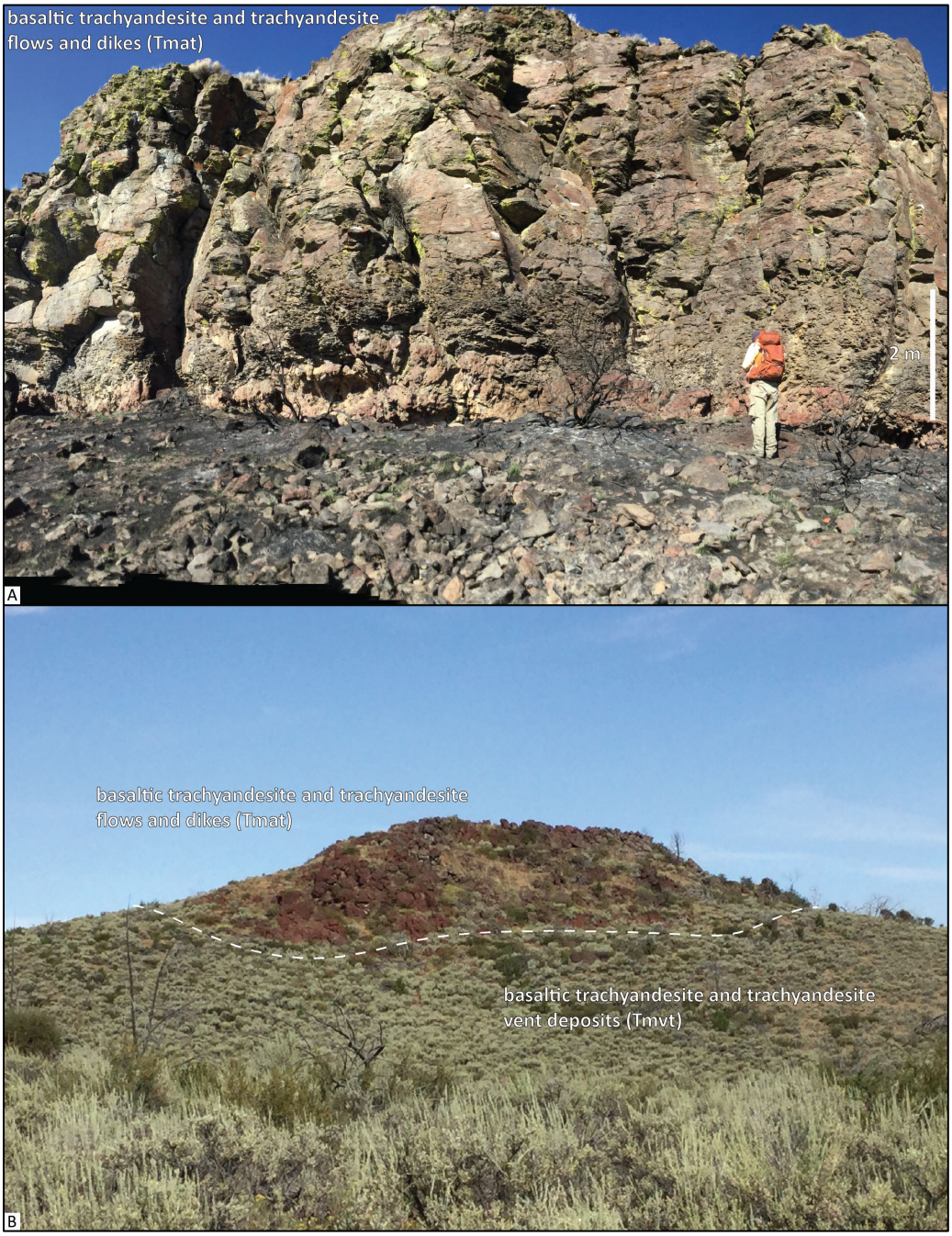

Figure 5-18. Hand sample and thin-section photographs showing textural variations in basaltic trachyandesite and trachyandesite lava flows (Tmat). (A) Hand sample of basaltic trachyandesite (Tmat) from the base of the exposed section shown in Figure 5-11A, sample 14 BBJ 19 (Map no. G21) (43.57409, −119.20769 WGS84 geographic coordinates; 4826937mN, 321736mE, WGS84 UTM Zone 11 coordinates). (B) Hand sample of trachyandesite (Tmat) exposed along the west-central edge of the Burns Butte 7.5′ quadrangle, sample 46 BBJ 19 (43.58948, −119.24969 WGS84 geographic coordinates; 4828737mN, 318391mE, WGS84 UTM Zone 11 coordinates). Scale bar in A-B is 2.5 cm (1 in) high. (C) Photomicrograph of sample 14 BBJ 19 under cross-polarized light. (D) Same view as (C), under plane-polarized light. (E) Photomicrograph of sample 46 BBJ 19 under cross-polarized light. (F) Same view as (E), under plane-polarized light. Scale bar in C–F is 1 mm (0.04 in) in length. Photo credits: (A–F) Jason D. McClaughry, 2018.

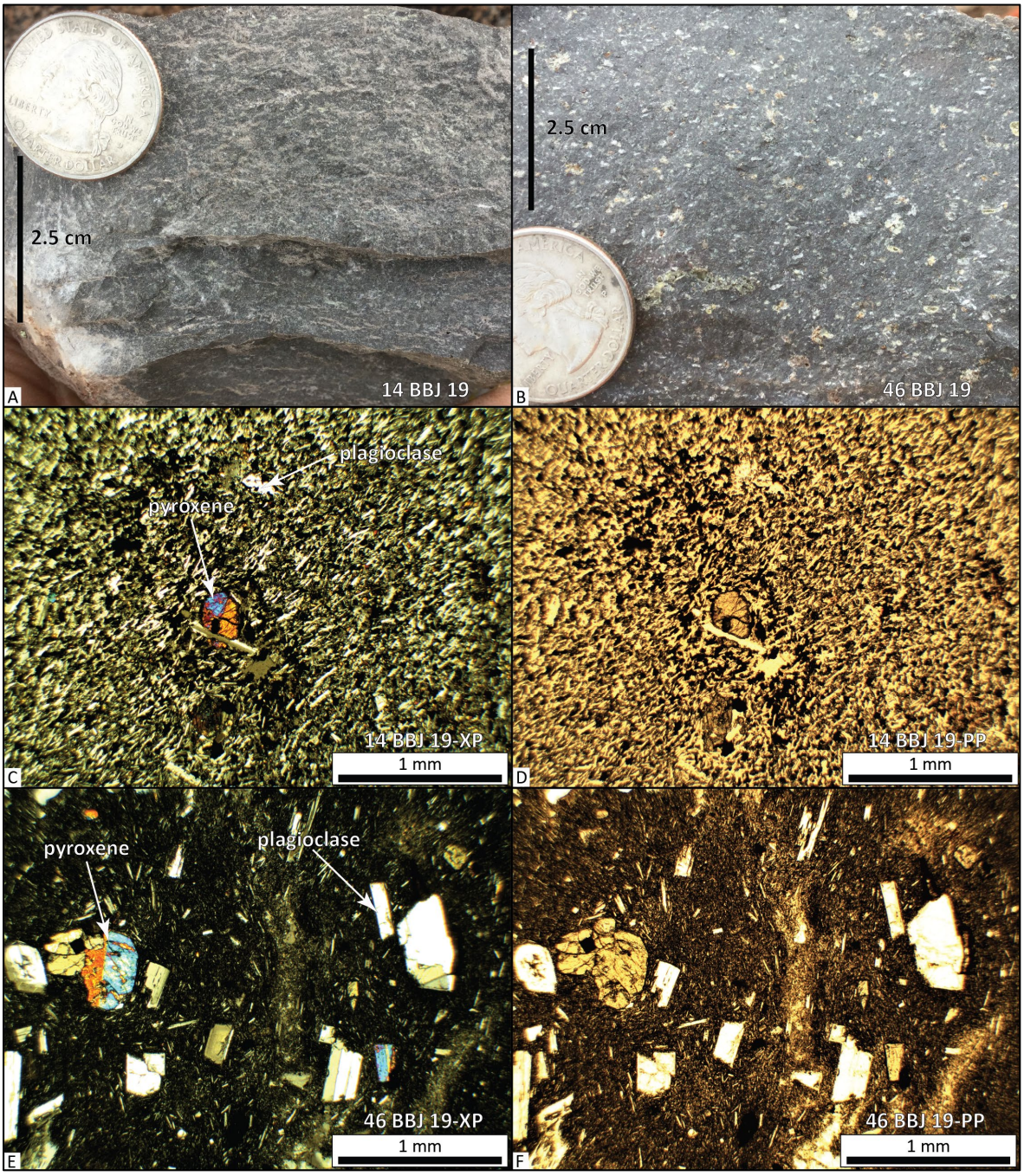

Tmvt **basaltic trachyandesite and trachyandesite vent deposits (upper Miocene)**—Weakly consolidated scoria, cinders, and palagonitic tuffs forming small shield volcanoes and still extant cinder- and dike-capped vents between Willow Creek Flats on the north and U.S. Highway 20 in the southwest corner of the Burns 7.5′ quadrangle (Plate 1; McClaughry and others, 2019, Plate 2). Other **Tmvt** deposits are mapped in the vicinity of the Federal 1-10 well in the northwest part of the Burns Butte 7.5′ quadrangle (**Figure 5-17b**) and west of the Silvies River in the Poison Creek 7.5′ quadrangle (McClaughry and others, 2019, Plate 1). Cinder deposits are moderate reddish brown (10R 4/6) to grayish black (N2) and typically massive to moderately bedded, containing numerous fluidal volcanic bombs (**Figure 5-19**). Samples of cinder and scoria obtained from the **Tmvt** outcrops by McClaughry and others (2019) have a basaltic trachyandesite or trachyandesite composition (SiO_2 = 55.62 to 57.33 weight percent; K_2O = 1.40 to 1.88 weight percent; *n* = 6 analyses), similar to flows in unit **Tmat**.

Tmvt vent deposits are assigned a late Miocene age on the basis of stratigraphic association with unit **Tmat** (**Figure 5-17b**). A significant component of unconsolidated cinders has been eroded and reworked as an important clast component in younger sedimentary rocks of unit **QTst.** The unit is extensively mined as an aggregate resource in the Burns Butte 7.5′ quadrangle (**Figure 5-19**; Plate 1). Partly equivalent to Qbh (late basalt) and Th (Harney Formation) of Piper and others (1939), QTmv (mafic vent complexes) of Greene (1972) and Greene and others (1972), Tob (olivine basalt) and Tmv (mafic vent rocks) of Walker (1977), QTmv (Upper Pliocene Mafic vent complexes) of Brown and others (1980a), and Tav (basaltic andesite vent complexes) of Brown (1982).

Figure 5-19. Unit Tmvt vent deposits. Moderate reddish brown (10R 4/6), massive to moderately bedded cinder deposit exposed in a borrow pit in the southeast part of Willow Flats in the northeast part of the Burns Butte 7.5′ quadrangle (43.60715, −119.17379 WGS84 geographic coordinates; 4830537mN, 324570mE WGS84 UTM Zone 11 coordinates). View is looking east. Scale bar is 1 m (3.3 ft) high. Photo credit: Carlie J.M. Duda, 2019.

Tmrb **rhyolite of Burns Butte (upper Miocene)** — Flow-banded, strongly flow-foliated aphyric rhyolite (SiO_2 = 74.35 to 77.20 weight percent; K_2O = 4.52 to 5.10 weight percent; *n* = 16 analyses) forming an extensive flow and dome sequence extending in a northwest trending belt between Sage Hen Valley northwest to Boone Canyon (9.3 km [5.8 mi] north of the map area) (Plate 1; **Figure 5-7**, **Figure 5-9**, **Table 5-2**; **Figure 5-20**; Appendix). Rhyolite exposed in the northeast corner of the map area is a variant containing higher amounts of SiO_2, Zr, and Nb (**Table 5-2**; see map no. G67). The rhyolite forms the high topography of Burns Butte and extends west into Willow Creek Canyon, where flows are overlain by trachyandesite lava flows (**Tmat**) and Rattlesnake Tuff (**Tmtr**) (**Figure 5-13**; **Figure 5-20a,b**). West of Willow Creek, Burns Butte rhyolite flows (**Tmrb**) thin to the extent that they are not present in the subsurface in the vicinity of the Federal 1-10 well (Plate 1, cross sections A-A′ and B-B′). The rhyolite commonly is exposed as expansive ledge- and cliff-forming outcrops up to tens of meters high; where incised by deep canyons, such as Willow Creek, prominent outcrops may extend up to 100 m (328 ft) high (**Figure 5-20a**). Outcrops typically are characterized by distinct flow banding and horizontal to subvertical and vertical flow foliation with complex recumbent flow folds up to 20 m (66 ft) high (**Figure 5-21**). The upper parts of flows are marked by faintly banded black (N9) to greenish black (5G 2/1) obsidian flow tops (Brown, 1982). Flow breccia, containing poorly sorted, faintly banded black (N9) to greenish black (5G 2/1) obsidian fragments, is present in a number of outcrops and may be related to carapace, basal, marginal, and internal autobrecciation (McClaughry and others, 2019). Chemical composition of the rhyolite of Burns Butte (**Tmrb**) is indistinguishable from analyses obtained from the underlying tuff of Wheeler Springs (**Tmtw**, **Tmtwh**) (**Figure 5-7**, **Figure 5-9**, **Table 5-2**).

Typical hand samples of the rhyolite are medium light gray (N6) to light brownish gray (5YR 6/1) and medium bluish gray (**Figure 5-22a**). The rhyolite is characteristically aphyric to very sparsely microporphyritic with <1 percent (vol.) subhedral, blocky to prismatic alkali feldspar, clinopyroxene/orthopyroxene, and quartz microphenocrysts ≤0.5 mm (0.02 in) contained within a cryptocrystalline, felty, and mottled groundmass of feldspar, pyroxene, and magnetite (**Figure 5-22c-d**). Plagioclase and pyroxene microphenocrysts occur as single crystals or in small clusters. Resorbed quartz grains up to 4.5 mm (0.2 in) are also present. Flow banding is apparent in thin section, defined by the trachytic alignment of plagioclase microlites alternating with bands of cryptocrystalline quartz. Hand sample textures range from strongly planar to contorted flow-banded, sugary-textured rhyolite, to devitrified obsidian, or brecciated rhyolite (**Figure 5-22a,b**).

The rhyolite of Burns Butte (**Tmrb**) has normal magnetic polarity and is assigned a late Miocene age on the basis of stratigraphic position above the 8.52 Ma intracaldera unit of the Prater Creek Ash-flow Tuff (**Tmtpi**) and below the 7.1 Ma Rattlesnake Tuff (**Tmtr**) (Plate 1). Unit **Tmrb** intrudes and directly overlies the tuff of Wheeler Springs (**Tmtw**, **Tmtwh**); the unit is in fault contact and overlies the 8.46 Ma rhyolite of Golden Ranch (**Tmrg**) southwest of Burns Butte (Plate 1). Isotopic ages of 7.68 ± 0.04 Ma ($^{40}Ar/^{39}Ar$ plateau; sanidine; sample HP-91-2; Jordan and others, 2004) and 7.74 ± 0.04 Ma (K-Ar; obsidian; sample M3-79; MacLeod and others, 1975; Fiebelkorn and others, 1982) were reported for samples of the rhyolite (**Tmrb**) obtained on Burns Butte (Plate 1; Appendix). Unit **Tmrb** is partly equivalent to Td (Danforth Formation) of Piper and others (1939), Tr (rhyodacite) of Greene (1972) and Greene and others (1972), Tvs (silicic vent rocks) of Walker (1977), Tmrb (rhyodacite of Burns Butte) of Brown and others (1980a), and Tmrb (rhyolite of Burns Butte) of Brown (1982).

Figure 5-20. Rhyolite of Burns Butte (Tmrb) exposed in the Burns Butte 7.5′ quadrangle. (A) Prominent outcrops in the Willow Creek drainage, in the south-central part of the map area, are typically up to tens of meters high and form at least two distinct benches. The rhyolite is characterized by horizontal to subvertical and vertical flow foliation and chaotic flow folding (43.55106, −119.19170 WGS84 geographic coordinates; 4824345mN, 322960mE WGS84 UTM Zone 11 coordinates). View is looking north. Scale bar is 1 m (3.3 ft) high. (B) Expansive outcrops of Tmrb forming the northeastern part of Burns Butte in the northeast part of the map area (43.56414, −119.13223 WGS84 geographic coordinates; 4825674mN, 327801mE WGS84 UTM Zone 11 coordinates). View is looking southeast toward the radio towers. Photo credits: (A) Carlie J.M. Duda, 2019; (B) Ian P. Madin, 2019.

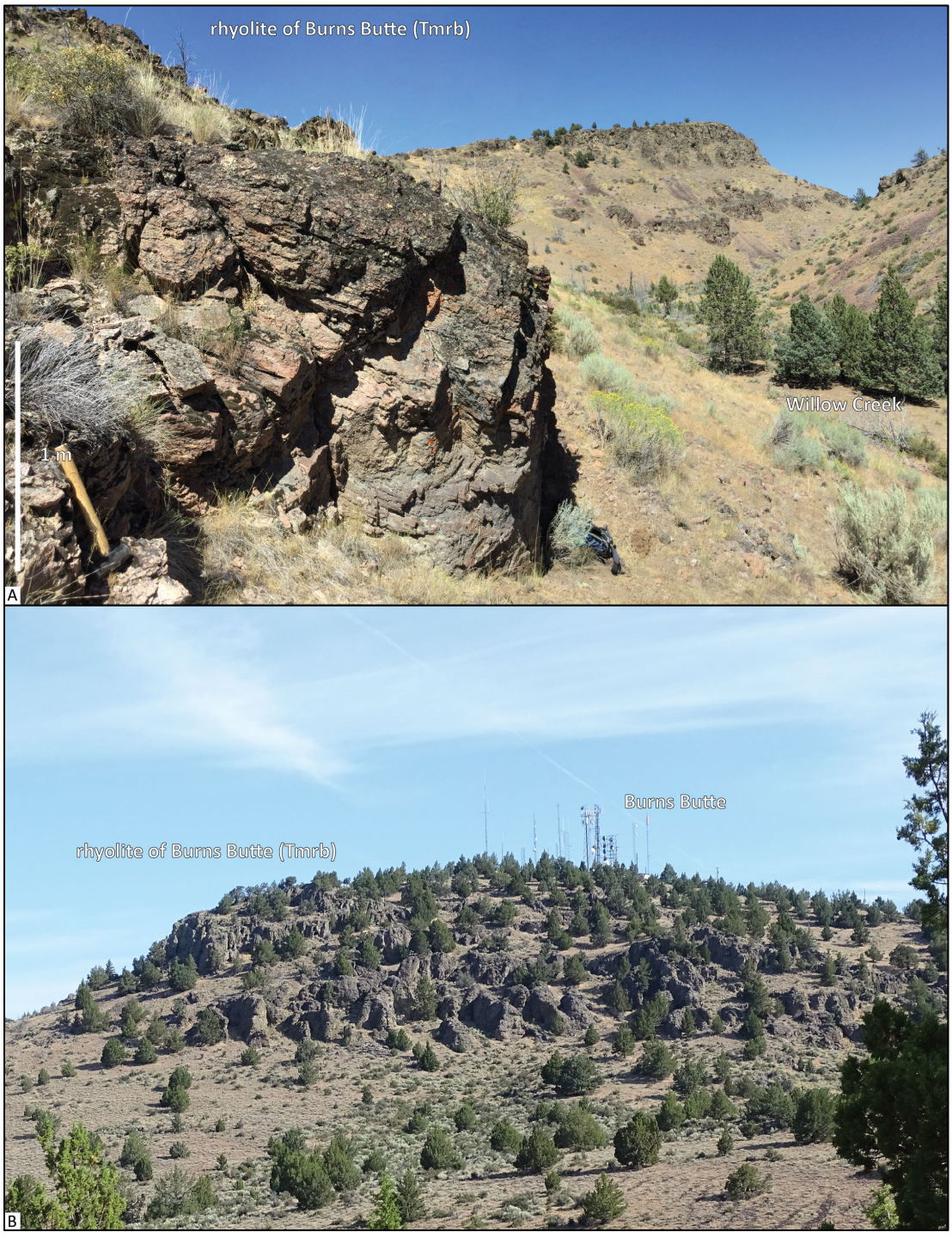

Figure 5-21. Flow banding in the rhyolite of Burns Butte (Tmrb). Canyon exposures of the rhyolite in the northeast part of the map area are characterized by chaotic flow folding on a centimeter scale (43.59561, −119.14905 WGS84 geographic coordinates; 4829203mN, 326533mE WGS84 UTM Zone 11 coordinates). View is looking north. Scale bar is 2.5 cm (1 in) high. Photo credit: Jason D. McClaughry, 2019.

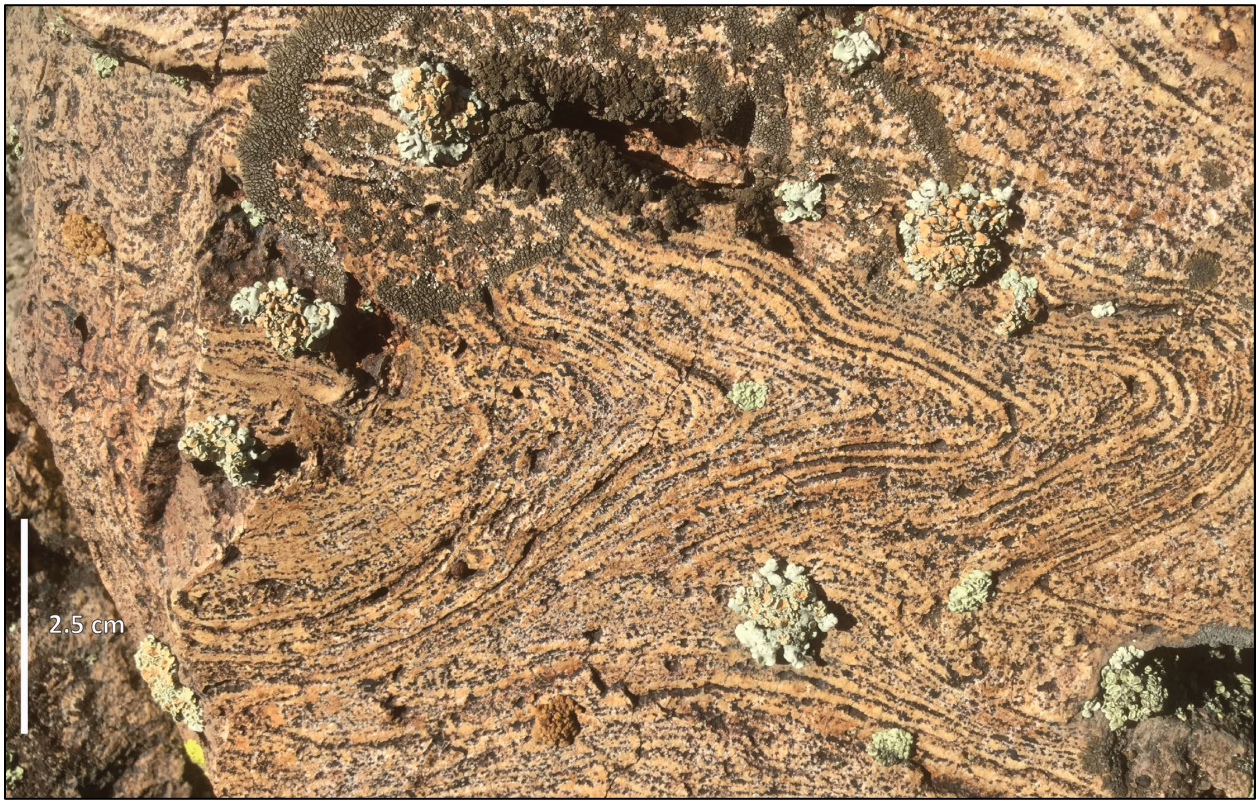

Figure 5-22. Hand sample and thin section photographs showing lithologic textures in the rhyolite of Burns Butte (Tmrb). (A) Planar flow-banded rhyolite, sample 191 BBJ 19 (43.59766, −119.15149 WGS84 geographic coordinates; 4829203mN, 326533mE WGS84 UTM Zone 11 coordinates). (B) Devitrified lithophysal rhyolite, sample 250 BBJ 19 (43.55466, −119.19209 WGS84 geographic coordinates; 4824745mN, 322939mE WGS84 UTM Zone 11 coordinates). Scale bar in A-B is 2.5 cm (1 in) high. (C) Photomicrograph of sample 29 BRHC 18 under cross-polarized light. (D) Same view as (C), under plane-polarized light. Scale bar in C-D is 1 mm (0.04 in) in length. Abbreviations: qtz – quartz, px – pyroxene. Photo credits: (A-F) Jason D. McClaughry, 2019.

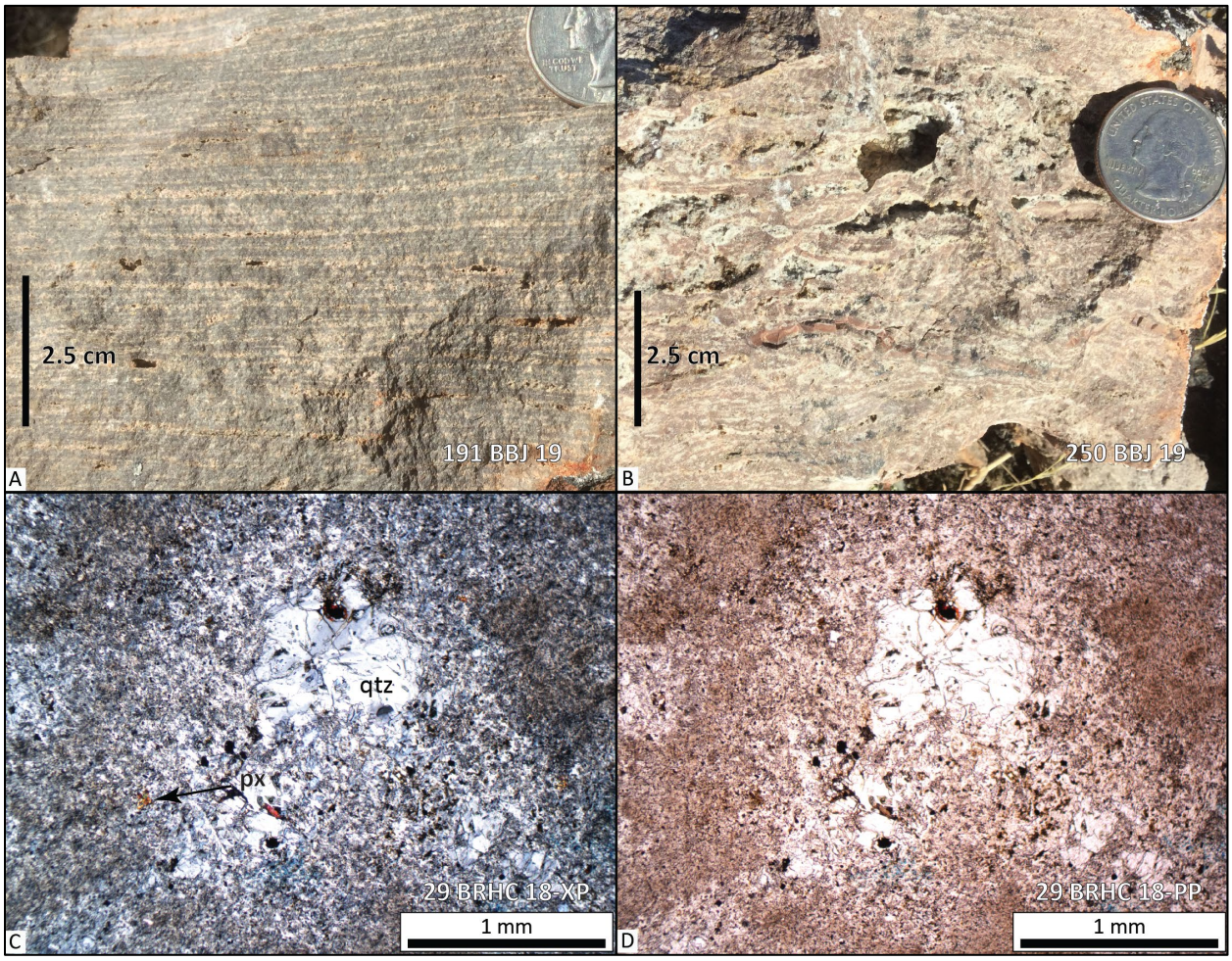

Tmrg **rhyolite of Golden Ranch (upper Miocene)**—Massive to flow-foliated rhyolite (SiO_2 = 71.94 to 72.30 weight percent; K_2O = 4.67 to 4.75 weight percent; *n* = 2 analyses) exposed above the tuff of Wheeler Springs (**Tmtw**; **Tmtwh**) and the rhyolite of Burns Butte (**Tmrb**) in the low hills between Burns Butte and U.S. Highway 20 (Plate 1; **Figure 5-7**, **Figure 5-9**, **Figure 5-23**; **Table 5-2**; Appendix). Outcrops of the rhyolite of Golden Ranch (**Tmrg**) also reach east into the Burns 7.5′ quadrangle (see Plate 2 in McClaughry and others, 2019). The rhyolite occurs in prominent outcrops up to 30 m (100 ft) high, characterized by blocky to subvertical to vertical tabular jointing (**Figure 5-23**). Outcrop surfaces observed in 1-m lidar DEMs south of U.S. Highway 20 in the Burns 7.5′ quadrangle retain complex compression ridges formed during lava flow emplacement (see Plate 2 in McClaughry and others, 2019).

Typical hand samples of the rhyolite are medium light gray (N6) and characteristically porphyritic (**Figure 5-24a**). The rhyolite contains ~3 to 5 percent (vol.) subhedral to anhedral, blocky to prismatic, seriate alkali feldspar and plagioclase phenocrysts ≤5 mm (0.2 in), 1 to 2 percent (vol.) subhedral biotite microphenocrysts ≤1 mm (0.04 in), trace amounts of clinopyroxene and orthopyroxene, ≤1 percent (vol.) alkali feldspar-biotite glomerocrysts ≤5 mm (0.2 in), and trace Fe-Ti oxides, contained within a glassy to spherulitic cryptocrystalline groundmass of feldspar, quartz, and magnetite (**Figure 5-24b,c**).

The rhyolite of Golden Ranch (**Tmrg**) is assigned a late Miocene age on the basis of stratigraphic position and a $^{40}Ar/^{39}Ar$ plateau age of 8.46 ± 0.03 Ma (groundmass; sample 148 BRHC 19; appendix). Unit **Tmrg** intrudes and directly overlies the tuff of Wheeler Springs (**Tmtw**, **Tmtwh**); the unit is in fault contact and underlies the 7.68 Ma rhyolite of Burns Butte (**Tmrb**) southwest of Burns Butte (Plate 1). Green and others (1972) reported a K/Ar age of 7.82 ± 0.26 Ma for the rhyolite of Golden Ranch (**Tmrg**) (recalculated to 8.03 ± 0.26 Ma by Fiebelkorn and others, 1982, 1983; Appendix). Unit **Tmrg** is partly equivalent to units Td (Danforth Formation) of Piper and others (1939), Tr (rhyodacite) of Greene (1972) and Greene and others (1972), Tvs (silicic vent rocks) of Walker (1977), Tmrb (rhyodacite of Burns Butte) of Brown and others (1980a), and Tmrg (rhyolite of Golden Ranch) of Brown (1982).

Figure 5-23. The rhyolite of Golden Ranch (Tmrg) (next page), cropping out in the southern part of the Burns Butte 7.5′ quadrangle. Massive to blocky-jointed, abundantly porphyritic rhyolite exposed in a roadcut on the north side of U.S. Highway 20 (43.51204, −119.14013 WGS84 geographic coordinates; 4827734mN, 329015mE WGS84 UTM Zone 11 coordinates). The outcrop corresponds to field site and sample number 148 BRHC 19 (map no. G1) which has an $^{40}Ar/^{39}Ar$ plateau age of 8.46 ± 0.03 Ma. View is looking north. Scale bar is 1 m (3.3 ft) high. Photo credit: Carlie J.M. Duda, 2019.

Figure 5-24. Hand sample and thin section photographs showing the rhyolite of Golden Ranch (Tmrg). (A) Alkali feldspar-biotite microporphyritic rhyolite with a devitrified, spherulitic groundmass. Sample 148 BRHC 19 (map no. G1). Scale bar in (A) is 2.5 cm (1 in) high. (B) Photomicrograph of sample 148 BRHC 19 under cross-polarized light. (C) Same view as (B), under plane-polarized light. Scale bar in (B) and (C) is 1 mm (0.04 in) in length. Abbreviations: af – alkali feldspar; bt- biotite; qtz – quartz. Photo credits: Jason D. McClaughry, 2019.

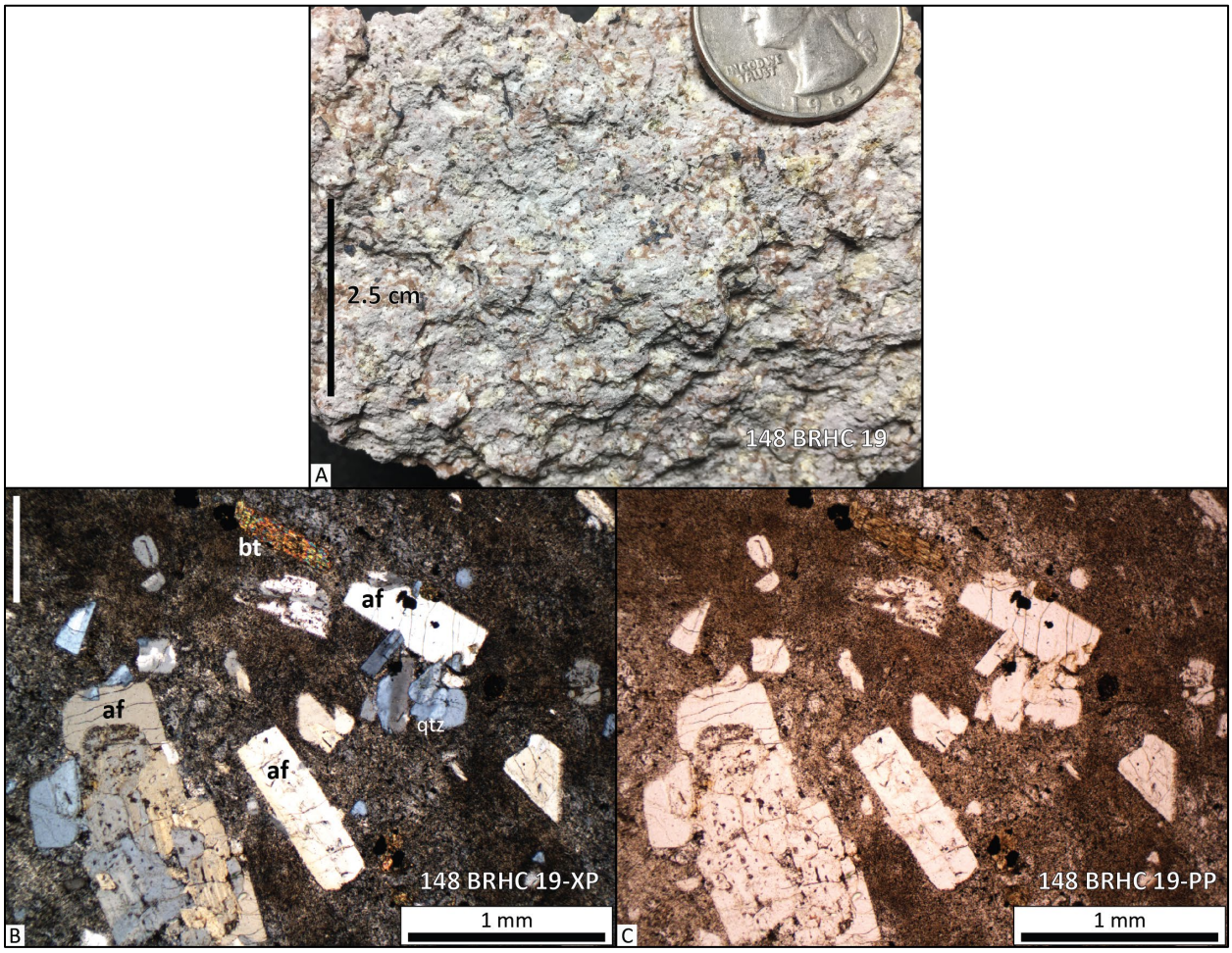

Tmri **rhyolite and trachydacite (upper Miocene)**—Light gray (N7) rhyolite intruding the tuff of Wheeler Springs (**Tmtw**) along the southeast-central edge of Burns Butte 7.5′ quadrangle (Plate 1). The distribution of unit **Tmri** along the east edge of the map area is based solely on the work of Brown (1982); access to the privately held outcrop area was not available during the course of this study. Brown (1982) considered **Tmri** cropping out along the east edge of the map area to represent a hypabyssal intrusive equivalent to the rhyolite of Golden Ranch (**Tmrg**). Unit **Tmri** includes a lone exposure of platy- to blocky-jointed porphyritic trachydacite (SiO_2 = 67.78 weight percent; K_2O = 3.90 weight percent; FeO* = 3.92 weight percent; *n* = 1 analysis) with zones of rubbly basal flow breccia, cropping out above the 7.68 Ma rhyolite of Burns Butte (**Tmrg**) and below the 7.1 Ma Rattlesnake Tuff (**Tmtr**), along the east side of Willow Creek (**Figure 5-13**; **Table 5-2**; Plate 1).

Tmtwh **tuff of Wheeler Springs, non-welded lapilli tuff (upper Miocene)**—Semi-consolidated to consolidated, unwelded lithic-rich to lithic-poor rhyolitic lapilli-fall and lapilli-flow with minor intercalated ash-fall and ash-flow tuff and epiclastic rocks exposed between Burns Butte and U.S. Highway 20 (**Figure 5-25**; Plate 1; McClaughry and others, 2019). The unit directly underlies the rhyolite of Burns Butte (**Tmrb**), rhyolite of Golden Ranch (**Tmrg**), and basaltic trachyandesite and trachyandesite flows (**Tmat**) and vent deposits (**Tmvt**). **Tmtwh** directly overlies and is associated with a series of underlying welded tuffs (**Tmtw**) exposed south of Burns Butte; the unit sits above the intracaldera unit of the Prater Creek Ash-flow Tuff (**Tmtpi**) in the Federal 1-10 well (Plate 1, cross sections A-A′ and B-B′). The non-welded tuff of Wheeler Springs (**Tmtwh**) is well exposed in 10- to 50-m-high (33 to 164 ft) outcrops in borrow pits, where it is characterized by massive to well-bedded meter-scale subunits (**Figure 5-25**). **Tmtwh** is identified by an abundance of white (N9) inflated pumices up to 30 cm (12 in) across, fresh, black (N1) obsidian nodules up to 5 cm (2.1 in) across, and pebble- to boulder-sized, angular basaltic andesite to rhyolitic lithic fragments (**Figure 5-25**). Both the non-welded and welded phases of the tuff of Wheeler Springs (**Tmtw**, **Tmtwh**) are restricted in distribution east of Willow Creek (Plate 1, cross section B-B′).

Pumices sampled from this unit in the Burns 7.5′ quadrangle have rhyolitic compositions with 73.04 to 74.25 weight percent SiO_2 and 4.71 to 5.75 weight percent K_2O (McClaughry and others, 2019; *n* = 5 analyses). The unit is chemically indistinguishable from the underlying welded phases of the tuff of Wheeler Springs (**Tmtw**). Chemical composition of pumices in the non-welded part of the tuff of Wheeler Springs (**Tmtwh**) and welded tuff (**Tmtw**) are also indistinguishable from whole-rock XRF analyses obtained from the overlying rhyolite of Burns Butte (**Tmrb**). Together, both non-welded and welded phases of the tuff of Wheeler Springs (**Tmtw**, **Tmtwh**) are chemically similar to the younger Rattlesnake Tuff (**Tmtr**) but are differentiated from the Rattlesnake Tuff (**Tmtr**) on the basis of their lower SiO_2, higher Al_2O_3, higher Sr, lower Y, and higher Rb (McClaughry and others, 2019).

The tuff of Wheeler Springs, non-welded lapilli tuff (**Tmtwh**) is assigned a late Miocene age on the basis of stratigraphic position above the 8.52 Ma intracaldera unit of the Prater Creek Ash-flow Tuff (**Tmtpi**) and below the 8.46 Ma rhyolite of Golden Ranch (**Tmrg**) and the 7.68 Ma rhyolite of Burns Butte (**Tmrb**) (Plate 1). The unit is used widely as a source of construction aggregate and crushed stone in the map area and can be mapped partially on the basis of prospect pits and mine excavations (Plate 1; McClaughry and others, 2020). Equivalent to Tmlh (Hotchkiss lapilli member of the tuff of Wheeler Springs) of Brown (1982).

Figure 5-25. The tuff of Wheeler Springs, non-welded lapilli tuff (Tmtwh) exposed in a gravel pit off of the Hines Logging Road in the west-central part of the map area (43.55894, −119.13685 WGS84 geographic coordinates; 4825250mN, 330428mE WGS84 UTM Zone 11 coordinates). (A) Massively bedded pumice lapilli tuff containing blocks of white (N9) inflated pumice up to 10 to 15 cm (4 to 6 in) across and scattered fresh black (N1) obsidian clasts. Scale bar is 0.5 m (1.6 ft) high. View is looking northwest. (B) Close-up photo of the outcrop in (A) showing fragmented black (N1) perlitic obsidian clasts. View is looking northwest. Scale bar is 5 cm (2 in) high. Photo credits: Carlie J.M. Duda, 2019.

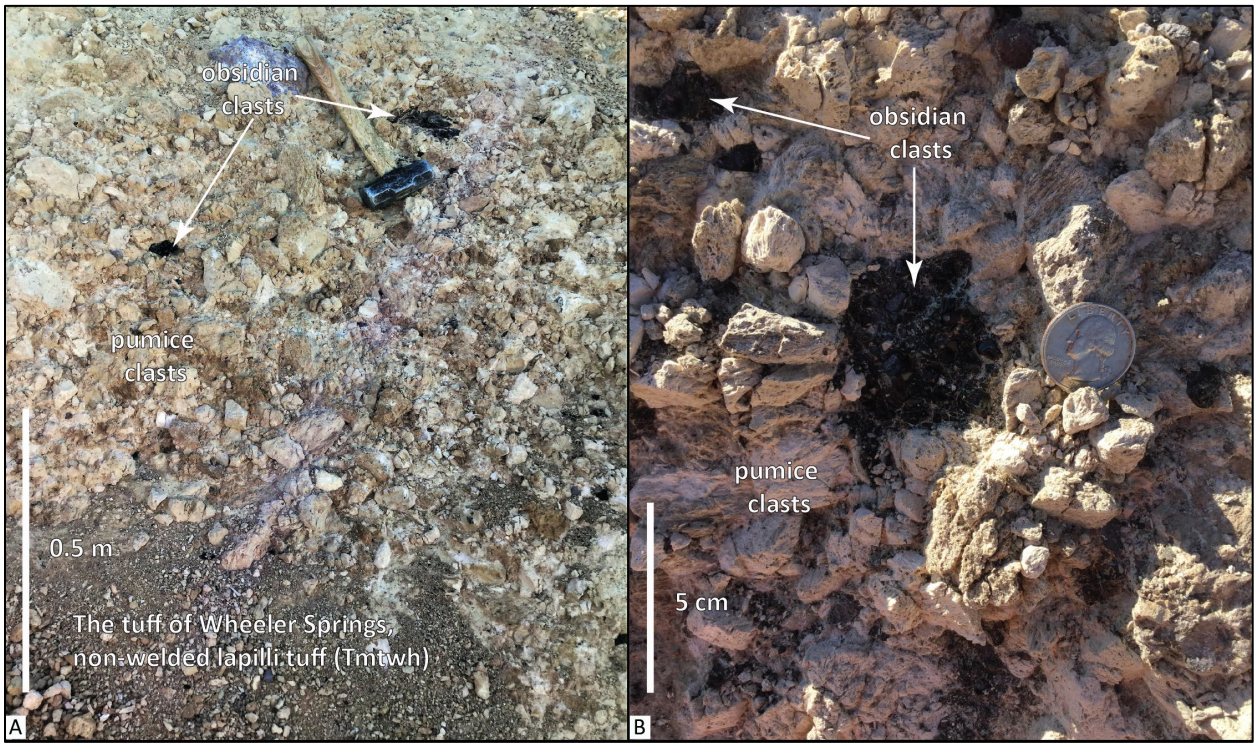

Tmtw **tuff of Wheeler Springs, welded tuff (upper Miocene)**—Sequence of devitrified, aphyric, crystal-vitric rhyolitic (SiO_2 = 73.47 to 76.86 weight percent; K_2O = 4.93 to 5.56 weight percent; *n* = 7 analyses; Appendix) welded ash-flow tuffs exposed between Burns Butte and U.S. Highway 20 in the southeast part of the Burns Butte 7.5′ quadrangle and Burns 7.5′ quadrangle (McClaughry and others, 2019) (Plate 1; **Figure 5-7**, **Figure 5-9**, **Table 5-2**). Brown (1982) subdivided the welded part of the tuff of Wheeler Springs (**Tmtw**) into five mappable units on the basis of lithologic criteria. We do not distinguish the units of Brown (1982) here as 1) key outcrops likely observed by Brown (1982) are on private ground closed to entry and 2) several geochemical analyses obtained from accessible outcrops of subdivided members are indistinguishable.

The unit is typically preserved in bench-forming outcrops ranging from 5 to 30 m (16.4 to 98.4 ft) high in the Burns Butte and Burns 7.5′ quadrangles (**Figure 5-26**; Plate 1; McClaughry and others, 2019, Plate 1). Outcrops show a range of welding facies from strongly welded devitrified tuff to highly expanded vitric tuff. Black hydrated obsidian in the groundmass is common in vitric zones. Locally, highly expanded areas show significant vapor-phase alteration of groundmass and pumice. In some cases, pumice has been completely altered to masses of crystobalite.

Typical hand samples of the tuff are moderate orange pink (10R 7/4), aphyric, and strongly welded, with pumice fiamme up to several centimeters (**Figure 5-27a**). Petrographically, the

welded tuff of Wheeler Springs (**Tmtw**) is devitrified, characterized by well-developed vitroclastic texture with moderately preserved, cuspate glass shards to variably altered glass shards and pumice fiamme overgrown and replaced by fibrous cryptocrystalline quartz and radiating growths of quartz and feldspar (axiolites) (**Figure 5-27b-c**). Thin sections typically contain scattered prismatic alkali feldspar crystals < 1 mm (0.02 in) long and flow-banded black-brown obsidian lithics.

The tuff of Wheeler Springs, welded tuff (**Tmtw**) is assigned a late Miocene age on the basis of stratigraphic position above the 8.52 Ma intracaldera unit of the Prater Creek Ash-flow Tuff (**Tmtpi**) and below the 8.46 Ma rhyolite of Golden Ranch (**Tmrg**) and the 7.68 Ma rhyolite of Burns Butte (**Tmrb**) (Plate 1). Equivalent to the tuff of Wheeler Springs (units Tmta, Tmtm, Tmtn, and Tmts) of Brown (1982).

Figure 5-26. Welded tuff of Wheeler Springs (Tmtw). Blocky-jointed outcrop of strongly welded, devitrified tuff exposed east-southeast of Burns Butte in the Burns Butte 7.5' quadrangle (43.54862, −119.13982 WGS84 geographic coordinates; 4823965mN, 327144mE, WGS84 UTM Zone 11 coordinates). Scale bar is 1 m (3.3 ft) high. View is looking north. Photo credit: Carlie J.M. Duda, 2019.

Figure 5-27. Hand sample and thin section photographs showing the welded tuff of Wheeler Springs (Tmtw). (A) Strongly welded tuff, containing pumice fiamme, sample 66 BRHC 18 (43.55670, −119.12275 WGS84 geographic coordinates; 328546mE, 4824827mN WGS84 UTM Zone 11 coordinates). Scale bar in photo A is 2.5 cm (1 in) high. (B) Photomicrograph of sample 66 BRHC 18 under cross-polarized light showing a mixture of microphenocrysts of alkali feldspar and an obsidian lithic in a groundmass of relict cuspate glass shards. (C) Same view as photo B, under plane-polarized light. Scale bar in photos B and C is 1 mm (0.04 in) in length. Abbreviation: af – alkali feldspar. Photo credits: Carlie J.M. Duda, 2019.

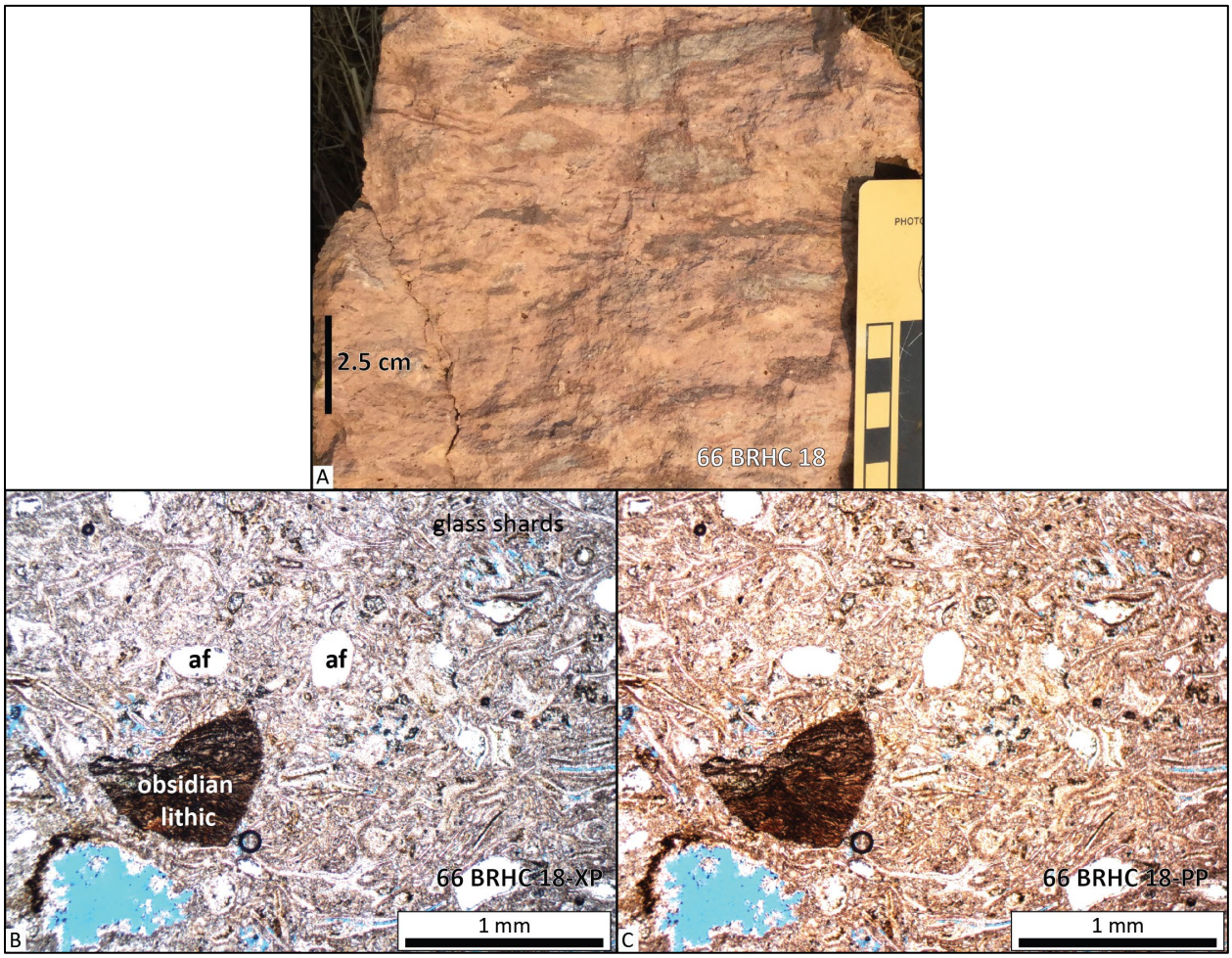

Tmatl **basaltic trachyandesite, trachyandesite, trachydacite flows and dikes (upper Miocene) (cross section only)**—Cryptic subsurface volcanic sequence of basaltic trachyandesite, trachyandesite, and trachydacite flows and intrusions(?) recognized from cuttings obtained from the Federal 1-10 exploration well between the 250 m (820 ft) and 899 m (2,950 ft) depth intervals (Plate 1). The unit lies stratigraphically below the tuff of Wheeler Springs (**Tmtwh**) and above the intracaldera unit of the Prater Creek Ash-flow Tuff (**Tmtpi**) in the Federal 1-10 well. The volcanic sequence is not exposed at the surface. On the basis of detailed lithologic inspection and interpretation, combined with geochemical analyses on cuttings from multiple intervals (e.g., 820 ft, 940 ft, 1,240 ft, 1,330 ft, 1,480 ft, 1,810 ft, 1,960 ft, 2,200 ft, 2,290 ft, 2,470 ft, 2,830 ft), the unit consists of the following subunits (**Figure 5-7**, **Figure 5-9**, **Table 5-2**; Appendix):

- Medium gray (N5) to medium dark gray (N4) and light brownish gray (5YR 6/1) interbedded basaltic trachyandesite lavas, with SiO_2 contents between 55.71 and 55.81 weight percent (*n* = 2 analyses) make up the section from 250 m (820 ft) to 332 m (1,090 ft). Lavas are separated by thin white (N9) tuffaceous and pale red (5R 6/2) mafic scoria interbeds.
- Mafic basaltic trachyandesite flows are underlain by a sequence of dark gray (N3) to very light gray (N8) to medium light gray (N6) trachyandesite flows extending from the depth interval of 332 m (1,090 ft) downward to 552 m (1,810 ft). The upper part of the trachyandesite flow sequence is marked by an ~27-m-thick (90 ft) interval of pale red (5R 6/2) aphyric, vesicular cinders. Analyzed cuttings from dense flow interiors at the 378, 405, and 451 m (1240, 1330, and 1,480 ft) depth intervals have trachyandesite chemical compositions characterized by SiO_2 contents from 56.88 to 58.91 weight percent (*n* = 3 analyses). The lowest interval (543 to 552 m [1,780 to 1,810 ft]) of the trachyandesite sequence includes light brownish gray (5YR 6/1) tuff fragments.
- The lower 348 m (1,140 ft) of the **Tmatl** section from 552 m (1,810 ft) down to ~899 m (2,950 ft) consists of an interbedded section of porphyritic trachydacite, basaltic trachyandesite, and trachyandesite. Analyzed samples from depth intervals of 552 m (1,810 ft), 598 m (1,960 ft), 753 m (2,470 ft), and 817 m (2,680 ft) are light brownish gray (5YR 6/1) to medium gray (N5) and medium dark gray (N4) holocrystalline porphyritic to aphyric trachydacite with SiO_2 contents from 64.69 to 68.28 weight percent (*n* = 4 analyses). Horizons at depths of 671 m (2,200 ft) and 698 (2,290 ft) are medium dark gray (N4) aphyric, holocrystalline basaltic trachyandesite with SiO_2 contents between 54.94 and 55.16 weight percent (*n* = 2 analyses). The base of the **Tmatl** section at the 899 m (2,950 ft) depth interval is a medium dark gray (N4), aphyric, holocrystalline trachyandesite with 59.51 weight percent SiO_2 (*n* = 1 analysis).
- The entire **Tmatl** section conspicuously lacks interbedded sedimentary rocks.

The unit is assigned a late Miocene age on the basis of stratigraphic position above the 8.52 Ma intracaldera unit of the Prater Creek Ash-flow Tuff (**Tmtpi**) and below the tuff of Wheeler Springs (**Tmtwh**) and 8.46 Ma rhyolite of Golden Ranch (**Tmrg**) (Plate 1).

Tmtp **Prater Creek Ash-flow Tuff (upper Miocene)**—Devitrified, welded, lithophysal, crystal-poor rhyolitic (SiO_2 = 76.55 to 77.10 weight percent; K_2O = 4.51 to 4.69 weight percent; *n* = 59 analyses in the Harney Basin) ash-flow tuff crops out in two isolated exposures between Burns Butte and Rimrock Springs, east of Willow Creek Flats (Plate 1; **Figure 5-7**, **Figure 5-9**, **Figure 5-28**; **Table 5-2**; Appendix). The two isolated exposures of Prater Creek Ash-flow Tuff (**Tmtp**) in the map area both lie beneath younger vent deposits of unit (**Tmvt**) and are now exposed through erosional windows projecting through the covering unit (Plate 1). The older 8.48/8.41 Ma Prater Creek Ash-flow Tuff (**Tmtp**) in the northern exposure near Willow Creek Flats gives the impression of lying out of stratigraphic sequence, appearing stratigraphically above the younger 7.68 Ma rhyolite of Burns Butte (**Tmrb**). The precise stratigraphic relationship between the two units is ambiguous in the northern exposure, as thick colluvium (**Qc**) obscures the contact (**Figure 5-2**). The southern exposure south of Rimrock Spring is more informative, as mapped vertical contacts between the Prater Creek Ash-flow Tuff (**Tmtp**) and the rhyolite of Burns Butte (**Tmrb**) indicate a relationship of the younger rhyolite intruding the older tuff (Plate 1). An intrusive relationship between the two units implies that the isolated and apparently stratigraphically high exposures of Prater Creek Ash-flow Tuff (**Tmtp**) are likely roof pendants of the older rock, uplifted during emplacement of extensive Burns Butte rhyolite (**Tmrb**) domes at 7.68 Ma.

Typical fresh hand samples of the Prater Creek Ash-flow Tuff (**Tmtpi**) in the map area are pale blue (5PB 7/2), pinkish gray (5YR 8/1), light brown (5YR 5/2), to moderate reddish brown (10R 4/6) when weathered. The tuff contains < 1 percent (vol.) crystal fragments of sanidine and quartz ≤0.5 mm (<0.01 in) in a devitrified glass-shard groundmass (**Figure 5-29a-d**). The strongly welded, devitrified tuff commonly exhibits a distinctive spotted appearance. Locally, the tuff is zeolitized.

The Prater Creek Ash-flow Tuff (**Tmtp**) is assigned a late Miocene age on the basis of stratigraphic position and isotopic ages. Jordan and others (2004) reported an $^{40}Ar/^{39}Ar$ isochron age of 8.41 ± 0.16 Ma and $^{40}Ar/^{39}Ar$ plateau and integrated ages of 8.46 ± 0.09 Ma (matrix; sample PC-1). Streck and others (1999) reported a similar $^{40}Ar/^{39}Ar$ age of 8.48 ± 0.05 Ma (devitrified whole rock) for the Prater Creek Ash-flow Tuff (**Tmtp**), obtained from unpublished data of A.L. Deino and A.L. Grunder. The tuff was informally named the welded tuff of Prater Creek by Greene (1972) and Greene and others (1972) and was formally recognized as the Prater Creek Ash-flow Tuff by Walker (1979). Unit **Tmtp** is partly equivalent to Td (Danforth Formation) of Piper and others (1939) and (silicic ash-flow tuff) of Walker (1977). Equivalent to Tmtp (Prater Creek Ash-flow Tuff) of Brown and others (1980a) and Brown (1982).

Figure 5-28. Lithophysal Prater Creek Ash-flow Tuff (Tmtp) exposed north of Radar Road, 6.1 km [3.8 mi] east of Federal 1-10 well (43.58856, –119.14429 WGS84 geographic coordinates; 4828410mN, 326898mE WGS84 UTM Zone 11 coordinates). View is looking northwest. Scale bar is 1 m (3.3 ft) high. Photo credit: Jason D. McClaughry, 2019.

Figure 5-29. Hand sample and thin section photographs showing the Prater Creek Ash-flow Tuff (Tmtp). (A) Hand sample of Prater Creek Tuff (Tmtp) from an outcrop west of the Silvies River in the Poison Creek 7.5′ quadrangle, sample 64 PCBJ 18 (43.66616, −119.11520 WGS84 geographic coordinates; 4836764mN, 329547mE WGS84 UTM Zone 11 coordinates) (McClaughry and others, 2019). (B) Hand sample of lithophysal Prater Creek Tuff (Tmtp) from the outcrop shown in Figure 5-27, sample 201 BBJ 19 (43.58856, −119.14429 WGS84 geographic coordinates; 4828410mN, 326898mE WGS84 UTM Zone 11 coordinates). Scale bar in (A) and (B) is 2.5 cm (1 in) high. (C) Thin section of sample 201 BBJ 19 under cross-polarized light. (D) Same view as (C), under plane-polarized light. Scale bar in (C) and (D) is 1 mm (0.04 in) in length. Abbreviation: af – alkali feldspar. Photo credits: Jason D. McClaughry, 2018, 2019.

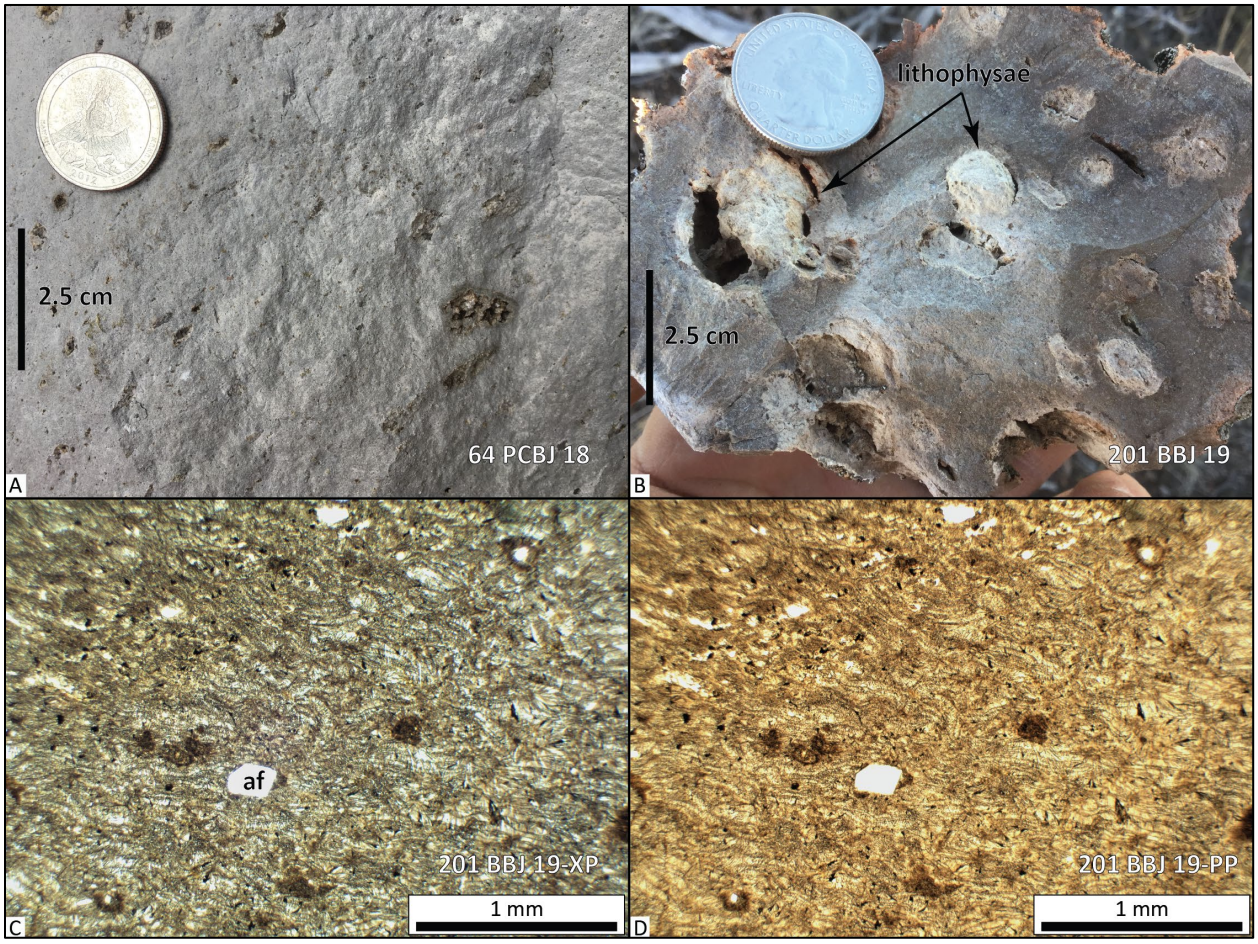

Tmtpi **Prater Creek Ash-flow Tuff, intracaldera unit (upper Miocene) (cross section only)**—Dusky yellow green (5GY 5/2) to light olive gray (5Y 5/2), fine-grained rhyolite tuff recovered from the Federal 1-10 well in the Burns Butte 7.5′ quadrangle (Plate 1, cross sections) and the CTI well in the Burns 7.5′ quadrangle (**Figure 5-30a,b**, **Table 2-1**; Appendix; McClaughry and others, 2019). The tuff is known only from drill cuttings and is not exposed at the surface. Unit **Tmtpi**, as defined here, forms a lithologically and geochemically monotonous interval exceeding 427 m (1,400 ft) in the Federal 1-10 well and >429 m (>1,406 ft) in the CTI well. The base of unit **Tmtpi** was not encountered in the CTI well; it may be of considerably greater thickness in that area.

The top of **Tmtpi** lies at an elevation of ~561 m (1,840 ft) above sea level (asl) in the Federal 1-10 well and at ~ 1,097 m (3,598 ft) asl in the CTI well. The **Tmtpi** sequence in the Federal 1-10

well is overlain by an ~762 m (2,130 ft) sequence of basaltic trachyandesite, trachyandesite, and trachydacite dacite **(Tmatl)**. Near the top of the mafic sequence, flows are overlain by an ~37 m (~120 ft) thick non-welded ash-flow tuff unit, correlative to the tuff of Wheeler Springs, non-welded lapilli tuff (**Tmtwh**). The upper part of the mafic sequence above the Wheeler Springs Tuff is correlative with basaltic trachyandesite and trachyandesite flows **(Tmat)**, widely exposed in the map area, beneath the Rattlesnake Tuff **(Tmtr)**. The uppermost part of the Federal 1-10 well was spudded into Rattlesnake Tuff (**Tmtr**). The base of the **Tmtpi** sequence in the Federal 1-10 well lies at an elevation of ~1,228 m (4,030 ft) asl, overlying a >1,114-m-thick (3,654 ft) section of geochemically variable rhyolite intrusions. In the CTI well, the **Tmtpi** sequence is directly overlain by ~61 m (200 ft) of silicic tuff correlated with the tuff of Wheeler Springs (**Tmtw**, **Tmtwh**), ~43 m (140 ft) of basaltic trachyandesite **(Tmat)**, and Rattlesnake Tuff (**Tmtr**).

Grain mount thin sections of cuttings from **Tmtpi** in both the Federal 1-10 and CTI wells are dominated by fragments of silicic tuff where former glass shards and pumice have been recrystallized to radiating intergrowths or quartz and alkali feldspar forming a pervasive granophyric texture (**Figure 5-30c–f**). Granophyric overgrowths are arranged about sparse remnant euhedral to subhedral alkali feldspar crystals. Sparse lithics of plagioclase-pyroxene andesite are scattered through the thin sections. Magnetic grain separation indicates that the intervals studied are ~95 percent (vol.) granophyric silicic tuff and ~5 percent (vol.) mafic lithics. Samples (n = 5) obtained from **Tmtpi** in the Federal 1-10 well, interval 899 to 1,320 m (2,950 to 4,330 ft), have a high-silica peraluminous rhyolitic composition with 75.44 to 78.15 weight percent SiO_2. The rhyolite tuff also contains 408 to 479 ppm Zr and 36.0 to 42.0 ppm Nb. Samples (n= 16) obtained from this unit in the CTI well, interval 152 m (500 ft) to 596 m (1956), have a high-silica peraluminous rhyolitic composition identical to the Federal Well with 75.37 to 77.40 weight percent SiO_2, 439 to 712 ppm Zr, and 35.8 to 47.5 ppm Nb (**Figure 5-7**, **Figure 5-9**, **Table 5-2**). Geochemical analyses from **Tmtpi** in the lower parts of the CTI and Federal 1-10 wells are indistinguishable from analyses obtained from surface outcrops of the wide-ranging Prater Creek Ash-flow Tuff (**Tmtp**) (**Figure 2-3**, **Figure 5-7**, **Figure 5-9**, **Table 5-2**).

The Prater Creek Ash-flow Tuff, intracaldera unit (**Tmtpi**) is assigned a late Miocene age on the basis of stratigraphic position and an $^{40}Ar/^{39}Ar$ plateau age of 8.52 ± 0.02 Ma (groundmass; sample F-1-10-3040) obtained from cuttings at the 927 m (3,040 ft) depth interval of the Federal 1-10 well (**Figure 5-31**). **Tmtpi** is considered the intracaldera tuff equivalent to the outflow unit forming the 8.48/8.41 Ma Prater Creek Ash-flow Tuff (**Tmtp**).

Figure 5-30. Representative cuttings and grain-mount thin sections from the Federal 1-10 and CTI wells. (A) Cuttings sample of silicic tuff from the 926 m (3,040 ft) depth interval of the Federal 1-10 well. This interval of the Federal 1-10 well has an $^{40}Ar/^{39}Ar$ plateau age of 8.52 ± 0.02 Ma. (B) Cuttings sample of silicic tuff from the 308 to 311 m (1,010 to 1,020 ft) depth interval of the CTI well. (C) Federal 1-10 grain mount thin section under cross-polarized light. Sample number F-1-10-3040. (D) Same view as (C), under plane-polarized light. (E) CTI well grain mount thin section under cross-polarized light. Sample number HARN 50087-1010-1020. (F) Same view as (E), under plane-polarized light. Scale bar is 1 mm (0.04 in) in length in photos C–F. Thin sections show grains of fine-grained tuff with granophyric textures and sparse lithics of andesite. Granophyric textures are related to slow cooling and crystallization of formerly glassy components (glass shards and pumice) in the central parts of very thick, densely welded ignimbrites (McPhie and others, 1993). Photo credits: (A–F) Jason D. McClaughry, 2019.

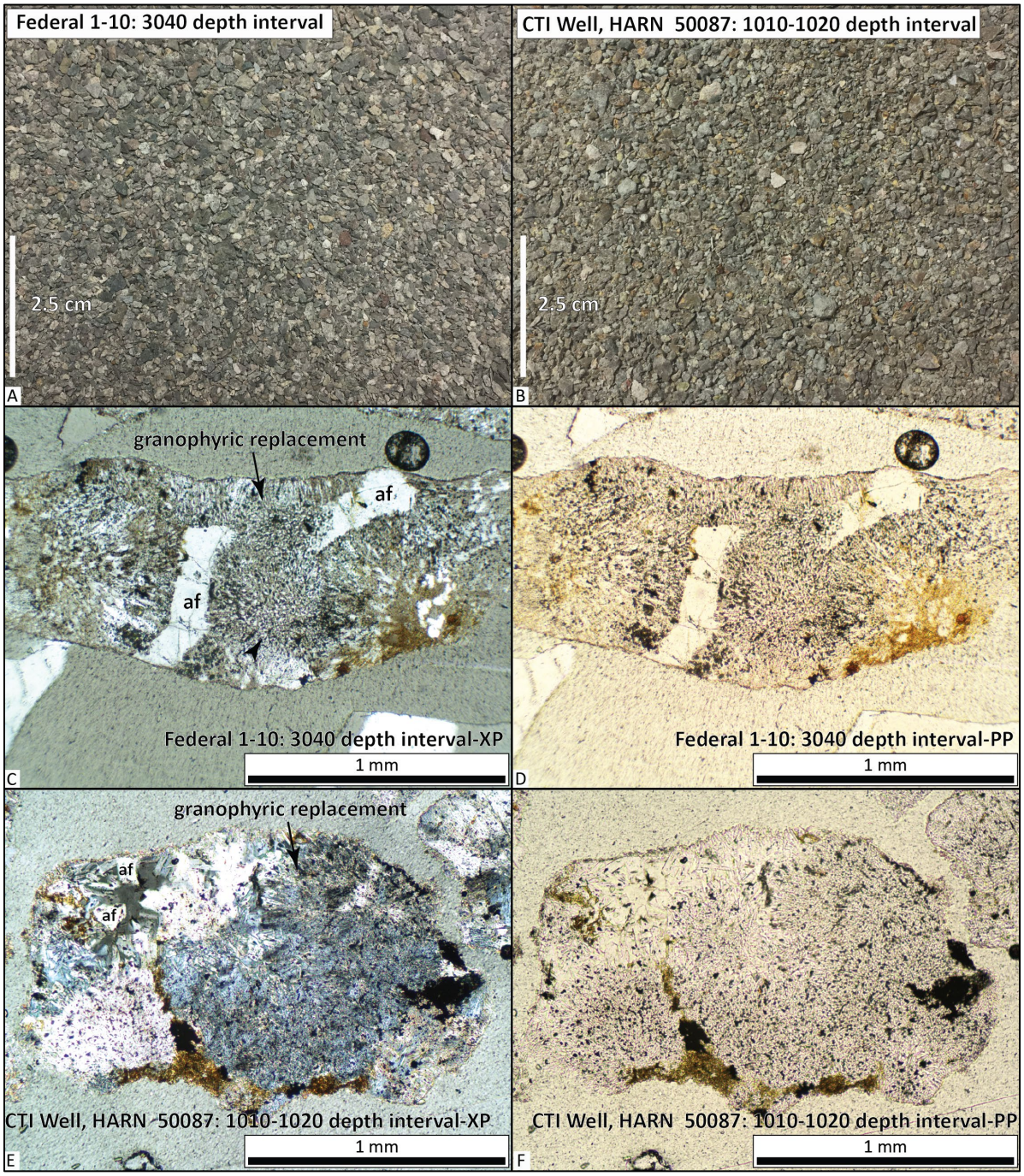

Figure 5-31. Analytical data for $^{40}Ar/^{39}Ar$ ages obtained from the intracaldera unit of the Prater Creek Ash-Flow Tuff (Tmtpi). See appendix folder, spreadsheets, subfolder NEW_$^{40}Ar^{39}Ar$_ANALYTICALDATA for complete analytical data.

Information on Analysis and Constants Used in Calculations

Project = **MCCLAUGHRY (19-20)**
Sample = **F-1-10-3040**
Material = **Groundmass**
Location = **Burns Butte**
Region = **Harney Basin**
Analyst = **Dan Miggins**
Irradiation = **20-OSU-04 (4B7-20)**
Position = **X: 0 | Y: 0 | Z/H: 8.393235 mm**
FCT-NM Age = **28.201 ± 0.023 Ma**
FCT-NM Reference = **Kuiper et al (2008)**
FCT-NM 40Ar/39Ar Ratio = **9.34095 ± 0.00448**
FCT-NM J-value = **0.00166209 ± 0.00000080**
Air Shot 40Ar/36Ar = **298.9570 ± 0.3438**
Air Shot MDF = **0.99966758 ± 0.00038761 (LIN)**
Experiment Type = **Incremental Heating**
Extraction Method = **Bulk Laser Heating**
Heating = **64 sec**
Isolation = **6.12 min**
Instrument = **ARGUS-VI-F**
Preferred Age = **Mini Plateau**
Age Classification = **Crystallization Age**
IGSN = Undefined
Rock Class = Undefined
Lithology = Undefined
Lat-Lon = Undefined - Undefined
Age Equations = **Min et al. (2000)**
Negative Intensities = **Allowed**
Collector Calibrations = **36Ar**
Decay 40K = **5.463 ± 0.107 E-10 1/a**
Decay 39Ar = **2.940 ± 0.016 E-07 1/h**
Decay 37Ar = **8.230 ± 0.012 E-04 1/h**
Decay 36Cl = **2.257 ± 0.015 E-06 1/a**
Decay 40K(EC,β^+) = **0.580 ± 0.014 E-10 1/a**
Decay 40K(β^-) = **4.884 ± 0.099 E-10 1/a**
Atmospheric 40/36(a) = **296.40 ± 0.51**
Atmospheric 38/36(a) = **0.1885 ± 0.0003**
Production 39/37(ca) = **0.0006425 ± 0.0000059**
Production 38/37(ca) = **0.0001800 ± 0.0000173**
Production 36/37(ca) = **0.0002703 ± 0.0000005**
Production 40/39(k) = **0.000607 ± 0.000059**
Production 38/39(k) = **0.012077 ± 0.000011**
Production 36/38(cl) = **262.80 ± 1.71**
Scaling Ratio K/Ca = **0.430**
Abundance Ratio 40K/K = **1.1700 ± 0.0100 E-04**
Atomic Weight K = **39.0983 ± 0.0001 g**

Subatmospheric Initial 40Ar/36Ar = 296.40 ± 0.17 (%SD).

Results	40(a)/36(a) ± 2σ	40(r)/39(k) ± 2σ	Age ± 2σ (Ma)	MSWD	39Ar(k) (%,n)	K/Ca ± 2σ
Age Plateau		2.80771 ± 0.00566	**8.52 ± 0.02**	1.82	30.43	4.70 ± 0.31
		± 0.20%	**± 0.22%**	5%	11	
		Full External Error ± 0.44		1.89	2σ Confidence Limit	
		Analytical Error ± 0.02		1.3506	Error Magnification	
Total Fusion Age		2.74809 ± 0.00283	**8.34 ± 0.01**		29	4.55 ± 0.00
		± 0.10%	**± 0.14%**			
		Full External Error ± 0.43				
		Analytical Error ± 0.01				
Normal Isochron	**296.44 ± 1.03**	2.80751 ± 0.00763	**8.52 ± 0.02**	2.54	30.43	
Error Chron	**± 0.35%**	± 0.27%	**± 0.29%**	1%	11	
		Full External Error ± 0.44		1.94	2σ Confidence Limit	
		Analytical Error ± 0.02		1.5943	Error Magnification	
Inverse Isochron	**296.40 ± 1.03**	2.80805 ± 0.00766	**8.52 ± 0.02**	2.55	30.43	
Error Chron	**± 0.35%**	± 0.27%	**± 0.29%**	1%	11	
		Full External Error ± 0.44		1.94	2σ Confidence Limit	
		Analytical Error ± 0.02		1.5953	Error Magnification	
				76%	Spreading Factor	

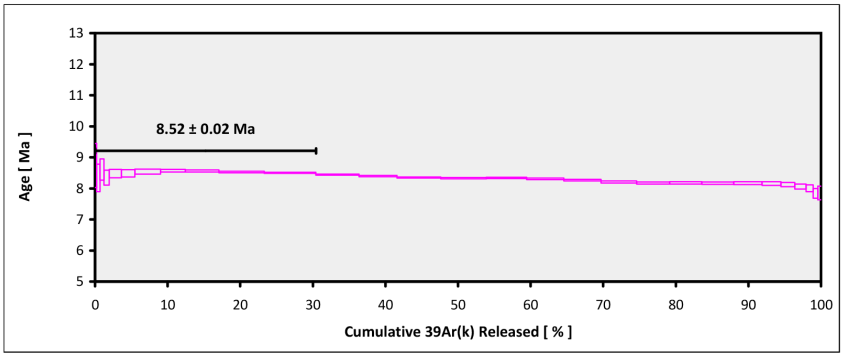

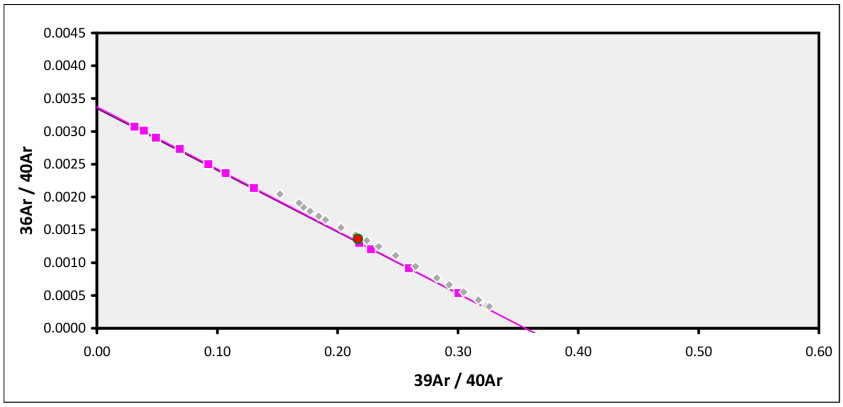

6.0 EXPLORATION WELLS

6.1 Introduction

Several deep wells have been drilled in the central and western parts of the Harney Basin, near the city of Burns, for the purposes of oil and gas exploration, geothermal testing, and groundwater monitoring (**Figure 6-1**, **Figure 6-2**; McClaughry and others, 2019). Cuttings retained for the Federal 1-10 and #1 Fay wells by DOGAMI and cuttings archived by OWRD for the CTI and HARN 52247 Eastern Oregon Agricultural Research Center (EOARC) wells provide direct and detailed evidence about subsurface stratigraphic relationships in this part of the western Harney Basin (**Figure 6-1**, **Figure 6-2**). Primary lithologic logs for other wells that do not have existing cuttings, like the Weed and Poteet #1 and Voglar #1 wells, can be reasonably, although not unequivocally, interpreted on the basis of knowledge of geologic relationships at the surface (**Figure 6-1**, **Figure 6-2**, McClaughry and others, 2019). **Table 2-1** shows a listing of exploration, test, and observation wells in this part of the Harney Basin. The following sections in this report describe well history and stratigraphic interpretations of both the Federal 1-10 and the CTI geothermal test wells; other exploration wells in the area were described in detail by McClaughry and others (2019). Additional information on these wells is available from DOGAMI and OWRD, and specific web links are provided in individual well descriptions below and in **Table 2-1**.

Figure 6-1. Locations of deep exploration wells in the west-central Harney Basin. Yellow circles are located oil and gas exploration, geothermal test, and groundwater observation wells. TD is total depth of well in feet (ft) and meters (m). Solid white line is the boundary of the Burns Butte 7.5′ quadrangle mapped during this study; B-B′ line is trend of B-B′ cross section on map plate. Black lines are the boundaries of the Poison Creek and Burns 7.5′ quadrangles (McClaughry and others, 2019). Dashed yellow line is the southernmost exposure-limit of Mesozoic rocks and the Devine Canyon Ash-flow Tuff; the area to the south is largely buried by Rattlesnake Tuff (Tmtr). Dashed white line is the concealed eastern margin of the Silvies River caldera. Basemap is an oblique Google Earth™ landscape image. View in the image is looking north. The Federal 1-10 and CTI wells are discussed in detail in this report. The reader is directed to McClaughry and others (2019) for additional discussion of the #1 Fay, Weed and Poteet #1 Voglar #1, and EOARC HARN 52747 wells. Labels are as follows – Mesozoic accreted terrane rocks (Jr), Oligocene rocks (O), Columbia River Basalt (CRB), Devine Canyon Ash-Flow Tuff (DC), Prater Creek Ash-Flow Tuff (PC).

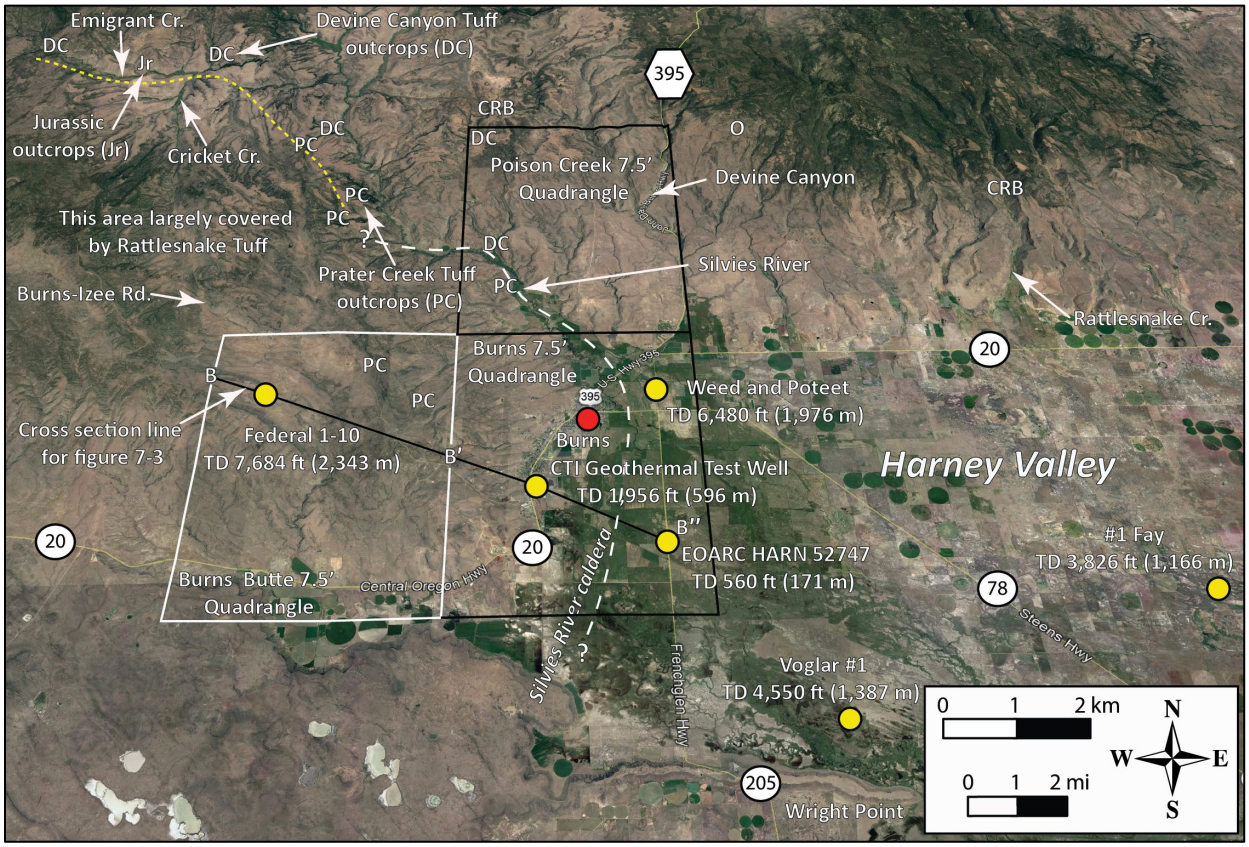

Figure 6-2. Interpreted stratigraphic logs for deep exploration wells in the west-central Harney Basin. Vertical scale bars show elevation and depth from collar of downhole intervals. Red-filled circles are stratigraphic horizons in exploration wells where XRF geochemical analyses have been obtained. Vertical red-dashed line separating the CTI and Weed and Poteet #1 wells is the concealed eastern margin of the Silvies River caldera as inferred by McClaughry and others (2019). The Federal 1-10 and CTI wells are discussed in detail in this report. The reader is directed to McClaughry and others (2019) for additional discussion of the #1 Fay and Weed and Poteet #1 wells.

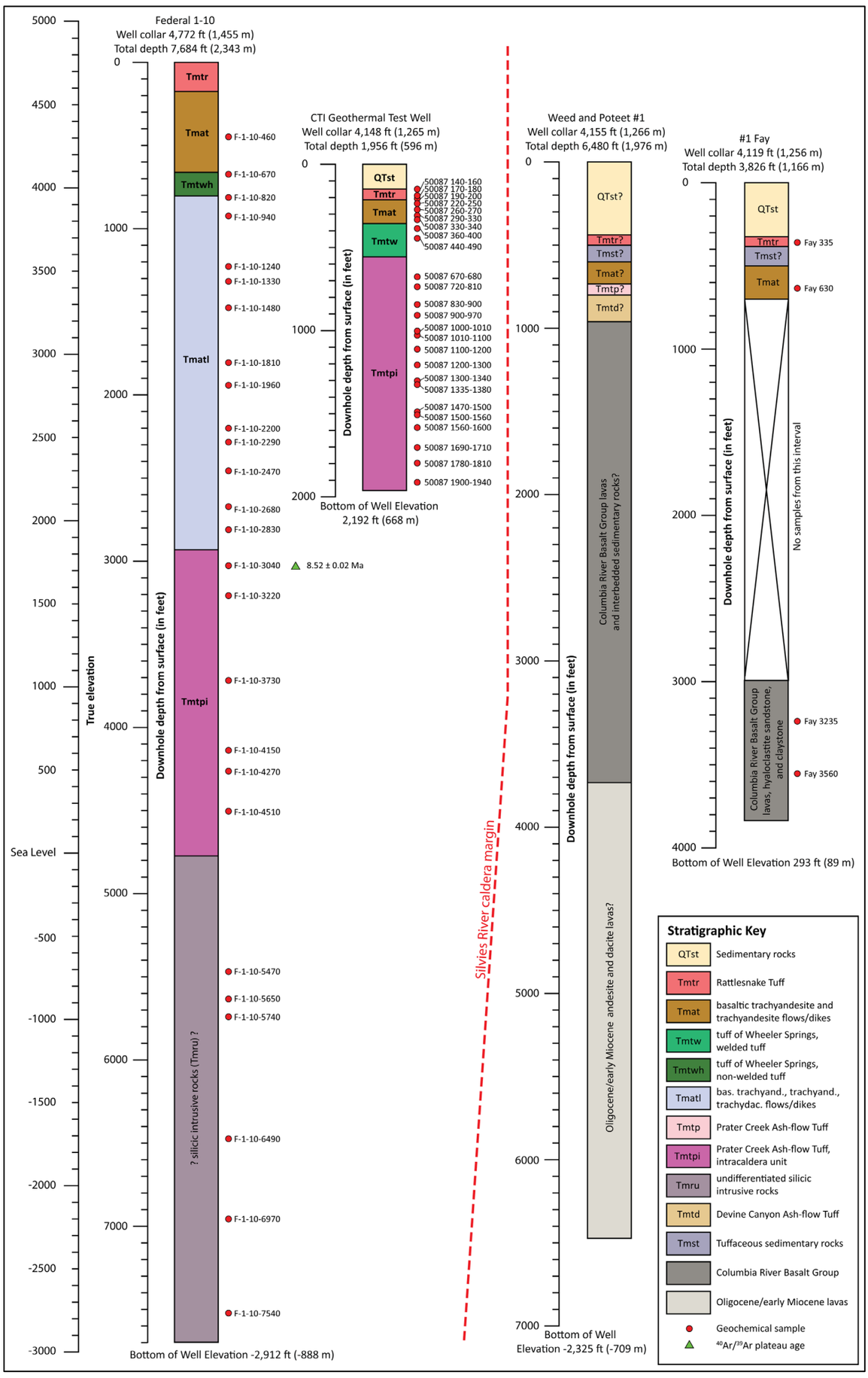

6.2 Michael T. Halbouty Federal 1-10 (HARN 52703)

The Michael T. Halbouty Federal 1-10 well was drilled by the Hunnicut and Camp Drilling Company ~13.5 km (~8.5 mi) west of Burns between June and September 1977 (Plate 1; **Table 2-1**; **Figure 2-3**, **Figure 6-1**, **Figure 6-2**). Total depth of the well is 2,343 m (7,684 ft). Elevation of the well collar is 1,455 m (4,772 ft, lidar) (Plate 1). Cuttings in DOGAMI archives exist for the depth interval between 131 m (430 ft) and 2,326 m (7,630 ft) below land surface. Available data from DOGAMI and OWRD include the notice of intention to drill new well, drilling proposal, application for permit to drill new well or stratigraphic hole, plat of a survey for a proposed oil well drilling site, history of oil or gas well, log and core record of oil or gas well, mud log, dip meter log, temperature-depth log, sundry notices, spontaneous potential/ conduction/resistivity logs, compensated neutron-formation density logs, and plugging record. Original log and core records report a section of undifferentiated Tertiary volcanics, including basalts, andesites, and tuffs. We reexamined the cuttings of the Federal 1-10 well and analyzed 26 stratigraphic intervals for major and trace element XRF geochemistry (**Figure 5-7**, **Figure 5-9**, **Figure 6-2**, **Table 5-2**; Appendix; McClaughry and others, 2019). Additionally. we obtained an $^{40}Ar/^{39}Ar$ age for the depth interval 927 m (3040 ft) (Appendix).

The Federal 1-10 well was spudded in Rattlesnake Tuff (**Tmtr**) and penetrated 2,343 m (7,684 ft) of volcanic rock (**Figure 6-2**; Appendix). The uppermost 140 m (460 ft) is unlogged and no cuttings exist from this section; stratigraphy through this part of the well is presumed to include Rattlesnake Tuff (**Tmtr**) and basaltic trachyandesite and trachyandesite lava flows (**Tmat**), equivalent to those units exposed at the surface.

Cuttings begin at a depth of 131 m (430 ft), where the borehole penetrated two mafic to intermediate lavas (**Tmat**), directly underlying the Rattlesnake Tuff (**Tmtr**) (**Figure 6-2**; Appendix). The uppermost sampled flow in the sequence (140 m [460 ft] interval) is a medium gray (N5) to medium dark gray (N4) aphyric basaltic trachyandesite with 54.48 weight percent SiO_2, 1.34 weight percent TiO_2, 698 ppm Ba, 128 ppm Zr, 9.1 ppm Nb, 20 ppm La, and 46 ppm Ce (**Table 5-2**; Appendix). Major and trace element abundances closely resemble lavas (**Tmat**) exposed at the surface directly below the Rattlesnake Tuff (**Tmtr**) in the area between Halfway Reservoir Flat Road and Willow Creek Flats and to flows exposed beneath the Rattlesnake Tuff (**Tmtr**) along Cricket Creek (Sample 37-BF-15), 16.6 km (10.3 mi) north-northeast of the Federal 1-10 well (Plate 1; **Figure 6-2**).

Mafic lavas (**Tmat**) extend downward to a depth of 195 m (640 ft) where they directly overlie a moderate reddish brown (10R 4/6) pumice tuff with very sparse feldspar microphenocrysts (**Figure 6-2**; Appendix). This horizon constitutes the upper part of an ~55 m thick (180 ft), non-welded, pumice tuff and obsidian-clast vitric ash-flow tuff that extends downward to a depth of 250 m (820 ft) depth. The ash-flow tuff sequence is distinguished by a conspicuous abundance of very fresh clear glass shards, black (N1) obsidian nodules, and medium gray (N5) to medium dark gray (N4) stony rhyolite fragments. Analyzed cuttings from the 204 to 213 m (670 to 700 ft) interval show the tuff to be a peraluminous rhyolite correlative with the non-welded phase of the tuff of Wheeler Springs (**Tmtwh**), with 73.86 weight percent SiO_2, 227 ppm Zr, 25.2 ppm Nb, 36 ppm La, and 76 ppm Ce (**Table 5-2**; Appendix).

Below the tuff of Wheeler Springs (**Tmtwh**), at a depth of 250 m (820 ft), the Federal 1-10 borehole entered a series of medium gray (N5) to medium dark gray (N4) and light brownish gray (5YR 6/1) interbedded basaltic trachyandesite and trachyandesite lavas, separated by thin white (N9) tuffaceous and pale red (5R 6/2) mafic scoria interbeds (**Tmatl**) (**Figure 6-2**; Appendix). Flows of unit **Tmatl** are nowhere exposed at the surface. Analyzed cuttings from the 250 m (820 ft) and 287 m (940 ft) depth

intervals are basaltic trachyandesite with 55.71 to 55.81 weight percent SiO_2, 1.26 to 1.36 weight percent TiO_2, 793 to 844 ppm Ba, 163 to 177 ppm Zr, 12.3 to 13.6 ppm Nb, 25 to 27 ppm La, and 51 to 53 ppm Ce (appendix). More mafic basaltic trachyandesite flows are underlain by a sequence of trachyandesite flows extending from the depth interval of 332 m (1,090 ft) downward to 552 m (1,810 ft). The upper part of the trachyandesite flow sequence is marked by an ~27 m thick (90 ft) interval of pale red (5R 6/2) aphyric, vesicular cinders. Analyzed cuttings from dense flow interiors at the 378, 405, and 451 m (1,240, 1,330, and 1,480 ft) depth intervals have trachyandesite chemical compositions characterized by 56.88 to 58.91 weight percent SiO_2, 0.98 to 1.01 weight percent TiO_2, 866 to 931 ppm Ba, 157 to 187 ppm Zr, 10.1 to 12.1 ppm Nb, 23 to 29 ppm La, and 52 to 54 ppm Ce (**Table 5-2**; Appendix). The lowest interval (543 to 552 m [1,780 to 1,810 ft]) of the trachyandesite sequence includes light brownish gray (5YR 6/1) tuff fragments.

The lower 348 m (1,140 ft) of the **Tmatl** section in the Federal 1-10, from 552 m (1,810 ft) down to ~899 m (2,950 ft), consists of an interbedded section of porphyritic trachydacite, basaltic trachyandesite, and trachyandesite (**Figure 6-2**; Appendix). Analyzed samples from depth intervals of 552 m (1,810 ft), 598 m (1,960 ft), 753 m (2,470 ft), and 817 m (2,680 ft) are light brownish gray (5YR 6/1) to medium gray (N5) and medium dark gray (N4) holocrystalline porphyritic to aphyric trachydacite with 64.69 to 68.28 weight percent SiO_2, 0.53 to 0.95 weight percent TiO_2, 995 to 1,061 ppm Ba, 154 to 345 ppm Zr, 22.1 to 24.9 ppm Nb, 29 to 35 ppm La, and 58 to 72 ppm Ce (**Table 5-2**; Appendix). Intervening horizons at depths of 671 m (2,200 ft) and 698 (2,290 ft) are medium dark gray (N4) aphyric, holocrystalline basaltic trachyandesite with 54.94 to 55.16 weight percent SiO_2, 1.12 weight percent TiO_2, 790 to 800 ppm Ba, 149 to 154 ppm Zr, 10.0 to 10.6 ppm Nb, 23 to 26 ppm La, and 48 to 55 ppm Ce (**Table 5-2**; Appendix). The base of the **Tmatl** section at the 863 m (2,830 ft) depth interval is a medium dark gray (N4), aphyric, holocrystalline trachyandesite with 59.51 weight percent SiO_2, 1.13 weight percent TiO_2, 882 ppm Ba, 238 ppm Zr, 17.8 ppm Nb, 27 ppm La, and 55 ppm Ce. The complete Federal 1-10 section from the top of the logged hole at 126 m (414 ft) to the base of the **Tmatl** section at 899 m (2,950 ft) conspicuously lacks interbedded sedimentary rocks.

The interval underlying **Tmatl** flows from 899 to 1,320 m (2,950 to 4,330 ft) consists of rhyolitic tuff, the top of which is defined by a banded rhyolite breccia (**Figure 6-2**; Appendix). Five analyzed samples over an interval extending from 927 to 1,320 m (3,040 to 4,330 ft) indicate a single, remarkably monotonous and homogenous tuff unit characterized chemically by 75.44 to 78.15 weight percent SiO_2, 408 to 479 ppm Zr, and 36.0 to 42.0 ppm Nb (**Table 5-2**; Appendix). Major and trace element abundances, particularly the Nb/Zr ratio, closely resemble those obtained from the Prater Creek Ash-flow Tuff (**Tmtp**) exposed and sampled widely across the Harney Basin (McClaughry and others, 2019; **Figure 5-7**, **Figure 5-9**, **Figure 6-2**, **Table 5-2**; Appendix). Grain mount thin sections of cuttings from this interval display granophyric textures, indicative of a devitrified densely welded rheomorphic tuff (**Figure 5-30**). A sample from the 927 m (3040 ft) depth interval has an $^{40}Ar/^{39}Ar$ plateau age of 8.52 ± 0.02 Ma (groundmass; sample F-1-10-3040; **Figure 5-31**). Cuttings from the underlying sequence that extends downward from 1,320 m (4,330 ft) to 1,448 m (4,750 ft) consist of fine-grained rheomorphic(?) crystal tuff displaying ghost vitroclastic textures, fiamme, and zones of lithophysae. Several horizons within this interval contain scattered sugary, fine-grained, holocrystalline, equigranular, olive gray (5Y 4/1) flow-banded rhyolite fragments and medium dark gray (N4) trachyandesite fragments. An analyzed sample of the tuff from the 1,375 m (4,510 ft) depth interval contains similar amounts of SiO_2 (77.00 weight percent) to the upper tuff section but lesser amounts of Zr (190 ppm) and Nb (32.5 ppm) (Appendix).

The underlying 895 m (2,934 ft) of the Federal 1-10 well section from 1,448 m (4,750 ft) down to the bottom of the hole at 2,343 m (7,684 ft) records a sequence of variably altered and compositionally diverse rhyolite to microgranitic intrusive complex (labeled as Tmru in the detailed well log) (**Figure 6-2**;

Appendix). The upper part of the rhyolite sequence from 1,448 to 1,567 m (4,750 to 5,140 ft) is relatively fresh, light brownish gray (5YR 6/1) to brownish gray (5YR 4/1) fine-grained, equigranular rhyolite or microgranite, with 2 to 3 percent clinopyroxene, intermixed with clear alkali feldspar and quartz. Below 1,567 m (5,140 ft) downward to 1,613 m (5,290 ft), the Federal 1-10 section transitions to white (N9) to very light gray (N8) and medium light gray (N6), variably altered, fine-grained, sugary, holocrystalline, equigranular rhyolite with quartz and K-feldspar. Clinopyroxene, conspicuous in the above interval, is rare in this section. Vapor phase sulfides are common in this interval. From 1,613 m (5,290 ft) down to 1,704 m (5,590 ft), the section continues through white (N9) to very light gray (N8) and medium light gray (N6), variably altered, fine-grained, sugary holocrystalline, equigranular rhyolite with 3 to 5 percent quartz and K-feldspar up to 1 mm, and occasional mica grains. A single analyzed sample from the 1,668 m (5,470 ft) depth interval consists of altered high-SiO_2 rhyolite with 84.29 weight percent SiO_2, 667 ppm Ba, 204 ppm Zr, 21.1 Nb, 30 ppm La, and 68 ppm Ce (Appendix).

The depth interval 1,704 m (5,590 ft) to 2,034 m (6,670 ft) consists of variably altered white (N9) to very light gray (N8) and medium light gray (N6), fine-grained, sugary holocrystalline rhyolite with 1 to 2 percent quartz and K-feldspar up to 1 mm (**Figure 6-2**; Appendix). Relict rhyolite textures, including flow banding, are common. An analyzed sample from the upper part of this section, at a depth interval of 1,723 m (5,650 ft), has a high-SiO_2 composition with 77.31 weight percent SiO_2, 88 ppm Ba, 657 ppm Zr, 44.3 ppm Nb, 77 ppm La, and 143 ppm Ce (Appendix). At a depth of 1,732 m (5,680 ft), the rhyolite section transitions from high-SiO_2/high-Ba to high-SiO_2/low-Ba rhyolite. The transition is imperceptible through examination of the cuttings but is recognized through several geochemical analyses across the boundary. Samples from the depth intervals 1,753 m (5,750 ft) and 1,979 m (6,490 ft) are compositionally high-SiO_2 rhyolite with 77.94 to 79.05 weight percent SiO_2, 238 to 273 ppm Zr, 1,468 to 1,490 ppm Ba, 31.4 to 34.0 ppm Nb, 43 to 45 ppm La, and 83 to 94 ppm Ce (Appendix). This high-SiO_2 rhyolite is distinguished from the upper rhyolites in this section by significantly higher Ba contents and less amounts of Zr.

The interval from 2,034 m (6,670 ft) down to the bottom of the hole at 2,343 m (7,684 ft) consists of white (N9) to very light gray (N8) and light gray (N7) fine-grained, sugary holocrystalline, equigranular rhyolite composed of <1 percent quartz, K-feldspar, and sparse clinopyroxene (**Figure 6-2**; Appendix). This section of the Federal 1-10 well is conspicuous for multiple intervals containing 10 to 30 percent white and black mica grains up to 3 mm (0.1 in) across. Analyzed samples from this section are compositionally low-SiO_2 rhyolite with 72.19 to 72.56 weight percent SiO_2, 107 to 554 ppm Zr, 35.3 to 46.8 ppm Nb, 11 to 42 ppm La, and 26 to 84 ppm Ce. Low-silica rhyolites, occurring in the deepest part of the Federal 1-10 well, also show a significant reduction in Ba content (383 to 386 ppm) as compared to high-SiO_2 (77.94 to 79.05 weight percent) and high-Ba (1,468 to 1,490 ppm) rhyolites occurring higher in the well at the 1,753 m (5,750 ft) and 1,979 m (6,490 ft) depth intervals (Appendix). The break between the high-SiO_2–high-Ba and low-SiO_2–low-Ba rhyolites occurs approximately at the 2,034 to 2,061 m (6,670 to 6,760 ft) depth interval, where grayish black (N2) holocrystalline trachyandesite is mixed with sparse medium light gray (N6) holocrystalline rhyolite and some pale yellowish orange (10YR 8/6) stony rhyolite(?).

Additional detailed information about this well is available from DOGAMI at https://www.oregongeology.org/mlrr/oilgas-logs.htm and from OWRD at https://apps.wrd.state.or.us/apps/gw/gw_info/gw_info_report/gw_details.aspx?gw_site_id=30493.

6.3 CTI Geothermal Test Well (HARN 50087)

The HARN 50087 CTI Geothermal Test Well was drilled at the old Edward Hines Lumber Company mill site at the south end of Hines between March and August 1996 (**Table 2-1**; **Figure 2-3**, **Figure 6-1**, **Figure**

6-2; Appendix). Total depth of the well is 596 m (1,956 ft). Elevation of the well collar is 1,265 m (4,148 ft, lidar). The primary purpose of the hole was exploration for geothermal water; it was situated to intersect a projected fault at depth. Cuttings for this well, at 3 m (10 ft) intervals, for well depth 43 to 596 m (140 to 1,956 ft) were archived by DOGAMI and OWRD. Available data from OWRD include the water supply well report, engineering schematics for the well, cuttings descriptions, and site photographs. We reexamined the cuttings of the CTI well and analyzed 25 stratigraphic intervals for major and trace element XRF geochemistry (**Figure 5-7**, **Figure 5-9**, **Figure 6-2**, **Table 5-2**; Appendix; McClaughry and others, 2019).

Cuttings begin at 43 m (140 ft), where the well penetrated a 6 m (20 ft) thick light brownish gray (5YR 6/1) welded ash-flow tuff with numerous lithic fragments and white feldspar crystals (**Figure 6-2**; Appendix). A single geochemical analysis from this interval shows the rock is altered, with very high loss on ignition (LOI) and low original analytical totals (Total_I). Trace element concentrations in the sample from this interval are similar to the Rattlesnake Tuff (**Tmtr**), but with lower Zr (206 ppm) and Nb (19.8) (see geochemical data in geodatabase and appendix). Samples between the depth interval of 48 and 64 m (160 and 210 ft) consist of a mixture of pinkish gray (5YR 8/1) to white (N9) semi-consolidated tuff and very pale orange (10YR 8/2) pumice. Two geochemical analyses from this interval have very high loss on ignition (LOI) and low original analytical totals (Total_I) and are therefore interpreted to have altered major element concentrations. Trace element concentrations of samples from this interval are comparable to the Rattlesnake Tuff (**Tmtr**) with 260 to 281 ppm Zr and 27.6 to 29.0 ppm Nb. Samples between the depth interval of 64 and 107 m (210 and 350 ft) are yellowish gray (5Y 8/1), medium gray (N6), and moderate orange pink (10R 7/4) to light brownish gray (5YR 6/1) dense basaltic trachyandesite and interbedded cinders. Analyzed fresh cuttings from this interval indicate a correlation with unit **Tmat** (basaltic trachyandesite and trachyandesite), with 56.37 to 57.10 weight percent SiO_2, 146 to 154 ppm Zr, and 10.3 to 10.7 ppm Nb. At 106 to 158 m (350 to 550 ft) the well intersects a 61 m (200 ft) thick section of very light gray (N8) to pinkish gray (5YR 8/12) strongly welded rheomorphic tuff with 73.47 to 75.25 weight percent SiO_2, 242 to 246 ppm Zr, and 27.3 to 29.8 ppm Nb. Geochemical analyses from this interval are identical to the tuff of Wheeler Springs (**Tmtw**) (**Figure 6-2**; Appendix). The interval from 168 to 596 m (550 to 1,956 ft) is lithologically homogeneous, but variably colored yellowish gray (5Y 8/1), pinkish gray (5YR 8/1), light brownish gray (5YR 6/1), medium light gray (N6), to dark gray (N3) rheomorphic ash-flow tuff. The tuff is grayish blue green (5BG 5/2) and dark reddish brown (10R 3/4) where altered. The top of the tuff is defined by a banded rhyolite breccia. Sixteen analyzed samples over this interval indicate a single, remarkably monotonous and homogenous unit with 75.37 to 77.40 weight percent SiO_2, 439 to 530 ppm Zr, and 35.8 to 44.0 ppm Nb. Major and trace element abundances closely resemble those in the Prater Creek Ash-flow Tuff (**Tmtp**) exposed widely across the Harney Basin (**Figure 2-3**, **Figure 5-7**, **Figure 5-9**, **Figure 6-2**, **Table 5-2**; Appendix; McClaughry and others, 2019). Like the Federal 1-10 well, grain mount thin sections of cuttings from this interval display granophyric textures (**Figure 5-30**). Three samples from the interval 515 to 591 m (1,690 to 1,940 ft) are lithologically identical and chemically similar to the above interval with 74.46 to 77.00 weight percent SiO_2 and 38.2 to 47.0 ppm Nb, but with slightly higher amounts of Zr (576 to 712 ppm) (Appendix). The intracaldera unit of the Prater Creek Ash-flow Tuff (**Tmtpi**) forms the base of the CTI well and may be of considerably greater thickness (**Figure 6-2**; Appendix).

Additional detailed information about this well is available from OWRD at https://apps.wrd.state.or.us/apps/gw/gw_info/gw_info_report/gw_details.aspx?gw_site_id=12735.

7.0 STRUCTURE

7.1 Introduction

Geologic structures in the Burns Butte 7.5′ quadrangle are recognized on the basis of offset between mapped geologic contacts, repeated sections, topographic lineaments (as observed in the field and in 1-m lidar DEMs, 10-m DEMs, and 2016 NAIP photographs), changes in bedding attitudes, alignment of springs, and subsurface lithologic data obtained from water and exploration wells (Plate 1). Primary structural features (e.g., slickensides or fault breccia) were not observed in the field area.

7.2 Structural setting

The Burns Butte 7.5′ quadrangle is located in the central part of the Harney Basin, at the eastern end of the High Lava Plains (HLP) of southeastern Oregon. The area is transitional between two structural fabrics preserved in the modern Harney Basin (**Figure 2-2**). Directly south of the map area, the Harney Basin is bisected by the regionally extensive Brothers Fault zone (BFZ), which separates the principal north-northeast-striking extensional faults of the Basin and Range Province (BRP) from the less extended terrain of the Blue Mountains Province (BMP) (**Figure 2-1**, **Figure 2-2**). The transition is manifested by a northward decrease in topographic and structural relief on fault-bounded range fronts, and an overall decrease northward in the amount of extension (Jordan and others, 2004; Meigs and others, 2009; Trench and others, 2012).

The BFZ is an ~40 km-wide (25 mi) diffuse zone of en echelon northwest-striking (~N. 40° W.) brittle faults, cutting ~250 km (155 mi) obliquely across the HLP (**Figure 2-1**; Walker, 1969). Individual fault strands within the BFZ are typically several kilometers long and closely spaced (1 to 2 km [0.6 to 1.2 mi]), with apparent normal offsets of ~10 to 100 m (32.8 to 328 ft) (Lawrence, 1976; Jordan and others, 2004). Vertical offset is usually in a down-on-the-northeast sense, down-dropping the Harney Basin and the region north of the BFZ down relative to the HLP (Lawrence, 1976; Trench, 2008). A smaller number of ~5- to 10-km-long (3.1 to 6.2 mi), ~N. 30° E.–striking fault strands shows mutually cross cutting relationships with the dominant northwest-striking faults (Lawrence, 1976; Johnson, 1995; Trench, 2008; Trench and others, 2012). Johnson (1995) and Johnson and Grunder (2000) indicated that both BRP and BFZ faults were active in the eastern HLP by ~10 m.y.a. Evidence presented by Trench (2008) and Iademarco (2009) suggested that the en echelon faults of the BFZ formed from ~7 to 5 Ma, concurrent with the peak of HLP volcanism after ~7.6 Ma (Millard, 2010). Walker and Nolf (1981) interpreted that displacement along a number of fault strands localized many basaltic and rhyolitic vents of late Miocene through Pleistocene age across the HLP.

The northern and eastern part of the Harney Basin is cut by a dominant set of steeply dipping, normal and normal oblique, north- and north-northwest-striking faults, and by a lesser number of north-striking and east-northeast–striking faults (**Figure 2-1**, **Figure 2-2**; Houston and others, 2018; Niewendorp and others, 2018). This deformation is responsible for the growth of extensional fault fabric along the northernmost part of the BRP, including development of the Crane Basin. Extensional fault fabric and associated depositional basins developed closely in space in time with heightened regional magmatic activity between ~15.5 to 9.63 Ma (Millard, 2010). In the Crane Basin, tectonic deformation ceased post-7.25 Ma (Millard, 2010).

Faulting and broad folding have tilted the rocks of the northern Harney Basin to the southwest. East of Poison Creek, in the Devine Ridge North and Devine Ridge South 7.5′ quadrangles, the south-dipping

section of ash-flow tuffs is cut by a predominant set of vertical to subvertical, north-striking dextral oblique strike-slip faults referred to as the Trout Creek and Soldier Creek fault zones, respectively (**Figure 2-1**, **Figure 2-2**; Houston and others, 2018; Niewendorp and others, 2018). Oblique strike-slip faults in the Trout Creek and Soldier Creek fault zones have a dominant down-on-the-west offset, with imbricate fault splays along narrow zones, leading to the duplexing of strata into negative and positive blocks (Houston and others, 2018; Niewendorp and others, 2018). Windows of older upper Oligocene stratigraphy in the Devine Ridge area are surrounded by younger rocks, suggesting the development of a significant paleo-topography prior to the deposition of the 9.74 Ma Devine Canyon Ash-flow Tuff. Faults in the Devine Ridge area cut Oligocene and Miocene rocks but are much less common in the late Miocene and younger rocks, suggesting that faulting may have been reactivated several times along selected structures through the late Miocene. West of Devine Canyon, to the Silvies River, few faults cut the south-dipping, upper Miocene stratigraphic section (McClaughry and others, 2019). Southwest of the Silvies River, into the Burns Butte 7.5′ quadrangle, a high concentration of north- to northwest-trending normal faults offset cliff- and bench-forming ash-flow tuffs, forming a series of paired north-northwest–trending horsts and grabens (Brown, 1982; Greene, 1972; Greene and others, 1972; McClaughry and others, 2019). Over the length of some longer faults in the vicinity northwest of Burns, structures are recognized as scissors faults where direction of offset varies along the strike of the individual strand. Most faults in this area cut and show activity postdating emplacement of the 7.1 Ma Rattlesnake Tuff (**Tmtr**), with offsets along individual fault strands ranging from centimeters to tens to hundreds of meters (**Figure 7-1**).

Figure 7-1. Faulted cliff- and bench-forming Rattlesnake Tuff (Tmtr) in the Poison Creek 7.5′ quadrangle (McClaughry and others, 2019). (43.63529, –119.11974 WGS84 geographic coordinates; 4833550mN, 329011mE WGS84 UTM Zone 11 coordinates). The section exposed here is offset by several small-displacement, down-on-the-west normal fault strands (solid white lines). Dashed white lines are geologic contacts between unit Tmtr and Tmst. U and D symbols are relative up and down movement along normal fault strands. View is looking northeast. Photo credit: Jason D. McClaughry, 2018.

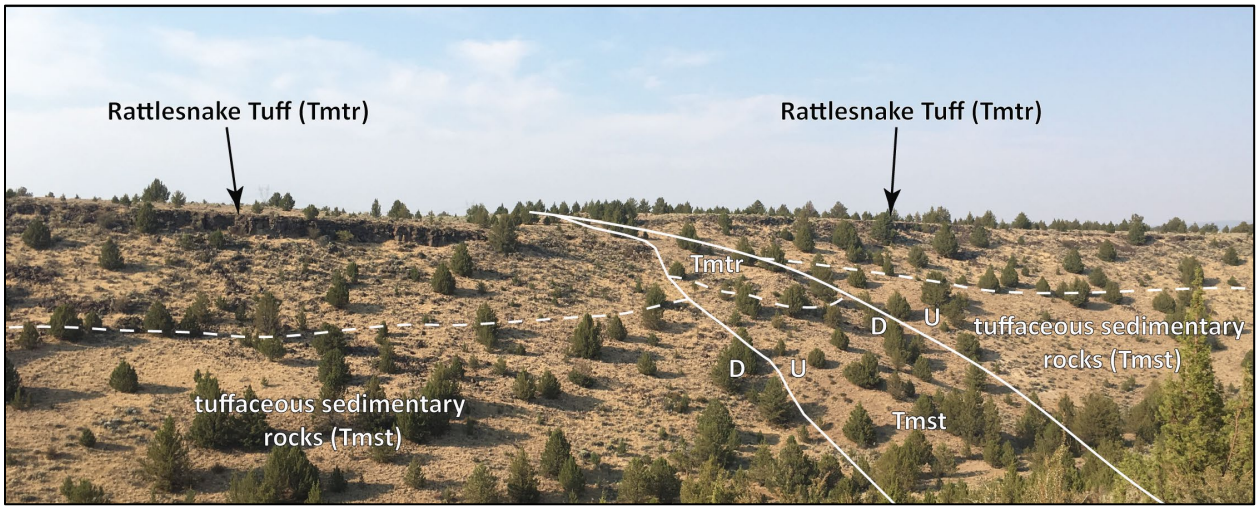

7.3 Structural geology in the Burns Butte 7.5′ quadrangle

Bedrock geology in the Burns Butte 7.5′ quadrangle consists of a relatively flat-lying section of Pleistocene to late Miocene(?) sedimentary rocks (**QTst**) and Pleistocene basaltic lava flows (**QTbw**), overlying the southwest-dipping Rattlesnake Tuff (**Tmtr**). These units sit above locally erupted mafic to intermediate lava flows and vent deposits (**Tmat**, **Tmvt**, **Tmatl**), rhyolite flows and domes (**Tmrg**, **Tmrb**), and ash-flow tuff (**Tmtw**, **Tmtwh**, **Tmtpi**) (Plate 1). Older rocks, including the Devine Canyon Tuff, early to middle Miocene Columbia River Basalt, late Oligocene to late Miocene calc-alkaline andesites and dacites, and pre-Cenozoic terranes, exposed beneath regional ash-flow tuffs in the highlands north and east of the city of Burns are not present at depth in the Burns Butte area (**Figure 6-2**; Houston and others, 2018; Niewendorp and others, 2018; McClaughry and others, 2019).

Normal faults in the map area collectively form part of a broad ~20 km-wide (12.4 mi), ~N. 20° W.-trending zone of normal faults, situated between the northeast margin of the BFZ near Sage Hen Powerline Road and Devils Garden in the Poison Creek 7.5′ quadrangle (**Figure 2-2**; Greene and others, 1972; Brown, 1982; see Plate 1 in McClaughry and others, 2019). The extent of the northern part of the zone is obscure north of Emigrant Creek, where the structural fabric meets northwest-trending faults cutting Columbia River Basalt and older accreted Mesozoic rocks; the southern extent of the zone is concealed beneath Quaternary sediments of the Harney Valley. At the southeastern part of the structural zone, mapped fault traces trend ~N. 10° W. to N. 30° W. (Plate 1). Northward fault traces curve to more northwesterly orientations of ~N. 60° W. to N. 65° W. (Plate 1). Northwest- and west-northwest–trending normal faults are associated with many subsidiary cross faults oriented ~N. 50° E. Structural offsets along faults range from several meters to tens of meters along subsidiary strands to offsets ranging from tens of meters up to ~220 m (728 feet) on main fault strands (**Figure 5-12**, **Figure 5-13**). The highest concentration of normal faults occurs in the area between Halfway Reservoir Flat Road and the city of Burns, where late Miocene geologic units are folded into a broad antiform (Plate 1, cross section A-A′; McClaughry and others, 2019). Normal faults have segmented the apex of this antiform into a number of elongate horst and graben blocks, which are representative of the modern topography of the area (Plate 1). Faults segmenting the antiform southwest of Willow Creek are dominantly northeast facing, down-on-the-northeast structures, whereas those mapped northeast of Willow Creek are dominantly southwest facing, down-on-the-southwest faults (Plate 1, cross section A-A′ and B-B′).

The mainstem Willow Creek and its tributaries largely occur within the Willow Creek graben, situated along the axis of this broad antiform in the north half of the map area. In Willow Creek Flats, and areas just to the southwest, the stream is characterized by a rectangular drainage pattern, where the distribution of polygonal channel reaches is controlled by linear faults and smaller grabens. South of the major horst-ridge, Willow Creek has incised an ~200-m-deep (656 ft) gorge through the resistant rhyolite of Burns Butte (**Tmrb**) (**Figure 5-20a**). South of the gorge, Willow Creek flows south down a dip slope of Rattlesnake Tuff (**Tmtr**). Incision of the drainage across the uplifted horst structure of relatively resistant bedrock implies that Willow Creek is an antecedent stream, carrying this general course since ~8.4 Ma.

Progressive relative uplift and normal faulting in the area generated the broad antiform across the northeast and eastern parts of the map area and the development of a number of linear horst ridges and grabens. All fault structures in the map area break the 7.1 Ma Rattlesnake Tuff (**Tmtr**). However, some normal faulting and formation of horsts and grabens could slightly predate emplacement of the 7.1 Ma Rattlesnake Tuff (**Tmtr**). Mapped field relationships show that the Rattlesnake Tuff (**Tmtr**) relatively thins across some horst structures and thickens into the associated grabens (Plate 1, cross section B-B′; see discussion of Willow Creek graben below). Segments of the Burns Butte fault, in the vicinity of Willow

Creek Flats, appear as lineaments cutting across older alluvial fan deposits (**Qoaf**) and colluvium (**Qc**), suggesting that some structures have been active in the Quaternary.

Figure 7-2. View looking northeast into the Willow Creek valley in the west-central part of the Burns Butte 7.5′ quadrangle, Harney County, Oregon (43.582108, −119.222403 WGS84 geographic coordinates; 4827859mN, 320572mE WGS84 UTM Zone 11 coordinates). The outcrops here expose a faulted sequence of trachyandesite lavas (Tmat) overlain by the 7.1 Ma Rattlesnake Tuff (Tmtr). The central part of the image is the fault-bounded Willow Creek graben, which contains Willow Creek. Dashed lines are geologic contacts; solid white lines represent fault traces. Labels U and D refer to relative up and down movement of fault blocks, respectively. Photo credit: Jason D. McClaughry, 2019.

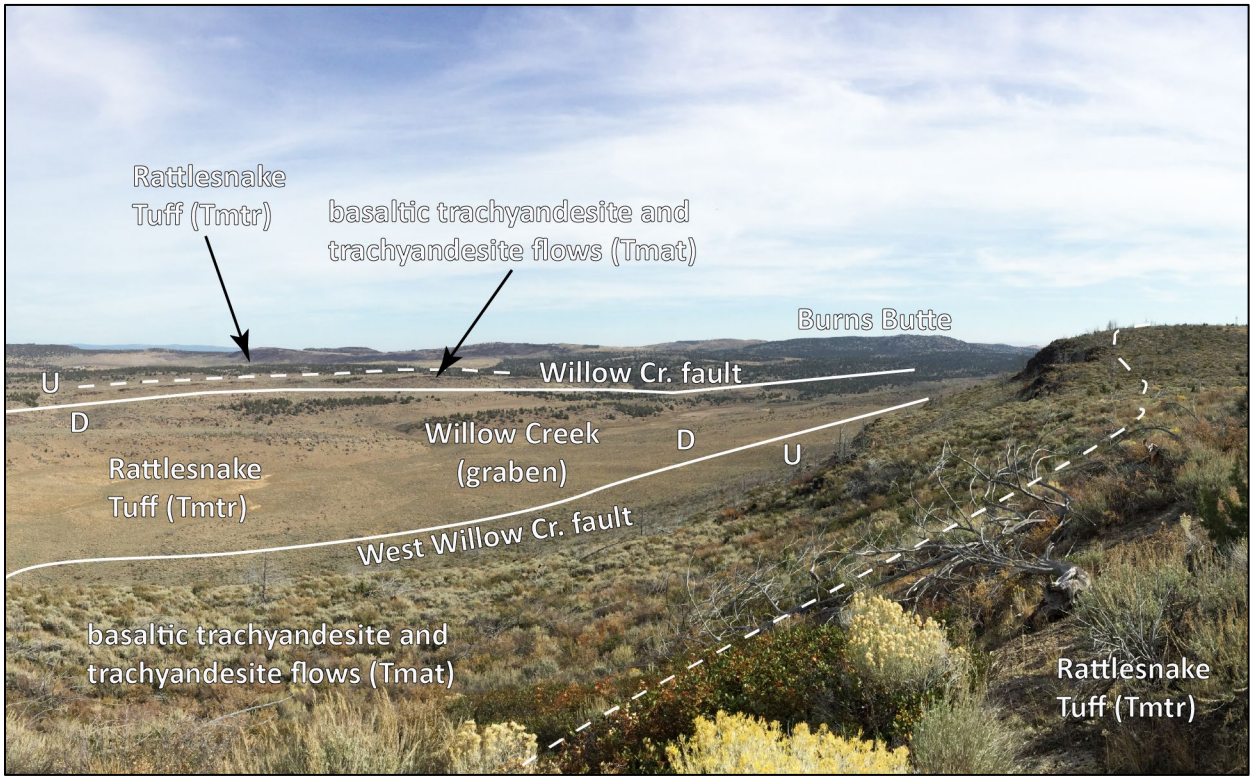

- ***West Willow Creek fault*** – The West Willow Creek fault extends for a length of ~12.9 km (8.0 mi), reaching from U.S. Highway 20 on the southeast to the head of West Willow Creek on the northwest. The overall geometry of the fault trends N. 32° W. beneath the Sage Hen Valley in the southeast part of the map area; the arcing fault trace is oriented N. 65° W. as the structure exits the Burn Butte 7.5′ quadrangle on the northwest. Down-on-the-northeast normal offset along the length of the fault has formed a prominent curvilinear, northeast-facing horst ridge exposing a sequence of rhyolite (**Tmrb**) and basaltic trachyandesite and trachyandesite flows (**Tmat**) capped by Rattlesnake Tuff (**Tmtr**) (Plate 1, cross section A-A′; **Figure 5-12**, **Figure 5-13**). Units **Tmtr** and **Tmat** underlying the horst ridge correlate to depth intervals of 0 to 52.4 m (0 to 172 ft) and 52.4 to 195 m (172 to 640 ft), respectively, in the Federal 1-10 well, drilled through the downthrown fault block (Plate 1). Correlation of horst ridge stratigraphy with that observed in the Federal 1-10 well indicates normal offset along this part of the West Willow Creek fault trace of ~192 m (630 ft).

- ***Halfway-Reservoir Flat Road fault*** – The Halfway-Reservoir Flat fault is a N. 63° W.-trending, normal fault extending for a length of ~5.9 km (3.7 mi), just north of the Federal 1-10 well (Plate 1). Down-on-the-northeast normal offset along the length of the fault has formed a north-northeast–facing horst ridge exposing a sequence of basaltic trachyandesite and trachyandesite flows (**Tmat**) capped by Rattlesnake Tuff (**Tmtr**) (Plate 1, cross section A-A′). Units **Tmtr** and **Tmat** underlying the horst ridge correlate to depth intervals of 0 to 52.4 m (0 to 172 ft) and 52.4 to 195 m (172 to 640 ft), respectively, in the Federal 1-10 well, drilled through the fault block (Plate 1). Normal offset along the Halfway-Reservoir Flat fault is ~138 m (452 ft) on the basis of cross section interpretation.
- ***Willow Creek fault*** – The Willow Creek fault stretches for a length of ~7 km (4.3 mi) from where it is concealed beneath the upper part of Willow Creek on the north, south to Wheeler Springs, where it merges with the Willow Creek Flats fault. Over the length of the fault, the trace trends N. 40° W. Down-on-the-southwest normal offset along the length of the fault has formed a southwest-facing horst ridge exposing a sequence of rhyolite (**Tmrb**; **Tmrg**) and basaltic trachyandesite and trachyandesite flows (**Tmat**) capped by Rattlesnake Tuff (**Tmtr**) (Plate 1, cross sections A-A′ and B-B′). Normal offset along this part of the Willow Creek fault trace ranges between ~9 and 50 m (30 and 164 ft).
- ***Willow Creek graben*** – The area between the West Willow Creek fault and the Willow Creek fault is a northwest-trending graben, formed at the apex of an overall antiformal structure extending between West Willow Creek and Skull Creek Road. On the basis of outcrop relationships along the east side of Willow Creek, graben formation began prior to emplacement of the Rattlesnake Tuff (**Tmtr**). Adjacent to the Willow Creek fault, Rattlesnake Tuff (**Tmtr**) lies both adjacent to and above older **Tmat** flows (Plate 1, cross section B-B′; see Rattlesnake Tuff [**Tmtr**] outcrops in the area of geochemical samples G22 and G23). The outcrop relationship, combined with thickening of lithophysal Rattlesnake Tuff (**Tmtr**) within the Willow Creek drainage, implies that structural paleotopography represented by a longitudinal graben existed prior to emplacement of the tuff. Continued faulting in post-Rattlesnake time has further modified the geometry of all geologic units and the graben itself (Plate 1).
- ***Willow Creek Flats fault*** – The Willow Creek Flats fault is a N. 36° W.- to N. 77° W.-trending fault stretching for a length of ~10.5 km (6.5 mi), from the northwest corner of the map area, south to where it merges with the Wheeler Springs fault, near Wheeler Springs (Plate 1). Down-on-the-southwest normal offset along the length of the fault has formed a southwest-facing horst ridge capped by Rattlesnake Tuff (**Tmtr**) (Plate 1, cross section A-A′). Along northern segments of the fault, the Rattlesnake Tuff (**Tmtr**) directly overlies basaltic trachyandesite and trachyandesite flows (**Tmat**), whereas the tuff rests directly on the rhyolite of Burns Butte (**Tmrb**) in the south (Plate 1, cross section B-B′). Normal offset along the Willow Creek Flats fault is ~134 m (440 ft) in the north along cross section A-A′. Interpreted fault offset, where the structure is intersected by cross section B-B′, is ~109 m (357 ft).
- ***Wheeler Springs fault*** – The Wheeler Springs fault includes several ~N. 30° W.-trending fault strands and extends for a length of ~9.3 km (5.8 mi), from Willow Creek Reservoir Road, south to where faults are concealed beneath the Harney Valley. Down-on-the-southwest normal offset along the length of the fault has exposed fault blocks composed of the rhyolite of Golden Ranch (**Tmrg**) and tuff of Wheeler Springs (**Tmtwh**, **Tmtw**) (Plate 1). Normal offset along the

Willow Creek Flats fault is as much as 76 m (250 ft) in the southeast part of the map area (Plate 1).

- ***Burns Butte fault/Radar Road fault*** – The Burns Butte and Radar Road faults are parallel, N. 35° W.-trending normal faults stretching for lengths of ~19.6 km (12.2 mi) and ~15.7 km (9.8 mi), respectively, from the area of Upper Willow Creek Reservoir (north of map area), south to where both faults cross U.S. Highway 20 and are concealed beneath the Harney Valley (Greene and others, 1972; Brown, 1982; see Plate 2 in McClaughry and others, 2019). Down-on-the-southwest normal offset along the length of both faults has formed southwest-facing ridges variably underlain by the tuff of Wheeler Springs (**Tmtw**, **Tmtwh**), rhyolite of Burns Butte (**Tmrb**), and basaltic trachyandesite and trachyandesite flows (**Tmat**) and vent deposits (**Tmvt**) (Plate 1, cross section A-A′). Along the north flank of Burns Butte, the **Tmrb /Tmtwh** contact is offset ~90 m (295 ft) in a down-on-the-southwest normal sense along the Burns Butte fault (Plate 1). Relative offset along the Radar Road fault appears to be greater. The cross section interpretation suggests at least 225 m (738 ft) of down-on-the-southwest normal offset of the rhyolite of Burns Butte east of Willow Creek Flats (Plate 1, cross section A-A′). Throughout their lengths, the Burns Butte and Radar Road faults are conspicuously associated with and cross cut vent deposits, dikes, and flows of units **Tmat** and **Tmvt** (Plate 1). This spatial association implies that the mafic to intermediate volcanics are surface manifestations of focused deformation on a larger deeply buried structure. In the vicinity of Willow Creek Flats, short and discontinuous linear features are observed in 1-m lidar DEMs, trending across Quaternary older alluvial fan deposits (**Qoaf**) and colluvium (**Qc**). These lidar-observed lineaments lie along the trace of the mapped Burns Butte fault, indicating local activity along strands of this fault continued into the Quaternary (Plate 1).

7.4 Silvies River caldera

Detailed geologic mapping of surface outcrops, examination of deep exploration wells, collection of whole-rock geochemical data, isotopic ages, and review and assessment of existing geophysical data define a concealed volcano-tectonic depression beneath the Burns Butte area. McClaughry and others (2019) named this structure the Silvies River caldera. The following section presents the salient geochemical, structural, and lithofacies observations related to this structure. Note, the following section references additional geologic units exposed outside the map area. These units include Mesozoic accreted terrane rocks (Jr), Oligocene rocks (O), Columbia River Basalt (CRB), and Devine Canyon Ash-Flow Tuff (DC). Some outcrop locations of these units are shown in **Figure 6-1**.

7.4.1 Observations

- A >427 m thick (1,400 ft) section of monotonous, lithologically, petrographically, and geochemically identical rhyolitic welded tuff is correlated between the Federal 1-10 and CTI wells (Plate 1; **Figure 5-7**, **Figure 5-9**, **Figure 2-3**, **Figure 5-30**, **Figure 6-1**; **Table 5-2**; Appendix). A pervasive granophyric texture characterizes the tuff (**Figure 5-30**).
- Geochemical analyses compared between surface exposures of the 8.48/8.41 Ma Prater Creek Ash-flow Tuff (**Tmtp**) and thick rhyolitic tuff intervals (**Tmtpi**) in the Federal 1-10 and CTI wells are indistinguishable (**Figure 5-7**, **Figure 5-9**, **Figure 2-3**, **Figure 5-30**, **Figure 6-1**, **Figure 6-2**, **Table 5-2**; Appendix; McClaughry and others, 2019).

- An $^{40}Ar/^{39}Ar$ plateau age of 8.52 ± 0.02 Ma (groundmass; sample F-1-10-3040) was obtained on a sample of rhyolitic tuff (**Tmtpi**) collected from the 927 m (3,040 ft) depth interval of the Federal 1-10 well.
- The lower 1,114 m (3,654 ft) of the Federal 1-10 well is a complex assemblage of rhyolitic ash-flow tuff, rhyolite (± muscovite), microgranite, and trachyandesite (Plate 1; **Figure 2-3**, **Figure 5-7**, **Figure 5-9**, **Figure 5-30**, **Figure 6-1**; **Table 5-2**; Appendix).
- The Burns Butte area, west of Silvies River and south of Emigrant Creek, is characterized by a surface of widespread Rattlesnake Tuff (**Tmtr**), with scattered erosional windows revealing underlying trachyandesite andesite lava flows (**Tmat**) (**Figure 6-1**; Green and others, 1972). Geologic units, including the late Miocene Devine Canyon Ash-flow Tuff (DC in **Figure 6-1**), middle Miocene Columbia River Basalt (CRB in **Figure 6-1**), Oligocene andesite and dacite (O in **Figure 6-1**), and older Mesozoic Rocks (Jr in **Figure 6-1)** are exposed at the surface beneath the Rattlesnake Tuff (**Tmtr**) east of the Silvies River (12.8 km [8 mi] northeast of the Federal 1-10 well; Niewendorp and others, 2018) and north of Emigrant Creek (24.6 km [15.3 mi] northwest of the Federal 1-10 well; Green and others, 1972). The Federal 1-10 well penetrated 2,343 m (7,684 ft) of mafic to intermediate lavas (**Tmatl, Tmat**), rhyolite flows and intrusions, and ash-flow tuff (Plate 1; **Figure 6-2**). The CTI well traversed 596 m (1,956 ft) of a stratigraphic section of similar lithology to that observed in the Federal 1-10 well. All regionally significant units (DC, CRB, O, and Jr), outlined above and shown in **Figure 6-1,** are absent in both drill holes, although they are exposed at the surface nearby (**Figure 6-2**).
- The Federal 1-10 well includes a 622-m-thick (2,040 ft) cryptic volcanic sequence of basaltic trachyandesite, trachyandesite, and trachydacite flows and intrusions (**Tmatl**) lying below the non-welded tuff of Wheeler Springs (**Tmtwh**) and above rhyolitic tuff of unit **Tmtpi** (Plate 1; **Figure 2-3**, **Figure 5-7**, **Figure 5-9**, **Figure 5-30**, **Figure 6-1**, **Figure 6-2**, **Table 5-2**; Appendix). This mafic to intermediate, flow-on-flow unit has no surface expression and is conspicuously absent in the CTI well drilled to a depth of 596 m (1,956 ft) below the city of Hines, ~12.1 km (7.5 mi) southeast of the Federal 1-10 well (**Figure 6-2**).
- The top of the thick rhyolitic tuff sequence (**Tmtpi**) lies at an elevation of 561 m (1,840 ft) asl in the Federal 1-10 well and at 1,096 m (3,598 ft) asl in the CTI well (Plate 1; **Figure 6-1**, **Figure 6-2**). The elevation of the top of the outflow Prater Creek Ash-flow Tuff (**Tmtp**) on the lower Silvies River, 12 km (7.3 mi) northeast of the Federal 1-10 well and 13.2 km (8.2 mi) north of the CTI well, is at 1,320 m (4,330 ft) asl. There is 760 m (2,493 ft) of vertical offset between the top of unit **Tmtpi** in the Federal 1-10 well and top of Prater (**Tmtp)** outcrops on the Silvies River, and 535 m (1,755 ft) of vertical offset between the top of **Tmtpi** in the Federal 1-10 well and top of **Tmtpi** in the CTI well (**Figure 6-1**, **Figure 6-2**). Two additional outcrops of lithophysal Prater Creek Ash-flow tuff are mapped in the Burns Butte 7.5′ quadrangle between Willow Creek Flats and Burns Butte lying at elevations of 1,485 m (4,870 ft) (6.1 km [3.8 mi] east of Federal 1-10 well) and 1,518 m (4,980 ft) (4.3 km [2.7 mi] northeast of Federal 1-10 well), respectively (Plate 1; **Figure 6-1**). These outcrops are at elevations ~932 m (3,060 ft) higher than the top of the Prater Creek Tuff caldera-fill sequence (**Tmtpi**) in the Federal 1-10 well and ~397 m (1,302 ft) higher than the caldera-fill sequence in the CTI well. The area between the wells and Silvies River outcrops is buried by Rattlesnake Tuff (**Tmtr**), basaltic trachyandesite and trachyandesite flows (**Tmat, Tmatl**), rhyolite flows and domes (**Tmrb, Tmrg**), and ash-flow tuff (**Tmtw, Tmtwh**). The younger cover units are faulted by a series of arcuate north-northwest-trending normal faults, between the Silvies River and the Federal 1-

10 well, but vertical offset along any individual fault strand in this intervening area does not exceed 225 m (738 ft).

- There is a noticeable stratigraphic discontinuity between the CTI well and the Weed and Poteet #1 well, located 6.9 km (4.3 mi) to the northeast of the city of Burns (**Figure 6-1**, **Figure 6-2**; McClaughry and others, 2019). In the CTI well, the **Tmtpi** rhyolitic tuff sequence is >429 m (>1,406 ft) thick and is directly overlain by ~58 m (190 ft) of silicic tuff correlated with the tuff of Wheeler Springs (**Tmtw**, **Tmtwh**) and farther upward by ~43 m (~140 ft) of basaltic trachyandesite and trachyandesite, and minor dacite **(Tmat)**; the upper part of the CTI well sequence is capped by Rattlesnake Tuff (**Tmtr**) (**Figure 6-2**). Stratigraphy in the Weed and Poteet #1 is inferred on the basis of lithologic logs (no cuttings are available) to include from top to bottom the local Harney Basin stratigraphic sequence including sedimentary rocks (**QTst**), Rattlesnake Tuff (**Tmtr**), basaltic trachyandesite and andesite lava flows (**Tmat**), outflow Prater Creek Ash-flow Tuff (**Tmtp**), Devine Canyon Ash-flow Tuff, and tuffaceous sedimentary rocks (**Tmst**) (McClaughry and others, 2019). These units overlie a >915 m (>3,000 ft) thick sequence of rocks presumed equivalent to the middle Miocene Columbia River Basalt, intercalated sedimentary rocks, and older Oligocene andesite and dacite (see Plate 2 in McClaughry and others, 2019).
- A bimodal suite of mafic to intermediate lava flows and vent deposits (**Tmat**, **Tmvt, Tmatl**), rhyolitic tuffs (**Tmtw**, **Tmtwh**), and exogenous rhyolite domes and flows (**Tmrg**, **Tmrb**) form a narrow volcanic field above unit **Tmtpi** rhyolitic tuff (Plate 1; **Figure 6-1**, **Figure 6-2**; McClaughry and others, 2019). Rhyolite units **Tmrg** and **Tmrb** have $^{40}Ar/^{39}Ar$ ages of 8.46 ± 0.03 Ma (groundmass; sample 148 BRHC 19) and 7.68 ± 0.04 Ma ($^{40}Ar/^{39}Ar$ plateau; sanidine; sample HP-91-2; Jordan and others, 2004), similar to the 8.52 Ma caldera-filling tuff (**Tmtpi**).
- Basaltic trachyandesite and trachyandesite flow (**Tmat**, **Tmatl**) and vent deposits (**Tmvt**) are almost exclusively confined in their distribution to areas west and south of the Silvies River in the map area (Plate 1; McClaughry and others, 2019).
- Crystal-rich rheomorphic rhyolitic tuff and rhyolite xenoliths contained within basaltic trachyandesite and trachyandesite flow (**Tmat**) and vent deposits (**Tmvt**) in the area directly south and west of the Silvies River (McClaughry and others, 2019) are geochemically similar to chemical compositions defining the Prater Creek Ash-flow Tuff (**Tmtp**) across the Harney Basin and those obtained from rhyolitic tuff (**Tmtp**) intervals in the Federal 1-10 and CTI wells.
- Most low-temperature geothermal wells are clustered in the southwestern part of the Burns 7.5′ quadrangle (McClaughry and others, 2019).
- In the Burns Butte and Burns NW 7.5′ quadrangles, normal fault strands are portrayed by Greene and others (1972), Brown (1982), and this report, as curvilinear structures transitioning from northwest-directed to west-northwest trends. The highest concentration of these normal faults is coincident with a broad antiform in the generally southwest dipping stratigraphic section (Plate 1, cross section A-A′). The faulted antiform is also associated with an area of focused mafic to intermediate volcanism (**Tmat**, **Tmvt**), extending southeast into the Burns 7.5′ quadrangle (McClaughry and others, 2019).
- Khatiwada and Keller (2015) show a seismic discontinuity at depth just to the east of the city of Burns (McClaughry and others, 2019). Their Figure 5F showing an east-west slice taken along 43.6° N. latitude, passing close to the Weed and Poteet, CTI, and Federal 1-10 wells, shows a discontinuity between the CTI and the Weed and Poteet wells (**Figure 6-1**, **Figure**

6-2; McClaughry and others, 2019). A similar although less pronounced discontinuity shows up to the west, near Capehart Lake.

- The Silvies River caldera lies just to the northeast of the younger postulated eruptive source for the Rattlesnake Tuff (**Tmtr**), centered on Capehart Lake (Streck, 1994; Streck and Grunder, 1995) (**Figure 2-3**).

7.4.2 Discussion of observations

Caldera sources for the Devine Canyon, Prater, and Rattlesnake tuffs have no surface expression and thus have been difficult to locate (**Figure 2-2**; **Figure 2-3**). Previous studies have inferred the likelihood of source calderas in the Harney Basin, although there has been no direct observation of such features (Parker, 1974; Walker, 1974, 1979; Walker and Nolf, 1981; Streck and Grunder, 1995, 2008; Cox, 2011; Cox and others, 2013; Ford and others, 2013; Khatiwada and Keller, 2015). Varying ideas about possible caldera locations have been made on the basis of mapped outcrop distribution, thickness changes, welding characteristics, and distance correlations with pumice-lithic size or shape (**Figure 2-3**). Additional suggestions about the locations of source calderas beneath the Harney Basin have come from geophysical studies by Cox (2011), Cox and others (2013), and Khatiwada and Keller (2015). No previous investigations, apart from Cox and others (2013), have incorporated deep well lithologic data, and no studies have physically examined or analyzed existing cuttings from historic Harney Basin exploration wells.

Careful geologic mapping combined with characterization of two deep exploration wells provides direct evidence, demonstrating the existence and identity of the Silvies River caldera and its linkage to the Prater Creek Ash-Flow Tuff (**Tmtp**) (McClaughry and others, 2019). Key evidence for the Silvies River caldera comes from a >427-m-thick (1,400 ft) section of rhyolitic welded tuff (**Tmtpi**) correlated between the Federal 1-10 and CTI wells. Unit **Tmtpi** is interpreted as an intracaldera tuff on the basis of a lithologically and geochemically monotonous nature of the silicic tuff from top to bottom, combined with its thickly ponded distribution (**Figure 7-3**). Pervasive granophyric texture in the tuff is consistent with slow cooling and crystallization of formerly glassy components (glass shards and pumice) in the central part of a very thick (several tens to hundreds of meters) or densely welded ignimbrite (McPhie and others, 1993).

The buried rhyolitic tuff (**Tmtpi**) shares a similar stratigraphic position to and is geochemically identical to surface exposures of the Prater Creek Ash-flow Tuff (**Tmtp**) (**Figure 5-7**, **Figure 5-9**, **Table 5-2**; McClaughry and others, 2019). An $^{40}Ar/^{39}Ar$ plateau age of 8.52 ± 0.02 Ma from unit **Tmtpi** is indistinguishable from $^{40}Ar/^{39}Ar$ ages of 8.41 ± 0.16 Ma (Jordan and others, 2004) and 8.48 ± 0.05 Ma (Deino and Grunder, unpublished data in Streck and others, 1999) reported for the Prater Creek Ash-Flow Tuff (**Tmtp**). These relationships provide a direct link that the source vent of the Prater Creek Ash-flow Tuff (**Tmtp**) is the Silvies River caldera (**Figure 2-3**).

The top of the caldera-filling tuff sequence (**Tmtpi**) is 760 m (2,493 ft) lower in the Federal 1-10 well than the top of Prater Creek tuff (**Tmtp)** outcrops on the Silvies River and 535 m (1,755 ft) lower than the top of unit **Tmtpi** in the CTI well (**Figure 6-1**, **Figure 6-2**; **Figure 7-3**). Younger cover units are faulted by a series of arcuate north-northwest-trending normal faults between the Silvies River and the Federal 1-10 well, but vertical offset along any individual fault strand in this intervening area does not exceed 225 m (738 ft). The lateral relationship between intracaldera unit **Tmtpi** and correlative Prater Creek Ash-flow tuff outcrops (**Tmtp**) is most plausibly explained by vertical offset and westward-deepening caldera collapse during formation of the Silvies River caldera at 8.52 Ma (Plate 1; **Figure 6-1**, **Figure 6-2**, **Figure**

7-3). Post-caldera faults, broad folding, and uplift of the area due a combination of normal faulting along the northern margin of the Brothers fault zone and probable resurgence during the emplacement of post-caldera intrusions have further modified the original geometry of the caldera structure (Plate 1; **Figure 7-3**). Two isolated outcrops of lithophysal Prater Creek Ash-flow Tuff (**Tmtp**) are present between Willow Creek Flats and Burns Butte, lying out of stratigraphic sequence, above the 7.68 Ma rhyolite of Burns (**Tmrb**). These outcrops are at elevations ~932 m (3,060 ft) higher than the top of the Prater Creek Tuff caldera-fill sequence (**Tmtpi**) in the Federal 1-10 well and ~397 m (1,302 ft) higher than the caldera-fill sequence in the CTI well (Plate 1). The isolated exposures of Prater Creek Ash-flow Tuff (**Tmtp**) are likely roof pendants of the older rock, uplifted during emplacement of extensive Burns Butte rhyolite (**Tmrb**) domes and flows.

Further evidence for the Silvies River caldera comes from missing regional stratigraphic units in the Federal 1-10 well, including the Mesozoic accreted terrane rocks, Oligocene volcanic rocks, Columbia River Basalt, and Devine Canyon Tuff. All of these units are exposed at the surface in areas 10 to 20 km (6.2 to 12.4 mi) north and northwest of the map area, yet are conspicuously absent in the 2343-m-deep (7,684 ft) Federal 1-10 well and the 596-m-deep (1,956 ft) CTI well (**Figure 6-1**, **Figure 6-2**, **Figure 7-3**).

The interval below unit **Tmtpi**, in the Federal 1-10 well instead consists of 1,114 m (3,654 ft) of rhyolitic ash-flow tuff, rhyolite (± muscovite), microgranite, and trachyandesite. On the basis of detailed examination of cuttings and stratigraphic relationships, we interpret these intervals as a variety of mafic to silicic intrusions emplaced beneath the caldera-filling tuff (**Tmtpi**) in post-Silvies River caldera time.

The 622-m-thick (2,040 ft) cryptic volcanic sequence of basaltic trachyandesite, trachyandesite, and dacite flows and intrusions (**Tmatl**) lying below the non-welded tuff of Wheeler Springs (**Tmtwh**) and above rhyolitic tuff of unit (**Tmtpi**) appear to be a series of lava flows, erupted from post-collapse caldera-related vents, that partially fill the structure (**Figure 6-2**; **Figure 7-3**). This mafic to intermediate, flow-on-flow unit has no surface expression and is conspicuously absent in the CTI well. Flows were erupted in over a narrow range of time between 8.52 and 8.46 Ma, and were confined on the east by a complex set of north-northwest–trending intracaldera ring faults. These now buried intracaldera fault structures are interpreted to lie beneath the northwest-trending belt of rhyolite domes and dikes (**Tmrb**, **Tmrg**) and mafic to intermediate vents and flows (**Tmat**, **Tmvt**) extending from the Sage Hen Valley to the south, northwest to Boone Canyon (9.4 km [5.8 mi]) (Plate 1; **Figure 7-3**).

West and northwest of the city of Burns, thick intracaldera unit **Tmtpi** deposits are spatially associated with a bimodal suite of late Miocene (8.52 to 8.46 Ma) rhyolitic tuffs (tuff of Wheeler Springs, **Tmtw**, **Tmtwh**), 8.46 to 7.68 Ma exogenous rhyolite domes and flows (rhyolite of Golden Ranch **Tmrg**, rhyolite of Burns Butte **Tmrb,** rhyolite intrusive rocks **Tmri**), and (7.68 to 7.1 Ma) basaltic trachyandesite and trachyandesite flows, dikes, and vent deposits (**Tmatu, Tmat**, **Tmvt, Tmatl**). These rocks define a narrow volcanic field of silicic domes and mafic shield volcanoes lying above caldera-filling tuffs (**Tmtpi**) along the eastern ring fracture zone of the Silvies River caldera (Plate 1; McClaughry and others, 2019). The restricted distribution of rhyolite domes and flows and intermediate lavas to areas exclusively west of the Silvies River indicates these units are confined by a structural-topographic depression. The controlling structural-topographic depression is interpreted to be the Silvies River caldera (**Figure 6-2**). It is also inferred that the main ring-fracture zone of the eastern part of the Silvies River caldera is a major volcanic-tectonic control determining the course of modern river entrenchment along the lower Silvies River as it enters the Harney Valley (McClaughry and others, 2019).

The tuff of Wheeler Springs (**Tmtw**, **Tmtwh**) is a complex pyroclastic unit, representing at least 20 discrete eruptive events (Brown, 1982). The tuff erupted from a vent either underlying or west of Burns Butte and has a distribution restricted to an area lying along the eastern margin of the Silvies River caldera

(Plate 1; **Figure 7-3**). Chemical composition of the tuff of Wheeler Springs (**Tmtw**, **Tmtwh**) is indistinguishable from analyses obtained from the overlying rhyolite of Burns Butte (**Tmrb**). (**Figure 5-7**, **Figure 5-9**, **Table 5-2**). Spatial and geochemical association of the silicic units indicates the tuff of Wheeler Springs represents pyroclastic eruptions directly preceding and genetically related to later effusive exogenous dome growth and flows forming the rhyolite of Burns Butte (**Tmrb**).

The lateral juxtaposition of markedly different stratigraphic units between the CTI and Weed and Poteet wells indicates the presence of a major structural boundary concealed beneath the Harney Valley, east of the city of Burns. This structure was portrayed and interpreted by McClaughry and others (2019) to be the concealed caldera-bounding fault of the Silvies River caldera (**Figure 6-1**; **Figure 6-2**; **Figure 7-3**). South of Burns this inferred caldera margin may extend to Double O Ranch, where Parker (1974) suggested a Prater Creek Ash-flow Tuff (**Tmtp**) source area associated with the 8.28 Ma rhyolite of Double O Ranch (red star in **Figure 2-3**; age by Jordan and others, 2004). A tomographic inversion velocity model along an east-west vertical slice at the general latitude of the Weed and Poteet well, shown in figure 5F of Khatiwada and Keller (2015) portrays a significant discontinuity in the same area (**Figure 7-4**). The imaged structure may correspond to the inferred eastern margin of the Silvies River caldera or, alternatively, a buried geologic structure of unknown origin and orientation.

Figure 7-3. Northwest to southeast geologic cross section, drawn through the Federal 1-10 well (HARN 52703), CTI geothermal test well (HARN 50087), and the EOARC Obs. Well (HARN 52747). Location of the cross section line B-B′-B″ is shown in Figure 6-1. Part B-B′ in the figure is the same as geologic cross section B-B′ shown on Plate 1.

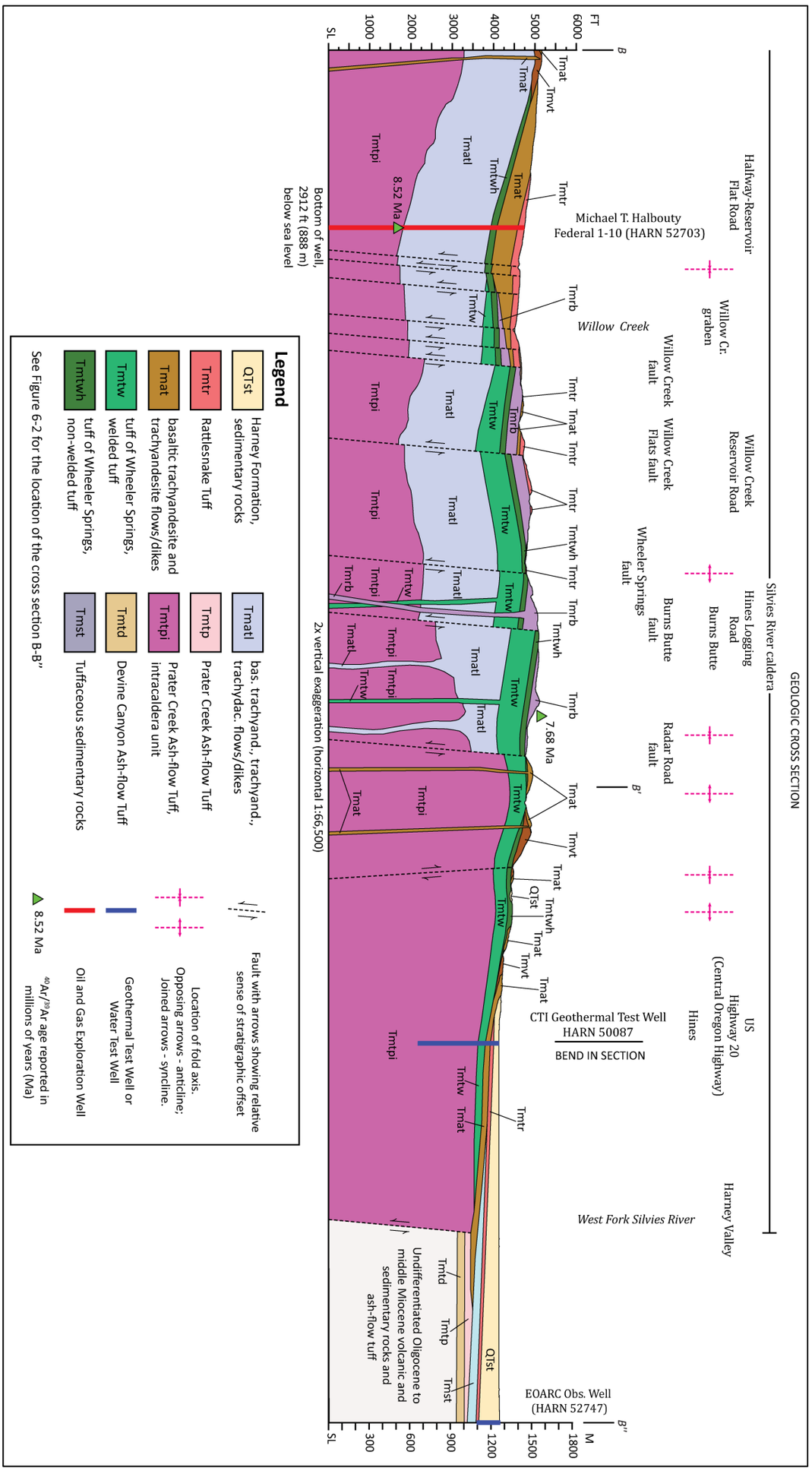

Figure 7-4. Geophysical interpretation of the eastern margin of the Silvies River caldera. Map view of the Silvies River caldera and located deep exploration wells superimposed on a tomographic inversion velocity model taken along an east-west vertical slice at 43.6° N. latitude. Vertical slice modified from Khatiwada and Keller (2015, figure 5F). Khatiwada and Keller (2015) imaged a subsurface feature here that appears to correspond to the eastern margin of the Silvies River caldera that we base on geologic mapping and lithologic and geochemical interpretation of deep exploration wells. White ellipses are deep exploration wells including the Federal 1-10 (F1-10), CTI (CTI), Weed and Poteet (WP), HARN 52747 EOARC (OBS), Voglar (VG), and #1 Fay (FAY) wells. Red solid line is the approximate location of the eastern margin of the Silvies River caldera.

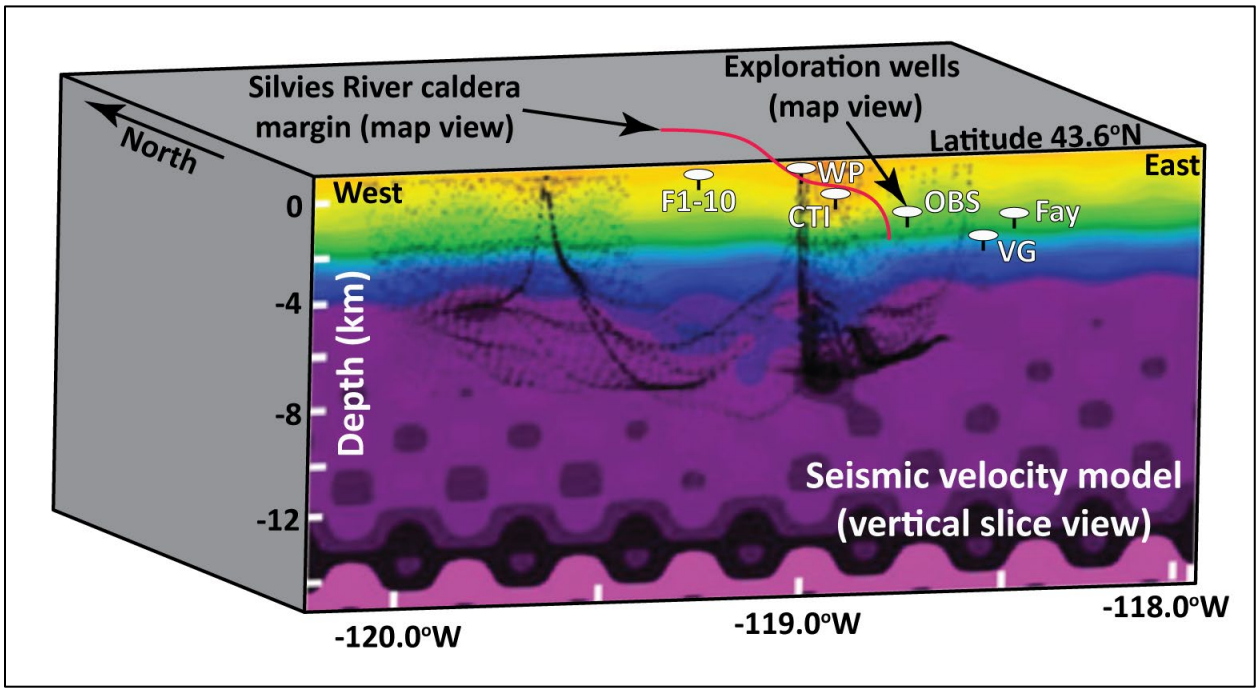

8.0 GEOLOGIC HISTORY

The "basement" rocks in the Harney Basin include parts of the Olds Ferry and Izee terranes (Brooks and Vallier, 1978; Silberling and others, 1984; Ave'Lallemant, 1995). The Olds Ferry Terrane, the most inboard of the Blue Mountains terranes, is an island arc terrane composed of a wide range of arc rocks (basalts to rhyolites, predominantly andesites) and volcanogenic sedimentary rocks of Middle Triassic to Early Jurassic ages. The Izee Terrane is a sedimentary cover sequence of Triassic/Jurassic flysch-like turbidites with ubiquitous volcanic flows in the lower part of the section. Pre-Cenozoic basement is overlain and/or intruded by a locally erupted late Oligocene (~25 to 22 Ma) sequence of dacites, rhyolites, and andesites, and early to middle Miocene basalt flows, displaying similarities to Grande Ronde, Steens, and Picture Gorge basalts of the Columbia River Basalt Group (CRBG) (Niewendorp and others, 2018; Houston and others, 2018). Locally, in the northern Harney Basin, early to middle Miocene lavas are overlain by the ~16 Ma Dinner Creek Tuff.

8.1 Late Miocene (9.74 Ma to 7.05 Ma)

Three voluminous late Miocene ash-flow tuffs are widely exposed and recognized across the Harney Basin above the CRBG and older rocks. The 8.52 Ma intracaldera unit of the Prater Creek Ash-flow Tuff (**Tmtpi**) and associated 8.48/8.41 Ma outflow deposits (**Tmtp**) are the oldest geologic units in the Burns Butte 7.5' quadrangle. The older 9.74 Ma Devine Canyon Ash-flow Tuff is not present in the map area, while the younger 7.1 Ma Rattlesnake Tuff (**Tmtr**) forms an extensive sheet, commonly concealing underlying geology (Plate 1; **Figure 6-2**, **Figure 7-3**; Walker, 1979; Streck, 1994; Streck and Grunder, 1995, 2008; Jordan and others, 2004; Ford and others, 2013; Isom, 2017). The three major late Miocene tuff units, each exceeding 200 km^3 (48 mi^3) in eruptive volume and covering areas ranging from ~9,615 km^2 (~3,713 mi^2) to >35,000 km^2 (>13,500 mi^2) are presumed to have originated from caldera sources lying buried beneath the Harney Basin, including the Silvies River caldera(**Figure 2-3**). Rapidly moving, incandescent pyroclastic flows, emanating from these calderas completely inundated the landscape of the late Miocene Harney Basin, largely burying evidence of older late Miocene calderas. Tuffaceous sedimentary rocks (**Tmst**) preserved between ash-flow tuffs represent erosion, remobilization, transport, and deposition of abundant tuffaceous material in the intervals between caldera-forming eruptions. Some **Tmst** horizons include air-fall tuffs, signaling continued regional eruptions, including pumice and tuff beds formed during pre-cursor eruptions to caldera-forming ash-flow tuff events.

The Silvies River caldera formed in the area of Burns Butte at ~8.52 to 8.41 Ma, with the eruption of the Prater Creek Ash-flow tuff (**Tmtp**, **Tmtpi**). Formation of the caldera resulted in the emplacement of ~200 km^3 (48 $mile^3$) of pyroclastic debris as ash flows that rapidly inundated more than 9,000 km^2 (>3,474 mi^2) of southeastern Oregon. Caldera-forming eruptions at the Silvies River caldera were followed by the emplacement of a 8.52 to 8.46 Ma bimodal suite of late Miocene basaltic trachyandesite, trachyandesite, and trachydacite flows and intrusions (**Tmatl**), 8.52 to 8.46 Ma rhyolitic tuffs (tuff of Wheeler Springs, **Tmtw**, **Tmtwh**), 8.46 to 7.68 Ma exogenous rhyolite domes and flows (rhyolite of Golden Ranch **Tmrg**, rhyolite of Burns Butte **Tmrb**), and 7.68 to 7.1 Ma basaltic trachyandesite and trachyandesite flows, dikes, and vent deposits (**Tmat**, **Tmvt**), now forming the low hills west of Burns (see Plate 2 in McClaughry and others, 2019). These rocks define a narrow volcanic field of prominent silicic domes and mafic shield volcanoes that formed above caldera-filling tuffs following caldera formation (Plate 1; McClaughry and others, 2019). At 7.1 Ma the Silvies River caldera and intracaldera volcanic fields were partially to completely buried by the Rattlesnake Tuff (**Tmtr**). Late Miocene trachyandesite flows (**Tmatu**) overlie the Rattlesnake Tuff (**Tmtr**) in the northeast part of the Burns Butte 7.5′ quadrangle (Plate 1).

8.2 Late Miocene to Recent

Uplift of the Blue Mountains to the north and Steens Mountain to the south and downwarping of the Harney Valley into a broad synclinal trough occurred through post-Rattlesnake (**Tmtr**) time (Buwalda, 1921). Drainages in the northern Harney Basin entrenched themselves into the southerly tilted dip-slope, flowing into the valley forming the shallow Harney and Malheur lakes. These drainages carried locally derived detritus into the basin in the form of clay, sand, and gravel building up basin-fill deposits of considerable thickness.

Late Miocene units in the marginal parts of the Harney Basin, including the southern part of the Burns Butte 7.5′ quadrangle, are covered by sequences of late Pliocene to Quaternary sedimentary rocks (**QTst**). These rocks represent fluvial and lacustrine deposits that partially filled the Harney Basin and followed ancestral drainages 61 to 183 m (200 to 600 ft) above the modern valley floor. Along Sage Hen Creek,

sedimentary units are interbedded with several basalt flows (**QTbw**), erupted from the area of Dog Mountain (Parker, 1974; Brown, 1982) at ~3.29 Ma (Plate 1). Neogene bedrock units in the area are locally covered by surficial units, including older fan deposits (**Qoaf**), colluvium (**Qc**), fan deposits (**Qaf**), stream channel alluvium (**Qa**), and modern fill (**Qf**). Landslide deposits (**Qls**) are also present in some areas.

9.0 GEOLOGIC RESOURCES

9.1 Aggregate materials and industrial minerals

Aggregate in the form of crushed rock and gravel is the major mineral resource mined in areas marginal to the Harney Basin. McClaughry and others (2020) provided regional locations for aggregate and crushed rock resources (https://www.oregongeology.org/milo/index.htm). In the map area, sand and gravel quarries are sited mainly in sedimentary rocks (**QTst**). Those quarries developing crushed rock and cinders are sited in basaltic trachyandesite and trachyandesite flows (**Tmat**), basaltic trachyandesite and trachyandesite vent deposits (**Tmvt**), and rarely Rattlesnake Tuff (**Tmtr**). Industrial mineral sites hosting pumice, pumicite, and obsidian are found in the tuff of Wheeler Springs, non-welded lapilli tuff (**Tmtwh**). Obsidian and gemstone localities are also reported from sedimentary rocks (unit **QTst**) northwest of the city of Burns. Presently, all quarries in the study area are small pit-run sources located on private lands and on lands administered by the Oregon Department of Transportation or the U.S. Bureau of Land Management. This material is used locally for road construction and maintenance. However, certain localities may provide material suitable for decorative stone and for use as riprap for stabilization and erosion control purposes.

9.2 Energy resources

9.2.1 Geothermal

Brown and others (1980a), in a reconnaissance study, investigated the geothermal resource potential of the northern Harney Basin. Two low-temperature resource areas were identified: 1) the area near the Soldier Creek shear zone, northeast of the city of Burns (Houston and others, 2018; Niewendorp and others, 2018), and 2) the area immediately south, west, and east of the city of Burns (see Plate 2 in McClaughry and others, 2019). The area surrounding the city of Burns is currently recognized as a Direct Use Geothermal Area, covering ~13,725 hectares (~33,917 acres) centered on the bimodal volcanic highlands southeast of Burns Butte (Niewendorp and others, 2012; https://www.oregongeology.org/gtilo/index.htm). Direct use areas are locations that because of their geologic history, presence of thermal springs, wells, geohydrologic settings favorable for the recovery of thermal water, and similarity to areas with known geothermal/hydrothermal systems, are expected to contain geothermal resources suitable for direct heat applications (20°C and above) (Niewendorp and others, 2012).

Several warm springs are documented in the area along U.S. Highway 20 just south of Hines, including the Millpond well (26°C, 78.8°F maximum recorded temperature), an unnamed well (25°C, 77°F maximum recorded temperature), Goodman Spring (21°C, 71.6°F maximum recorded temperature), and Roadland Spring (22°C, 71.6°F maximum recorded temperature).

Fifty-two low-temperature geothermal wells are present in the Burns area. Low-temperature wells are wells that have temperatures < 90°C (194°F). Recorded maximum temperatures on these wells range

between 18.3° and 35°C (64.9 to 95°F). Higher maximum temperatures of are associated with the Federal 1-10 well (17°C [62.6°F]) and with the Weed and Poteet well (58° to 71°C [136.4° and 159.8° F]).

Most low-temperature geothermal wells in this part of the Harney Basin are clustered in the southwestern part of the Burns 7.5′ quadrangle (McClaughry and others, 2019), associated with the eastern ring-fracture zone of the Silvies River caldera and late Miocene bimodal basaltic trachyandesite and rhyolite volcanic vent complexes forming the low hills west of Burns. Additional low-temperature geothermal wells are present in Sage Hen Valley in the southern part of the Burns Butte 7.5′ quadrangle. Temperatures from four wells located in this area range between 18.3° and 20°C (65° and 68°F). Two additional wells, one on Burns Butte proper and the other within the Wheeler Springs fault zone, have reported temperatures of 21°C (69.8°F).

Six geothermal prospect wells have been drilled in the adjacent Burns 7.5′ quadrangle including the BN-12, BN-13, Weed and Poteet #1, Hotchkiss 1, Hines Mill No. 1, and Burns High School wells (see Plate 2 in McClaughry and others, 2019). These wells were largely drilled in the 1970s and 1980s to gather temperature observation data. Data are contained in the unpublished permit files of the Oregon Department of Geology and Mineral Industries' Mineral Land Reclamation and Regulation program.

9.2.2 Oil and gas

Several oil and gas exploration wells were drilled in the central and western regions of the Harney Basin in the vicinity of the city of Burns starting around 1900 and then from the late 1940s into the late 1970s (**Figure 6-1**). Oil and gas well locations and drilling logs are available at https://www.oregongeology.org/mlrr/oilgas-logs.htm. Many of the wells reported shows of gas. A show is the appearance of oil and/or gas in cuttings, samples, or cores from drilling a well. Drilling records indicate that these wells were plugged and abandoned shortly after completion. This suggests that not all elements of a petroleum system for production of oil and/or gas are associated with the rocks within the Harney Basin, e.g., 1) a source rock for petroleum, 2) migration path(s), 3) reservoir rock, 4) seal, 5) trap, and 6) the geologic processes that form these elements. Therefore, the oil and gas potential for the area is low. **Table 2-1** shows a listing of Oil and Gas exploration wells in the Burns/Burns Butte area. The history of the wells is described by McClaughry and others (2019) and in preceding section 6.0, Exploration Wells.

9.2.3 Mercury

A single location for a cinnabar prospect in the map area is reported by Brooks (1963) and in the compilation of McClaughry and others (2020) in SW ¼, sec. 26, T.23S., R.29E. Brooks (1963) reported that the property was first worked for gold and then abandoned. Cinnabar, associated with small bodies of opalite, was discovered in 1939. The site was developed with several cuts and an ~ 8-m-deep (25 ft) shaft.

Evidence for hydrothermal alteration is conspicuously absent throughout the Burns Butte 7.5′ quadrangle, with just a few narrow lenses of porcelainous opaline quartz in the vicinity of the reported prospect. Glassy volcanic rocks appear pristine with no indications of clay alteration or silicification associated with the Burns Butte rhyolites.

9.3 Water resources

A full discussion of the geologic controls on surface and groundwater resources in the study area is beyond the scope of this report. Field observations and preliminary findings on geologic parameters controlling water resources within the study area are briefly summarized below. The reader is referred to previous

hydrogeologic investigations by Piper and others (1939), Leonard (1970), Walker (1979), Whitehead (1994), and Gonthier (1985) for more in-depth discussions.

The Harney Basin is a dominantly agricultural area, with water resources allocated for a combination of domestic use, irrigated agriculture, livestock, and fish and wildlife needs. A database of 61 located wells accompanies the geodatabase for this report (see WellPoints data in geodatabase and appendix). Most of these wells are sited along the Sage Hen Valley and in the area of Willow Creek Flats. Most water wells are drilled in units **QTst** and **Tmtr** across the Sage Hen Valley; in Willow Creek Flats, wells penetrate **Tmrb** and **Tmat**.

Unconsolidated to partly consolidated alluvial sand and gravel deposits preserved in terraces and floodplains (**Qa**) and on alluvial and debris fans (**Qoaf**, **Qaf**) likely contain groundwater that typically saturates sediments just above the underlying bedrock platform and is usually in hydraulic connection with nearby streams (Plate 1 ; Piper and others, 1939; Leonard, 1970). The deposits are typically thin (<10 m [30 ft]) and likely sinuous but may be very permeable except where they contain large amounts of clay and silt (Piper and others, 1939; Leonard, 1970). Alluvial wells developed in higher-permeability sand and gravel intervals, with yields depending on annual precipitation, as compared to lower-permeability silt-rich sedimentary intervals, are likely favorable targets (Piper and others, 1939).

Other water-bearing horizons in the study area may generally be found at the basal contacts of Rattlesnake Tuff (**Tmtr**) and Prater Creek Ash-flow Tuff (**Tmtp**) rock types, although few wells are sited in these strata (Plates 1). These horizons serve as lateral pathways for groundwater flow. Tuffaceous sedimentary rocks (**Tmst**) between ash-flow tuffs appear to act as either confining units or porous media serving as pathways for lateral transport of groundwater depending on percent clays.

10.0 GEOLOGIC HAZARDS

10.1 Landslide hazards

The downslope movement of rock and soil, in the form of landslides, rock falls, and debris flows, may present a geologic hazard to residents, infrastructure, and transportation corridors in the Burns Butte 7.5′ quadrangle.

10.1.1 Typical and colluvial landslides

Eleven landslide deposits (**Qls**) were recognized and mapped in the study area during the course of this study. Those landslide deposits (**Qls**) recognized cover ~0.002 percent of the map area and range from larger slides covering up to 15 hectares (37 acres) to the smallest mapped landslide deposit covering just 0.2 hectares (0.05 acres). A majority of mapped landslide deposits are simple rotational or translational slides or shallow-seated earthflow-type features occurring along all major drainages. Landslides typically originate on sparsely vegetated, moderate to steep slopes underlain by weakly consolidated tuffaceous sedimentary rocks (**QTst**) forming interbeds between cliff- and bench-forming basaltic lava flows (**QTbw**) (Plate 1). Other slides occur where Rattlesnake Tuff (**Tmtr**) overlies lava flows (**Tmat**) or where vent deposits cover the Prater Creek Ash-flow Tuff (**Tmtp**) (Plate 1). Many of these slides can be attributed to the combined influences of parallel topographic slope and faulting or bedding dip, undercutting by streams, intermittent heavy precipitation, groundwater conditions, and rock type. The generally weakly consolidated nature of the tuffaceous sedimentary rocks (**QTst**) makes this unit especially prone to landslides. Future landslides should be expected in **QTst** deposits, particularly in areas of changing

vegetation resulting from rangeland fires or changes in land use that may alter local groundwater conditions.

Unstable colluvium (**Qc**; wedges of soil and rock) mantles many slopes in the study area. These deposits typically form when weathered rock particles accumulate along a hillside. When the mass of the accumulated material reaches a critical size, a triggering event such as heavy rainfall or a seismogenic event may initiate the rapid downslope movement of this mass. Areas denuded by fire or other anthropogenic devegetation can especially be at risk from such events.

10.1.2 Rock fall

Rock fall and rockslide (**Qc**) hazards may be present in the study area where steep slopes and cliff exposures occur (Plate 1). Potential natural triggering mechanisms for rock fall events include freeze-thaw cycles, heavy rainfall, earthquakes, or extensive devegetation due to fire.

10.1.3 Alluvial fan deposits

Alluvial fan and debris fan (**Qaf**, **Qoaf**) deposits in the study area have been mapped along all drainages (Plate 1). Rapidly moving landslides in the form of debris flows may be expected on both alluvial and debris fans that lie at the mouths of steep-sided, colluvium-filled canyons and upland drainages. The potential for inundation of fan areas by rapidly moving debris flows increases during episodes of intense rainfall that occur after soils have been saturated by fall and early winter rainfall. Redirected drainage and poor construction practices are human activities that could initiate debris flows. Debris flows have the potential to threaten life and may cause extensive damage to property and transportation corridors.

10.2 Earthquake hazards

There has been little in the way of recorded historic (1896 to 2002) seismic activity in the Burns area (Niewendorp and Neuhaus, 2003). Three historic earthquake epicenters have been recorded in the greater area of Harney County, with events ranging in magnitude from M4.0 to M4.9 (Richter scale). Approximately 10 smaller events (<M4.0) have been documented in the southern part of the county in historical times (Niewendorp and Neuhaus, 2003). Weldon and others (2003), in their active fault map for central and eastern Oregon, show two fault strands in the Burns Butte 7.5' quadrangle (fault identification numbers 3797 and 1060; corresponds to the Burns Butte fault shown on Plate 1 and discussed herein), as well as a number of northwest-trending fault strands in the Brothers Fault Zone west of Wrights Point as possibly active during the Quaternary (2.58 Ma and younger). These workers also show a major north-south trending fault stand along the eastern edge of the Harney Valley (fault #1244), extending from Crane north through Buchanan, interpreted as active through the middle to late Quaternary (<0.78 Ma). In the northeast part of the Burns Butte 7.5' quadrangle (Plate 1) we portray several northwest-trending fault strands to offset Quaternary fans (**Qoaf**; **Qaf**) and colluvium (**Qc**) of unit **QTst**. USGS probabilistic ground shaking estimates for the area range from 10 to 14 percent G for the peak ground acceleration with a 2 percent chance of exceedance in 50 years (USGS Earthquake Hazards Program, https://earthquake.usgs.gov/static/lfs/nshm/conterminous/2014/2014pga2pct.pdf).

11.0 ACKNOWLEDGMENTS

Discovery of the Silvies River caldera would not have been possible without the availability of historic oil and gas and geothermal well cuttings archived by DOGAMI as part of agency statute (ORS 516.030 [11]). This project and publication were supported through the STATEMAP component of the National Cooperative Geologic Mapping Program under cooperative agreement number G19AC00160. Additional matching funds were provided by the State of Oregon. XRF geochemical analyses were prepared and analyzed by Dr. Ashley Steiner at the GeoAnalytical Lab at Washington State University, Pullman. New $^{40}Ar/^{39}Ar$ ages were prepared and analyzed by Dr. Dan Miggins at the College of Oceanic and Atmospheric Sciences, Oregon State University, Corvallis. The authors acknowledge several area landowners who provided local knowledge and graciously allowed access to private holdings within the study area. Ian Madin digitized and contributed linework for an early version of surficial geology in the Burns Butte area. Cartography for the map plate was provided by Jon Franczyk. The authors sincerely appreciate field assistance and discussions with Darrick Boschmann, Jon Franczyk, and Ian Madin about the geology of southeast Oregon. Critical and insightful reviews by Darrick Boschmann (OWRD), Andrew Meigs (OSU), Ian Madin (DOGAMI), and Christina Appleby (DOGAMI) greatly enriched the final manuscript, geologic map, and geodatabase.

12.0 REFERENCES

Ave'Lallemant, H. G., 1995, Pre-Cretaceous tectonic evolution of the Blue Mountains Province, Northeastern Oregon, *in* Vallier, T. C., and Brooks, H. C., eds., Geology of the Blue Mountains Region, U.S. Geological Survey Professional Paper 1438, p. 291–304.

Boschmann, D. E., 2012, Structural and volcanic evolution of the Glass Buttes area, High Lava Plains, Oregon: Corvallis, Oreg., Oregon State University, M.S. thesis, 100 p. https://ir.library.oregonstate.edu/concern/graduate_thesis_or_dissertations/47429d66f

Brooks, H.C., 1963, Quicksilver in Oregon: Oregon Department of Geology and Mineral Industries Bulletin 55, 223 p. https://www.oregongeology.org/pubs/B/B-055.pdf

Brooks, H. C., and Vallier, T. L., 1978, Mesozoic rocks and tectonic evolution of eastern Oregon and western Idaho, in Howell, D. G., and McDougall, K. A., eds., Mesozoic paleogeography of the western United States: Pacific Coast Paleogeography Symposium 2, Sacramento, Calif., Society of Economic Paleontologists and Mineralogists, Pacific Section, p. 133–136.

Brown, D. E., 1982, Map showing geology and geothermal resources of the southern half of the Burns 15-minute quadrangle, Oregon: Oregon Department of Geology and Mineral Industries Geological Map Series GMS-20, 1 pl., scale 1:24,000. https://www.oregongeology.org/pubs/gms/GMS-020.pdf

Brown, D. E., McLean, G. D., and Black, G. L., 1980a, Preliminary geology and geothermal resource potential of the northern Harney Basin, Oregon: Oregon Department of Geology and Mineral Industries Open-File Report 80-6, 52 p., 4 pl., scale 1:62,500. Zipped file: https://www.oregongeology.org/pubs/ofr/O-80-06.zip

Brown, D. E., McLean, G. D., and Black, G. L., 1980b, Preliminary geology and geothermal resource potential of the southern Harney Basin, Oregon: Oregon Department of Geology and Mineral Industries Open-File Report 80-7, 90 p. 8 pl. Zipped file: https://www.oregongeology.org/pubs/ofr/O-80-07.zip

Buwalda, J. P., 1921, Report on oil and gas possibilities of eastern Oregon: Oregon Bureau of Mines and Geology, Mineral Resources of Oregon, v. 3, no. 2, July 1921.

Cahoon, E. B., Streck, M. J., Koppers, A.A.P., and Miggins, D.P., 2020, Reshuffling the Columbia River Basalt chronology-Picture Gorge Basalt, the earliest- and longest-erupting formation: Geology, v. 48, no. 4, p. 348-352.

Camp, V. E., Ross, M. E., and Hanson, W. E., 2003, Genesis of flood basalts and Basin and Range volcanic rocks from Steens Mountain to the Malheur River Gorge, Oregon: Geological Society of America Bulletin, v. 115, no. 1, p. 105–128. https://doi.org/10.1130/0016-7606(2003)115<0105:GOFBAB>2.0.CO;2

Camp, V. E., Ross, M. E., Duncan, R. A., Jarboe, N. A., Coe, R. S., Hanan, B. B., and Johnson, J. A., 2013, The Steens Basalt: Earliest lavas of the Columbia River Basalt Group, *in* Reidel, S. P., Camp, V. E., Ross, M. E., Wolff, J. A., Martin, B. S., Tolan, T. L., and Wells, R. E., The Columbia River Flood Basalt Province: Geological Society of America Special Paper 497, p. 87–116. https://doi.org/10.1130/2013.2497(04)

Cande, S. C., and Kent, D. V., 1992, A new geomagnetic polarity time scale for the Late Cretaceous and Cenozoic: Journal of Geophysical Research, v. 97, p. 13,917–13,951.

Cohen, K. M., Finney, S. C., Gibbard, P. L., and Fan, J.-X., 2013, The ICS International Chronostratigraphic Chart: Episodes, v. 36, no. 3, 199–204. Available at https://stratigraphy.org/icschart/Cohen2013_Episodes.pdf

Colgan, J.P., Shuster, D. L., Reiners, P.W., 2008, Two-phase Neogene extension in the northwestern Basin and Range recorded in a single thermochronology sample: Geology v. 36, p. 631–634.

Cox, C., 2011, A controlled-source seismic and gravity study of the High Lava Plains (HLP): Norman, Okla., University of Oklahoma, M.S. thesis, 110 p.

Cox, C., Keller, G. R., and Harder, S. H., 2013, A controlled-source seismic and gravity study of the High Lava Plains (HLP) of eastern Oregon: Geochemistry, Geophysics, Geosystems, v. 14, no. 12, p. 5208–5226. https://doi.org/10.1002/2013GC004870

Cox, K. G., Bell, J. D., and Pankhurst, R. J., 1979, The interpretation of igneous rocks: London, George Allen and Unwin, 450 p.

Dicken, S. N., 1965, Oregon Geography: The people, the place, and the time, 4th ed: Ann Arbor, Mich., Edwards Brothers, 147 p.

Duda, C. J. M., McClaughry, J. D., Houston, R. A., and Niewendorp, C. A., 2018, Lidar and structure from motion-enhanced geologic mapping, examples from Oregon, *in* Thorleifson, L. H., ed., Geologic Mapping Forum 2018 Abstracts, Minnesota Geological Survey Open File Report OFR-18-1, 107 p. http://www.mngs.umn.edu/

Duda, C. J. M., McClaughry, J. D., and Madin, I. P., 2019, Building the modern geologic map in Oregon: a multi-faceted field- and technology-based approach: Geological Society of America Abstracts with Programs. Vol. 51, No. 4, ISSN 0016-7592, doi: 10.1130/abs/2019CD-329552. https://gsa.confex.com/gsa/2019CD/meetingapp.cgi/Paper/329552

Duncan, R.A. and Keller, R.A., 2004, Radiometric ages for basement rocks from the Emperor Seamounts, ODP Leg 197. Geochemistry, Geophysics, Geosystems, v. 5. doi:10.1029/ 2004GC000704.

Ferns, M. L., and McClaughry, J. D., 2013, Stratigraphy and volcanic evolution of the middle Miocene to Pliocene La Grande–Owyhee eruptive axis in eastern Oregon, *in* Reidel, S. P., Camp, V. E., Ross, M. E., Wolff, J. A., Martin, B. S., Tolan, T. L., and Wells, R. E., eds., The Columbia River Flood Basalt Province: Geological Society of America Special Paper 497, p. 401–427. https://doi.org/10.1130/2013.2497(16)

Fiebelkorn, R. B., Walker, G. W., MacLeod, N. S., McKee, E. H., and Smith, J. G., 1982, Index to K-Ar age determinations for the state of Oregon: U.S. Geological Survey Open File Report 82-596, 42 p. 1 plate.

Fiebelkorn, R. B., Walker, G. W., MacLeod, N. S., McKee, E. H., and Smith, J. G., 1983, Index to K-Ar age determinations for the state of Oregon: Isochron/West, no. 37, p. 3–60.

Ford, M. T., 2012, Rhyolitic magmatism of the High Lava Plains and adjacent northwest Basin and Range, Oregon: Implications for the evolution of continental crust: Corvallis, Oreg., Oregon State University, Ph.D. dissertation, 111 p. https://ir.library.oregonstate.edu/concern/graduate_thesis_or_dissertations/p5547t57d

Ford, M. T., Grunder, A. L., and Duncan, R. A., 2013, Bimodal volcanism of the High Lava Plains and northwestern Basin and Range of Oregon: Distribution and tectonic implications of age-progressive rhyolites: Geochemistry, Geophysics, Geosystems, v. 14, no. 8, p. 2837–2857. https://doi.org/10.1002/ggge.20175

Geological Society of America Rock-Color Chart Committee, 1991, Rock color chart, 7th printing: Boulder, Colo.

Gillespie, M. R., and Styles, M. T., 1999, BGS rock classification scheme, v. 1, Classification of igneous rocks: Keyworth, U.K., British Geological Survey Research Report RR 99-06 (reformatted), 52 p. http://nora.nerc.ac.uk/3223/1/RR99006.pdf

Gonthier, J. B., 1985, A description of aquifer units in eastern Oregon: U.S. Geological Survey Water-Resources Investigations Report 84-4095, 39 p., 4 pl., scale 1:500,000. https://doi.org/10.3133/wri844095

Gradstein, F. M., and others. 2004, A geologic time scale 2004: Cambridge University Press, 589 p.

Greene, R. C., 1972, Preliminary geologic map of the Burns and West Myrtle Butte 15-minute quadrangles, Oregon: U.S. Geological Survey Miscellaneous Field Studies Map MF-320, scale 1:62,500. https://ngmdb.usgs.gov/Prodesc/proddesc_2743.htm

Greene, R. C., 1973, Petrology of the welded tuff of Devine Canyon, southeast Oregon: U.S. Geological Survey Professional Paper 797, 26 p. https://doi.org/10.3133/pp797

Greene, R. C., Walker, G. W., and Corcoran, R. E., 1972, Geologic map of the Burns quadrangle, Oregon: U.S. Geological Survey Miscellaneous Geologic Investigations Map I-680, scale 1:250,000. https://ngmdb.usgs.gov/Prodesc/proddesc_9455.htm

Hallsworth, C. R., and Knox, R. W. O'B., 1999, BGS rock classification scheme, v. 3, Classification of sediments and sedimentary rocks: Keyworth, U.K., British Geological Survey Research Report RR 99-03, 44 p. http://nora.nerc.ac.uk/3227/1/RR99003.pdf

Houston, R. A., McClaughry, J. D., Duda, C. J. M., and Niewendorp, C. A., 2018, Geologic map of the Devine Ridge North 7.5′ quadrangle, Harney County, Oregon: Oregon Department of Geology and Mineral Industries Geologic Map Series GMS-121, 115 p., 1 pl., scale 1:24,000. https://www.oregongeology.org/pubs/gms/p-GMS-121.htm

Iademarco, M. J., 2009, Volcanism and faulting along the northern margin of Oregon's High Lava Plains: Hampton Butte to Dry Mountain: Corvallis, Oreg., Oregon State University, M.S. thesis, 158 p., 1 pl. https://ir.library.oregonstate.edu/concern/graduate_thesis_or_dissertations/t435gj391

Isom, S. L., 2017, Compositional and physical gradients in the magmas of the Devine Canyon Tuff, eastern Oregon: constraints for evolution models of voluminous high-silica rhyolites: Portland, Oreg., Portland State University, M.S. thesis, 147 p. https://pdxscholar.library.pdx.edu/open_access_etds/3885/

Johnson, D. M., Hooper, P. R., and Conrey, R. M., 1999, XRF analysis of rocks and minerals for major and trace elements on a single low dilution Li-tetraborate fused bead: Advances in X-ray Analysis, v. 41, p. 843–867. Available at: https://s3.wp.wsu.edu/uploads/sites/2191/2017/06/Johnson-Hooper-and-Conrey.pdf

Johnson, J. A., 1994, Geologic map of the Krumbo Reservoir quadrangle, Harney County, southeastern Oregon: U.S. Geological Survey Miscellaneous Field Studies Map MF-2267, 11 p., 1 pl., scale 1:24,000. https://pubs.er.usgs.gov/publication/mf2267

Johnson, J. A, 1995, Geologic evolution of the Duck Creek Butte eruptive center, High Lava Plains, southeastern Oregon: Corvallis, Oreg., Oregon State University, M.S. thesis, 151 p., 2 pl. https://ir.library.oregonstate.edu/concern/graduate_thesis_or_dissertations/bn999b569?locale=en

Johnson, J. A., 1996, Geologic map of the Page Springs quadrangle, Harney County, southeastern Oregon: U.S. Geological Survey Open-File Report OF-96-675, 1 pl., scale 1:24,000. https://ngmdb.usgs.gov/Prodesc/proddesc_18672.htm

Johnson, J. A., and A. L. Grunder, 2000, The making of intermediate composition magma in a bimodal suite: Duck Butte Eruptive Center, Oregon, USA: Journal of Volcanology and Geothermal Research, 95, 175–195.

Jordan, B. T., 2001, Basaltic volcanism and tectonics of the High Lava Plains, southeastern Oregon: Corvallis, Oreg., Oregon State University, Ph.D. dissertation, 218 p., https://ir.library.oregonstate.edu/concern/graduate_thesis_or_dissertations/nv935579s?locale=en

Jordan, B. T., Streck, M. J., and Grunder, A. L., 2002, Bimodal volcanism and tectonism of the High Lava Plains, Oregon, *in* Moore, G. W., ed., Field guide to geologic processes in Cascadia, Field trips to accompany the 98th Annual Meeting of the Cordilleran Section of the Geological Society of America, May 13–15, 2002, Corvallis, Oregon: Oregon Department of Geology and Mineral Industries Special Paper 36, p. 23–46. https://www.oregongeology.org/pubs/sp/SP-36.pdf

Jordan, B. T., Grunder, A. L., Duncan, R. A., and Deino, A. L., 2004, Geochronology of age-progressive volcanism of the Oregon High Lava Plains: implications for the plume interpretation of Yellowstone: Journal of Geophysical Research, v. 109, no. B10, B10202, 19 p. https://doi.org/10.1029/2003JB002776

Kasbohm, J., and Schoene, B., 2018, Rapid eruption of the Columbia River flood basalt and correlation with mid-Miocene climate optimum; Science Advances v. 4, no. 9. https://advances.sciencemag.org/content/4/9/eaat8223

Khatiwada, M., and Keller, G. R., 2015, An integrated geophysical imaging of the upper crustal features in the Harney Basin, southeast Oregon: Geosphere, v. 11, no. 1, p. 185–200. https://doi.org/10.1130/GES01046.1

Langer, V. W., 1991, Geology and petrologic evolution of the silicic to intermediate volcanic rocks underneath Steens Mountain basalt, SE Oregon: Corvallis, Oreg., Oregon State University, M.S. thesis, 109 p., 1 pl., scale 1:24,000. https://ir.library.oregonstate.edu/concern/graduate_thesis_or_dissertations/p8418q421

Lawrence, R. D., 1976, Strike-slip faulting terminates the Basin and Range province in Oregon: Geological Society of America Bulletin, v. 87, no. 6, p. 846–850. https://doi.org/10.1130/0016-7606(1976)87<846:SFTTBA>2.0.CO;2

Le Bas, M. J., and Streckeisen, A. L., 1991, The IUGS systematics of igneous rocks: Journal of the Geological Society, v. 148, no. 5, p. 825–833. https://doi.org/10.1144/gsjgs.148.5.0825

Le Bas, M. J., Le Maitre, R. W., Streckeisen, A., and Zanettin, B., 1986, A chemical classification of volcanic rocks based on the total alkali-silica diagram: Journal of Petrology, v. 27, no. 3, p. 745–750. https://doi.org/10.1093/petrology/27.3.745

Le Maitre, R. W., and others, 1989, A classification of igneous rocks and glossary of terms: Recommendations of the International Union of Geological Sciences Subcommission on the Systematics of Igneous Rocks: Oxford, Blackwell, 193 p.

Le Maitre, R. W. (ed.), and others, 2004, Igneous rocks: a classification and glossary of terms: recommendations of the International Union of Geological Sciences, Subcommission on the Systematics of Igneous Rocks: Cambridge, Cambridge University Press, 236 p.

Leonard, A. R., 1970, Ground-water resources in Harney Valley, Harney County, Oregon: Salem, Oreg., Oregon Water Resources Department, Ground Water Report 16, 65 p., 3 pl., scale 1:125,000. https://www.oregon.gov/owrd/wrdreports/gw_report_16_harney.pdf

Mackenzie, W. S., Donaldson, C. H., and Guilford, C., 1997, Atlas of igneous rocks and their textures (7th ed.): Addison Wesley Longman, 148 p.

MacLean, J. W., 1994, Geology and geochemistry of Juniper Ridge, Horsehead Mountain, and Burns Butte: implications for the petrogenesis of silicic magma on the high lava plains, southeastern Oregon: Corvallis, Oreg., Oregon State University, M.S. thesis, 141 p. https://ir.library.oregonstate.edu/concern/graduate_thesis_or_dissertations/zp38wf64g?locale=en

MacLeod, N.S., and Sherrod, D.R., 1992, Reconnaissance geologic map of the west half of the Crescent 1° by 2° quadrangle, central Oregon: U.S. Geological Survey Miscellaneous Investigations Map I-2215, scale 1:250,000.

MacLeod, N.S., Walker, G.W., and McKee, E.H., 1975, Geothermal significance of eastward increase in age of Upper Cenozoic rhyolitic domes in southeastern Oregon: U.S. Geological Survey Open-File Report 75-348, 21 p.

MacLeod, N. S., Walker, G. W., and McKee, E. H., 1976, Geothermal significance of eastward increase in age of upper Cenozoic rhyolitic domes in southeastern Oregon, *in* Second United Nations Symposium on the Development and Use of Geothermal Resources, v. 1: Washington D.C., Government Printing Office, p. 465–474.

McClaughry, J.D., Duda, C. J. M., and Ferns, M. L., 2019, Geologic map of the Poison Creek and Burns 7.5' quadrangles, Harney County, Oregon: Oregon Department of Geology and Mineral Industries Geological Map Series GMS 123, 127 p., 2 plates, scale 1:24,000, Esri format geodatabase; shapefiles, metadata; spreadsheet (4 sheets). https://www.oregongeology.org/pubs/gms/p-GMS-123.htm

McClaughry, J. D., Niewendorp, C.A., Franczyk, J. J., Duda, C. J. M., and Madin, I. P., 2020, Mineral Information Layer for Oregon, release 3 [MILO-3]: Oregon Department of Geology and Mineral Industries Digital Data Series MILO-3, Esri geodatabase. https://www.oregongeology.org/milo/index.htm

McGrane, D. J., 1985, Geology of the Idol City area: a volcanic-hosted, disseminated precious-metal occurrence in east-central Oregon: Missoula, Mont., University of Montana, M.S. thesis, 88 p. https://scholarworks.umt.edu/etd/7536

McPhie, J., Doyle, M., Allen, R. L., and Allen, R., 1993, Volcanic textures: A guide to the interpretation of textures in volcanic rocks: Centre for Ore Deposit and Exploration Studies, University of Tasmania, 198 p.

Meigs, A., Scarberry, K., Grunder, A., Carlson, R., Ford, M. T., Fouch, M., Grove, T., Hart, W. K., Iademarco, M., Jordan, B., and Milliard, J., 2009, Geological and geophysical perspectives on the magmatic and tectonic development, High Lava Plains and northwest Basin and Range, *in* O'Connor, J. E., Dorsey, R. J., and Madin, I. P., GSA Field Guide 15, Volcanoes to Vineyards: Boulder, Colo., Geological Society of America. https://doi.org/10.1130/2009.fld015(21)

Milliard, J. B., 2010, Two-stage opening of the northwestern Basin and Range in eastern Oregon: Evidence from the Miocene Crane Basin: Corvallis, Oreg., Oregon State University, M.S. thesis, 82 p. https://ir.library.oregonstate.edu/concern/graduate_thesis_or_dissertations/fn107319d

Minor, S. A., Rytuba, J. J., Meulen Vander, D. B., Grubensky, M. J., and Tegtmeyer, K. J., 1987a, Geologic map of the Wildhorse Lake quadrangle, Harney County, Oregon: U.S. Geological Survey Miscellaneous Field Studies Map MF-1915, 1 sheet, scale 1:24,000.

Minor, S. A., Rytuba, J. J., Goeldner, C. A., and Tegtmeyer, K. J., 1987b, Geologic map of the Alvord Hot Springs quadrangle, Harney County, Oregon: U.S. Geological Survey Miscellaneous Field Studies Map MF-1916, 1 sheet, scale 1:24,000.

Moore, N. E., Grunder, A. L., and Bohrson, W. A., 2018, The three-stage petrochemical evolution of the Steens Basalt (southeast Oregon, USA) compared to large igneous provinces and layered mafic intrusions: Geosphere, v. 14, no. 6, p. 2505-2532.

Niem, A. R., 1974, Wright's Point, Harney County, Oregon: an example of inverted topography: Ore Bin, v. 36, no. 3, 33–49. https://www.oregongeology.org/pubs/OG/OBv36n03.pdf

Niewendorp, C. A., and Neuhaus, M. E., 2003, Map of selected earthquakes for Oregon, 1841 through 2002: Oregon Department of Geology and Mineral Industries Open-File Report O-03-02, 1 pl. https://www.oregongeology.org/pubs/ofr/p-O-03-02.htm

Niewendorp, C. A., and Ricker, T. R., Rabjohns, K. W., and Brodie, S. H., 2012, Geothermal Information Layer for Oregon, release 2 [GTILO-2]: Oregon Department of Geology and Mineral Industries Digital Data Series, GIS files, 1:100,000-scale. https://www.oregongeology.org/gtilo/index.htm.

Niewendorp, C. A., Duda, C. J. M., Houston, R. A., and McClaughry, J. D., 2018, Geologic map of the Devine Ridge South 7.5′ quadrangle, Harney County, Oregon: Oregon Department of Geology and Mineral Industries Geologic Map Series GMS-120, 65 p., 1 pl., scale 1:24,000. https://www.oregongeology.org/pubs/gms/p-GMS-120.htm

Ogg, J. G., Ogg, G., and Gradstein, F. M., 2008, The concise geologic time scale: Cambridge University Press, 150 p.

Parker, D. J., 1974, Petrology of selected volcanic rocks of the Harney Basin, Oregon: Corvallis, Oreg., Oregon State University, Ph.D. dissertation, 153 p., 1 pl. https://ir.library.oregonstate.edu/concern/graduate_thesis_or_dissertations/r494vn606

Personius, S. F., and Haller, K. M., compilers, 2016, Fault number 856c, Steens fault zone, Alvord section, *in* Quaternary fault and fold database of the United States: U.S. Geological Survey website, https://earthquakes.usgs.gov/hazards/qfaults

Piper, A. M., Robinson, T. W., and Park C. F., 1939, Geology and ground-water resources of the Harney Basin, Oregon: U.S. Geological Survey Water Supply Paper 841, 189 p., 1 pl., scale 1:125,000. https://pubs.er.usgs.gov/publication/wsp841

Robertson, S., 1999, BGS rock classification scheme, v. 2, Classification of metamorphic rocks: Keyworth, U.K., British Geological Survey Research Report RR 99-02, 24 p. http://nora.nerc.ac.uk/id/eprint/3226/1/RR99002.pdf

Russell, I. C., 1884, A geological reconnaissance in southern Oregon: U.S. Geological Survey Annual Report 4 (1882-1883), p. 431–464. https://doi.org/10.3133/ar4

Scarberry, K., Meigs, A., and Grunder, A., 2009, Faulting in a propagating continental rift: Insight from the late Miocene structural development of the Abert Rim fault, southern Oregon, USA: Tectonophysics, v. 488, no. 1–4, p. 71–86. https://doi.org/10.1016/j.tecto.2009.09.025

Sheppard, R. A., 1994, Zeolitic diagenesis of tuffs in Miocene lacustrine rocks near Harney Lake, Harney County, Oregon: U.S. Geological Survey Bulletin 2108, 28 p. https://pubs.usgs.gov/bul/2108/report.pdf

Sherrod, D. R., and Johnson, J. A., 1994, Geologic map of the Irish Lake quadrangle, Harney County, south-central Oregon: U.S. Geological Survey Miscellaneous Field Studies Map MF-2256, 1 sheet, scale 1:24,000. https://ngmdb.usgs.gov/Prodesc/proddesc_5877.htm

Silberling, N. J., Jones, D. L., and Blake, M. C., Jr., 1984, Lithotectonic terrane map of the conterminous western United States, Pt C *of* Silberling, N. J., and Jones D. L., eds., Lithotectonic terrane maps of northern Cordillera: U.S. Geological Survey Open-File Report 84-523, 43 p. https://doi.org/10.3133/ofr84523

Smith, G. A., 1986a, Stratigraphy, sedimentology, and petrology of Neogene rocks in the Deschutes Basin, central Oregon: a record of continental margin volcanism and its influence on fluvial sedimentation in an arc-adjacent basin: Corvallis, Oreg., Oregon State University, Ph.D. dissertation, 467 p, 3 pl., scale 1:24,000. https://ir.library.oregonstate.edu/concern/graduate_thesis_or_dissertations/c247dw09t

Smith, G. A., 1986b, Stratigraphy, sedimentology, and the petrology of Neogene rocks in the Deschutes Basin, central Oregon: A record of continental-margin volcanism and its influence on fluvial sedimentation in an arc-adjacent basin: Richland, Wash., U.S. Department of Energy Basalt Waste Isolation Project, Rockwell Hanford Operations Publication RHO-BW-SA-555-P, 1 pl., scale 1:24,000.

Smith, R. L., and Roe, W. P., 2015, Oregon geologic data compilation [OGDC], release 6 (statewide): Oregon Department of Geology and Mineral Industries Digital Data Series OGDC-6, geodatabase. https://www.oregongeology.org/pubs/dds/p-OGDC-6.htm

Streck, M. J., 1994, Volcanology and petrology of the Rattlesnake Ash-flow Tuff, eastern Oregon: Corvallis, Oreg., Oregon State University, Ph.D. dissertation, 184 p. https://ir.library.oregonstate.edu/concern/graduate_thesis_or_dissertations/kh04ds239

Streck, M., and Ferns, M. L., 2004, The Rattlesnake Tuff and other Miocene silicic volcanism in eastern Oregon, chap. 1 *of* Haller, K. M., and Wood, S. H., Geological field trips in southern Idaho, eastern Oregon, and northern Nevada: U.S. Geological Survey Open-File Report 2004-1222, p. 4–19. https://pubs.usgs.gov/of/2004/1222/

Streck, M. J., and Grunder, A. L., 1995, Crystallization and welding variations in a widespread ignimbrite sheet; the Rattlesnake Tuff, eastern Oregon, USA: Bulletin of Volcanology, v. 57, no. 3, p. 151–169. https://doi.org/10.1007/BF00265035

Streck, M. J., and Grunder, A. L., 2008, Phenocryst-poor rhyolites of bimodal, tholeiitic provinces: The Rattlesnake Tuff and implications for mush extraction models: Bulletin of Volcanology, v. 70, no. 3, p. 385–401. https://doi.org/10.1007/s00445-007-0144-3

Streck, M. J., and A. L. Grunder (2012), Temporal and crustal effects on differentiation of tholeiite to calcalkaline and ferrotrachytic suites, High Lava Plains, Oregon, USA: Geochemistry, Geophysics, Geosystems, 13, Q0AN02, doi:10.1029/2012GC004237.

Streck, M. J., Johnson, J. A., and Grunder, A. L., 1999, Field guide to the Rattlesnake Tuff and High Lava Plains near Burns, Oregon: Ore Bin, v. 61, no. 3, 64–76. https://www.oregongeology.org/pubs/og/OGv61n03.pdf

Streck, M. J., Ferns, M. L., and McIntosh, W., 2015, Large, persistent rhyolitic magma reservoirs above Columbia River Basalt storage sites: The Dinner Creek Tuff Eruptive Center, eastern Oregon: Geological Society of America, Geosphere, v. 11, no. 2, 226–235. https://doi.org/10.1130/GES01086.1

Thormahlen, D. J., 1984, Geology of the northwest one-quarter of the Prineville quadrangle, central Oregon: Corvallis, Oreg., Oregon State University, M.S. thesis, 106 p. 1 pl., scale 1:24,000.

Trench, D., 2008, The termination of the Basin and Range Province into a clockwise rotating region of transtension and volcanism, central Oregon: Corvallis, Oreg., Oregon State University, M.S. thesis, 64 p. https://ir.library.oregonstate.edu/concern/graduate_thesis_or_dissertations/qr46r331w

Trench, D., Meigs, A., and Grunder, A., 2012, Termination of the northwestern Basin and Range Province into a clockwise rotating region of transtension and volcanism, southeast Oregon: Structural Geology, v. 39, p. 52-65.

U.S. Geological Survey National Cooperative Geologic Mapping Program, 2010, NCGMP09—Draft standard format for digital publication of geologic maps, version 1.1, *in* Soller, D. R., ed., Digital Mapping Techniques '09—Workshop Proceedings: U.S. Geological Survey Open-File Report 2010–1335, p. 93–146. https://ngmdb.usgs.gov/Info/standards/GeMS/#docs

U.S. Geological Survey National Cooperative Geologic Mapping Program, 2018, GeMS (Geologic Map Schema)—a standard format for digital publication of geologic maps: U.S. Geological Survey, version 2, draft 7, 78 p. https://ngmdb.usgs.gov/Info/standards/GeMS/#docs

Walker, G. W., 1969, Geology of the High Lava Plains province, *in* A. E. Weissenborn, ed., Mineral and Water Resources of Oregon: Oregon Department of Geology and Mineral Industries Bulletin 64, 77–79. https://www.oregongeology.org/pubs/B/B-064.pdf

Walker, G. W., 1970, Cenozoic ash-flow tuffs of Oregon: Ore Bin, v. 32, no. 6, 97–115. https://www.oregongeology.org/pubs/OG/OBv32n06.pdf

Walker, G. W., 1974, Some implications of Late Cenozoic volcanism to geothermal potential in the High Lava Plains of south-central Oregon: Ore Bin, v. 36, no. 7, p. 109–119. https://www.oregongeology.org/pubs/og/OBv36n07.pdf

Walker, G. W., 1977, Geologic map of Oregon east of the 121st meridian: U.S. Geological Survey Miscellaneous Investigations Map I-902, 2 sheets, scale 1:500,000. https://ngmdb.usgs.gov/Prodesc/proddesc_9795.htm

Walker, G. W., 1979, Revisions to the Cenozoic stratigraphy of Harney Basin, southeastern Oregon: U.S. Geological Survey Bulletin 1475, 35 p., 1 pl. https://doi.org/10.3133/b1475

Walker, G. W., and MacLeod, N. S., 1991, Geologic map of Oregon: U.S. Geological Survey, scale 1:500,000. https://ngmdb.usgs.gov/Prodesc/proddesc_16259.htm

Walker, G. W., and Nolf, B., 1981, High Lava Plains, Brothers fault zone to Harney Basin, Oregon, *in* Johnson, D.A., and Donnelly-Nolan, J., eds., Guides to Some Volcanic Terranes in Washington, Idaho, Oregon, and Northern California: U.S. Geological Survey Circular 838, p. 105–111. https://doi.org/10.3133/cir838

Weldon, R. J., II, Fletcher, D. K., Weldon, E. M., Scharer, K. M., and McCrory, P. A., 2003, An update of Quaternary faults of central and eastern Oregon: U.S. Geological Survey Open-File Report 02-301. http://pubs.usgs.gov/of/2002/of02-301/

Wentworth, C. K., 1922, A scale of grade and class terms of clastic sediments: Journal of Geology, v. 30, no. 5, p. 377–392. https://www.jstor.org/stable/30063207

Whitehead, R. L., 1994, Ground water atlas of the United States: Segment 7, Idaho, Oregon, Washington: U.S. Geological Survey Hydrologic Atlas 730-H, 31 p. https://doi.org/10.3133/ha730H

Zakšek, K., Oštir, K., and Kokalj, Ž., 2011, Sky-view factor as a relief visualization technique: Remote Sensing, v. 3, no. 2, p. 398–415. https://doi.org/10.3390/rs3020398

13.0 APPENDIX

This appendix contains a summary of the geodatabase along with a description of analytical and field methods and the list of attribute fields for spreadsheets (see page 5 of this report). The appendix is divided into two sections:

- Section 13.1 describes the digital databases included with this publication.
- Section 13.2 contains a summary of analytical and field methods. Accompanying tables explain the fields listed in various spreadsheets.

13.1 Geographic Information Systems (GIS) database

Geodatabase specifications

Digital data created for the Burns Butte 7.5′ quadrangle is stored in an Esri format geodatabase. The geodatabase structure follows that outlined by the U.S. Geological Survey (USGS) Geologic Map Schema (GeMS), version 2.7 (USGS National Cooperative Geologic Mapping Program, 2018). The following information describes the overall database structure, the feature classes, and supplemental tables (**Figure 13-1**, **Figure 13-2**, **Figure 13-3**, **Table 13-1**, and **Table 13-2**).

The data are stored in a file geodatabase feature dataset (GeologicMap). Accessory file geodatabase tables (DataSources, DescriptionOfMapUnits, GeoMaterialDict, and Glossary) were created by using ArcGIS version 10.7 (SP 1). The GeologicMap feature dataset contains all the spatially oriented data (feature classes) created for the Burns Butte 7.5′ quadrangle. The file geodatabase tables are used to hold additional geologic attributes. Additional information and complete descriptions of the "GeMS" — Geologic Map Schema (formerly "NCGMP09") can be found at https://ngmdb.usgs.gov/Info/standards/GeMS/#docs.

Figure 13-1. Burns Butte 7.5′ quadrangle geodatabase feature dataset and data tables.

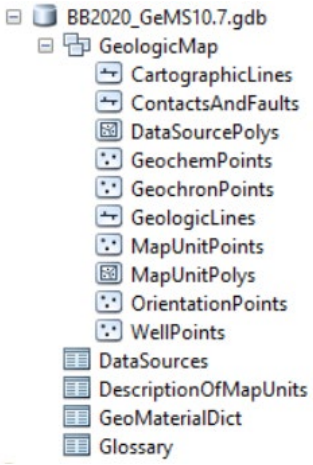

Geodatabase feature class specifications

Each feature class within the GeologicMap feature dataset in the geodatabase contains detailed metadata. Please see the embedded metadata for detailed information such as process descriptions, accuracy specifications, and entity attribute descriptions.

Figure 13-2. Burns Butte 7.5' quadrangle geodatabase feature classes and descriptions.

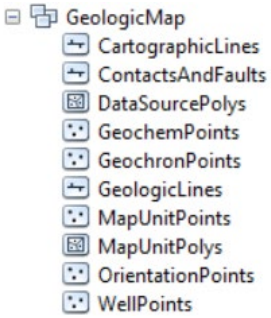

Table 13-1. Feature class description.

Name	Description
CartographicLines	Vector lines that have no real-world physical existence and do not participate in map-unit topology. The feature class includes cross section lines used for cartography for the quadrangle.
ContactsAndFaults	The vector lines in this feature class contain geologic content including contacts and fault locations used to create the map unit polygon boundaries. The existence and location confidence values for the contacts and faults are provided in the feature class attribute table.
DataSourcePolys	This feature class contains polygons that delineate data sources for all parts of the geologic map. These sources may be a previously published map, new mapping, or mapping with a certain technique. For a map with one data source, for example all new mapping, this feature class contains one polygon that encompasses the map area.
GeochemPoints	This feature class represents point locations where whole-rock samples have been analyzed by X-ray fluorescence (XRF) techniques in the quadrangle. Includes data collected by the authors during this study or compiled from previous studies. These data are also contained in the geochemistry spreadsheet described in more detail below.
GeochronPoints	This feature class represents point locations where $^{40}Ar/^{39}Ar$ isotopic ages have been obtained for rock samples in the quadrangle. Includes data collected by the authors during this study or compiled from previous studies. These data are also contained in the geochronology spreadsheet described in more detail below.
GeologicLines	These vector lines represent known fold axis locations in the quadrangle. The existence and location confidence for the fold axes are provided in the feature class attribute table.
MapUnitPoints	This feature class represents points used to generate the MapUnitPolys feature class from the ContactsAndFaults feature class.
MapUnitPolys	This polygon feature class represents the geologic map units as defined by the authors.
OrientationPoints	This feature class represents point locations in the quadrangle where structural measurements were made or were compiled from previous studies. These data are also contained in the bedding (strike and dip) spreadsheet described in more detail below.
WellPoints	This feature class represents point locations of water wells in the quadrangle. Includes data obtained by the authors from the Oregon Department of Water Resources (OWRD). These data are also contained in the Wells spreadsheet described in more detail below.

Geodatabase table specifications

Figure 13-3. Burns Butte 7.5' quadrangle geodatabase data tables.

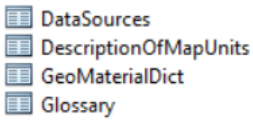

Table 13-2. Geodatabase tables.

Name	Description
DataSources	Data table that contains information about data sources used to compile the geology of the area.
DescriptionOfMapUnits	Data table that captures the content of the Description of Map Units (DMU), or equivalent List of Map Units and associated pamphlet text, included in a geologic map.
GeoMaterialDict	Data table providing definitions and hierarchy for GeoMaterial names prescribed by the GeMS database schema.
Glossary	Data table that contains information about the definitions of terms used in the geodatabase.

Geodatabase projection specifications

All spatial data are stored in the Oregon Statewide Lambert Conformal Conic projection. The datum is NAD83 HARN. The linear unit is international feet. See detailed projection parameters below:

Projection: Lambert_Conformal_Conic
False_Easting: 1312335.958005
False_Northing: 0.0
Central_Meridian: -120.5
Standard_Parallel_1: 43.0
Standard_Parallel_2: 45.5
Latitude_Of_Origin: 41.75
Linear Unit: Foot (0.3048)

Geographic Coordinate System: GCS_North_American_1983_HARN
Angular Unit: Degree (0.0174532925199433)
Prime Meridian: Greenwich (0.0)
Datum: D_North_American_1983_HARN
Spheroid: GRS_1980
Semimajor Axis: 6378137.0
Semiminor Axis: 6356752.314140356
Inverse Flattening: 298.257222101

Geologic map

This report is accompanied by a single map plate displaying the surficial and bedrock geology at a scale of 1:24,000 and geologic cross sections (see Plate 1 facsimile below) for the Burns Butte 7.5′ quadrangle. The map plate was generated from detailed geologic data (scale of 1:8,000 or better) contained in the accompanying Esri format geodatabase. Both bedrock and surficial geologic interpretations can be recovered from the geodatabase and can be used to create a variety of additional thematic maps.

Figure 13-4. Reproduction of the geologic map of the Burns Butte 7.5′ quadrangle, Harney County, Oregon (Plate 1). Plate dimensions are 35 by 47 inches, scale 1;24,000. See digital folder for map plate.

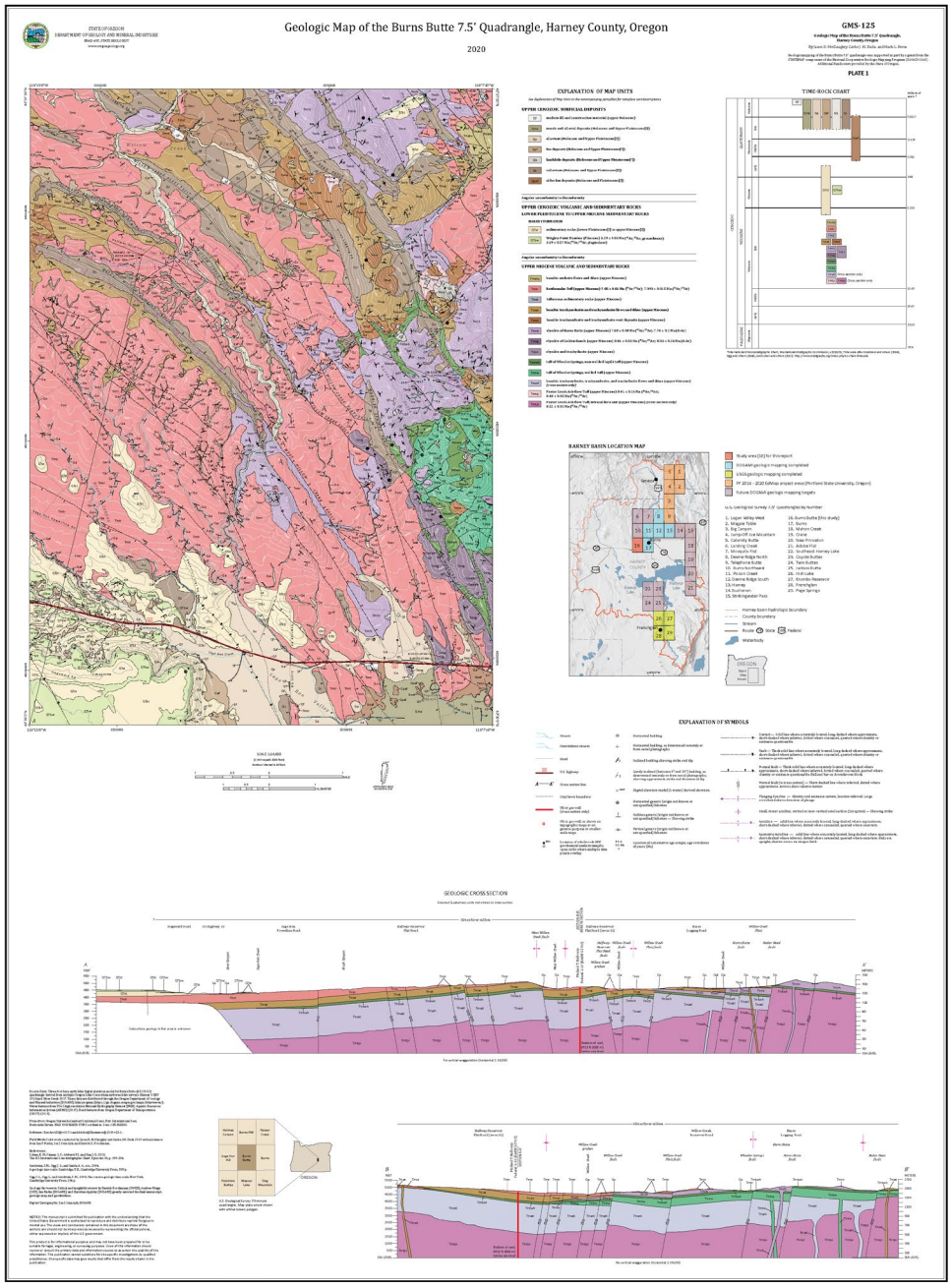

13.2 Methods

Geochemical analytical methods

Geologic mapping in the Burns Butte 7.5′ quadrangle was supported by numerous new and compiled X-ray fluorescence (XRF) geochemical analyses of whole-rock samples. Descriptive rock unit names for igneous rocks are based on normalized major element analyses plotted on the total alkalis ($Na_2O + K_2O$) versus silica (SiO_2) diagram (TAS) of Le Bas and others (1986), Le Bas and Streckeisen (1991), and Le Maitre and others (1989, 2004). New and compiled XRF-geochemical analyses are included in the geodatabase, in a separate shapefile named BB2020_Geochemistry, and in Microsoft Excel® workbook BB2020_DATA.xls (sheet BB2020_Geochemistry). **Table 13-3** describes the fields listed in the spreadsheet. The locations of all geochemical samples are given in five coordinate systems: UTM Zone 11 (datum = NAD 27, NAD 83, units = meters), Geographic (datum = NAD 27, NAD 83, units = decimal degrees), and Oregon Lambert (datum = NAD 83, HARN, units = international feet).

Samples denoted by lab abbreviation WSU were analyzed by XRF at the Washington State University GeoAnalytical Lab, Pullman, Washington. Analytical procedures for the Washington State University GeoAnalytical Lab are described by Johnson and others (1999) and are available online at https://environment.wsu.edu/facilities/geoanalytical-lab/technical-notes/. The location of each sample is given in five coordinate systems: UTM Zone 11 (datum = NAD 27, NAD 83, units = meters), Geographic (datum = NAD 27, NAD 83, units = decimal degrees), and Oregon Lambert (datum = NAD 83, HARN, units = international feet). Notes for spreadsheet: −9 equals no data for numerical fields for analytical data; nd equals no data in text fields; na equals information not applicable for text fields; samples shown with an "R" (e.g., 121 BBJ 19R) are a repeat analysis of a single sample.

Table 13-3. Geochemistry spreadsheet field names and descriptions.

Field	Description
Type	The geochemical method used by laboratory that analyzed the sample – e.g., XRF, ICP-MS
FieldSampleID	Unique alpha-numeric id applied to the sample at time of collection– e.g., 21 BBJ 19.
AlternateSampleID	Alternate unique alpha-numeric id applied to the sample by lab, museum, etc. – e.g., 21 BBJ 19R.
Symbol	References a FGDC symbol in the GeMS style file – e.g., 31.21.
Label	Free text. A unique number identifying the sample on the map plates – e.g., G1.
LocationConfidenceMeters	Radius in meters of positional uncertainty envelope for the observation locale. Null values not permitted. Recommended value is -9 if value is not otherwise available.
PlotAtScale	Cartographic map scale or larger that the observation or analysis should be plotted at. Value is scale denominator.
Quadrangle	The USGS 7.5' quadrangle in which the sample is located – e.g., Burns Butte.
Elevation	Elevation of data location in feet – e.g., 22.
MapUnit	Map unit from which the analyzed sample was collected – e.g., Tmrb.
MaterialAnalyzed	Type of material analyzed – e.g., whole rock.
TASLithology	Rock name assigned based on the total alkalis ($Na_2O + K_2O$) versus silica (SiO_2) diagram (TAS) of Le Bas and others (1986), Le Bas and Streckeisen (1991), and Le Maitre and others (1989) – e.g., basalt, rhyolite.
MajorElements	SiO_2, Al_2O_3, TiO_2, FeOTotal, MnO, CaO, MgO, K_2O, Na_2O, P_2O_5. In wt. percent.
TraceElements	Ni, Cr, Sc, V, Ba, Rb, Sr, Zr, Y, Nb, Ga, Cu, Zn, Pb, La, Ce, Th, Nd, U, Cs, Co, Hf, Sm, Eu, Yb, Lu. In ppm.
TotalInitial	Original analytical total as reported by the lab.
LossOnIgnition	Value for loss on ignition as reported by the laboratory.
FE2O3	Iron (III) oxide or ferric oxide reported in original analysis.
FeO	Iron (II) oxide or ferrous oxide reported in original analysis.
UTMNorthingNAD27	Meters north in NAD 27 UTM projection, zone 11.
UTMEastingNAD27	Meters east in NAD 27 UTM projection, zone 11.
LatitudeNAD27	Latitude in NAD 27 geographic coordinates.
LongitudeNAD27	Longitude in NAD 27 geographic coordinates.
UTMNorthingNAD83	Meters north in NAD 83 UTM projection, zone 11.
UTMEastingNAD83	Meters east in NAD 83 UTM projection, zone 11.
LatitudeNAD83	Latitude in NAD 83 geographic coordinates.
LongitudeNAD83	Longitude in NAD 83 geographic coordinates.
Northing83HARN	Feet north in Oregon Lambert NAD 83, HARN, international feet.
Easting83HARN	Feet east in Oregon Lambert NAD 83, HARN, international feet.
LocationSourceID	Unique data source from which the data was obtained – e.g., McClJD2020.
AnalysisSourceID	Foreign key to DataSources. Identifies source of analytical data for this sample. Null values not permitted – e.g., WSU.
Notes	Special information about certain samples – e.g., alteration.
GeochemPoints_ID	Primary key. e.g., GCM01

Geochronology analytical methods

Three K/Ar and $^{40}Ar/^{39}Ar$ isotopic ages were compiled for this study. Three new samples were analyzed by the $^{40}Ar/^{39}Ar$ method at the College of Oceanic and Atmospheric Sciences, Oregon State University, Corvallis (OSU), under the direction of Dr. Dan Miggins. The methodology for $^{40}Ar/^{39}Ar$ geochronology at OSU is summarized on the Web at http://geochronology.coas.oregonstate.edu/ and in Duncan and Keller (2004). Geochronological data are included in the geodatabase, in a separate shapefile named BB2020_Geochronology, and in Microsoft Excel® workbook BB2020_DATA.xls (sheet BB2020_Geochronology). **Table 13-4** describes the fields listed in the spreadsheet. The location of each isotopic age is given in five coordinate systems: UTM Zone 11 (datum = NAD 27, NAD 83, units = meters), Geographic (datum = NAD 27, NAD 83, units = decimal degrees), and Oregon Lambert (datum = NAD 83, HARN, units = international feet). Notes for spreadsheet: −9 equals no data for numerical fields for analytical data; nd equals no data in text fields; na equals information not applicable for text fields.

Table 13-4. Geochronology spreadsheet field names and descriptions.

Field	Description
Type	The geochronological method – e.g., $^{40}Ar/^{39}Ar$, K-Ar, radiocarbon, mineral - whole-rock Rb-Sr isochron, etc.) used to estimate the age.
FieldSampleID	Unique alpha-numeric id applied to the sample – e.g., 21 BBJ 19.
AlternateSampleID	Alternate unique alpha-numeric id applied to the sample by lab, museum, etc. – e.g., 21 BBJ 19R.
MapUnit	Map unit from which the analyzed sample was collected.
Symbol	References a symbol in the GeMS style file.
Label	Isotopic age of sample with error – e.g., 8.52 ± 0.02 Ma
LocationConfidenceMeters	Radius in meters of positional uncertainty envelope for the observation locale. Null values not permitted. Recommended value is -9 if value is not otherwise available.
PlotAtScale	Cartographic map scale or larger that the observation or analysis should be plotted at. Value is scale denominator.
MaterialAnalyzed	Type of material analyzed – e.g., amphiboles, plagioclase.
NumericAge	Interpreted (preferred) age calculated from geochronological analysis, not necessarily the date calculated from a single set of measurements.
AgePlusError	The maximum potential error before the numerical age.
AgeMinusError	The maximum potential error after the numerical age.
AgeUnits	Values = years, Ma, ka, radiocarbon ka, calibrated ka, etc.
UTMNorthingNAD27	Meters north in NAD 27 UTM projection, zone 11.
UTMEastingNAD27	Meters east in NAD 27 UTM projection, zone 11.
LatitudeNAD27	Latitude in NAD 27 geographic coordinates.
LongitudeNAD27	Longitude in NAD 27 geographic coordinates.
UTMNorthingNAD83	Meters north in NAD 83 UTM projection, zone 11.
UTMEastingNAD83	Meters east in NAD 83 UTM projection, zone 11.
LatitudeNAD83	Latitude in NAD 83 geographic coordinates.
LongitudeNAD83	Longitude in NAD 83 geographic coordinates.
Northing83HARN	Feet north in Oregon Lambert NAD 83, HARN, international feet.
Easting83HARN	Feet east in Oregon Lambert NAD 83, HARN, international feet.
StationID	Foreign key to Stations point feature class.
LocationSourceID	Unique data source from which the data was obtained; e.g., McClJD2020.
AnalysisSourceID	Foreign key to DataSources. Identifies source of analytical data for this sample. Null values not permitted – e.g., OSU.
Notes	Special information about certain samples – e.g., alteration.
GeochronPoints_ID	e.g., GCR1

Orientation points

Structural measurements of inclined bedding and igneous foliation were taken in the Burns Butte 7.5′ quadrangle during the course of this study by traditional compass and clinometer methods. Additional structural measurements were determined from interpretation of lidar imagery. DOGAMI has developed a routine and model in Esri ArcGIS™ Model Builder to calculate three-point solutions for lidar-derived bedding. The modeling process incorporates the use of 1) a 1-m lidar-derived DEM (digital elevation model); 2) the registration of three non-collinear points picked along the trace of a geological plane or contact discernable from a 1-m lidar DEM; 3) updating these points with their lidar-derived elevation values; and 4) creating a TIN (triangular irregular network) facet of the three points. The aspect of the TIN facet is equivalent to the dip direction, and the slope corresponds to the dip (0 to 90 degrees). The strike is then determined from the dip direction, subtracting or adding 90 degrees on the basis of the right-hand rule (described in below).

The factors influencing the certainty of lidar-derived bedding are the subjectivity of the digitizer and the clarity of the feature presumed to be indicative of bedding. To improve the clarity of lidar visualization, lidar-derived bedding was compiled using both a hillshade and a slopeshade image, each at 50 percent transparency, draped over a Sky-View Factor (SVF) image. Sky-View Factor images are enhanced 1-m lidar DEMs, processed using the Sky-View Factor computation tool. The Sky-View Factor computation tool is part of the Relief Visualization Toolbox (RVT), open-source processing software produced by the Institute of Anthropological and Spatial Studies (http://iaps.zrc-sazu.si/en) at the Research Centre of the Slovenian Academy of Sciences and Arts (ZRCSAZU), to help visualize raster elevation model datasets. Sky-View visualizes hillshade models using diffuse illumination, overcoming the common problem of direct illumination, which can obscure linear objects that lie parallel to the direction of the light source and saturation of shadow areas. This brings improvements in detection of linear structures because the method exposes edges and holes (Zakšek and others, 2011). DOGAMI's visualization routine, combining a lidar-derived hillshade, slopeshade, and SVF imagery, helps illuminate shadows and amplifies the edges/ridges related to bedding features. Where possible, aerial photography, combined with a contextual knowledge of the geology of the area, was used to verify bedding features interpreted from lidar.

Strikes and dips are reported in both quadrant format (e.g., N. 30° W., 15° NE.) and azimuthal format using the right-hand rule (e.g., 330°, 15° NE., American convention). Field-measured bedding is coded by its appropriate Federal Geographic Data Committee (FGDC) reference number for geologic map symbolization. The measured point data are included in the geodatabase, in a separate shapefile named BB2020_Orientation, and in Microsoft Excel® workbook BB2020_DATA.xls (sheet BB2020_Orientation). **Table 13-5** describes the fields listed in the spreadsheet. The locations of these point data are given in five coordinate systems: UTM Zone 10 (datum = NAD 27, NAD 83, units = meters), Geographic (datum = NAD 27, NAD 83, units = decimal degrees), and Oregon Lambert (datum = NAD 83, HARN, units = international feet). Strike and dip symbols can be properly drawn by the Esri ArcMap product by opening the layer properties, categorizing by type, choosing the appropriate symbol, and rotating the symbol based on the "Strike_Azi" field. (The Advanced button allows one to select the rotation field.) The rotation style should be set to geographic in order to maintain the right-hand rule property. Azimuths are given in true north; an additional clockwise correction of about 1.6 degrees is needed to plot strikes and dips properly on the Oregon Lambert conformal conic projection in this area. Notes for spreadsheet: nd, no data.

Table 13-5. Orientation points spreadsheet field names and descriptions.

Field	Description
Type	Type of geologic structure from which feature was determined – e.g., Inclined bedding.
Azimuth	Strike or trend, measured in degrees clockwise from geographic North. Values limited to range 0-360. Use right-hand rule (dip is to right of azimuth direction). Horizontal planar features may have any azimuth – e.g., 20.
Inclination	Dip or plunge, measured in degrees down from horizontal. Values limited to range -90 to 90. Types defined as horizontal (e.g., horizontal bedding) have Inclination=0. Null values not Data type=float – e.g., 45.
StrikeQuadrant	Strike direction of the inclined plane, stated in a north-directed quadrant format – e.g., N35E.
DipQuadrant	Amount of dip, degrees from horizontal, with direction – e.g., 45SE.
Symbol	References a FGDC symbol in the GeMS style file – e.g., 6.40.
Label	Amount of dip, degrees from horizontal – e.g., 45.
LocationConfidenceMeters	Radius in meters of positional uncertainty envelope for the observation locale. Null values not permitted. Recommended value is -9 if value is not otherwise available.
IdentityConfidence	Specifies confidence that observed structure is of the type specified; e.g., 'certain', 'questionable', 'unspecified'.
OrientationConfidenceDegrees	Estimated circular error, in degrees – e.g., 20.
PlotAtScale	Cartographic map scale or larger that the observation or analysis should be plotted at. Value is scale denominator.
Quadrangle	The USGS 7.5' quadrangle in which the sample is located – e.g., Burns Butte.
Elevation	Elevation of data location in feet – e.g., 22.
MapUnit	Map unit from which the analyzed sample was collected.
UTMNorthingNAD27	Meters north in NAD 27 UTM projection, zone 11.
UTMEastingNAD27	Meters east in NAD 27 UTM projection, zone 11.
LatitudeNAD27	Latitude in NAD 27 geographic coordinates.
LongitudeNAD27	Longitude in NAD 27 geographic coordinates.
UTMNorthingNAD83	Meters north in NAD 83 UTM projection, zone 11.
UTMEastingNAD83	Meters east in NAD 83 UTM projection, zone 11.
LatitudeNAD83	Latitude in NAD 83 geographic coordinates.
LongitudeNAD83	Longitude in NAD 83 geographic coordinates.
Northing83HARN	Feet north in Oregon Lambert NAD 83, HARN, international feet.
Easting83HARN	Feet east in Oregon Lambert NAD 83, HARN, international feet.
LocationSourceID	Unique data source from which the data was obtained – e.g., McClJD2020.
OrientationSourceID	Unique data source from which the data was obtained – e.g., McClJD2020.
Notes	Special information about the point – e.g., lidar derived.
OrientationPoints_ID	Primary key – e.g., ORP001.
PTTYPE	e.g., Bedding
RuleID1	Rule ID used for cartographic representation – e.g., 6.40.

Water well logs

The well log spreadsheet is derived from written drillers' logs provided by Oregon Department of Water Resources (OWRD). Well logs vary greatly in completeness and accuracy, so the utility of subsurface interpretations based upon these data can be limited. Water well logs compiled and used for interpretation during this study were not field located. The approximate locations were estimated using taxlot maps, street addresses (coordinates obtained from Google Earth™), and aerial photographs to plot locations on the map. The accuracy of the locations ranges widely, from errors of one-half mile possible for wells located only by section and plotted at the section centroid to a few tens of feet for wells located by address or taxlot number on a city lot with bearing and distance from a corner. At each mapped location the number of the well log is indicated. This number can be combined with the first four letters of the county name (e.g., HARN 5473), to retrieve an image of the well log from the OWRD website.

Point data are included in the geodatabase, in a separate shapefile named BB2020_Wells, and in Microsoft Excel® workbook BB2020_DATA.xls (sheet BB2020_Wells).

Table 13-6 describes the fields listed in the spreadsheet. The locations of water well point data are given in six coordinate systems: UTM Zone 11 (datum = WGS 84, NAD 27, NAD 83, units = meters), Geographic (datum = NAD 27, NAD 83, units = decimal degrees), and Oregon Lambert (datum = NAD 83, HARN, units = international feet).

Lithologies in well intervals listed in the well log spreadsheet can alternate between consolidated and unconsolidated and may be listed as alternating between bedrock and surficial geologic units. This may occur where bedrock units are soft, where paleosols or weak zones lie within bedrock, or where cemented or partly cemented zones alternate with unconsolidated zones in surficial deposits.

Lithologic abbreviations (alphabetical by group)

Unconsolidated Surficial Units	
Abbreviation	**Description**
a	ash
bd	boulders
c	clay
ch	clay, hard (often logged as claystone but probably not bedrock)
g	gravel
gc	cemented gravel
gs	gravel and sand (also sandy gravel)
m	mud
s	sand
sg	sand and gravel (also gravelly sand)
st	silt
Rock, sedimentary	
bc	breccia
cg	conglomerate
cs	claystone
sh	shale
ss	sandstone
Rock, igneous	
an	andesite
b	basalt
ba	basaltic andesite
cd	cinders
da	dacite
pu	pumice
gr	granite
l	lava
r	rhyolite
sc	scoria
t	tuff
v	volcanic, undivided
vb	volcanic breccia
Other	
af	artificial fill
cl	coal (lignite)
dg	decomposed granite
o	other (drillers unit listed in notes column of spreadsheet)
rk	rock
sl	soil
u	unknown (typically used where a well has been deepened)

Table 13-6. Water well log spreadsheet field names and descriptions.

Field	*Description and Example
Type	Type of well located; e.g., well used for domestic-water supply, well used for irrigation-water supply, drill hole for hydrocarbon exploration or exploitation- Showing name and number.
Symbol	References a FGDC symbol in the GeMS style file – e.g., 26.1.25.
Label	A unique label identifying the well, if applicable – e.g., Federal 1-10.
IdentityConfidence	Specifies confidence that observed structure is of the type specified; e.g., 'certain', 'questionable', 'unspecified'.
LocationConfidenceMeters	Radius in meters of positional uncertainty envelope for the observation locale. Null values not permitted. Recommended value is -9 if value is not otherwise available.
PlotAtScale	Cartographic map scale or larger that the observation or analysis should be plotted at. Value is scale denominator.
TownshipRangeSection	Two digits for township, two digits for range, and two for section; negative if township is south of Willamette baseline. Exception for township and range if they contain a decimal – e.g., −2132.503.
County	Harney County – e.g., HARN.
Grid	Well log number for well records assigned by the Oregon Water Resources Department. Wells in Harney County preceded by acronym HARN – e.g., HARN 53799.
WellElevation	Wellhead elevation in feet as given by Google Earth™ at corresponding WGS 84 location. e.g., 1978.
LocatedBy	Google Earth™ elevation for cursor location at a given address – e.g., Google. Google Earth™ elevation at house in vicinity of given address – e.g., House. Pad identifying approximate well location, visible in air photo – e.g., Pad. Approximate taxlot centroid or other best guess for well location using a combination of taxlot maps and aerial photographs – e.g., Taxlot. Owner name – e.g., Owner. Address of well listed on Oregon Water Resources Department (OWRD) Start Card. Wells located by Oregon Water Resources Department (OWRD) using handheld GPS – e.g., OWRD. GPS coordinates of wellhead included with well log – e.g., GPS. Approximate quarter-quarter-quarter section centroid – e.g., QQQ. Approximate quarter-quarter-section centroid – e.g., QQ. Approximate quarter-section centroid – e.g., Q. Approximate fit to sketch map included with well log – e.g., map.
Lithology	Best interpretation of driller's log using abbreviations above – e.g., g.
Base	Record base of driller's interval or, if lithology abbreviation would not change, similar intervals, in feet below wellhead – e.g., 17.
Top	Calculated top of driller's interval or similar intervals, in feet below wellhead – e.g., 14.
TopElevation	Calculated elevation at top of driller's interval, or similar intervals, in feet above sea level – e.g., 86.
BaseElevation	Calculated elevation at base of driller's interval, or similar intervals, in feet above sea level – e.g., 83.
BedrockLithology	Lists bedrock lithologies, when encountered, abbreviations listed above – e.g., b.
BedrockElevation	Calculated elevation at which bedrock or soil over bedrock was first encountered, in feet above sea level – e.g., 1924.
TaxLot	Taxlot number. Where it is determined that a taxlot number is used more than once in the section then the appropriate subdivision of the section is indicated in the notes field – e.g., 800.
Color	Color of interval as reported by the well driller – e.g., green.
MapUnit	Geologic unit interpreted in subsurface based on drillers log and designated by map unit label used in accompanying geodatabase. Intervals labeled "suna" (surface unit not applicable) are those where the lithology as interpreted by the original drillers' log do not correspond; also denotes intervals in the subsurface where a precise unit label cannot be applied – e.g., Tb.
Quadrangle	The USGS 7.5' quadrangle in which the sample is located – e.g., Burns Butte.
UTMNorthingWGS84	Meters north in WGS84 UTM projection, zone 11.
UTMEastingWGS84	Meters east in WGS84 UTM projection, zone 11.
UTMNorthingNAD27	Meters north in NAD 27 UTM projection, zone 11.
UTMEastingNAD27	Meters east in NAD 27 UTM projection, zone 11.
LatitudeNAD27	Latitude in NAD 27 geographic coordinates.
LongitudeNAD27	Longitude in NAD 27 geographic coordinates.
UTMNorthingNAD83	Meters north in NAD 83 UTM projection, zone 11.

UTMEastingNAD83	Meters east in NAD 83 UTM projection, zone 11.
LatitudeNAD83	Latitude in NAD 83 geographic coordinates.
LongitudeNAD83	Longitude in NAD 83 geographic coordinates.
Northing83HARN	Feet north in Oregon Lambert NAD 83, HARN, international feet.
Easting83HARN	Feet east in Oregon Lambert NAD 83, HARN, international feet.
LocationSourceID	Unique data source from which the data was obtained – e.g., OWRD2020.
WellSourceID	Unique data source from which the data was obtained – e.g., OWRD2020.
Notes	Notes about the stratigraphic interval as originally described by the well driller or observer.
WellPoints_ID	Primary key – e.g., WLP593
PTTYPE	– e.g., Water Well, Oil and Gas.

*Well location given in six coordinate systems calculated by reprojecting original WGS 84 UTM, zone 11 locations.

Michael T. Halbouty Federal 1-10 Exploration Well (HARN 52703) – cuttings and log

This section of the report 1) shows cuttings samples from the HARN 52703 Michael T. Halbouty Federal 1-10 Exploration Well west of Burns Butte, 2) provides tabulated geochemical data for samples obtained from the well (**Table 13-7**), and 3) provides detailed log of cuttings by J.D. McClaughry and M. L. Ferns (**Table 13-8).**

Name of Well: HARN 52703 - Michael T. Halbouty Federal 1-10 **Year well drilled**: 1977
Location of Well: Burns Butte, Oregon **Latitude, Longitude (NAD83)**: 43.59241, -119.21974
Elevation of well collar: 1,455 m (4,772 ft) asl
Total depth drilled: 2,343 m (7,684 ft), depth intervals of retrieved cuttings shown in feet (e.g., 430-460).
Cuttings shown are from depth intervals 430 to 1030 ft.

Name of Well: HARN 52703 - Michael T. Halbouty Federal 1-10 **Year well drilled**: 1977
Location of Well: Burns Butte, Oregon **Latitude, Longitude (NAD83)**: 43.59241, -119.21974
Elevation of well collar: 1,455 m (4,772 ft) asl
Total depth drilled: 2,343 m (7,684 ft), depth intervals of retrieved cuttings shown in feet (e.g., 430-460).
Cuttings shown are from depth intervals 1030 to 1630 ft.

Name of Well: HARN 52703 - Michael T. Halbouty Federal 1-10 **Year well drilled**: 1977
Location of Well: Burns Butte, Oregon **Latitude, Longitude (NAD83)**: 43.59241, -119.21974
Elevation of well collar: 1,455 m (4,772 ft) asl
Total depth drilled: 2,343 m (7,684 ft), depth intervals of retrieved cuttings shown in feet (e.g., 430-460).
Cuttings shown are from depth intervals 1630 to 2230 ft.

Name of Well: HARN 52703 - Michael T. Halbouty Federal 1-10 **Year well drilled**: 1977
Location of Well: Burns Butte, Oregon **Latitude, Longitude (NAD83)**: 43.59241, -119.21974
Elevation of well collar: 1,455 m (4,772 ft) asl
Total depth drilled: 2,343 m (7,684 ft), depth intervals of retrieved cuttings shown in feet (e.g., 430-460).

Cuttings shown are from depth intervals 2230 to 2830 ft.

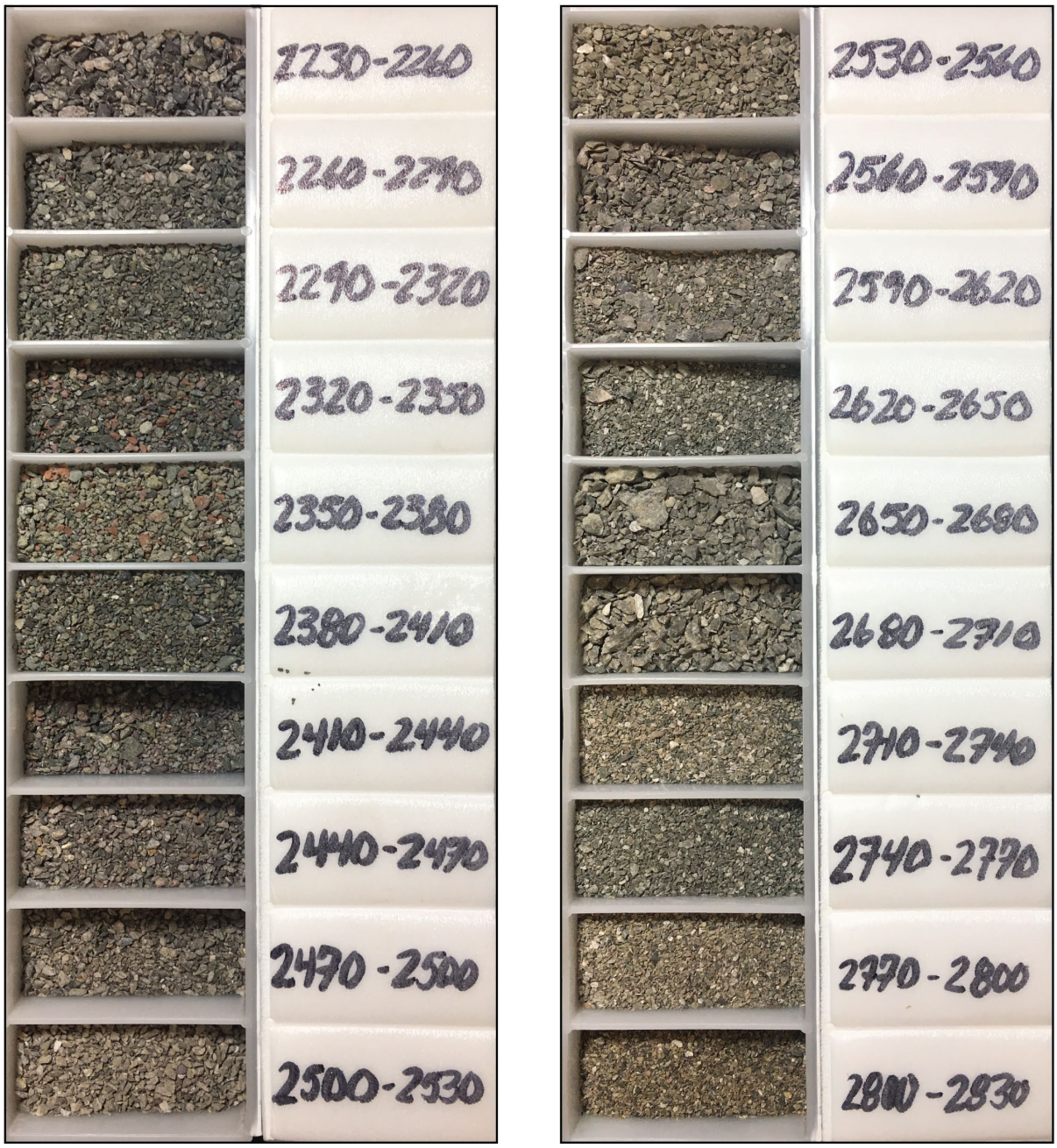

Name of Well: HARN 52703 - Michael T. Halbouty Federal 1-10 **Year well drilled**: 1977
Location of Well: Burns Butte, Oregon **Latitude, Longitude (NAD83)**: 43.59241, -119.21974
Elevation of well collar: 1,455 m (4,772 ft) asl
Total depth drilled: 2,343 m (7,684 ft), depth intervals of retrieved cuttings shown in feet (e.g., 430-460).

Cuttings shown are from depth intervals 2830 to 3430 ft.

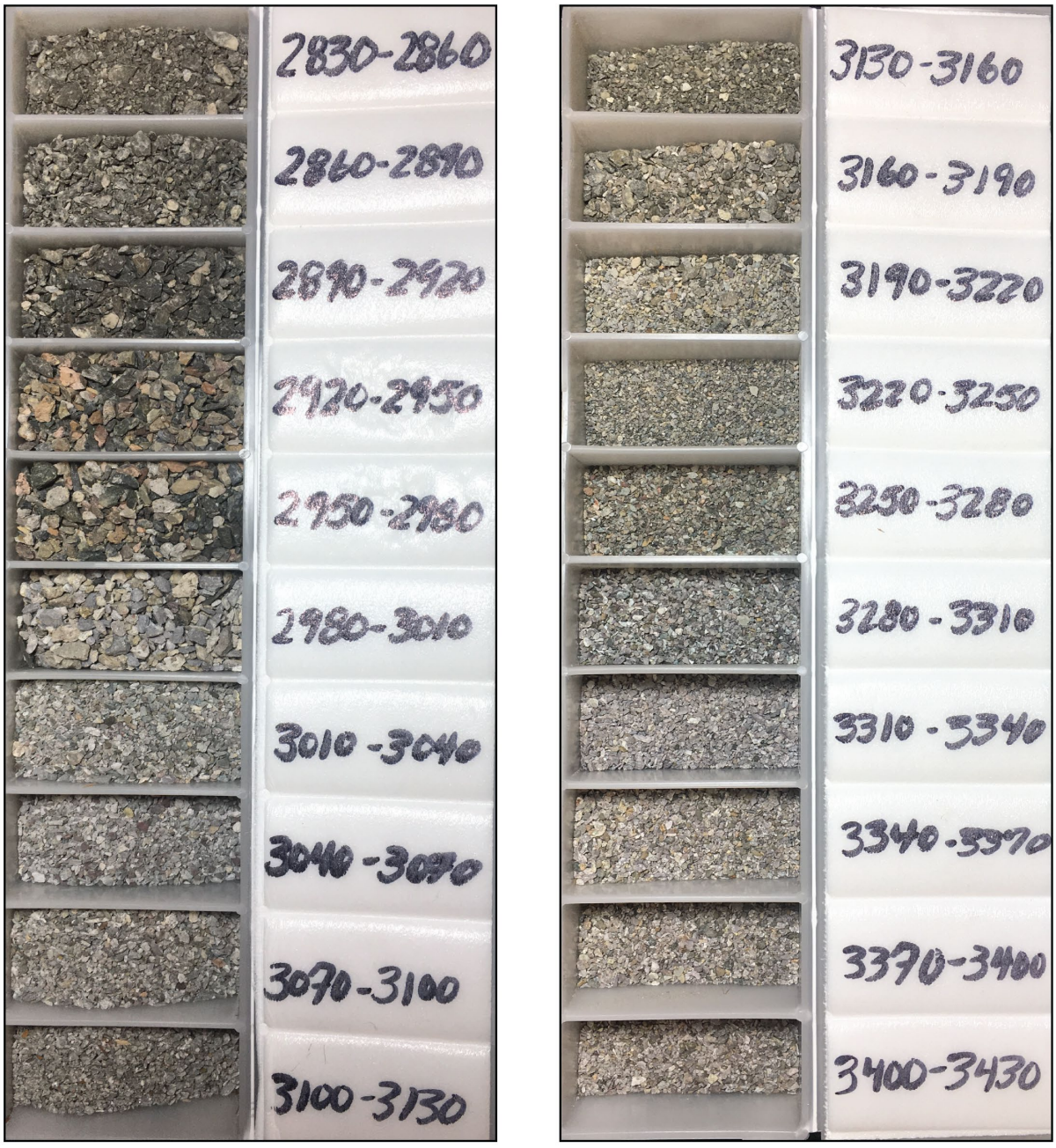

Name of Well: HARN 52703 - Michael T. Halbouty Federal 1-10 **Year well drilled**: 1977
Location of Well: Burns Butte, Oregon **Latitude, Longitude (NAD83)**: 43.59241, -119.21974
Elevation of well collar: 1,455 m (4,772 ft) asl
Total depth drilled: 2,343 m (7,684 ft), depth intervals of retrieved cuttings shown in feet (e.g., 430-460).

Cuttings shown are from depth intervals 3430 to 4030 ft.

Name of Well: HARN 52703 - Michael T. Halbouty Federal 1-10 **Year well drilled**: 1977
Location of Well: Burns Butte, Oregon **Latitude, Longitude (NAD83)**: 43.59241, -119.21974
Elevation of well collar: 1,455 m (4,772 ft) asl
Total depth drilled: 2,343 m (7,684 ft), depth intervals of retrieved cuttings shown in feet (e.g., 430-460).

Cuttings shown are from depth intervals 4030 to 4630 ft.

Name of Well: HARN 52703 - Michael T. Halbouty Federal 1-10 **Year well drilled**: 1977
Location of Well: Burns Butte, Oregon **Latitude, Longitude (NAD83)**: 43.59241, -119.21974
Elevation of well collar: 1,455 m (4,772 ft) asl
Total depth drilled: 2,343 m (7,684 ft), depth intervals of retrieved cuttings shown in feet (e.g., 430-460).

Cuttings shown are from depth intervals 4630 to 5230 ft.

5 cm

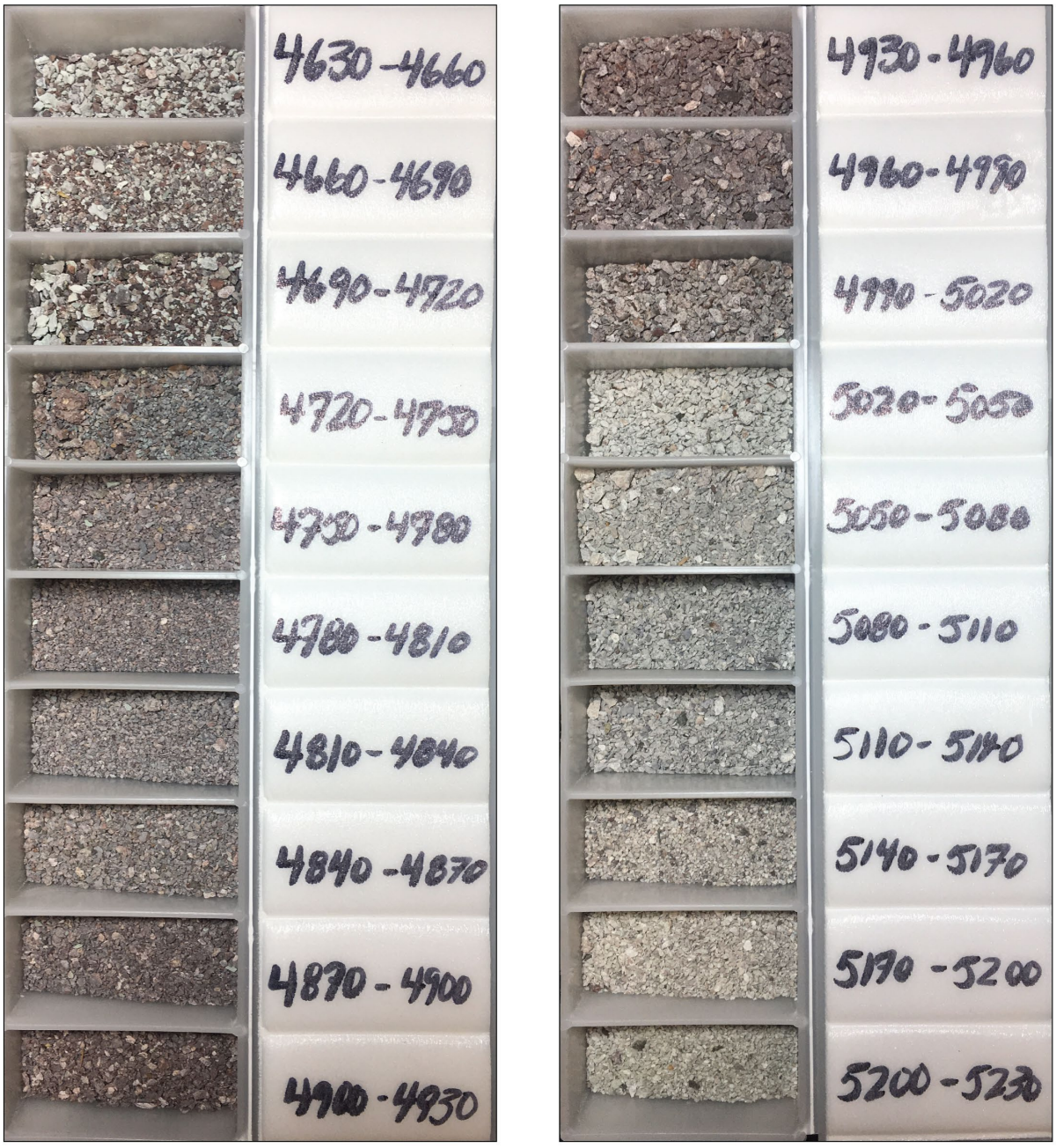

Name of Well: HARN 52703 - Michael T. Halbouty Federal 1-10 **Year well drilled**: 1977
Location of Well: Burns Butte, Oregon **Latitude, Longitude (NAD83)**: 43.59241, -119.21974
Elevation of well collar: 1,455 m (4,772 ft) asl
Total depth drilled: 2,343 m (7,684 ft), depth intervals of retrieved cuttings shown in feet (e.g., 430-460).
Cuttings shown are from depth intervals 5230 to 5830 ft.

Name of Well: HARN 52703 - Michael T. Halbouty Federal 1-10 **Year well drilled**: 1977
Location of Well: Burns Butte, Oregon **Latitude, Longitude (NAD83)**: 43.59241, -119.21974
Elevation of well collar: 1,455 m (4,772 ft) asl
Total depth drilled: 2,343 m (7,684 ft), depth intervals of retrieved cuttings shown in feet (e.g., 430-460).
Cuttings shown are from depth intervals 5830 to 6430 ft.

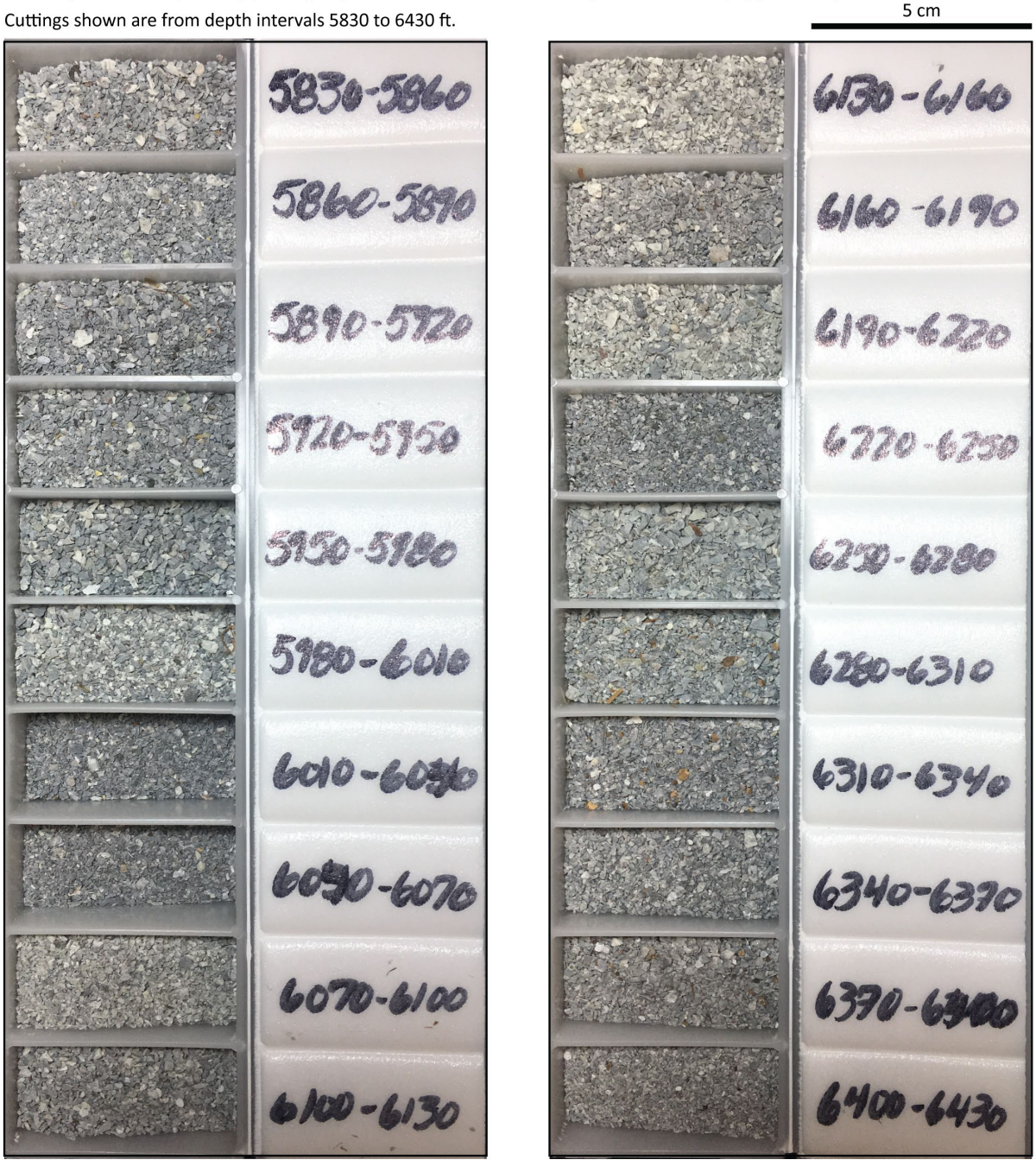

Name of Well: HARN 52703 - Michael T. Halbouty Federal 1-10 **Year well drilled**: 1977
Location of Well: Burns Butte, Oregon **Latitude, Longitude (NAD83)**: 43.59241, -119.21974
Elevation of well collar: 1,455 m (4,772 ft) asl
Total depth drilled: 2,343 m (7,684 ft), depth intervals of retrieved cuttings shown in feet (e.g., 430-460).

Cuttings shown are from depth intervals 6430 to 7030 ft.

5 cm

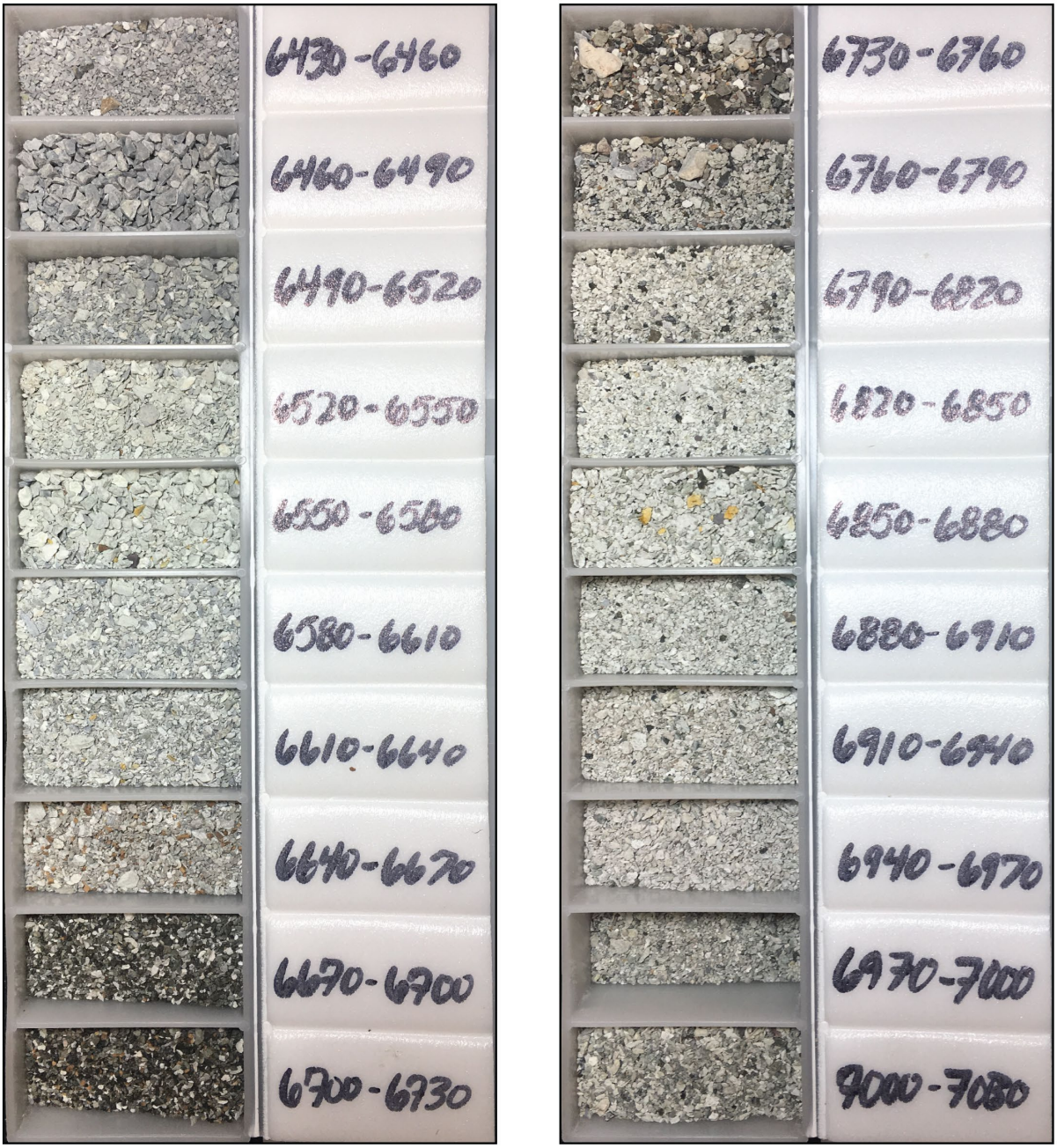

Name of Well: HARN 52703 - Michael T. Halbouty Federal 1-10 **Year well drilled**: 1977
Location of Well: Burns Butte, Oregon **Latitude, Longitude (NAD83)**: 43.59241, -119.21974
Elevation of well collar: 1,455 m (4,772 ft) asl
Total depth drilled: 2,343 m (7,684 ft), depth intervals of retrieved cuttings shown in feet (e.g., 430-460).
Cuttings shown are from depth intervals 7030 to 7630 ft.

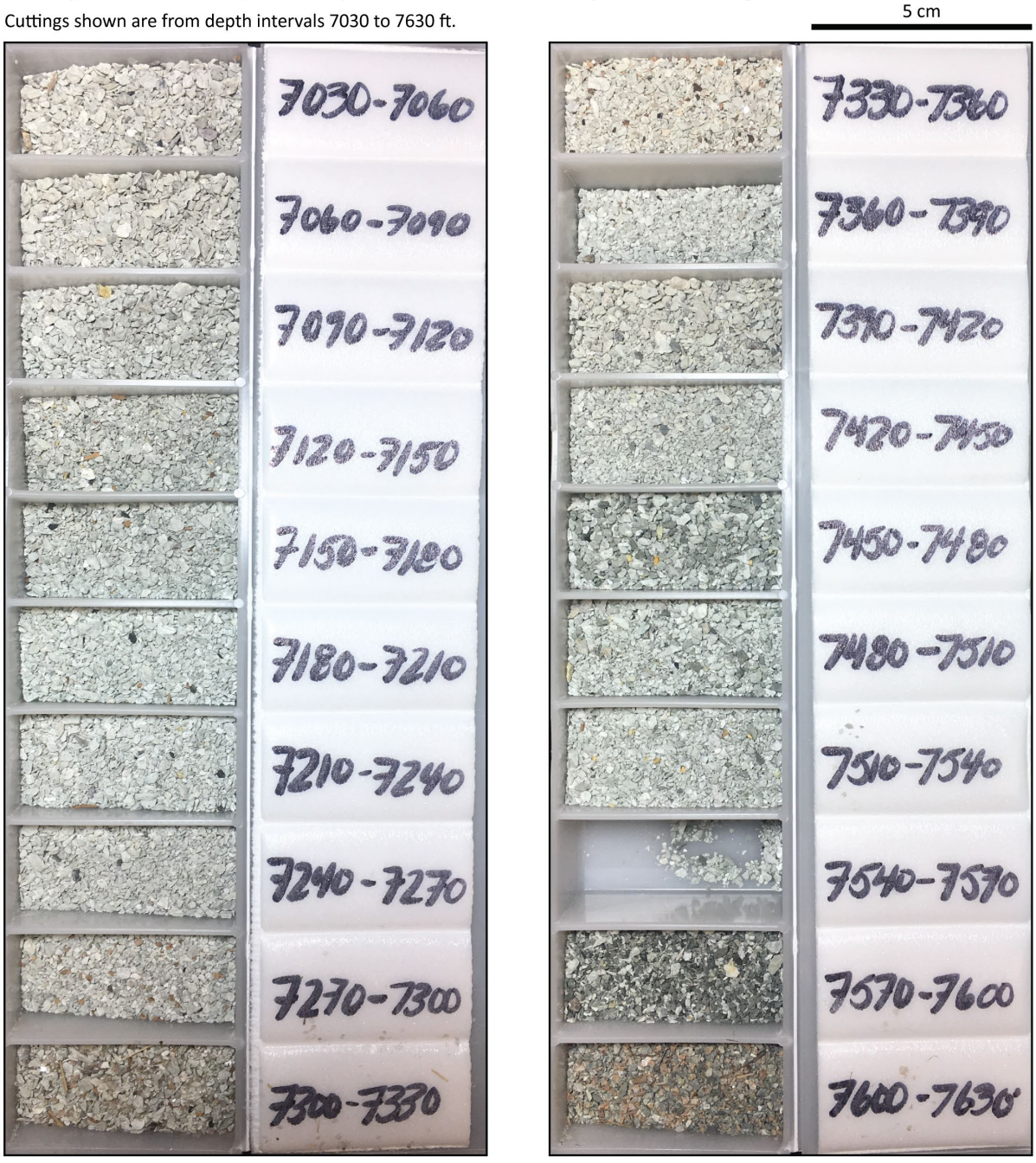

Name of Well: HARN 52703 - Michael T. Halbouty Federal 1-10 **Year well drilled**: 1977
Location of Well: Burns Butte, Oregon **Latitude, Longitude (NAD83)**: 43.59241, -119.21974
Elevation of well collar: 1,455 m (4,772 ft) asl
Total depth drilled: 2,343 m (7,684 ft), depth intervals of retrieved cuttings shown in feet (e.g., 430-460).
Cuttings shown are from depth intervals 7630 to 7684 ft.

5 cm

Table 13-7. Geochemical analyses obtained from HARN 52073 Michael T. Halbouty Federal 1-10 Well cuttings (3 tables, 1 of 3).

Sample	F-1-10-460	F-1-10-670	F-1-10-820	F-1-10-940	F-1-10-1240	F-1-10-1330	F-1-10-1480	F-1-10-1810	F-1-10-1960	F-1-10-2200	F-1-10-2290
Geographic Area	West Willow Cr.	West Willow Cr.	West Willow Cr.	West Willow Cr.	West Willow Cr.	West Willow Cr.	West Willow Cr.	West Willow Cr.	West Willow Cr.	West Willow Cr.	West Willow Cr.
MapUnit	bas. trachand. & trachand. flows	Tuff of Wheeler Springs, non-welded tuff	lower bas. trachand. & trachand. flows	lower bas. trachand. & trachand. flows	lower bas. trachand. & trachand. flows	lower bas. trachand. & trachand. flows	lower bas. trachand. & trachand. flows	lower bas. trachand. & trachand. flows	lower bas. trachand. & trachand. flows	lower bas. trachand. & trachand. flows	lower bas. trachand. & trachand. flows
Label	Tmat	Tmtwh	Tmatl	Tmatl	Tmatl	Tmatl	Tmatl	Tmatl	Tmatl	Tmatl	Tmatl
UTMNorthing NAD83	4828998	4828998	4828998	4828998	4828998	4828998	4828998	4828998	4828998	4828998	4828998
UTMEastingNAD83	320818	320818	320818	320818	320818	320818	320818	320818	320818	320818	320818
Age (Ma)	nd	nd	nd	nd	nd	nd	nd	nd	nd	nd	nd
Map No.	G29	G30	G31	G32	G33	G34	G35	G36	G37	G38	G39
Oxides, weight percent											
SiO_2	54.48	73.86	55.71	55.81	58.91	58.77	56.88	68.28	65.80	55.16	54.94
Al_2O_3	17.06	13.53	17.08	16.75	16.98	17.06	17.33	14.99	15.29	17.20	17.42
TiO_2	1.34	0.23	1.26	1.36	0.98	0.98	1.01	0.53	0.67	1.12	1.12
FeO*	8.83	1.95	8.24	8.42	7.03	6.84	7.21	3.54	4.41	8.11	8.21
MnO	0.16	0.05	0.16	0.15	0.12	0.11	0.13	0.06	0.08	0.15	0.15
CaO	7.85	0.92	7.47	7.42	6.19	6.52	7.37	2.21	3.23	7.55	7.49
MgO	4.13	0.43	4.19	3.67	2.93	2.81	3.55	1.16	1.69	4.30	4.39
K_2O	1.62	5.22	1.77	2.07	2.35	2.41	2.09	4.73	4.14	1.83	1.71
Na_2O	3.98	3.77	3.58	3.72	4.02	4.02	3.92	4.31	4.44	4.03	4.03
P_2O_5	0.55	0.04	0.55	0.63	0.49	0.48	0.52	0.18	0.25	0.55	0.55
LOI	nd	4.37	nd	nd	nd	nd	nd	nd	nd	nd	nd
Total_I	98.13	94.65	96.96	98.01	97.68	98.20	96.40	97.46	97.19	97.07	97.04
Trace Elements, parts per million											
Ni	27	4	27	21	19	19	26	10	17	37	37
Cr	38	6	49	40	14	17	49	16	23	63	65
Sc	25	6	23	25	19	18	21	9	11	21	23
V	216	14	178	222	160	157	166	50	70	184	183
Ba	698	399	793	844	928	931	866	995	997	800	790
Rb	20	106	28	34	44	44	33	86	77	24	20
Sr	529	42	452	457	443	450	485	139	173	470	465
Zr	128	227	163	177	177	187	157	317	310	154	149
Y	25	41	27	28	25	25	23	36	35	25	25
Nb	9.1	25.2	12.3	13.6	11.4	12.1	10.1	22.8	22.1	10.6	10.0
Ga	19	17	16	19	18	19	17	17	18	18	18
Cu	88	8	58	53	45	38	63	19	22	75	75
Zn	86	43	86	86	78	79	83	48	52	82	82
Pb	5	16	7	7	8	8	8	13	9	5	7
La	20	36	25	27	26	29	23	33	29	26	23
Ce	46	76	53	51	54	54	52	62	58	55	48
Th	2	9	2	1	2	3	2	6	6	2	3
Nd	25	30	27	29	29	24	23	29	26	24	25
U	1	3	2	1	2	2	3	2	1	2	2

Major element determinations have been normalized to a 100-percent total on a volatile-free basis and recalculated with total iron expressed as FeO*; nd - no data or element not analyzed; na - not applicable or no information. LOI, Loss on Ignition; Total_I, original analytical total.

Table 13-7, continued. Geochemical analyses obtained from cuttings from the HARN 52073 Michael T. Halbouty Federal 1-10 Well (3 tables, 2 of 3).

Sample	F-1-10-2470	F-1-10-2680	F-1-10-2830	F-1-10-3040	F-1-10-3220	F-1-10-3730	F-1-10-4150	F-1-10-4270	F-1-10-4510	F-1-10-5470	F-1-10-5650
Geographic Area	West Willow Cr.	West Willow Cr.	West Willow Cr.	West Willow Cr.	West Willow Cr.	West Willow Cr.	West Willow Cr.	West Willow Cr.	West Willow Cr.	West Willow Cr.	West Willow Cr.
MapUnit	lower bas. trachand. & trachand. flows	lower bas. trachand. & trachand. flows	lower bas. trachand. & trachand. flows	Prater Creek Ash-flow Tuff, intracald. Unit	Prater Creek Ash-flow Tuff, intracald. Unit	Prater Creek Ash-flow Tuff, intracald. Unit	Prater Creek Ash-flow Tuff, intracald. Unit	Prater Creek Ash-flow Tuff, intracald. Unit	Undiff. rhyolite intrusives and ash-flow tuff	Undiff. rhyolite intrusives and ash-flow tuff	Undiff. rhyolite intrusives and ash-flow tuff
Label	Tmatl	Tmatl	Tmatl	Tmtpi	Tmtpi	Tmtpi	Tmtpi	Tmtpi	Tmru	Tmru	Tmru
UTMNorthing NAD83	4828998	4828998	4828998	4828998	4828998	4828998	4828998	4828998	4828998	4828998	4828998
UTMEastingNAD83	320818	320818	320818	320818	320818	320818	320818	320818	320818	320818	320818
Age (Ma)	nd	nd	nd	8.52 Ma	nd	nd	nd	nd	nd	nd	nd
Map No.	G40	G41	G42	G43	G44	G45	G46	G47	G48	G49	G50
Oxides, weight percent											
SiO_2	64.69	66.32	59.51	77.11	75.44	77.60	78.15	78.00	77.00	84.29	77.31
Al_2O_3	15.59	15.29	16.32	10.79	10.36	11.10	11.16	11.37	12.51	8.65	11.62
TiO_2	0.95	0.81	1.13	0.14	0.15	0.12	0.11	0.12	0.13	0.15	0.16
FeO*	5.02	4.29	6.74	2.01	2.18	2.14	1.60	1.55	1.20	0.89	2.23
MnO	0.09	0.09	0.12	0.05	0.04	0.04	0.03	0.03	0.03	0.05	0.05
CaO	3.14	3.10	5.77	1.40	4.05	0.25	0.47	0.37	0.44	0.75	0.20
MgO	1.69	1.42	3.23	0.13	0.24	0.10	0.06	0.07	0.09	0.08	0.03
K_2O	3.88	3.82	2.55	5.14	4.17	5.02	5.13	4.79	5.00	1.75	4.86
Na_2O	4.61	4.63	4.26	3.23	3.34	3.61	3.28	3.69	3.59	3.39	3.53
P_2O_5	0.33	0.23	0.37	0.02	0.03	0.01	0.01	0.01	0.01	0.01	0.01
LOI	nd	nd	nd	nd	4.45	nd	nd	nd	0.79	1.28	0.72
Total_I	97.32	97.58	97.18	97.49	94.89	98.43	97.64	97.73	98.42	98.10	98.83
Trace Elements, parts per million											
Ni	3	7	28	5	1	1	1	1	5	3	8
Cr	12	14	46	11	17	3	5	4	3	6	4
Sc	12	12	19	1	2	1	1	1	3	6	1
V	83	68	137	17	24	6	5	4	4	7	2
Ba	1061	1034	882	86	110	24	27	23	128	667	88
Rb	68	70	42	124	100	127	127	121	106	41	111
Sr	223	200	352	18	59	9	15	10	22	24	13
Zr	325	345	238	447	431	479	410	408	190	204	657
Y	41	41	33	59	66	73	68	68	46	44	109
Nb	23.0	24.9	17.8	38.5	36.0	42.0	40.5	37.2	32.5	21.1	44.3
Ga	19	18	18	21	20	22	18	19	17	13	22
Cu	14	14	35	9	13	5	4	6	5	4	4
Zn	67	52	70	92	100	116	73	76	32	61	130
Pb	11	9	8	19	24	18	17	14	17	14	22
La	34	35	27	50	51	58	49	46	48	30	77
Ce	72	69	55	100	100	106	96	88	91	68	143
Th	6	6	4	8	7	8	11	9	10	3	10
Nd	35	33	30	46	46	48	42	40	35	33	71
U	1	2	3	4	3	3	2	2	3	2	4

Major element determinations have been normalized to a 100-percent total on a volatile-free basis and recalculated with total iron expressed as FeO*; nd - no data or element not analyzed; na - not applicable or no information. LOI, Loss on Ignition; Total_I, original analytical total.

Table 13-7, continued. Geochemical analyses obtained from cuttings from the HARN 52073 Michael T. Halbouty Federal 1-10 Well (3 tables, 3 of 3).

Sample	F-1-10-5740	F-1-10-6490	F-1-10-6970	F-1-10-7540
Geographic Area	West Willow Cr.	West Willow Cr.	West Willow Cr.	West Willow Cr.
MapUnit	Undiff. rhyolite intrusives and ash-flow tuff	Undiff. rhyolite intrusives and ash-flow tuff	Undiff. rhyolite intrusives and ash-flow tuff	Undiff. rhyolite intrusives and ash-flow tuff
Label	Tmru	Tmru	Tmru	Tmru
UTMNorthingNAD83	4828998	4828998	4828998	4828998
UTMEastingNAD83	320818	320818	320818	320818
Age (Ma)	nd	nd	nd	nd
Map No.	G51	G52	G53	G54
Oxides, weight percent				
SiO_2	79.05	77.94	72.19	72.56
Al_2O_3	11.89	12.46	12.85	13.66
TiO_2	0.20	0.18	0.49	0.44
FeO*	0.85	0.93	3.82	2.65
MnO	0.02	0.04	0.08	0.09
CaO	0.19	0.36	2.64	2.00
MgO	0.00	0.02	1.22	0.95
K_2O	3.49	3.28	3.41	4.43
Na_2O	4.28	4.77	3.19	3.11
P_2O_5	0.02	0.02	0.10	0.10
LOI	0.40	0.58	2.46	1.55
Total_I	98.98	98.50	96.97	97.78
Trace Elements, parts per million				
Ni	5	4	27	20
Cr	3	5	23	26
Sc	7	6	8	10
V	4	2	53	50
Ba	1490	1468	386	383
Rb	67	61	98	107
Sr	23	26	119	136
Zr	273	238	554	107
Y	79	67	79	53
Nb	32.0	31.4	46.8	35.3
Ga	17	16	19	15
Cu	1	1	28	8
Zn	83	71	109	60
Pb	13	16	21	18
La	45	43	42	11
Ce	94	83	84	26
Th	5	7	10	10
Nd	47	41	41	16
U	2	2	4	6

Major element determinations have been normalized to a 100-percent total on a volatile-free basis and recalculated with total iron expressed as FeO*; nd - no data or element not analyzed; na - not applicable or no information. LOI, Loss on Ignition; Total_I, original analytical total.

Table 13-8. Descriptions and interpretations of downhole lithologies from the HARN 52073 Michael T. Halbouty Federal 1-10 Well. Cuttings described and interpreted by J. D. McClaughry and M. L. Ferns during 2018 to 2020.

Depth Interval (Ft)		Elevation Interval (Ft)		Geochemical Sample	Color	Interval Description	Label
0	430	4772	4342		no cuttings	no cuttings	na
430	460	4342	4312		Medium gray (N5) to Medium dark gray (N4)	Aphyric, holocrystalline andesite.	Tmat
460	490	4312	4282	**F-1-10-460**	Medium gray (N5) to Medium dark gray (N4)	Aphyric, holocrystalline basaltic trachyandesite, with pinkish vesicular zones.	Tmat
490	520	4282	4252		Medium gray (N5) to Medium dark gray (N4) and Moderate reddish brown (10R 4/6)	Mottled aphyric, holocrystalline andesite, with Grayish orange pink (10R 8/2) vesicular zones.	Tmat
520	550	4252	4222		Medium gray (N5) to Medium dark gray (N4) and Moderate reddish brown (10R 4/6)	Mottled aphyric, holocrystalline andesite, with Grayish orange pink (10R 8/2) vesicular zones.	Tmat
550	580	4222	4192		Medium gray (N5) to Medium dark gray (N4)	Aphyric, holocrystalline andesite.	Tmat
580	610	4192	4162		Medium gray (N5) to Medium dark gray (N4)	Aphyric, holocrystalline andesite.	Tmat
610	640	4162	4132		Medium gray (N5) to Medium dark gray (N4)	Aphyric, holocrystalline andesite.	Tmat
640	670	4132	4102		Moderate reddish brown (10R 4/6)	Pumiceous tuff with very sparse feldspar microphenocrysts. Medium dark gray (N4) andesite fragments.	Tmtwh
670	700	4102	4072	**F-1-10-670**	Medium gray (N5) to Medium dark gray (N4), Black (N1), Very light gray (N8)	Crystal vitric tuff with very fresh clear glass and Black (N1) obsidian, minor feldspar.	Tmtwh
700	730	4072	4042		Medium gray (N5) to Medium dark gray (N4), Black (N1), Very light gray (N8)	Crystal vitric tuff with very fresh clear glass and Black (N1) obsidian, minor feldspar.	Tmtwh
730	760	4042	4012		Medium gray (N5) to Medium dark gray (N4), Black (N1), Very light gray (N8)	Vitric tuff with very fresh clear glass and Black (N1) obsidian, stony Medium gray (N5) and Medium dark gray (N4) rhyolite, feldspar and quartz.	Tmtwh
760	790	4012	3982		Medium gray (N5) to Medium dark gray (N4), Black (N1), Very light gray (N8)	Vitric tuff with very fresh clear glass and Black (N1) obsidian, Medium gray (N5) and Medium dark gray (N4) stony rhyolite, feldspar and quartz.	Tmtwh
790	820	3982	3952		Moderate reddish brown (10R 4/6) to Medium gray (N5) and Medium dark gray (N4)	Vitric tuff with very fresh clear glass and Black (N1) obsidian, Medium gray (N5) and Medium dark gray (N4) stony rhyolite, feldspar and quartz.	Tmtwh
820	850	3952	3922	**F-1-10-820**	Medium gray (N5) to Medium dark gray (N4)	Mottled, very sparsely porphyritic (feldspar), holocrystalline basaltic trachyandesite.	Tmatl
850	880	3922	3892		Medium gray (N5) to Medium dark gray (N4) and Moderate reddish brown (10R 4/6)	Very sparsely porphyritic (feldspar), holocrystalline basaltic trachyandesite, with Grayish orange pink (10R 8/2) vesicular zones. Minor zeolite in vesicles.	Tmatl
880	910	3892	3862		Medium gray (N5) to Medium dark gray (N4)	Very sparsely porphyritic (feldspar), holocrystalline basaltic trachyandesite, with glassy rock fragments, White (N9) tuff.	Tmatl
910	940	3862	3832		Pale red (5R (6/2) to Medium gray (N5) and Medium dark gray (N4)	Very sparsely porphyritic (feldspar), holocrystalline, vesicular basaltic trachyandesite, with Grayish orange pink (10R 8/2) vesicular zones. Minor zeolite in vesicles.	Tmatl

Depth Interval (Ft)		Elevation Interval (Ft)		Geochemical Sample	Color	Interval Description	Label
940	970	3832	3802	**F-1-10-940**	Medium gray (N5) to Medium dark gray (N4) and Moderate reddish brown (10R 4/6)	Aphyric, holocrystalline basaltic trachyandesite, with Grayish orange pink (10R 8/2) vesicular fragments.	Tmatl
970	1000	3802	3772		Medium gray (N5) to Medium dark gray (N4)	Aphyric, holocrystalline basaltic trachyandesite, with White (N9) rhyolite rock fragments.	Tmatl
1000	1030	3772	3742		Moderate reddish brown (10R 4/6) to Medium gray (N5) and Medium dark gray (N4)	Aphyric, glassy basaltic trachyandesite, with aphyric rock fragments.	Tmatl
1030	1060	3742	3712		Moderate reddish brown (10R 4/6) to Medium gray (N5) and Medium dark gray (N4)	Aphyric, glassy, vesicular basaltic trachyandesite, with minor rhyolite fragments.	Tmatl
1060	1090	3712	3682		Moderate reddish brown (10R 4/6) to Medium gray (N5) and Medium dark gray (N4)	Aphyric, glassy, vesicular basaltic trachyandesite, with minor zeolite in vesicles.	Tmatl
1090	1120	3682	3652		Pale red (5R 6/2)	Fine, aphyric, vesicular cinders.	Tmatl
1120	1150	3652	3622		Pale red (5R 6/2)	Fine, aphyric, vesicular cinders.	Tmatl
1150	1180	3622	3592		Pale red (5R 6/2)	Fine, aphyric, vesicular cinders. Some flow fragments.	Tmatl
1180	1210	3592	3562		Pale red (5R 6/2) to Medium gray (N5) and Medium dark gray (N4)	Aphyric trachyandesite. Some vesicular.	Tmatl
1210	1240	3562	3532		Dark gray (N3)	Aphyric trachyandesite.	Tmatl
1240	1270	3532	3502	**F-1-10-1240**	Dark gray (N3)	Aphyric trachyandesite.	Tmatl
1270	1300	3502	3472		Dark gray (N3)	Aphyric trachyandesite.	Tmatl
1300	1330	3472	3442		Very light gray (N8) to Medium light gray (N6)	Aphyric trachyandesite, with fine White (N9), very sparsely feldspar microphyric tuff.	Tmatl
1330	1360	3442	3412	**F-1-10-1330**	Medium light gray (N6)	Aphyric trachyandesite.	Tmatl
1360	1390	3412	3382		Medium gray (N5)	Aphyric trachyandesite.	Tmatl
1390	1420	3382	3352		Pale red (5R (6/2) to Medium gray (N5)	Aphyric trachyandesite, with Grayish orange pink (10R 8/2) vesicular zones. Zeolite in vesicles and groundmass.	Tmatl
1420	1450	3352	3322		Medium gray (N5) to Pale red (5R (6/2)	Aphyric trachyandesite.	Tmatl
1450	1480	3322	3292		Light brownish gray (5YR 6/1)	Aphyric trachyandesite.	Tmatl
1480	1510	3292	3262	**F-1-10-1480**	Light brownish gray (5YR 6/1)	Aphyric trachyandesite.	Tmatl
1510	1540	3262	3232		Light brownish gray (5YR 6/1)	Aphyric trachyandesite.	Tmatl

Depth Interval (Ft)		Elevation Interval (Ft)		Geochemical Sample	Color	Interval Description	Label
1540	1570	3232	3202		Light brownish gray (5YR 6/1)	Aphyric trachyandesite.	Tmatl
1570	1600	3202	3172		Light brownish gray (5YR 6/1)	Aphyric trachyandesite mixed with fine White (N9) tuff.	Tmatl
1600	1630	3172	3142		Light brownish gray (5YR 6/1)	Aphyric trachyandesite.	Tmatl
1630	1660	3142	3112		Pale red (5R (6/2) to Medium gray (N5)	Aphyric trachyandesite.	Tmatl
1660	1690	3112	3082		Medium dark gray (N4)	Aphyric trachyandesite.	Tmatl
1690	1720	3082	3052		Medium dark gray (N4)	Aphyric trachyandesite.	Tmatl
1720	1750	3052	3022		Medium dark gray (N4)	Aphyric trachyandesite.	Tmatl
1750	1780	3022	2992		Light brownish gray (5YR 6/1)	Aphyric trachyandesite.	Tmatl
1780	1810	2992	2962		Medium gray (N5) to Light brownish gray (5YR 6/1)	Mix of trachyandesite and tuff.	Tmatl
1810	1840	2962	2932	**F-1-10-1810**	Light brownish gray (5YR 6/1)	Porphyritic dacite with feldspar and quartz(?). Terminated quartz in cavities.	Tmatl
1840	1870	2932	2902		Light brownish gray (5YR 6/1)	Porphyritic dacite with feldspar and quartz(?). Clear quartz veining.	Tmatl
1870	1900	2902	2872		Light brownish gray (5YR 6/1)	Sugary, holocrystalline dacite with minor feldspar crystals.	Tmatl
1900	1930	2872	2842		Light brownish gray (5YR 6/1) to Medium dark gray (N4)	Sugary, holocrystalline dacite with minor feldspar crystals.	Tmatl
1930	1960	2842	2812		Medium dark gray (N4)	Sugary, holocrystalline dacite with minor feldspar crystals and amphibole(?).	Tmatl
1960	1990	2812	2782	**F-1-10-1960**	Medium dark gray (N4)	Sugary, holocrystalline dacite with minor feldspar crystals.	Tmatl
1990	2020	2782	2752		Medium dark gray (N4)	Sugary, holocrystalline dacite with minor feldspar crystals.	Tmatl
2020	2050	2752	2722		Light brownish gray (5YR 6/1)	Sugary, holocrystalline dacite with minor feldspar crystals.	Tmatl
2050	2080	2722	2692		Light brownish gray (5YR 6/1)	Sugary, holocrystalline dacite with minor feldspar crystals.	Tmatl
2080	2110	2692	2662		Light brownish gray (5YR 6/1)	Sugary, holocrystalline dacite with minor feldspar crystals.	Tmatl
2110	2140	2662	2632		Light brownish gray (5YR 6/1)	Sugary, holocrystalline dacite with minor feldspar crystals.	Tmatl

Depth Interval (Ft)		Elevation Interval (Ft)		Geochemical Sample	Color	Interval Description	Label
2140	2170	2632	2602		Medium gray (N5)	Sugary, holocrystalline dacite with fine White (N9) tuff.	Tmatl
2170	2200	2602	2572		Medium dark gray (N4)	Sugary, holocrystalline dacite with fine White (N9) tuff.	Tmatl
2200	2230	2572	2542	**F-1-10-2200**	Medium dark gray (N4)	Aphyric, holocrystalline basaltic trachyandesite.	Tmatl
2230	2260	2542	2512		Medium dark gray (N4)	Aphyric, holocrystalline basaltic trachyandesite.	Tmatl
2260	2290	2512	2482		Medium dark gray (N4)	Aphyric, holocrystalline basaltic trachyandesite.	Tmatl
2290	2320	2482	2452	**F-1-10-2290**	Medium dark gray (N4)	Aphyric, holocrystalline basaltic trachyandesite.	Tmatl
2320	2350	2452	2422		Medium dark gray (N4) to Moderate reddish brown (10R 4/6)	Sugary, aphyric, holocrystalline trachyandesite, with Grayish orange pink (10R 8/2) vesicular zones.	Tmatl
2350	2380	2422	2392		Light brownish gray (5YR 6/1) to Moderate reddish brown (10R 4/6)	Sugary, aphyric, holocrystalline trachyandesite, with Grayish orange pink (10R 8/2) vesicular zones. Flow boundary	Tmatl
2380	2410	2392	2362		Medium dark gray (N4)	Sugary, aphyric, holocrystalline dacite, with Medium Gray (N5) vesicular zones.	Tmatl
2410	2440	2362	2332		Medium gray (N5) to Medium dark gray (N4)	Sugary, aphyric, holocrystalline dacite, with gray glassy and vesicular zones.	Tmatl
2440	2470	2332	2302		Medium gray (N5) to Medium dark gray (N4)	Sugary, aphyric, holocrystalline dacite, with rare plagioclase phenocrysts.	Tmatl
2470	2500	2302	2272	**F-1-10-2470**	Medium gray (N5) to Medium dark gray (N4)	Sugary, aphyric, holocrystalline dacite.	Tmatl
2500	2530	2272	2242		Medium gray (N5) to Medium dark gray (N4)	Sugary, porphyritic, holocrystalline dacite, with sparse feldspars. Flow boundary	Tmatl
2530	2560	2242	2212		Medium gray (N5) to Medium light gray (N6)	Sugary, porphyritic, glassy dacite, with sparse feldspars. Perlitic glass.	Tmatl
2560	2590	2212	2182		Medium gray (N5) to Medium light gray (N6)	Sugary dacite, with sparse feldspars. Sparse pyroxenes.	Tmatl
2590	2620	2182	2152		Medium gray (N5) to Medium light gray (N6)	Sugary dacite, with sparse feldspars.	Tmatl
2620	2650	2152	2122		Medium gray (N5) to Medium light gray (N6)	Sugary dacite, with sparse feldspars.	Tmatl
2650	2680	2122	2092		Medium gray (N5) to Medium light gray (N6)	Sugary, porphyritic dacite, with sparse feldspars.	Tmatl
2680	2710	2092	2062	**F-1-10-2680**	Medium gray (N5) to Medium light gray (N6)	Sugary, porphyritic dacite, with sparse feldspars.	Tmatl
2710	2740	2062	2032		Light brownish gray (5YR 6/1)	Sugary, porphyritic dacite, with sparse feldspars.	Tmatl

Depth Interval (Ft)		Elevation Interval (Ft)		Geochemical Sample	Color	Interval Description	Label
2740	2770	2032	2002		Medium dark gray (N4)	Sugary, porphyritic dacite, with sparse feldspars.	Tmatl
2770	2800	2002	1972		Light brownish gray (5YR 6/1)	Sugary, porphyritic dacite, with sparse feldspars. Sparse pyroxenes.	Tmatl
2800	2830	1972	1942		Dark yellowish brown (10YR 4/2)	Sugary, porphyritic dacite, with sparse feldspars. Sparse pyroxenes. Flow boundary.	Tmatl
2830	2860	1942	1912	**F-1-10-2830**	Medium dark gray (N4)	Aphyric, holocrystalline trachyandesite.	Tmatl
2860	2890	1912	1882		Medium dark gray (N4)	Aphyric, holocrystalline trachyandesite.	Tmatl
2890	2920	1882	1852		Medium dark gray (N4)	Aphyric, holocrystalline trachyandesite.	Tmatl
2920	2950	1852	1822		Medium dark gray (N4) to Medium gray (N5) and Pale red (5R (6/2)	Sugary, aphyric, holocrystalline trachyandesite mixed with rhyolite or welded tuff fragments. Transition horizon.	Tmatl
2950	2980	1822	1792		Medium dark gray (N4) to Medium gray (N5) and Pale red (5R (6/2)	Welded rhyolite tuff mixed with trachyandesite fragments. Transition horizon.	Tmtpi
2980	3010	1792	1762		Medium light gray (N6)	Welded rhyolite tuff. Opaline quartz in open-spaces.	Tmtpi
3010	3040	1762	1732		White (N9) to Very light gray (N8) and Medium light gray (N6)	Fine crystal tuff, sparsely microphyric 1 to 2 percent blocky clear alkali feldspar (<0.5 mm), quartz, and clinopyroxene.	Tmtpi
3040	3070	1732	1702	**F-1-10-3040**	White (N9) to Very light gray (N8) and Medium light gray (N6)	Fine crystal tuff, sparsely microphyric 1 to 2 percent blocky clear alkali feldspar (<0.5 mm), quartz, and clinopyroxene.	Tmtpi
3070	3100	1702	1672		White (N9) to Very light gray (N8) and Medium light gray (N6)	Fine crystal tuff, sparsely microphyric 1 to 2 percent blocky clear alkali feldspar (<0.5 mm), quartz, and clinopyroxene.	Tmtpi
3100	3130	1672	1642		White (N9) to Very light gray (N8) and Medium light gray (N6)	Fine crystal tuff, sparsely microphyric 1 to 2 percent blocky clear alkali feldspar (<0.5 mm), quartz, and clinopyroxene.	Tmtpi
3130	3160	1642	1612		White (N9) to Very light gray (N8) and Medium light gray (N6)	Fine crystal tuff, sparsely microphyric 1 to 2 percent blocky clear alkali feldspar (<0.5 mm), quartz, and clinopyroxene. Includes trachyandesite (?).	Tmtpi
3160	3190	1612	1582		White (N9) to Very light gray (N8) and Medium light gray (N6)	Fine crystal tuff, sparsely microphyric 1 to 2 percent blocky clear alkali feldspar, quartz, and clinopyroxene. Includes trachyandesite (?).	Tmtpi
3190	3220	1582	1552		White (N9) to Very light gray (N8) and Medium light gray (N6)	Fine crystal tuff, sparsely microphyric 1 to 2 percent blocky clear alkali feldspar (<0.5 mm), quartz, and clinopyroxene.	Tmtpi
3220	3250	1552	1522	**F-1-10-3220**	White (N9) to Very light gray (N8) and Medium light gray (N6)	Fine crystal tuff, sparsely microphyric 1 to 2 percent blocky clear alkali feldspar (<0.5 mm), quartz, and clinopyroxene.	Tmtpi
3250	3280	1522	1492		White (N9) to Very light gray (N8) and Medium light gray (N6)	Fine crystal tuff, sparsely microphyric 1 to 2 percent blocky clear alkali feldspar (<0.5 mm), quartz, and clinopyroxene. Devitrified glass textures.	Tmtpi
3280	3310	1492	1462		White (N9) to Very light gray (N8) and Medium light gray (N6)	Fine crystal tuff, sparsely microphyric 1 to 2 percent blocky clear alkali feldspar, quartz, and clinopyroxene.	Tmtpi
3310	3340	1462	1432		White (N9) to Very light gray (N8) and Medium light gray (N6)	Fine crystal tuff, sparsely microphyric 1 to 2 percent blocky clear alkali feldspar (<0.5 mm), quartz, and clinopyroxene. Sulfides.	Tmtpi

Depth Interval (Ft)		Elevation Interval (Ft)		Geochemical Sample	Color	Interval Description	Label
3340	3370	1432	1402		White (N9) to Very light gray (N8) and Medium light gray (N6)	Fine crystal tuff, sparsely microphyric 1 to 2 percent blocky clear alkali feldspar, quartz, and clinopyroxene.	Tmtpi
3370	3400	1402	1372		White (N9) to Very light gray (N8) and Medium light gray (N6)	Fine crystal tuff, sparsely microphyric 1 to 2 percent blocky clear alkali feldspar (<0.5 mm), quartz, and clinopyroxene.	Tmtpi
3400	3430	1372	1342		White (N9) to Very light gray (N8) and Medium light gray (N6)	Fine crystal tuff, sparsely microphyric 1 to 2 percent blocky clear alkali feldspar (<0.5 mm), quartz, and clinopyroxene.	Tmtpi
3430	3460	1342	1312		White (N9) to Very light gray (N8) and Medium light gray (N6)	Fine crystal tuff, sparsely microphyric 1 to 2 percent blocky clear alkali feldspar (<0.5 mm), quartz, and clinopyroxene.	Tmtpi
3460	3490	1312	1282		White (N9) to Very light gray (N8) and Medium light gray (N6)	Fine crystal tuff, sparsely microphyric 1 to 2 percent blocky clear alkali feldspar (<0.5 mm), quartz, and clinopyroxene.	Tmtpi
3490	3520	1282	1252		White (N9) to Very light gray (N8) and Medium light gray (N6)	Fine crystal tuff, sparsely microphyric 1 to 2 percent blocky clear alkali feldspar (<0.5 mm), quartz, and clinopyroxene.	Tmtpi
3520	3550	1252	1222		White (N9) to Very light gray (N8) and Medium light gray (N6)	Fine crystal tuff, sparsely microphyric 1 to 2 percent blocky clear alkali feldspar (<0.5 mm), quartz, and clinopyroxene.	Tmtpi
3550	3580	1222	1192		White (N9) to Very light gray (N8) and Medium light gray (N6)	Fine crystal tuff, sparsely microphyric 1 to 2 percent blocky clear alkali feldspar (<0.5 mm), quartz, and clinopyroxene.	Tmtpi
3580	3610	1192	1162		Medium gray (N5)	Fine crystal tuff, sparsely microphyric 1 to 2 percent blocky clear alkali feldspar (<0.5 mm), quartz, and clinopyroxene. Rare quartz porphyry.	Tmtpi
3610	3640	1162	1132		Medium gray (N5)	Fine crystal tuff, sparsely microphyric 1 to 2 percent blocky clear alkali feldspar, quartz, and clinopyroxene.	Tmtpi
3640	3670	1132	1102		Medium gray (N5)	Fine crystal tuff, sparsely microphyric 1 to 2 percent blocky clear alkali feldspar (<0.5 mm), quartz, and clinopyroxene.	Tmtpi
3670	3700	1102	1072		Medium gray (N5)	Fine crystal tuff, sparsely microphyric 1 to 2 percent blocky clear alkali feldspar (<0.5 mm), quartz, and clinopyroxene.	Tmtpi
3700	3730	1072	1042		White (N9) to very light gray (N8) and medium light gray (N6)	Fine crystal tuff, sparsely microphyric 1 to 2 percent blocky clear alkali feldspar (<0.5 mm), quartz, and clinopyroxene.	Tmtpi
3730	3760	1042	1012	**F-1-10-3730**	White (N9) to very light gray (N8) and medium light gray (N6)	Fine crystal tuff, sparsely microphyric 1 to 2 percent blocky clear alkali feldspar (<0.5 mm), quartz, and clinopyroxene.	Tmtpi
3760	3790	1012	982		Medium gray (N5)	Fine-grained, holocrystalline, equigranular rhyolite or rhyolite tuff with quartz, K-feldspar, and clinopyroxene.	Tmtpi
3790	3820	982	952		Medium gray (N5)	Fine-grained, holocrystalline, equigranular rhyolite or rhyolite tuff with quartz, K-feldspar, and clinopyroxene.	Tmtpi
3820	3850	952	922		Medium gray (N5)	Fine-grained, holocrystalline, equigranular rhyolite or rhyolite tuff with quartz, K-feldspar, and clinopyroxene. Some breccia fragments.	Tmtpi
3850	3880	922	892		Medium gray (N5)	Welded Fine crystal tuff, sparsely microphyric 1 to 2 percent blocky clear alkali feldspar (<0.5 mm), quartz, and clinopyroxene.	Tmtpi
3880	3910	892	862		Grayish orange pink (5YR 7/2)	Welded Fine crystal tuff, sparsely microphyric 1 to 2 percent blocky clear alkali feldspar (<0.5 mm), quartz, and clinopyroxene.	Tmtpi
3910	3940	862	832		Grayish orange pink (5YR 7/2)	Welded Fine crystal tuff, sparsely microphyric 1 to 2 percent blocky clear alkali feldspar (<0.5 mm), quartz, and clinopyroxene. Spherulites.	Tmtpi

Depth Interval (Ft)		Elevation Interval (Ft)		Geochemical Sample	Color	Interval Description	Label
3940	3970	832	802		Grayish orange pink (5YR 7/2)	Welded Fine crystal tuff, sparsely microphyric 1 to 2 percent blocky clear alkali feldspar (<0.5 mm), quartz, and clinopyroxene. Spherulites.	Tmtpi
3970	4000	802	772		Grayish orange pink (5YR 7/2)	Fine crystal tuff, sparsely microphyric 1 to 2 percent blocky clear alkali feldspar (<0.5 mm), quartz, and clinopyroxene.	Tmtpi
4000	4030	772	742		Olive gray (5Y 4/1)	Fine-grained, holocrystalline, equigranular trachyandesite. Intermixed fine tuff fragments.	Tmtpi
4030	4060	742	712		White (N9) to Very light gray (N8) and Medium light gray (N6), Olive gray (5Y 4/1)	Fine crystal tuff, sparsely microphyric 1 to 2 percent blocky clear alkali feldspar (<0.5 mm), quartz, and clinopyroxene.	Tmtpi
4060	4090	712	682		White (N9) to Very light gray (N8) and Medium light gray (N6)	Fine crystal tuff, sparsely microphyric 1 to 2 percent blocky clear alkali feldspar (<0.5 mm), quartz, and clinopyroxene.	Tmtpi
4090	4120	682	652		White (N9) to Very light gray (N8) and Medium light gray (N6)	Fine crystal tuff, sparsely microphyric 1 to 2 percent blocky clear alkali feldspar (<0.5 mm), quartz, and clinopyroxene.	Tmtpi
4120	4150	652	622		White (N9) to Very light gray (N8) and Medium light gray (N6)	Fine crystal tuff, sparsely microphyric 1 to 2 percent blocky clear alkali feldspar (<0.5 mm), quartz, and clinopyroxene.	Tmtpi
4150	4180	622	592	**F-1-10-4150**	White (N9) to Very light gray (N8) and Medium light gray (N6)	Fine crystal tuff, sparsely microphyric 1 to 2 percent blocky clear alkali feldspar (<0.5 mm), quartz, and clinopyroxene.	Tmtpi
4180	4210	592	562		White (N9) to Very light gray (N8) and Medium light gray (N6)	Fine crystal tuff, sparsely microphyric 1 to 2 percent blocky clear alkali feldspar (<0.5 mm), quartz, and clinopyroxene.	Tmtpi
4210	4240	562	532		White (N9) to Very light gray (N8) and Medium light gray (N6)	Fine crystal tuff, sparsely microphyric 1 to 2 percent blocky clear alkali feldspar (<0.5 mm), quartz, and clinopyroxene.	Tmtpi
4240	4270	532	502		White (N9) to Very light gray (N8) and Medium light gray (N6)	Fine crystal tuff, sparsely microphyric 1 to 2 percent blocky clear alkali feldspar (<0.5 mm), quartz, and clinopyroxene.	Tmtpi
4270	4300	502	472	**F-1-10-4270**	White (N9) to Very light gray (N8) and Medium light gray (N6)	Fine crystal tuff, sparsely microphyric 1 to 2 percent blocky clear alkali feldspar (<0.5 mm), quartz, and clinopyroxene.	Tmtpi
4300	4330	472	442		White (N9) to Very light gray (N8) and Medium light gray (N6)	Fine crystal tuff, sparsely microphyric 1 to 2 percent blocky clear alkali feldspar (<0.5 mm), quartz, and clinopyroxene.	Tmtpi
4330	4360	442	412		Grayish orange pink (5YR 7/2)	Fine crystal tuff, very sparsely microphyric with rare blocky clear alkali feldspar (<0.5 mm), quartz, and clinopyroxene. Vitroclastic textures	Tmtpi
4360	4390	412	382		Pale brown (5YR 5/2)	Fine crystal tuff, very sparsely microphyric with rare blocky clear alkali feldspar (<0.5 mm), quartz, and clinopyroxene. Vitroclastic textures	Tmtpi
4390	4420	382	352		White (N9) to Very light gray (N8) and Medium light gray (N6)	Fine crystal tuff, very sparsely microphyric with rare blocky clear alkali feldspar (<0.5 mm), quartz, and clinopyroxene. Vitroclastic textures	Tmtpi
4420	4450	352	322		White (N9) to Very light gray (N8) and Medium light gray (N6)	Fine crystal tuff, very sparsely microphyric with rare blocky clear alkali feldspar (<0.5 mm), quartz, and clinopyroxene. Vitroclastic textures	Tmtpi
4450	4480	322	292		White (N9) to Very light gray (N8) and Medium light gray (N6)	Fine crystal tuff, very sparsely microphyric with rare blocky clear alkali feldspar (<0.5 mm), quartz, and clinopyroxene. Vitroclastic textures	Tmtpi
4480	4510	292	262		Medium dark gray (N4) to Light gray (N7), Olive gray (5Y 4/1)	Fine crystal tuff, very sparsely microphyric with rare blocky clear alkali feldspar (<0.5 mm), quartz, and clinopyroxene. Vitroclastic textures. Sugary, fine-grained, holocrystalline, equigranular olive gray (5Y 4/1) flow-banded rhyolite fragments. Intermixed medium dark gray (N4) trachyandesite fragments.	Tmru

Depth Interval (Ft)		Elevation Interval (Ft)		Geochemical Sample	Color	Interval Description	Label
4510	4540	262	232	**F-1-10-4510**	Light brownish gray (5YR 6/1)	Fine crystal tuff, very sparsely microphyric with rare blocky clear alkali feldspar (<0.5 mm), quartz, and clinopyroxene. Vitroclastic textures. Sugary, fine-grained, holocrystalline, equigranular olive gray (5Y 4/1) flow-banded rhyolite fragments. Intermixed medium dark gray (N4) trachyandesite fragments.	Tmtpi
4540	4570	232	202		Medium gray (N5)	Fine crystal tuff, very sparsely microphyric with rare blocky clear alkali feldspar (<0.5 mm), quartz, and clinopyroxene. Vitroclastic textures. Sugary, fine-grained, holocrystalline, equigranular olive gray (5Y 4/1) flow-banded rhyolite fragments. Very sparse quartz and alkali feldspar. Perlitic and sparse trachytic textures.	Tmtpi
4570	4600	202	172		White (N9) to Very light gray (N8) and Medium light gray (N6)	Fine crystal tuff, very sparsely microphyric with rare blocky clear alkali feldspar (<0.5 mm), quartz, and clinopyroxene. Vitroclastic textures, fiamme, flow banding, spherulites. Gray vapor phase crystals.	Tmtpi
4600	4630	172	142		White (N9) to Very light gray (N8) and Medium light gray (N6)	Fine crystal tuff, very sparsely microphyric with rare blocky clear alkali feldspar (<0.5 mm), quartz, and clinopyroxene. Vitroclastic textures, fiamme, flow banding, spherulites. Gray vapor phase crystals.	Tmtpi
4630	4660	142	112		Light brownish gray (5YR 6/1) to Brownish gray (5YR 4/1) and Very light gray (N8)	Fine crystal tuff, sparsely microphyric 1 to 2 percent blocky clear alkali feldspar (<0.5 mm), quartz, and clinopyroxene. Mixed with Brownish gray (5YR 4/1) amorphous rhyolite fragments.	Tmtpi
4660	4690	112	82		Light brownish gray (5YR 6/1) to Brownish gray (5YR 4/1) and Very light gray (N8)	Brownish gray (5YR 4/1) amorphous rhyolite fragments mixed with fine crystal tuff, sparsely microphyric 1 to 2 percent blocky clear alkali feldspar (<0.5 mm), quartz, and clinopyroxene.	Tmtpi
4690	4720	82	52		Light brownish gray (5YR 6/1) to Brownish gray (5YR 4/1) and Very light gray (N8)	Brownish gray (5YR 4/1) amorphous rhyolite fragments mixed with fine crystal tuff, sparsely microphyric 1 to 2 percent blocky clear alkali feldspar (<0.5 mm), quartz, and clinopyroxene.	Tmtpi
4720	4750	52	22		Light brownish gray (5YR 6/1) to Brownish gray (5YR 4/1)	Fine-grained, holocrystalline, equigranular lithophysal rhyolite tuff with quartz.	Tmtpi
4750	4780	22	-8		Light brownish gray (5YR 6/1) to Brownish gray (5YR 4/1)	Relatively fresh, fine-grained equigranular rhyolite or microgranite with 2 to 3 percent clinopyroxene, intermixed with clear alkali feldspar and quartz.	Tmru
4780	4810	-8	-38		Light brownish gray (5YR 6/1) to Brownish gray (5YR 4/1)	Relatively fresh, fine-grained equigranular rhyolite or microgranite with 2 to 3 percent clinopyroxene, intermixed with clear alkali feldspar and quartz.	Tmru
4810	4840	−38	−68		Light brownish gray (5YR 6/1) to Brownish gray (5YR 4/1)	Relatively fresh, fine-grained equigranular rhyolite or microgranite with 2 to 3 percent clinopyroxene, intermixed with clear alkali feldspar and quartz.	Tmru
4840	4870	−68	−98		Light brownish gray (5YR 6/1) to Brownish gray (5YR 4/1)	Relatively fresh, fine-grained equigranular rhyolite or microgranite with 2 to 3 percent clinopyroxene, intermixed with clear alkali feldspar and quartz.	Tmru
4870	4900	−98	−128		Light brownish gray (5YR 6/1) to Brownish gray (5YR 4/1)	Relatively fresh, fine-grained equigranular rhyolite or microgranite with 2 to 3 percent clinopyroxene, intermixed with clear alkali feldspar and quartz.	Tmru
4900	4930	−128	−158		Light brownish gray (5YR 6/1) to Brownish gray (5YR 4/1)	Relatively fresh, fine-grained equigranular rhyolite or microgranite with 2 to 3 percent clinopyroxene, intermixed with clear alkali feldspar and quartz.	Tmru
4930	4960	−158	−188		Light brownish gray (5YR 6/1) to Brownish gray (5YR 4/1)	Relatively fresh, fine-grained equigranular rhyolite or microgranite with 2 to 3 percent clinopyroxene, intermixed with clear alkali feldspar and quartz.	Tmru

Depth Interval (Ft)		Elevation Interval (Ft)		Geochemical Sample	Color	Interval Description	Label
4960	4990	−188	−218		Light brownish gray (5YR 6/1) to Brownish gray (5YR 4/1)	Relatively fresh, fine-grained equigranular rhyolite or microgranite with 2 to 3 percent clinopyroxene, intermixed with clear alkali feldspar and quartz.	Tmru
4990	5020	−218	−248		Light brownish gray (5YR 6/1) to Brownish gray (5YR 4/1)	Relatively fresh, fine-grained equigranular rhyolite or microgranite with 2 to 3 percent clinopyroxene, intermixed with clear alkali feldspar and quartz.	Tmru
5020	5050	−248	−278		White (N9) to Very light gray (N8) and Medium light gray (N6)	Relatively fresh, fine-grained equigranular rhyolite or microgranite with 2 to 3 percent clinopyroxene, intermixed with clear alkali feldspar and quartz.	Tmru
5050	5080	−278	−308		White (N9) to Very light gray (N8) and Medium light gray (N6)	Relatively fresh, fine-grained equigranular rhyolite or microgranite with 2 to 3 percent clinopyroxene, intermixed with clear alkali feldspar and quartz. Fine-grained amorphous rhyolite fragments.	Tmru
5080	5110	−308	−338		White (N9) to Very light gray (N8) and Medium light gray (N6)	Relatively fresh, fine-grained equigranular rhyolite or microgranite with 2 to 3 percent clinopyroxene, intermixed with clear alkali feldspar and quartz. Fine-grained amorphous rhyolite fragments.	Tmru
5110	5140	−338	−368		White (N9) to Very light gray (N8) and Medium light gray (N6)	Relatively fresh, fine-grained equigranular rhyolite or microgranite with 2 to 3 percent clinopyroxene, intermixed with clear alkali feldspar and quartz. Fine-grained amorphous rhyolite fragments.	Tmru
5140	5170	−368	−398		White (N9) to Very light gray (N8) and Medium light gray (N6)	Variably altered, fine-grained, sugary holocrystalline, equigranular rhyolite with quartz, K-feldspar. Very rare clinopyroxene. Sparse fragments of Brownish gray (5YR 4/1) amorphous rhyolite and trachyandesite. Sulfides.	Tmru
5170	5200	−398	−428		White (N9) to Very light gray (N8) and Medium light gray (N6)	Variably altered, fine-grained, sugary holocrystalline, equigranular rhyolite with quartz, K-feldspar. Very rare clinopyroxene. Sparse fragments of Brownish gray (5YR 4/1) amorphous rhyolite and trachyandesite. Sulfides.	Tmru
5200	5230	−428	−458		White (N9) to Very light gray (N8) and Medium light gray (N6)	Variably altered, fine-grained, sugary holocrystalline, equigranular rhyolite with quartz, K-feldspar. Very rare clinopyroxene. Sparse fragments of Brownish gray (5YR 4/1) amorphous rhyolite and trachyandesite. Sulfides.	Tmru
5230	5260	−458	−488		White (N9) to Very light gray (N8) and Medium light gray (N6)	Variably altered, fine-grained, sugary holocrystalline, equigranular rhyolite with quartz, K-feldspar. Very rare clinopyroxene. Sparse fragments of Brownish gray (5YR 4/1) amorphous rhyolite. Sulfides.	Tmru
5260	5290	−488	−518		White (N9) to Very light gray (N8) and Medium light gray (N6)	Variably altered, fine-grained, sugary holocrystalline, equigranular rhyolite with quartz, K-feldspar. Very rare clinopyroxene. Sparse fragments of Brownish gray (5YR 4/1) amorphous rhyolite. Some lithophysal fragments.	Tmru
5290	5320	−518	−548		White (N9) to Very light gray (N8) and Medium light gray (N6)	Variably altered, fine-grained, sugary holocrystalline, equigranular rhyolite with quartz, K-feldspar. Very rare clinopyroxene. Sparse fragments of Brownish gray (5YR 4/1) amorphous rhyolite. Some lithophysal fragments. Vapor phase sulfides.	Tmru
5320	5350	−548	−578		White (N9) to Very light gray (N8) and Medium light gray (N6)	Variably altered, fine-grained, sugary holocrystalline, equigranular rhyolite or with 3 to 5 percent quartz and K-feldspar up to 1 mm.	Tmru
5350	5380	−578	−608		White (N9) to Very light gray (N8) and Medium light gray (N6)	Variably altered, fine-grained, sugary holocrystalline, equigranular rhyolite with 3 to 5 percent quartz and K-feldspar up to 1 mm. Very sparse white mica.	Tmru

Depth Interval (Ft)		Elevation Interval (Ft)		Geochemical Sample	Color	Interval Description	Label
5380	5410	−608	−638		White (N9) to Very light gray (N8) and Medium light gray (N6)	Variably altered, fine-grained, sugary holocrystalline, equigranular rhyolite with 3 to 5 percent quartz and K-feldspar up to 1 mm. Rare sulfides.	Tmru
5410	5440	−638	−668		White (N9) to Very light gray (N8) and Medium light gray (N6)	Variably altered, fine-grained, sugary holocrystalline, equigranular rhyolite with 3 to 5 percent quartz and K-feldspar up to 1 mm.	Tmru
5440	5470	−668	−698		White (N9) to Very light gray (N8) and Medium light gray (N6)	Variably altered, fine-grained, sugary holocrystalline, equigranular rhyolite with 3 to 5 percent quartz and K-feldspar up to 1 mm.	Tmru
5470	5500	−698	−728	**F-1-10-5470**	White (N9) to Very light gray (N8) and Medium light gray (N6)	Variably altered, fine-grained, sugary holocrystalline, equigranular rhyolite with 3 to 5 percent quartz and K-feldspar up to 1 mm. Very sparse white mica.	Tmru
5500	5530	−728	−758		White (N9) to Very light gray (N8) and Medium light gray (N6)	Variably altered, fine-grained, sugary holocrystalline, equigranular rhyolite with 1 to 2 percent quartz and K-feldspar up to 1 mm.	Tmru
5530	5560	−758	−788		White (N9) to Very light gray (N8) and Medium light gray (N6)	Variably altered, fine-grained, sugary holocrystalline, equigranular rhyolite with 1 to 2 percent quartz and K-feldspar up to 1 mm. Miarolitic cavities.	Tmru
5560	5590	−788	−818		White (N9) to Very light gray (N8) and Medium light gray (N6)	Fine-grained, sugary holocrystalline, equigranular rhyolite with 1 to 2 percent quartz and K-feldspar up to 1 mm. Miarolitic cavities.	Tmru
5590	5620	−818	−848		White (N9) to Very light gray (N8) and Medium light gray (N6)	Variably altered, fine-grained, sugary holocrystalline, equigranular rhyolite with 1 to 2 percent quartz and K-feldspar up to 1 mm. Relict rhyolite textures. Flow banding. Miarolitic cavities.	Tmru
5620	5650	−848	−878		White (N9) to Very light gray (N8) and Medium light gray (N6)	Variably altered, fine-grained, sugary holocrystalline, equigranular rhyolite with 1 to 2 percent quartz and K-feldspar up to 1 mm. Relict rhyolite textures. Flow banding.	Tmru
5650	5680	−878	−908	**F-1-10-5650**	White (N9) to Very light gray (N8) and Medium light gray (N6)	Variably altered, fine-grained, sugary holocrystalline, equigranular rhyolite with 1 to 2 percent quartz and K-feldspar up to 1 mm. Relict rhyolite textures. Flow banding.	Tmru
5680	5710	−908	−938		White (N9) to Very light gray (N8) and Medium light gray (N6)	Variably altered, fine-grained, sugary holocrystalline rhyolite with 1 to 2 percent quartz and K-feldspar up to 1 mm.	Tmru
5710	5740	−938	−968		White (N9) to Very light gray (N8) and Medium light gray (N6)	Variably altered, fine-grained, sugary holocrystalline rhyolite with 1 to 2 percent quartz and K-feldspar up to 1 mm. Sparse white mica.	Tmru
5740	5770	−968	−998	**F-1-10-5740**	White (N9) to Very light gray (N8) and Medium light gray (N6)	Variably altered, fine-grained, sugary holocrystalline rhyolite or with 1 to 2 percent quartz and K-feldspar up to 1 mm. Relict rhyolite textures. Flow banding	Tmru
5770	5800	−998	−1028		White (N9) to Very light gray (N8) and Medium light gray (N6)	Variably altered, fine-grained, sugary holocrystalline rhyolite with 1 to 2 percent quartz and K-feldspar up to 1 mm. Relict rhyolite textures. Some orange quartzite?	Tmru
5800	5830	−1028	−1058		White (N9) to Very light gray (N8) and Medium light gray (N6)	Variably altered, fine-grained, sugary holocrystalline rhyolite with 1 to 2 percent quartz and K-feldspar up to 1 mm. Relict rhyolite textures.	Tmru
5830	5860	−1058	−1088		Medium gray (N5) to Medium light gray (N6) and Light gray (N7)	Variably altered, fine-grained, sugary mottled holocrystalline rhyolite with 1 to 2 percent quartz and K-feldspar up to 1 mm. Relict rhyolite textures.	Tmru

Depth Interval (Ft)		Elevation Interval (Ft)		Geochemical Sample	Color	Interval Description	Label
5860	5890	−1088	−1118		Medium gray (N5) to Medium light gray (N6) and Light gray (N7)	Variably altered, fine-grained, sugary mottled holocrystalline rhyolite with 1 to 2 percent quartz and K-feldspar up to 1 mm. Very rare clinopyroxene. Relict rhyolite textures.	Tmru
5890	5920	−1118	−1148		Medium gray (N5) to Medium light gray (N6) and Light gray (N7)	Variably altered, fine-grained, sugary mottled holocrystalline rhyolite with 1 to 2 percent quartz and K-feldspar up to 1 mm. Very rare clinopyroxene. Relict rhyolite textures.	Tmru
5920	5950	−1148	−1178		Medium gray (N5) to Medium light gray (N6) and Light gray (N7)	Variably altered, fine-grained, sugary mottled holocrystalline rhyolite with 1 to 2 percent quartz and K-feldspar up to 1 mm. Very rare clinopyroxene. Relict rhyolite textures. Sulfides.	Tmru
5950	5980	−1178	−1208		Medium gray (N5) to Medium light gray (N6) and Light gray (N7)	Variably altered, fine-grained, sugary mottled holocrystalline rhyolite with 1 to 2 percent quartz and K-feldspar up to 1 mm. Very rare clinopyroxene. Relict rhyolite textures. Sulfides.	Tmru
5980	6010	−1208	−1238		Medium gray (N5) to Medium light gray (N6) and Light gray (N7)	Variably altered, fine-grained, sugary mottled holocrystalline rhyolite with 1 to 2 percent quartz and K-feldspar up to 1 mm. Very rare clinopyroxene. Relict rhyolite textures. Sulfides.	Tmru
6010	6040	−1238	−1268		Medium light gray (N6)	Variably altered, fine-grained, sugary mottled holocrystalline rhyolite with 1 to 2 percent quartz and K-feldspar up to 1 mm. Very rare clinopyroxene. Relict rhyolite textures. Sparse white tuff fragments.	Tmru
6040	6070	−1268	−1298		Medium light gray (N6)	Variably altered, fine-grained, sugary mottled holocrystalline rhyolite with 1 to 2 percent quartz and K-feldspar up to 1 mm. Very rare clinopyroxene. Relict rhyolite textures.	Tmru
6070	6100	−1298	−1328		Medium gray (N5) to Medium light gray (N6) and Light gray (N7)	Variably altered, fine-grained, sugary mottled holocrystalline rhyolite with 1 to 2 percent quartz and K-feldspar up to 1 mm. Very rare clinopyroxene. Relict rhyolite textures.	Tmru
6100	6130	−1328	−1358		Medium gray (N5) to Medium light gray (N6) and Light gray (N7)	Variably altered, fine-grained, sugary mottled holocrystalline rhyolite with 1 to 2 percent quartz and K-feldspar up to 1 mm. Very rare clinopyroxene. Relict rhyolite textures. Sulfides.	Tmru
6130	6160	−1358	−1388		Medium gray (N5) to Medium light gray (N6) and Light gray (N7)	Variably altered, fine-grained, sugary mottled holocrystalline rhyolite with 1 to 2 percent quartz and K-feldspar up to 1 mm. Sparse clinopyroxene. Relict rhyolite textures. Sulfides.	Tmru
6160	6190	−1388	−1418		Medium gray (N5) to Medium light gray (N6) and Light gray (N7)	Variably altered, fine-grained, sugary mottled holocrystalline rhyolite with 1 to 2 percent quartz and K-feldspar up to 1 mm. Sparse clinopyroxene. Relict rhyolite textures. Sulfides.	Tmru
6190	6220	−1418	−1448		Medium gray (N5) to Medium light gray (N6) and Light gray (N7)	Variably altered, fine-grained, sugary mottled holocrystalline rhyolite with 1 to 2 percent quartz and K-feldspar up to 1 mm. Sparse clinopyroxene. Relict rhyolite textures. Sulfides.	Tmru
6220	6250	−1448	−1478		Medium gray (N5) to Medium light gray (N6) and Light gray (N7)	Variably altered, fine-grained, sugary mottled holocrystalline rhyolite with 1 to 2 percent quartz and K-feldspar up to 1 mm. Sparse clinopyroxene. Relict rhyolite textures. Sulfides.	Tmru
6250	6280	−1478	−1508		Medium gray (N5) to Medium light gray (N6) and Light gray (N7)	Variably altered, fine-grained, sugary mottled holocrystalline rhyolite with 1 to 2 percent quartz and K-feldspar up to 1 mm. Sparse clinopyroxene. Relict rhyolite textures.	Tmru
6280	6310	−1508	−1538		Medium gray (N5) to Medium light gray (N6) and Light gray (N7)	Variably altered, fine-grained, sugary mottled holocrystalline rhyolite with 1 to 2 percent quartz and K-feldspar up to 1 mm. Sparse clinopyroxene. Relict rhyolite textures.	Tmru

Depth Interval (Ft)		Elevation Interval (Ft)		Geochemical Sample	Color	Interval Description	Label
6310	6340	−1538	−1568		Medium gray (N5) to Medium light gray (N6) and Light gray (N7)	Variably altered, fine-grained, sugary mottled holocrystalline rhyolite with 1 to 2 percent quartz and K-feldspar up to 1 mm. Sparse clinopyroxene. Relict rhyolite textures.	Tmru
6340	6370	−1568	−1598		Medium gray (N5) to Medium light gray (N6) and Light gray (N7)	Variably altered, fine-grained, sugary mottled holocrystalline rhyolite with 1 to 2 percent quartz and K-feldspar up to 1 mm. Sparse clinopyroxene. Relict rhyolite textures.	Tmru
6370	6400	−1598	−1628		Medium gray (N5) to Medium light gray (N6) and Light gray (N7)	Variably altered, fine-grained, sugary mottled holocrystalline rhyolite with 1 to 2 percent quartz and K-feldspar up to 1 mm. Sparse clinopyroxene. Relict rhyolite textures.	Tmru
6400	6430	−1628	−1658		Medium gray (N5) to Medium light gray (N6) and Light gray (N7)	Variably altered, fine-grained, sugary mottled holocrystalline rhyolite with 1 to 2 percent quartz and K-feldspar up to 1 mm. Sparse clinopyroxene. Relict rhyolite textures. Very sparse white mica.	Tmru
6430	6460	−1658	−1688		Medium light gray (N6)	Variably altered, fine-grained, sugary mottled holocrystalline rhyolite with 1 to 2 percent quartz and K-feldspar up to 1 mm. Sparse clinopyroxene. Relict rhyolite textures.	Tmru
6460	6490	−1688	−1718		Medium light gray (N6)	Variably altered, fine-grained, sugary mottled holocrystalline rhyolite with 1 to 2 percent quartz and K-feldspar up to 1 mm. Sparse clinopyroxene. Relict rhyolite textures.	Tmru
6490	6520	−1718	−1748	**F-1-10-6490**	Medium light gray (N6)	Variably altered, fine-grained, holocrystalline, equigranular rhyolite with < 1 percent quartz, K-feldspar, and clinopyroxene.	Tmru
6520	6550	−1748	−1778		White (N9) to Very light gray (N8) and Medium light gray (N6)	Variably altered, fine-grained, holocrystalline, equigranular tuff with < 1 percent quartz, K-feldspar, and clinopyroxene.	Tmru
6550	6580	−1778	−1808		White (N9) to Very light gray (N8) and Medium light gray (N6)	Variably altered, fine-grained, holocrystalline, equigranular tuff with < 1 percent quartz, K-feldspar, and clinopyroxene. Relict welded tuff textures.	Tmru
6580	6610	−1808	−1838		White (N9) to Very light gray (N8) and Medium light gray (N6)	Variably altered, fine-grained, holocrystalline, equigranular tuff with < 1 percent quartz, K-feldspar, and clinopyroxene. Relict welded tuff textures.	Tmru
6610	6640	−1838	−1868		White (N9) to Very light gray (N8) and Medium light gray (N6)	Variably altered, fine-grained, holocrystalline, equigranular tuff with < 1 percent quartz, K-feldspar, and clinopyroxene.	Tmru
6640	6670	−1868	−1898		White (N9) to Very light gray (N8) and Medium light gray (N6)	Variably altered, fine-grained, holocrystalline, equigranular tuff with < 1 percent quartz, K-feldspar, and clinopyroxene.	Tmru
6670	6700	−1898	−1928		Grayish black (N2)	Grayish black (N2) holocrystalline trachyandesite mixed with sparse Medium light gray (N6) holocrystalline rhyolite and some Pale yellowish orange (10YR 8/6) stony rhyolite?	Tmatl
6700	6730	−1928	−1958		Grayish black (N2)	Grayish black (N2) holocrystalline trachyandesite mixed with sparse Medium light gray (N6) holocrystalline rhyolite and some Pale yellowish orange (10YR 8/6) stony rhyolite?	Tmatl
6730	6760	−1958	−1988		Grayish black (N2) to Light gray (N7)	Grayish black (N2) holocrystalline trachyandesite mixed with sparse Medium light gray (N6) holocrystalline rhyolite and some Pale yellowish orange (10YR 8/6) stony rhyolite?	Tmatl

Depth Interval (Ft)		Elevation Interval (Ft)		Geochemical Sample	Color	Interval Description	Label
6760	6790	−1988	−2018		White (N9) to Very light gray (N8) and Medium light gray (N6)	Variably altered, fine-grained, equigranular rhyolite with quartz, K-feldspar. Scattered Grayish black (N2) holocrystalline mafic rock fragments.	Tmru
6790	6820	−2018	−2048		White (N9) to Very light gray (N8) and Medium light gray (N6)	Variably altered, fine-grained, sugary holocrystalline, equigranular rhyolite with 3 to 5 percent quartz and K-feldspar up to 1 mm. clinopyroxene. Scattered Grayish black (N2) holocrystalline mafic rock fragments.	Tmru
6820	6850	−2048	−2078		White (N9) to Very light gray (N8) and Medium light gray (N6)	Variably altered, fine-grained, sugary holocrystalline, equigranular rhyolite with 3 to 5 percent quartz and K-feldspar up to 1 mm. clinopyroxene. Scattered Grayish black (N2) holocrystalline mafic rock fragments. Relict tuff textures.	Tmru
6850	6880	−2078	−2108		White (N9) to Very light gray (N8) and Medium light gray (N6)	Variably altered, fine-grained, sugary holocrystalline, equigranular rhyolite with 3 to 5 percent quartz and K-feldspar up to 1 mm. clinopyroxene. Scattered Grayish black (N2) holocrystalline mafic rock fragments. Some orange matrix.	Tmru
6880	6910	−2108	−2138		White (N9) to Very light gray (N8) and Medium light gray (N6)	Variably altered, fine-grained, sugary holocrystalline, equigranular rhyolite with 3 to 5 percent quartz and K-feldspar up to 1 mm. clinopyroxene. Scattered Grayish black (N2) holocrystalline mafic rock fragments.	Tmru
6910	6940	−2138	−2168		White (N9) to Very light gray (N8) and Medium light gray (N6)	Variably altered, fine-grained, sugary holocrystalline, equigranular rhyolite with 3 to 5 percent quartz and K-feldspar up to 1 mm. clinopyroxene. Scattered Grayish black (N2) holocrystalline mafic rock fragments.	Tmru
6940	6970	−2168	−2198	**F-1-10-6970**	White (N9) to Very light gray (N8) and Medium light gray (N6)	Variably altered, fine-grained, sugary holocrystalline, equigranular rhyolite with 3 to 5 percent quartz and K-feldspar up to 1 mm. clinopyroxene. Scattered Grayish black (N2) holocrystalline mafic rock fragments.	Tmru
6970	7000	−2198	−2228		White (N9) to Very light gray (N8) and Medium light gray (N6)	Variably altered, fine-grained, sugary holocrystalline, equigranular rhyolite with 3 to 5 percent quartz and K-feldspar up to 1 mm. clinopyroxene. Scattered Grayish black (N2) holocrystalline mafic rock fragments.	Tmru
7000	7030	−2228	−2258		White (N9) to Very light gray (N8) and Medium light gray (N6)	Variably altered, fine-grained, sugary holocrystalline, equigranular rhyolite with 3 to 5 percent quartz and K-feldspar up to 1 mm. clinopyroxene. Scattered Grayish black (N2) holocrystalline mafic rock fragments and pinkish silicic rhyolite fragments.	Tmru
7030	7060	−2258	−2288		White (N9) to Very light gray (N8) and Light gray (N7)	Variably altered, fine-grained, sugary holocrystalline, equigranular rhyolite with < 1 percent quartz and K-feldspar up to 1 mm. Very sparse clinopyroxene and white mica. Very rare Grayish black (N2) holocrystalline mafic rock fragments.	Tmru
7060	7090	−2288	−2318		White (N9) to Very light gray (N8) and Light gray (N7)	Variably altered, fine-grained, sugary holocrystalline, equigranular rhyolite with < 1 percent quartz and K-feldspar up to 1 mm. Very sparse clinopyroxene. Very rare Grayish black (N2) holocrystalline mafic rock fragments.	Tmru
7090	7120	−2318	−2348		White (N9) to Very light gray (N8) and Light gray (N7)	Variably altered, fine-grained, sugary holocrystalline, equigranular rhyolite with < 1 percent quartz and K-feldspar up to 1 mm. Very sparse clinopyroxene. Very rare Grayish black (N2) holocrystalline mafic rock fragments.	Tmru
7120	7150	−2348	−2378		White (N9) to Very light gray (N8) and Light gray (N7)	Variably altered, fine-grained, sugary holocrystalline, equigranular rhyolite with < 1 percent quartz and K-feldspar up to 1 mm. Very sparse clinopyroxene. Very rare Grayish black (N2) holocrystalline mafic rock fragments.	Tmru

Depth Interval (Ft)		Elevation Interval (Ft)		Geochemical Sample	Color	Interval Description	Label
7150	7180	−2378	−2408		White (N9) to Very light gray (N8) and Light gray (N7)	Variably altered, fine-grained, sugary holocrystalline, equigranular rhyolite with < 1 percent quartz and K-feldspar up to 1 mm. Very sparse clinopyroxene and mica. Very rare Grayish black (N2) holocrystalline mafic rock fragments.	Tmru
7180	7210	−2408	−2438		White (N9) to Very light gray (N8) and Light gray (N7)	Variably altered, fine-grained, sugary holocrystalline, equigranular rhyolite with < 1 percent quartz and K-feldspar up to 1 mm. Very sparse clinopyroxene. Sulfides. Very rare Grayish black (N2) holocrystalline mafic rock fragments.	Tmru
7210	7240	−2438	−2468		White (N9) to Very light gray (N8) and Light gray (N7)	Variably altered, fine-grained, sugary holocrystalline, equigranular rhyolite with < 1 percent quartz and K-feldspar up to 1 mm. Very sparse clinopyroxene. Very rare Grayish black (N2) holocrystalline mafic rock fragments. Relict tuff textures.	Tmru
7240	7270	−2468	−2498		White (N9) to Very light gray (N8) and Light gray (N7)	Variably altered, fine-grained, sugary holocrystalline, equigranular rhyolite with < 1 percent quartz and K-feldspar up to 1 mm. Very sparse clinopyroxene. Very rare Grayish black (N2) holocrystalline mafic rock fragments. Relict tuff textures.	Tmru
7270	7300	−2498	−2528		White (N9) to Very light gray (N8) and Light gray (N7)	Variably altered, fine-grained, sugary holocrystalline, equigranular rhyolite with < 1 percent quartz and K-feldspar up to 1 mm. Very sparse clinopyroxene. Very rare Grayish black (N2) holocrystalline mafic rock fragments. Relict tuff textures.	Tmru
7300	7330	−2528	−2558		White (N9) to Very light gray (N8) and Light gray (N7)	Variably altered, fine-grained, sugary holocrystalline, equigranular rhyolite with < 1 percent quartz and K-feldspar up to 1 mm and >30 percent white and black mica up to 2 to 3 mm. Very sparse clinopyroxene. Very rare Grayish black (N2) holocrystalline mafic rock fragments.	Tmru
7330	7360	−2558	−2588		White (N9) to Very light gray (N8) and Light gray (N7)	Variably altered, fine-grained, sugary holocrystalline, equigranular rhyolite with < 1 percent quartz and K-feldspar up to 1 mm and >15 percent white and black mica up to 1 to 2 mm. Very sparse clinopyroxene. Very rare Grayish black (N2) holocrystalline mafic rock fragments.	Tmru
7360	7390	−2588	−2618		White (N9) to Very light gray (N8) and Light gray (N7)	Variably altered, fine-grained, sugary holocrystalline, equigranular rhyolite with < 1 percent quartz and K-feldspar up to 1 mm and <5 percent white and black mica up to 1 to 2 mm. Very sparse clinopyroxene. Very rare Grayish black (N2) holocrystalline mafic rock fragments.	Tmru
7390	7420	−2618	−2648		White (N9) to Very light gray (N8) and Light gray (N7)	Variably altered, fine-grained, sugary holocrystalline, equigranular rhyolite with < 1 percent quartz and K-feldspar up to 1 mm and <5 percent white and black mica up to 1 to 2 mm. Very sparse clinopyroxene. Very rare Grayish black (N2) holocrystalline mafic rock fragments.	Tmru
7420	7450	−2648	−2678		White (N9) to Very light gray (N8) and Light gray (N7)	Variably altered, fine-grained, sugary holocrystalline, equigranular rhyolite with < 1 percent quartz and K-feldspar up to 1 mm and <1 percent white and black mica up to 1 to 2 mm. Very sparse clinopyroxene. Sparse Grayish red purple (5RP 4/2) silicic rhyolite rock fragments.	Tmru
7450	7480	−2678	−2708		White (N9) to Very light gray (N8) to Light gray (N7) and Medium light gray (N6)	Variably altered, fine-grained, equigranular rhyolite with quartz, K-feldspar, and clinopyroxene.	Tmru
7480	7510	−2708	−2738		White (N9) to Very light gray (N8) and Light gray (N7)	Variably altered, fine-grained, equigranular rhyolite with quartz, K-feldspar, and clinopyroxene.	Tmru
7510	7540	−2738	−2768		White (N9) to Very light gray (N8) and Light gray (N7)	Variably altered, fine-grained, equigranular rhyolite with quartz, K-feldspar, and clinopyroxene. Very rare Grayish black (N2) holocrystalline mafic rock fragments.	Tmru

Depth Interval (Ft)		Elevation Interval (Ft)		Geochemical Sample	Color	Interval Description	Label
7540	7570	−2768	−2798	**F-1-10-7540**	White (N9) to Very light gray (N8) and Light gray (N7)	Variably altered, fine-grained, equigranular rhyolite with quartz, K-feldspar, and clinopyroxene.	Tmru
7570	7600	−2798	−2828		Medium gray (N5) and Light gray (N7)	Variably altered, fine-grained, equigranular rhyolite with quartz, K-feldspar, and clinopyroxene.	Tmru
7600	7630	−2828	−2858		Medium gray (N5)	Variably altered, fine-grained, equigranular rhyolite with quartz, K-feldspar, and clinopyroxene. >15 percent White (N9) and Black (N1) mica up to 2 to 3 mm.	Tmru
7630	7660	−2858	−2888		Medium dark gray (N4)	Variably altered, fine-grained, equigranular rhyolite with quartz, K-feldspar, and clinopyroxene. >15 percent White (N9) and Black (N1) mica up to 2 to 3 mm. >15 percent orange quartzite fragments. Rhyolite fragments are veined by White (N9) amorphous quartz.	Tmru
7660	7684	−2888	−2912		Medium dark gray (N4)	Variably altered, fine-grained, equigranular rhyolite with quartz, K-feldspar, and clinopyroxene. >15 percent White (N9) and Black (N1) mica up to 2 to 3 mm. >15 percent Pale yellowish orange (10YR 8/6) quartzite fragments. Rhyolite fragments are veined by White (N9) amorphous quartz.	Tmru

CTI Geothermal Test Well (HARN 50087) – cuttings and log

The following section shows 1) cuttings samples from the HARN 50087 CTI Geothermal Test Well in Hines, 2) provides tabulated geochemical data for samples obtained from the well (**Table 13-9**), and 3) provides a detailed log of cuttings by J. D. McClaughry (**Table 13-10**). Note that slight editorial revisions have been made to the original log description and interpretation reported by McClaughry and others (2019).

Name of Well: HARN 50087 - CTI Geothermal Test Well **Year well drilled**: 1996
Location of Well: Hines, Oregon **Latitude, Longitude (NAD83)**: 43.55013, -119.08158
Elevation of well collar: 1264 (4148 ft) asl
Total depth drilled: 596 m (1956 ft), depth intervals of retrieved cuttings shown in feet (e.g., 140-150).

Cuttings shown are from depth intervals 140 to 340 ft.

Name of Well: HARN 50087 - CTI Geothermal Test Well **Year well drilled**: 1996
Location of Well: Hines, Oregon **Latitude, Longitude (NAD83)**: 43.55013, -119.08158
Elevation of well collar: 1264 (4148 ft) asl
Total depth drilled: 596 m (1956 ft), depth intervals of retrieved cuttings shown in feet (e.g., 140-150).

Cuttings shown are from depth intervals 340 to 500 ft.

Name of Well: HARN 50087 - CTI Geothermal Test Well **Year well drilled**: 1996
Location of Well: Hines, Oregon **Latitude, Longitude (NAD83)**: 43.55013, -119.08158
Elevation of well collar: 1264 (4148 ft) asl
Total depth drilled: 596 m (1956 ft), depth intervals of retrieved cuttings shown in feet (e.g., 140-150).

Cuttings shown are from depth intervals 500 to 700 ft.

5 cm

Name of Well: HARN 50087 - CTI Geothermal Test Well **Year well drilled**: 1996
Location of Well: Hines, Oregon **Latitude, Longitude (NAD83)**: 43.55013, -119.08158
Elevation of well collar: 1264 (4148 ft) asl
Total depth drilled: 596 m (1956 ft), depth intervals of retrieved cuttings shown in feet (e.g., 140-150).

Cuttings shown are from depth intervals 700 to 900 ft.

5 cm

Name of Well: HARN 50087 - CTI Geothermal Test Well **Year well drilled**: 1996
Location of Well: Hines, Oregon **Latitude, Longitude (NAD83)**: 43.55013, -119.08158
Elevation of well collar: 1264 (4148 ft) asl
Total depth drilled: 596 m (1956 ft), depth intervals of retrieved cuttings shown in feet (e.g., 140-150).

Cuttings shown are from depth intervals 900 to 1100 ft; no returns for interval 970 to 1000.

5 cm

Name of Well: HARN 50087 - CTI Geothermal Test Well **Year well drilled**: 1996
Location of Well: Hines, Oregon **Latitude, Longitude (NAD83)**: 43.55013, -119.08158
Elevation of well collar: 1264 (4148 ft) asl
Total depth drilled: 596 m (1956 ft), depth intervals of retrieved cuttings shown in feet (e.g., 140-150).

Cuttings shown are from depth intervals 1100 to 1300 ft.

5 cm

Name of Well: HARN 50087 - CTI Geothermal Test Well **Year well drilled**: 1996
Location of Well: Hines, Oregon **Latitude, Longitude (NAD83)**: 43.55013, -119.08158
Elevation of well collar: 1264 (4148 ft) asl
Total depth drilled: 596 m (1956 ft), depth intervals of retrieved cuttings shown in feet (e.g., 140-150).

Cuttings shown are from depth intervals 1335 to 1500 ft.

5 cm

Name of Well: HARN 50087 - CTI Geothermal Test Well **Year well drilled**: 1996
Location of Well: Hines, Oregon **Latitude, Longitude (NAD83)**: 43.55013, -119.08158
Elevation of well collar: 1264 (4148 ft) asl
Total depth drilled: 596 m (1956 ft), depth intervals of retrieved cuttings shown in feet (e.g., 140-150).

Cuttings shown are from depth intervals 1500 to 1700 ft.

Name of Well: HARN 50087 - CTI Geothermal Test Well **Year well drilled**: 1996
Location of Well: Hines, Oregon **Latitude, Longitude (NAD83)**: 43.55013, -119.08158
Elevation of well collar: 1264 (4148 ft) asl
Total depth drilled: 596 m (1956 ft), depth intervals of retrieved cuttings shown in feet (e.g., 140-150).

Cuttings shown are from depth intervals 1700 to 1900 ft.

5 cm

Name of Well: HARN 50087 - CTI Geothermal Test Well **Year well drilled**: 1996
Location of Well: Hines, Oregon **Latitude, Longitude (NAD83)**: 43.55013, -119.08158
Elevation of well collar: 1264 (4148 ft) asl
Total depth drilled: 596 m (1956 ft), depth intervals of retrieved cuttings shown in feet (e.g., 140-150).
Cuttings shown are from depth intervals 1900 to 1956 ft.

5 cm

Table 13-9. Geochemical analyses obtained from HARN 50087 CTI Geothermal Test Well cuttings (3 tables, 1 of 3). "R" sample numbers indicate repeat analyses.

Sample	HARN 50087 140-160	HARN 50087 170-180	HARN 50087 170-180R	HARN 50087 190-200	HARN 50087 220-250	HARN 50087 260-270	HARN 50087 290-330	HARN 50087 330-340	HARN 50087 360-400	HARN 50087 440-490	HARN 50087 670-680
Geographic Area	Hines	Hines	Hines	Hines	Hines	Hines	Hines	Hines	Hines	Hines	Hines
MapUnit	sed. rocks	Rattlesn. Tuff	Rattlesn. Tuff	Rattlesn. Tuff	bas. trachand. & trachand. flows	bas. trachand. & trachand. flows	bas. trachand. & trachand. flows	bas. trachand. & trachand. flows	Tuff of Wheeler Springs, welded tuff	Tuff of Wheeler Springs, welded tuff	Prater Creek Ash-Flow Tuff, intracald. unit
Label	QTst	Tmtr	Tmtr	Tmtr	Tmat	Tmat	Tmat	Tmat	Tmtw	Tmtw	Tmtpi
UTMNorthingNAD83	4824014	4824014	4824014	4824014	4824014	4824014	4824014	4824014	4824014	4824014	4824014
UTMEastingNAD83	331853	331853	331853	331853	331853	331853	331853	331853	331853	331853	331853
Age (Ma)	nd	nd	nd	nd	nd	nd	nd	nd	nd	nd	nd
Map_No	nd	nd	nd	nd	nd	nd	nd	nd	nd	nd	nd
Oxides, weight percent											
SiO_2	80.65	68.71	68.73	69.15	61.04	56.37	64.26	57.10	73.47	75.25	76.47
Al_2O_3	10.37	18.62	18.56	18.11	15.75	17.53	14.42	17.49	14.15	13.21	12.27
TiO_2	0.16	0.29	0.29	0.25	1.06	1.06	0.96	1.15	0.23	0.22	0.12
FeO*	1.27	2.41	2.48	2.04	8.70	7.53	6.83	8.21	1.67	1.50	1.77
MnO	0.02	0.06	0.06	0.06	0.12	0.14	0.14	0.13	0.04	0.03	0.03
CaO	0.56	2.85	2.84	2.66	5.52	7.46	5.25	7.99	1.03	0.71	0.25
MgO	0.16	5.95	5.95	5.11	4.31	3.97	4.96	3.20	0.38	0.31	0.10
K_2O	3.88	0.56	0.55	1.33	1.65	1.85	2.06	1.16	5.02	4.93	4.95
Na_2O	2.91	0.52	0.50	1.27	1.62	3.63	0.63	2.87	3.97	3.80	4.01
P_2O_5	0.03	0.03	0.03	0.03	0.23	0.46	0.49	0.70	0.04	0.04	0.02
LOI	1.81	19.56	19.56	16.87	12.47	0.95	15.44	6.92	3.74	1.11	1.22
Total_I	97.57	80.00	80.20	82.48	86.78	98.48	84.15	92.59	95.83	98.42	98.48
Trace Elements, parts per million											
Ni	7	7	3	7	29	37	21	35	4	5	4
Cr	4	4	5	4	41	52	26	64	4	4	3
Sc	2	5	5	5	17	20	16	21	3	3	0
V	14	40	42	43	75	165	46	113	11	12	8
Ba	477	125	128	208	2087	788	563	714	695	549	228
Rb	91	19	19	31	104	30	105	32	101	108	109
Sr	33	82	83	81	424	527	477	550	63	43	46
Zr	206	276	281	260	134	154	128	146	242	246	501
Y	29	40	41	40	17	23	20	23	40	42	65
Nb	19.8	27.6	28.3	29.0	8.9	10.3	9.5	10.7	27.3	29.8	42.8
Ga	13	18	17	18	15	19	14	17	17	17	22
Cu	6	29	28	15	77	69	36	73	5	5	7
Zn	23	69	69	56	68	79	58	82	36	29	95
Pb	10	20	21	20	7	7	6	7	19	13	35
La	30	49	49	45	21	20	18	25	40	38	58
Ce	55	93	90	99	34	47	37	46	71	73	92
Th	7	10	10	11	2	3	2	2	10	9	9
Nd	22	37	37	35	19	26	21	22	29	30	37
U	2	0	1	1	1	1	3	2	3	3	4

Major element determinations have been normalized to a 100-percent total on a volatile-free basis and recalculated with total iron expressed as FeO*; nd - no data or element not analyzed; na - not applicable or no information. LOI, Loss on Ignition; Total_I, original analytical total.

Table 13-9, continued. Geochemical analyses obtained from cuttings from the HARN 50087 CTI Geothermal Test Well (2 of 3).

Sample	HARN 50087 720-810	HARN 50087 830-900	HARN 50087 900-970	HARN 50087 1000-1010	HARN 50087 1010-1100	HARN 50087 1100-1200	HARN 50087 1200-1300	HARN 50087 1300-1340	HARN 50087 1335-1380	HARN 50087 1470-1500	HARN 50087 1500-1560
Geographic Area	Hines	Hines	Hines	Hines	Hines	Hines	Hines	Hines	Hines	Hines	Hines
MapUnit	Prater Creek Ash-Flow Tuff, intracald. unit	Prater Creek Ash-Flow Tuff, intracald. unit	Prater Creek Ash-Flow Tuff, intracald. unit	Prater Creek Ash-Flow Tuff, intracald. unit	Prater Creek Ash-Flow Tuff, intracald. unit	Prater Creek Ash-Flow Tuff, intracald. unit	Prater Creek Ash-Flow Tuff, intracald. unit	Prater Creek Ash-Flow Tuff, intracald. unit	Prater Creek Ash-Flow Tuff, intracald. unit	Prater Creek Ash-Flow Tuff, intracald. unit	Prater Creek Ash-Flow Tuff, intracald. unit
Label	Tmtpi	Tmtpi	Tmtpi	Tmtpi	Tmtpi	Tmtpi	Tmtpi	Tmtpi	Tmtpi	Tmtpi	Tmtpi
UTMNorthingNAD83	4824014	4824014	4824014	4824014	4824014	4824014	4824014	4824014	4824014	4824014	4824014
UTMEastingNAD83	331853	331853	331853	331853	331853	331853	331853	331853	331853	331853	331853
Age (Ma)	nd	nd	nd	nd	nd	nd	nd	nd	nd	nd	nd
Map_No	nd	nd	nd	nd	nd	nd	nd	nd	nd	nd	nd
Oxides, weight percent											
SiO_2	75.37	77.29	77.40	77.28	76.38	77.12	76.85	76.98	76.82	76.76	77.04
Al_2O_3	12.40	11.60	11.52	11.73	11.40	11.60	11.64	11.66	12.08	11.57	11.48
TiO_2	0.14	0.13	0.13	0.12	0.12	0.12	0.12	0.12	0.12	0.11	0.12
FeO*	2.05	2.04	2.08	1.74	1.87	1.91	2.19	2.24	1.92	2.65	2.17
MnO	0.05	0.04	0.04	0.03	0.03	0.04	0.11	0.03	0.03	0.05	0.03
CaO	0.42	0.18	0.18	0.40	1.77	0.61	0.28	0.18	0.13	0.10	0.48
MgO	0.14	0.07	0.06	0.03	0.07	0.06	0.07	0.06	0.08	0.08	0.08
K_2O	5.09	4.77	4.75	4.81	4.67	4.67	4.70	4.69	4.82	4.72	4.81
Na_2O	4.20	3.86	3.82	3.85	3.66	3.85	3.97	4.01	3.99	3.93	3.78
P_2O_5	0.15	0.03	0.03	0.02	0.02	0.02	0.05	0.03	0.02	0.02	0.02
LOI	1.34	0.80	0.67	0.52	1.99	1.20	0.93	0.68	0.81	0.76	1.12
Total_I	98.37	98.72	98.74	99.26	97.57	98.13	98.71	98.82	98.51	99.04	98.32
Trace Elements, parts per million											
Ni	5	8	8	2	4	8	10	10	9	9	6
Cr	5	35	23	3	16	20	19	12	28	14	8
Sc	0	1	0	0	0	1	2	1	1	1	0
V	10	11	8	6	7	5	4	5	3	5	3
Ba	212	182	181	177	187	173	177	167	169	163	171
Rb	121	112	107	110	105	107	109	110	117	118	111
Sr	17	15	15	12	21	16	16	12	13	12	15
Zr	530	487	486	483	448	461	442	444	439	488	498
Y	80	72	71	70	66	67	65	61	61	59	64
Nb	44.0	41.6	41.7	40.9	37.4	38.3	39.4	37.3	35.8	39.7	38.8
Ga	23	21	21	21	20	20	21	21	21	21	20
Cu	9	10	11	7	12	10	16	17	84	14	20
Zn	118	97	95	149	119	123	107	97	158	103	116
Pb	18	19	18	17	27	28	38	16	42	18	20
La	61	63	57	54	55	55	53	56	50	50	50
Ce	116	113	115	100	106	109	107	110	103	98	98
Th	9	9	8	9	8	8	8	8	7	9	7
Nd	54	51	52	44	49	51	49	51	48	44	46
U	3	1	1	3	3	3	2	3	3	3	3

Major element determinations have been normalized to a 100-percent total on a volatile-free basis and recalculated with total iron expressed as FeO*; nd - no data or element not analyzed; na - not applicable or no information. LOI, Loss on Ignition; Total_I, original analytical total.

Table 13-9, continued. Geochemical analyses obtained from cuttings from the HARN 50087 CTI Geothermal Test Well (3 of 3).

Sample no.	HARN 50087 1560-1600	HARN 50087 1690-1710	HARN 50087 1780-1810	HARN 50087 1900-1940
Geographic Area	Hines	Hines	Hines	Hines
MapUnit	Prater Creek Ash-Flow Tuff, intracald. unit	Prater Creek Ash-Flow Tuff, intracald. unit	Prater Creek Ash-Flow Tuff, intracald. unit	Prater Creek Ash-Flow Tuff, intracald. unit
Label	Tmtpi	Tmtpi	Tmtpi	Tmtpi
UTMNorthingNAD83	4824014	4824014	4824014	4824014
UTMEastingNAD83	331853	331853	331853	331853
Age (Ma)	nd	nd	nd	nd
Oxides, weight percent		nd	nd	nd
SiO_2	76.72	74.46	77.00	76.78
Al_2O_3	11.92	12.23	11.17	11.18
TiO_2	0.13	0.17	0.16	0.15
FeO*	2.11	3.14	2.70	3.12
MnO	0.05	0.08	0.05	0.08
CaO	0.37	0.31	0.31	0.20
MgO	0.04	0.12	0.17	0.09
K_2O	4.55	5.86	4.70	4.63
Na_2O	4.11	3.61	3.72	3.74
P_2O_5	0.01	0.02	0.02	0.02
LOI	3.42	1.94	1.31	1.43
Total_I	96.17	97.63	98.45	98.29
Trace Elements, parts per million				
Ni	4	4	6	5
Cr	5	5	7	14
Sc	1	1	2	0
V	1	12	4	8
Ba	194	106	48	64
Rb	112	119	105	104
Sr	12	21	13	19
Zr	497	712	640	576
Y	73	68	81	75
Nb	41.1	47.5	37.9	38.2
Ga	21	22	20	22
Cu	13	7	43	17
Zn	103	141	124	122
Pb	24	24	24	24
La	56	66	61	58
Ce	110	131	125	127
Th	9	9	8	8
Nd	52	60	57	53
U	3	5	4	1

Major element determinations have been normalized to a 100-percent total on a volatile-free basis and recalculated with total iron expressed as FeO*; nd - no data or element not analyzed; na - not applicable or no information. LOI, Loss on Ignition; Total_I, original analytical total.

Table 13-10. Descriptions and interpretations of downhole lithologies from HARN 50087 CTI Geothermal Test Well cuttings. Cuttings described and interpreted by J.D. McClaughry during 2018 to 2019.

Depth Interval (Ft)		Elevation Interval (Ft)		Geochemical Sample	Color	Interval description	Label
0	23	4148	4125		Brown	Sand.	Qoaf
23	36	4125	4112		Blue	Clay.	Qoaf
36	102	4112	4046		Brown	Clay.	Qoaf
102	126	4046	4022		Brown	Clay/sand.	QTst
126	134	4022	4014		Brown/red	Cinders.	QTst
134	140	4014	4008		Gray	Volcanic rock.	QTst
140	150	4008	3998		Light brownish gray (5YR 6/1)	Welded tuff, numerous lithic fragments and white feldspar crystals.	QTst
150	160	3998	3988	**HARN 50087 140-160**	Light brownish gray (5YR 6/1)	Welded tuff, numerous lithic fragments and white feldspar crystals.	QTst
160	170	3988	3978		Pinkish gray (5YR 8/1)	Semi-consolidated tuff.	Tmtr
170	180	3978	3968	**HARN 50087 170-180**	White (N9)	Semi-consolidated tuff.	Tmtr
180	190	3968	3958		Very pale orange (10YR 8/2)	Highly expanded pumice.	Tmtr
190	200	3958	3948	**HARN 50087 190-200**	White (N9)	Semi-consolidated tuff.	Tmtr
200	210	3948	3938		Yellowish gray (5Y 8/1)	Semi-consolidated tuff.	Tmtr
210	220	3938	3928		Medium gray (N5)	Vesicular trachyandesite with microlite plagioclase.	Tmat
220	230	3928	3918	**HARN 50087 220-250**	Medium gray (N5) to White (N9)	Mixed vesiculated trachyandesite and crystal tuff. Bleached white, hydrothermally altered.	Tmat
230	240	3918	3908		Medium gray (N5)	Vesicular trachyandesite. Bleached white, hydrothermally altered.	Tmat
240	250	3908	3898		Medium gray (N5)	Vesicular trachyandesite. Bleached white, hydrothermally altered.	Tmat
250	260	3898	3888		Moderate reddish brown (10R 3/4)	Vesicular, microcrystalline cinders.	Tmat
260	270	3888	3878	**HARN 50087 260-270**	Moderate orange pink (10R 7/4) to Light brownish gray (5YR 6/1)	Vesicular to dense trachyandesite. Silica, botryoidal zeolite.	Tmat
270	280	3878	3868		Moderate orange pink (10R 7/4) to White (N9)	Vesicular to dense trachyandesite. Silica, botryoidal zeolite.	Tmat
280	290	3868	3858		Yellowish gray (5Y 8/1)	Crystal tuff, clear blocky feldspar, ash shards. Zeolite.	Tmat
290	300	3858	3848	**HARN 50087 290-330**	Yellowish gray (5Y 8/1)	Crystal tuff, clear blocky feldspar, ash shards. Zeolite.	Tmat
300	310	3848	3838		Yellowish gray (5Y 8/1)	Crystal tuff, clear blocky feldspar, ash shards. Zeolite.	Tmat
310	320	3838	3828		Yellowish gray (5Y 8/1)	Crystal tuff, clear blocky feldspar, ash shards.	Tmat
320	330	3828	3818		Yellowish gray (5Y 8/1)	Crystal tuff, abundant clear blocky feldspar, prismatic black pyroxene, ash shards.	Tmat
330	340	3818	3808	**HARN 50087 330-340**	Brownish gray (5YR 4/1) to White (N9)	Microcrystalline cinders. Bleached white where altered. Bladed zeolite.	Tmat
340	350	3808	3798		Medium gray (N6) to White (N9)	Vesicular to dense trachyandesite. Fragments of bleached white, crystal-rich volcaniclastic sandstone. Zeolite.	Tmat
350	360	3798	3788		Light gray N7 to Medium dark gray (N4)	Mixed crystalline welded tuff, microcrystalline trachyandesite. Zeolite.	Tmtw

360	370	3788	3778	**HARN 50087 360-400**	Clear to Very light gray (N8)	Perlitic, very sparsely pyroxene microphyric obsidian.	Tmtw
370	380	3778	3768		Clear to Very light gray (N8)	Perlitic, very sparsely pyroxene microphyric obsidian.	Tmtw
380	390	3768	3758		Clear to Very light gray (N8)	Perlitic, very sparsely pyroxene microphyric obsidian.	Tmtw
390	400	3758	3748		Clear to Very light gray (N8) to Pinkish gray (5YR 8/1)	Perlitic, very sparsely pyroxene microphyric obsidian, crystalline rhyolite fragments.	Tmtw
400	410	3748	3738		Very light gray (N8) to Pinkish gray (5YR 8/2)	Crystal tuff, sparse blocky clear feldspar and Black (N1) pyroxene microphenocrysts, perlitic obsidian fragments.	Tmtw
410	420	3738	3728		Very light gray (N8) to Pinkish gray (5YR 8/2)	Crystal tuff, sparse blocky clear feldspar and Black (N1) pyroxene microphenocrysts, perlitic obsidian fragments.	Tmtw
420	430	3728	3718		Very light gray (N8) to Pinkish gray (5YR 8/2)	Crystal tuff, sparse blocky clear feldspar and Black (N1) pyroxene microphenocrysts, perlitic obsidian fragments.	Tmtw
430	440	3718	3708		Very light gray (N8) to Pinkish gray (5YR 8/2)	Crystal tuff, sparse blocky clear feldspar and Black (N1) pyroxene microphenocrysts, perlitic obsidian fragments.	Tmtw
440	450	3708	3698	**HARN 50087 440-490**	Very light gray (N8) to Pinkish gray (5YR 8/2)	Crystal tuff, sparse blocky clear feldspar and Black (N1) pyroxene microphenocrysts, perlitic obsidian fragments.	Tmtw
450	460	3698	3688		Very light gray (N8) to Pinkish gray (5YR 8/2)	Crystal tuff, sparse blocky clear feldspar and Black (N1) pyroxene microphenocrysts, perlitic obsidian fragments.	Tmtw
460	470	3688	3678		Very light gray (N8) to Pinkish gray (5YR 8/2)	Crystal tuff, sparse blocky clear feldspar and Black (N1) pyroxene microphenocrysts, perlitic obsidian fragments.	Tmtw
470	480	3678	3668		Very light gray (N8) to Pinkish gray (5YR 8/2)	Crystal tuff, sparse blocky clear feldspar and Black (N1) pyroxene microphenocrysts, perlitic obsidian fragments.	Tmtw
480	490	3668	3658		Very light gray (N8) to Pinkish gray (5YR 8/2)	Crystal tuff, sparse blocky clear feldspar and Black (N1) pyroxene microphenocrysts, perlitic obsidian fragments.	Tmtw
490	500	3658	3648		Very light gray (N8) to Pinkish gray (5YR 8/2)	Crystal tuff, sparse blocky clear feldspar and Black (N1) pyroxene microphenocrysts, perlitic obsidian fragments.	Tmtw
500	510	3648	3638		Very light gray (N8) to Pinkish gray (5YR 8/2)	Crystal tuff, sparse blocky clear feldspar and Black (N1) pyroxene microphenocrysts, perlitic obsidian fragments.	Tmtw
510	520	3638	3628		Medium light gray (N6)	Crystal tuff, sparse blocky clear feldspar and Black (N1) pyroxene microphenocrysts, perlitic obsidian fragments.	Tmtw
520	530	3628	3618		Medium light gray (N6)	Crystal tuff, sparse blocky clear feldspar and Black (N1) pyroxene microphenocrysts, perlitic obsidian fragments.	Tmtw
530	540	3618	3608		Medium light gray (N6) to Light brownish gray (5YR 6/1) to White (N9)	Crystal tuff. Sparse blocky clear feldspar and Black (N1) pyroxene microphenocrysts. Eutaxitic texture.	Tmtw
540	550	3608	3598		Medium light gray (N6) to Light brownish gray (5YR 6/1) to White (N9)	Crystal tuff. Sparse blocky clear feldspar and Black (N1) pyroxene microphenocrysts. Eutaxitic texture.	Tmtw
550	560	3598	3588		White (N9) to yellowish gray (5Y 8/1) to moderate reddish brown (10R 3/4)	Mixed crystal tuff, feldspar and pyroxene microphenocrysts. Dark yellowish orange (10YR 6/6) iron staining on fragments.	Tmtpi
560	570	3588	3578		White (N9) to yellowish gray (5Y 8/1) to moderate reddish brown (10R 3/4)	Mixed crystal tuff, feldspar and pyroxene microphenocrysts. Dark yellowish orange (10YR 6/6) iron staining on fragments.	Tmtpi
570	580	3578	3568		White (N9) to yellowish gray (5Y 8/1) to moderate reddish brown (10R 3/4)	Mixed crystal tuff, feldspar and pyroxene microphenocrysts. Dark yellowish orange (10YR 6/6) iron staining on fragments.	Tmtpi
580	590	3568	3558		White (N9) to yellowish gray (5Y 8/1) to moderate reddish brown (10R 3/4)	Mixed crystal tuff, feldspar and pyroxene microphenocrysts. Dark yellowish orange (10YR 6/6) iron staining on fragments.	Tmtpi
590	600	3558	3548		White (N9) to Yellowish gray (5Y 8/1)	Aphyric crystal tuff.	Tmtpi
600	610	3548	3538		White (N9) to Yellowish gray (5Y 8/1)	Aphyric crystal tuff, scattered mafic lithics.	Tmtpi
610	620	3538	3528		White (N9) to Yellowish gray (5Y 8/2) to Light gray (N7)	Aphyric crystal tuff.	Tmtpi

620	630	3528	3518		White (N9) to Yellowish gray (5Y 8/2) to Light gray (N7)	Aphyric crystal tuff.	Tmtpi
630	640	3518	3508		White (N9) to Yellowish gray (5Y 8/1)	Aphyric crystal tuff, sparse blocky clear feldspar and prismatic pyroxene microphenocrysts.	Tmtpi
640	650	3508	3498		White (N9) to Yellowish gray (5Y 8/2) to Greenish gray (5GY 4/1)	Mixed crystal tuff and perlitic obsidian fragments.	Tmtpi
650	660	3498	3488		White (N9) to Yellowish gray (5Y 8/2) to Greenish gray (5GY 4/1)	Mixed crystal tuff and perlitic obsidian fragments.	Tmtpi
660	670	3488	3478		White (N9) to Yellowish gray (5Y 8/2) to Greenish gray (5GY 4/1)	Mixed crystal tuff and perlitic obsidian fragments. Light brownish gray (5YR 6/1) spherulites common.	Tmtpi
670	680	3478	3468	**HARN 50087 670-680**	Medium light gray (N6) to Light brownish gray (5YR 6/1)	Spherulitic to lithophysal welded tuff. Some fragments with 1 to 2 mm blocky clear feldspar crystals.	Tmtpi
680	690	3468	3458		Medium light gray (N6) to Light brownish gray (5YR 6/1)	Spherulitic to lithophysal welded tuff. Some fragments with 1 to 2 mm blocky clear feldspar crystals.	Tmtpi
690	700	3458	3448		Medium light gray (N6) to Light brownish gray (5YR 6/1)	Spherulitic to lithophysal welded tuff. Some fragments with 1 to 2 mm blocky clear feldspar crystals.	Tmtpi
700	710	3448	3438		White (N9)	Fine crystal tuff, sparsely microphyric, < 1 percent blocky clear alkali feldspar 1 to 2 mm. Variably lithophysal.	Tmtpi
710	720	3438	3428		White (N9)	Fine crystal tuff, sparsely microphyric, < 1 percent blocky clear alkali feldspar 1 to 2 mm. Variably lithophysal.	Tmtpi
720	730	3428	3418	**HARN 50087 720-810**	White (N9)	Fine crystal tuff, sparsely microphyric, < 1 percent blocky clear alkali feldspar 1 to 2 mm. Variably lithophysal.	Tmtpi
730	740	3418	3408		White (N9)	Fine crystal tuff, sparsely microphyric, < 1 percent blocky clear alkali feldspar 1 to 2 mm. Variably lithophysal.	Tmtpi
740	750	3408	3398		White (N9)	Fine crystal tuff, sparsely microphyric, < 1 percent blocky clear alkali feldspar 1 to 2 mm. Variably lithophysal.	Tmtpi
750	760	3398	3388		White (N9)	Fine crystal tuff, sparsely microphyric, < 1 percent blocky clear alkali feldspar 1 to 2 mm. Variably lithophysal.	Tmtpi
760	770	3388	3378		White (N9)	Fine crystal tuff, sparsely microphyric, < 1 percent blocky clear alkali feldspar 1 to 2 mm. Variably lithophysal.	Tmtpi
770	780	3378	3368		White (N9)	Fine crystal tuff, sparsely microphyric, < 1 percent blocky clear alkali feldspar 1 to 2 mm. Variably lithophysal.	Tmtpi
780	790	3368	3358		White (N9)	Fine crystal tuff, sparsely microphyric, < 1 percent blocky clear alkali feldspar 1 to 2 mm. Variably lithophysal.	Tmtpi
790	800	3358	3348		White (N9)	Fine crystal tuff, sparsely microphyric, < 1 percent blocky clear alkali feldspar 1 to 2 mm. Variably lithophysal.	Tmtpi
800	810	3348	3338		White (N9)	Fine crystal tuff, sparsely microphyric, < 1 percent blocky clear alkali feldspar 1 to 2 mm. Variably lithophysal.	Tmtpi
810	820	3338	3328		White (N9)	Fine crystal tuff, sparsely microphyric, < 1 percent blocky clear alkali feldspar 1 to 2 mm. Variably lithophysal.	Tmtpi
820	830	3328	3318		White (N9)	Fine crystal tuff, sparsely microphyric, < 1 percent blocky clear alkali feldspar 1 to 2 mm. Variably lithophysal.	Tmtpi
830	840	3318	3308	**HARN 50087 830-900**	White (N9)	Fine crystal tuff, sparsely microphyric, < 1 percent blocky clear alkali feldspar 1 to 2 mm. Variably lithophysal.	Tmtpi
840	850	3308	3298		White (N9) to medium light gray (N6)	Fine crystal tuff, sparsely microphyric, < 1 percent blocky clear alkali feldspar 1 to 2 mm. Variably lithophysal.	Tmtpi
850	860	3298	3288		White (N9) to medium light gray (N6)	Fine crystal tuff, sparsely microphyric, < 1 percent blocky clear alkali feldspar 1 to 2 mm. Variably lithophysal.	Tmtpi
860	870	3288	3278		White (N9) to medium light gray (N6)	Fine crystal tuff, sparsely microphyric, < 1 percent blocky clear alkali feldspar 1 to 2 mm. Variably lithophysal.	Tmtpi
870	880	3278	3268		White (N9) to medium light gray (N6)	Fine crystal tuff, sparsely microphyric, < 1 percent blocky clear alkali feldspar 1 to 2 mm. Variably lithophysal.	Tmtpi

880	890	3268	3258		White (N9) to medium light gray (N6)	Fine crystal tuff, sparsely microphyric, < 1 percent blocky clear alkali feldspar 1 to 2 mm. Variably lithophysal.	Tmtpi
890	900	3258	3248		White (N9)	Fine crystal tuff, sparsely microphyric 1 to 2 percent blocky clear alkali feldspar 1 to 2 mm. Variably lithophysal.	Tmtpi
900	910	3248	3238	**HARN 50087 900-970**	White (N9) to medium light gray (N6)	Fine crystal tuff, sparsely microphyric 1 to 2 percent blocky clear alkali feldspar 1 to 2 mm. Variably lithophysal.	Tmtpi
910	920	3238	3228		White (N9) to medium light gray (N6)	Fine crystal tuff, sparsely microphyric 1 to 2 percent blocky clear alkali feldspar 1 to 2 mm. Variably lithophysal.	Tmtpi
920	930	3228	3218		White (N9) to medium light gray (N6)	Fine crystal tuff, sparsely microphyric 1 to 2 percent blocky clear alkali feldspar 1 to 2 mm. Variably lithophysal.	Tmtpi
930	940	3218	3208		White (N9) to medium light gray (N6)	Fine crystal tuff, sparsely microphyric 1 to 2 percent blocky clear alkali feldspar 1 to 2 mm. Variably lithophysal.	Tmtpi
940	950	3208	3198		White (N9) to medium light gray (N6)	Fine crystal tuff, sparsely microphyric 1 to 2 percent blocky clear alkali feldspar 1 to 2 mm. Variably lithophysal.	Tmtpi
950	960	3198	3188		White (N9) to medium light gray (N6)	Fine crystal tuff, sparsely microphyric 1 to 2 percent blocky clear alkali feldspar 1 to 2 mm. Variably lithophysal.	Tmtpi
960	970	3188	3178		White (N9) to medium light gray (N6)	Fine crystal tuff, sparsely microphyric 1 to 2 percent blocky clear alkali feldspar 1 to 2 mm. Variably lithophysal.	Tmtpi
970	980	3178	3168		No sample	No sample	No sample
980	990	3168	3158		No sample	No sample	No sample
990	1000	3158	3148		No sample	No sample	No sample
1000	1010	3148	3138	**HARN 50087 1000-1010**	White (N9) to Medium light gray (N6)	Fine crystal tuff, sparsely microphyric 1 to 2 percent blocky clear alkali feldspar 1 to 2 mm. Variably lithophysal.	Tmtpi
1010	1020	3138	3128	**HARN 50087 1010-1100**	White (N9) to Medium light gray (N6)	Fine crystal tuff, sparsely microphyric 1 to 2 percent blocky clear alkali feldspar 1 to 2 mm. Variably lithophysal.	Tmtpi
1020	1030	3128	3118		White (N9) to Medium light gray (N6)	Fine crystal tuff, sparsely microphyric 1 to 2 percent blocky clear alkali feldspar 1 to 2 mm. Variably lithophysal.	Tmtpi
1030	1040	3118	3108		White (N9) to Medium light gray (N6)	Fine crystal tuff, sparsely microphyric 1 to 2 percent blocky clear alkali feldspar 1 to 2 mm. Variably lithophysal.	Tmtpi
1040	1050	3108	3098		White (N9) to Medium light gray (N6)	Silicified variably zeolitized, fine crystal tuff, sparsely microphyric < 1 percent blocky, clear alkali feldspar 1 to 2 mm.	Tmtpi
1050	1060	3098	3088		White (N9) to Medium light gray (N6)	Silicified variably zeolitized, fine crystal tuff, sparsely microphyric < 1 percent blocky, clear alkali feldspar 1 to 2 mm.	Tmtpi
1060	1070	3088	3078		White (N9) to Medium light gray (N6)	Silicified variably zeolitized, fine crystal tuff, sparsely microphyric < 1 percent blocky, clear alkali feldspar 1 to 2 mm.	Tmtpi
1070	1080	3078	3068		White (N9) to Medium light gray (N6)	Silicified variably zeolitized, fine crystal tuff, sparsely microphyric < 1 percent blocky, clear alkali feldspar 1 to 2 mm.	Tmtpi
1080	1090	3068	3058		White (N9) to Medium light gray (N6)	Silicified variably zeolitized, fine crystal tuff, sparsely microphyric < 1 percent blocky, clear alkali feldspar 1 to 2 mm.	Tmtpi
1090	1100	3058	3048		White (N9) to Medium light gray (N6)	Silicified variably zeolitized, fine crystal tuff, sparsely microphyric < 1 percent blocky, clear alkali feldspar 1 to 2 mm.	Tmtpi
1100	1110	3048	3038	**HARN 50087 1100-1200**	Medium light gray (N6)	Silicified variably zeolitized, fine crystal tuff, sparsely microphyric < 1 percent blocky, clear alkali feldspar 1 to 2 mm.	Tmtpi
1110	1120	3038	3028		Medium light gray (N6)	Silicified variably zeolitized, fine crystal tuff, sparsely microphyric < 1 percent blocky, clear alkali feldspar 1 to 2 mm.	Tmtpi
1120	1130	3028	3018		Medium light gray (N6)	Silicified variably zeolitized, fine crystal tuff, sparsely microphyric < 1 percent blocky, clear alkali feldspar 1 to 2 mm.	Tmtpi

1130	1140	3018	3008		Medium light gray (N6)	Silicified variably zeolitized, fine crystal tuff, sparsely microphyric < 1 percent blocky, clear alkali feldspar 1 to 2 mm.	Tmtpi
1140	1150	3008	2998		Medium light gray (N6)	Silicified variably zeolitized, fine crystal tuff, sparsely microphyric < 1 percent blocky, clear alkali feldspar 1 to 2 mm.	Tmtpi
1150	1160	2998	2988		Medium light gray (N6)	Silicified variably zeolitized, fine crystal tuff, sparsely microphyric < 1 percent blocky, clear alkali feldspar 1 to 2 mm.	Tmtpi
1160	1170	2988	2978		Medium light gray (N6)	Silicified variably zeolitized, fine crystal tuff, sparsely microphyric < 1 percent blocky, clear alkali feldspar 1 to 2 mm.	Tmtpi
1170	1180	2978	2968		Medium light gray (N6)	Silicified variably zeolitized, fine crystal tuff, sparsely microphyric < 1 percent blocky, clear alkali feldspar 1 to 2 mm.	Tmtpi
1180	1190	2968	2958		Medium light gray (N6)	Silicified variably zeolitized, fine crystal tuff, sparsely microphyric < 1 percent blocky, clear alkali feldspar 1 to 2 mm.	Tmtpi
1190	1200	2958	2948		Medium light gray (N6)	Silicified variably zeolitized, fine crystal tuff, sparsely microphyric < 1 percent blocky, clear alkali feldspar 1 to 2 mm.	Tmtpi
1200	1210	2948	2938	**HARN 50087 1200-1300**	Medium light gray (N6)	Silicified variably zeolitized, fine crystal tuff, sparsely microphyric < 1 percent blocky, clear alkali feldspar 1 to 2 mm.	Tmtpi
1210	1220	2938	2928		Medium light gray (N6)	Silicified variably zeolitized, fine crystal tuff, sparsely microphyric < 1 percent blocky, clear alkali feldspar 1 to 2 mm.	Tmtpi
1220	1230	2928	2918		Medium light gray (N6)	Silicified variably zeolitized, fine crystal tuff, sparsely microphyric < 1 percent blocky, clear alkali feldspar 1 to 2 mm.	Tmtpi
1230	1240	2918	2908		Medium light gray (N6)	Silicified variably zeolitized, fine crystal tuff, sparsely microphyric < 1 percent blocky, clear alkali feldspar 1 to 2 mm.	Tmtpi
1240	1250	2908	2898		Medium light gray (N6)	Silicified variably zeolitized, fine crystal tuff, sparsely microphyric < 1 percent blocky, clear alkali feldspar 1 to 2 mm.	Tmtpi
1250	1260	2898	2888		Medium light gray (N6)	Silicified variably zeolitized, fine crystal tuff, sparsely microphyric < 1 percent blocky, clear alkali feldspar 1 to 2 mm.	Tmtpi
1260	1270	2888	2878		Medium light gray (N6)	Silicified variably zeolitized, fine crystal tuff, sparsely microphyric < 1 percent blocky, clear alkali feldspar 1 to 2 mm.	Tmtpi
1270	1280	2878	2868		Medium light gray (N6)	Silicified variably zeolitized, fine crystal tuff, sparsely microphyric < 1 percent blocky, clear alkali feldspar 1 to 2 mm.	Tmtpi
1280	1290	2868	2858		Medium light gray (N6)	Silicified variably zeolitized, fine crystal tuff, sparsely microphyric < 1 percent blocky, clear alkali feldspar 1 to 2 mm.	Tmtpi
1290	1300	2858	2848		Medium light gray (N6)	Silicified variably zeolitized, fine crystal tuff, sparsely microphyric < 1 percent blocky, clear alkali feldspar 1 to 2 mm.	Tmtpi
1300	1310	2848	2838	**HARN 50087 1300-1340**	Medium light gray (N6)	Silicified, variably zeolitized fine crystal tuff, aphyric.	Tmtpi
1310	1320	2838	2828		Medium light gray (N6)	Silicified, variably zeolitized fine crystal tuff, aphyric.	Tmtpi
1320	1330	2828	2818		Medium light gray (N6)	Silicified, variably zeolitized fine crystal tuff, aphyric.	Tmtpi
1330	1340	2818	2808	**HARN 50087 1335-1380**	Medium light gray (N6)	Silicified, variably zeolitized fine crystal tuff, aphyric.	Tmtpi
1340	1350	2808	2798		Medium light gray (N6)	Silicified, variably zeolitized fine crystal tuff, aphyric.	Tmtpi
1350	1360	2798	2788		Medium light gray (N6)	Silicified variably zeolitized fine crystal tuff, rare blocky subhedral, clear alkali feldspar.	Tmtpi
1360	1370	2788	2778		Medium light gray (N6)	Silicified variably zeolitized fine crystal tuff, aphyric.	Tmtpi
1370	1380	2778	2768		Medium light gray (N6)	Silicified variably zeolitized fine crystal tuff, aphyric.	Tmtpi
1380	1390	2768	2758		Medium gray (N5)	Fine crystal tuff, sparsely microphyric < 1 percent blocky, clear alkali feldspar 1 to 2 mm. Variably lithophysal.	Tmtpi

1390	1400	2758	2748		Medium gray (N5)	Silicified fine crystal tuff, aphyric.	Tmtpi
1400	1410	2748	2738		Medium gray (N5)	Silicified fine crystal tuff, aphyric.	Tmtpi
1410	1420	2738	2728		Medium gray (N5)	Silicified fine crystal tuff, aphyric.	Tmtpi
1420	1430	2728	2718		Medium gray (N5)	Silicified fine crystal tuff, aphyric.	Tmtpi
1430	1440	2718	2708		Medium gray (N5)	Silicified fine crystal tuff, aphyric.	Tmtpi
1440	1450	2708	2698		Medium gray (N5)	Silicified fine crystal tuff, aphyric. Abundant iron staining on fragments.	Tmtpi
1450	1460	2698	2688		Medium gray (N5)	Silicified fine crystal tuff, aphyric. Abundant iron staining on fragments.	Tmtpi
1460	1470	2688	2678		Medium gray (N5)	Silicified fine crystal tuff, aphyric. Abundant iron staining on fragments.	Tmtpi
1470	1480	2678	2668	**HARN 50087 1470-1500**	Medium gray (N5)	Silicified fine crystal tuff, aphyric. Abundant iron staining on fragments.	Tmtpi
1480	1490	2668	2658		Medium gray (N5)	Silicified fine crystal tuff, aphyric. Abundant iron staining on fragments.	Tmtpi
1490	1500	2658	2648		Medium gray (N5)	Silicified fine crystal tuff, aphyric. Abundant iron staining on fragments.	Tmtpi
1500	1510	2648	2638	**HARN 50087 1500-1560**	Medium gray (N5)	Silicified variably zeolitized fine crystal tuff, aphyric.	Tmtpi
1510	1520	2638	2628		Medium gray (N5)	Silicified variably zeolitized fine crystal tuff, aphyric.	Tmtpi
1520	1530	2628	2618		Medium gray (N5)	Silicified variably zeolitized fine crystal tuff, aphyric.	Tmtpi
1530	1540	2618	2608		Medium gray (N5)	Silicified fine crystal tuff, aphyric. Abundant iron staining on fragments.	Tmtpi
1540	1550	2608	2598		Medium gray (N5)	Silicified fine crystal tuff, aphyric. Flow banded. Abundant iron staining on fragments.	Tmtpi
1550	1560	2598	2588		Medium gray (N5)	Fine crystal tuff, sparsely microphyric < 1 percent blocky, clear alkali feldspar 1 to 2 mm. Variably lithophysal. Flow banded.	Tmtpi
1560	1570	2588	2578	**HARN 50087 1560-1600**	Pale pink (5RP 8/2) to Grayish black (N2)	Silicified aphyric tuff mixed with fresh perlitic obsidian.	Tmtpi
1570	1580	2578	2568		Grayish black (N2)	Perlitic obsidian.	Tmtpi
1580	1590	2568	2558		Grayish black (N2)	Perlitic obsidian.	Tmtpi
1590	1600	2558	2548		Grayish black (N2)	Perlitic obsidian.	Tmtpi
1600	1610	2548	2538		Grayish black (N2)	Perlitic obsidian.	Tmtpi
1610	1620	2538	2528		Very pale green (10G 8/2)	Fine aphyric crystal tuff mixed with fresh perlitic obsidian.	Tmtpi
1620	1630	2528	2518		Very pale green (10G 8/2)	Fine aphyric crystal tuff mixed with fresh perlitic obsidian.	Tmtpi
1630	1640	2518	2508		Very pale green (10G 8/2)	Fine aphyric crystal tuff mixed with fresh perlitic obsidian.	Tmtpi
1640	1650	2508	2498		Very pale green (10G 8/2)	Fine aphyric crystal tuff mixed with fresh perlitic obsidian.	Tmtpi
1650	1660	2498	2488		Very pale green (10G 8/2)	Fine aphyric crystal tuff mixed with fresh perlitic obsidian.	Tmtpi
1660	1670	2488	2478		Very pale green (10G 8/2)	Fine aphyric crystal tuff mixed with fresh perlitic obsidian.	Tmtpi
1670	1680	2478	2468		Very pale green (10G 8/2)	Fine aphyric crystal tuff mixed with fresh perlitic obsidian.	Tmtpi
1680	1690	2468	2458		Very pale green (10G 8/2)	Fine aphyric crystal tuff mixed with fresh perlitic obsidian.	Tmtpi
1690	1700	2458	2448	**HARN 50087 1690-1710**	Yellowish gray (5Y 8/1)	Fine aphyric crystal tuff pink rhyolite lithics.	Tmtpi

1700	1710	2448	2438		Yellowish gray (5Y 8/1)	Fine aphyric crystal tuff pink rhyolite lithics.	Tmtpi
1710	1720	2438	2428		Medium gray (N5)	Zeolitized variably silicified crystal tuff, aphyric.	Tmtpi
1720	1730	2428	2418		Medium gray (N5)	Zeolitized variably silicified crystal tuff, aphyric.	Tmtpi
1730	1740	2418	2408		Medium gray (N5)	Zeolitized variably silicified crystal tuff, aphyric.	Tmtpi
1740	1750	2408	2398		Medium gray (N5)	Zeolitized variably silicified crystal tuff, aphyric.	Tmtpi
1750	1760	2398	2388		Medium gray (N5)	Zeolitized variably silicified crystal tuff, aphyric.	Tmtpi
1760	1770	2388	2378		Medium gray (N5)	Zeolitized to variably silicified crystal tuff, aphyric. Abundant iron staining on fragments.	Tmtpi
1770	1780	2378	2368		Medium gray (N5)	Zeolitized to variably silicified crystal tuff, aphyric.	Tmtpi
1780	1790	2368	2358	**HARN 50087 1780-1810**	Medium gray (N5)	Zeolitized to variably silicified crystal tuff, aphyric.	Tmtpi
1790	1800	2358	2348		Medium gray (N5)	Zeolitized to variably silicified crystal tuff, aphyric.	Tmtpi
1800	1810	2348	2338		Medium light gray (N6)	Zeolitized to variably silicified crystal tuff, aphyric.	Tmtpi
1810	1820	2338	2328		Medium light gray (N6)	Zeolitized to variably silicified crystal tuff, aphyric. Abundant iron staining on fragments.	Tmtpi
1820	1830	2328	2318		Medium light gray (N6)	Zeolitized to variably silicified crystal tuff, aphyric.	Tmtpi
1830	1840	2318	2308		Medium light gray (N6)	Zeolitized to variably silicified crystal tuff, aphyric. Iron staining on fragments.	Tmtpi
1840	1850	2308	2298		Medium light gray (N6)	Zeolitized to variably silicified crystal tuff, aphyric.	Tmtpi
1850	1860	2298	2288		Medium light gray (N6)	Zeolitized to variably silicified crystal tuff, aphyric.	Tmtpi
1860	1870	2288	2278		Medium light gray (N6)	Zeolitized to variably silicified crystal tuff, aphyric. Abundant iron staining on fragments.	Tmtpi
1870	1880	2278	2268		Medium light gray (N6)	Zeolitized to variably silicified crystal tuff, aphyric.	Tmtpi
1880	1890	2268	2258		Medium light gray (N6)	Zeolitized to variably silicified crystal tuff, aphyric. Abundant iron staining on fragments.	Tmtpi
1890	1900	2258	2248		Medium light gray (N6)	Zeolitized to variably silicified crystal tuff, aphyric. Abundant iron staining on fragments.	Tmtpi
1900	1910	2248	2238	**HARN 50087 1900-1940**	Medium light gray (N6)	Fine crystal tuff, aphyric.	Tmtpi
1910	1920	2238	2228		Medium light gray (N6)	Fine crystal tuff, aphyric.	Tmtpi
1920	1930	2228	2218		Medium light gray (N6)	Fine crystal tuff, aphyric.	Tmtpi
1930	1940	2218	2208		Medium light gray (N6)	Fine crystal tuff, aphyric.	Tmtpi
1940	1950	2208	2198		Medium light gray (N6)	Fine crystal tuff, aphyric. Abundant iron staining on fragments.	Tmtpi
1950	1956	2198	2192		Medium light gray (N6)	Fine crystal tuff, aphyric.	Tmtpi